

BULLETIN OF RUSSIAN STATE MEDICAL UNIVERSITY

BIOMEDICAL JOURNAL OF PIROGOV RUSSIAN NATIONAL
RESEARCH MEDICAL UNIVERSITY

EDITOR-IN-CHIEF Denis Rebrikov, DSc, professor

DEPUTY EDITOR-IN-CHIEF Alexander Oettinger, DSc, professor

EDITORS Valentina Geidebrekht, Nadezda Tikhomirova

TECHNICAL EDITOR Evgeny Lukyanov

TRANSLATORS Natalia Usman

DESIGN AND LAYOUT Marina Doronina

EDITORIAL BOARD

Averin VI, DSc, professor (Minsk, Belarus)
Alipov NN, DSc, professor (Moscow, Russia)
Belousov VV, DSc, professor (Moscow, Russia)
Bogomilskiy MR, corr. member of RAS, DSc, professor (Moscow, Russia)
Bozhenko VK, DSc, CSc, professor (Moscow, Russia)
Bylova NA, CSc, docent (Moscow, Russia)
Gainetdinov RR, CSc (Saint-Petersburg, Russia)
Gendlin GYe, DSc, professor (Moscow, Russia)
Ginter EK, member of RAS, DSc (Moscow, Russia)
Gorbacheva LR, DSc, professor (Moscow, Russia)
Gordeev IG, DSc, professor (Moscow, Russia)
Gudkov AV, PhD, DSc (Buffalo, USA)
Gulyaeva NV, DSc, professor (Moscow, Russia)
Gusev EI, member of RAS, DSc, professor (Moscow, Russia)
Danilenko VN, DSc, professor (Moscow, Russia)
Zarubina TV, DSc, professor (Moscow, Russia)
Zatevakhin II, member of RAS, DSc, professor (Moscow, Russia)
Kagan VE, professor (Pittsburgh, USA)
Kzyzhkowska YuG, DSc, professor (Heidelberg, Germany)
Kobriniskii BA, DSc, professor (Moscow, Russia)
Kozlov AV, MD PhD (Vienna, Austria)
Kotelevtsev YuV, CSc (Moscow, Russia)
Lebedev MA, PhD (Darem, USA)
Manturova NE, DSc (Moscow, Russia)
Milushkina OYu, DSc, professor (Moscow, Russia)
Mitupov ZB, DSc, professor (Moscow, Russia)
Moshkovskii SA, DSc, professor (Moscow, Russia)
Munblit DB, MSc, PhD (London, Great Britain)

Negrebetsky VV, DSc, professor (Moscow, Russia)
Novikov AA, DSc (Moscow, Russia)
Pivovarov YuP, member of RAS, DSc, professor (Moscow, Russia)
Polunina NV, corr. member of RAS, DSc, professor (Moscow, Russia)
Poryadin GV, corr. member of RAS, DSc, professor (Moscow, Russia)
Razumovskii AYU, corr. member of RAS, DSc, professor (Moscow, Russia)
Rebrova OYu, DSc (Moscow, Russia)
Rudoy AS, DSc, professor (Minsk, Belarus)
Rylova AK, DSc, professor (Moscow, Russia)
Savelieva GM, member of RAS, DSc, professor (Moscow, Russia)
Semiglazov VF, corr. member of RAS, DSc, professor (Saint-Petersburg, Russia)
Skoblina NA, DSc, professor (Moscow, Russia)
Slavyanskaya TA, DSc, professor (Moscow, Russia)
Smirnov VM, DSc, professor (Moscow, Russia)
Spallone A, DSc, professor (Rome, Italy)
Starodubov VI, member of RAS, DSc, professor (Moscow, Russia)
Stepanov VA, corr. member of RAS, DSc, professor (Tomsk, Russia)
Suchkov SV, DSc, professor (Moscow, Russia)
Takhchidi KhP, member of RAS, DSc, professor (Moscow, Russia)
Trufanov GE, DSc, professor (Saint-Petersburg, Russia)
Favorova OO, DSc, professor (Moscow, Russia)
Filipenko ML, CSc, leading researcher (Novosibirsk, Russia)
Khazipov RN, DSc (Marsel, France)
Chundukova MA, DSc, professor (Moscow, Russia)
Shimanovskii NL, corr. member of RAS, DSc, professor (Moscow, Russia)
Shishkina LN, DSc, senior researcher (Novosibirsk, Russia)
Yakubovskaya RI, DSc, professor (Moscow, Russia)

SUBMISSION <http://vestnikrgmu.ru/login?lang=en>

CORRESPONDENCE editor@vestnikrgmu.ru

COLLABORATION manager@vestnikrgmu.ru

ADDRESS ul. Ostrovityanova, d. 1, Moscow, Russia, 117997

Indexed in Scopus. CiteScore 2021: 0.5

Scopus[®]

SCImago Journal & Country Rank 2020: 0.14

SJR

Scimago Journal & Country Rank

Indexed in WoS. JCR 2021: 0.5

WEB OF SCIENCE[™]

Listed in HAC 31.01.2020 (№ 507)



**ВЫСШАЯ
АТТЕСТАЦИОННАЯ
КОМИССИЯ (ВАК)**

Five-year h-index is 8

Google
scholar

Open access to archive

CYBERLENINKA

Issue DOI: 10.24075/brsmu.2022-04

The mass media registration certificate № 012769 issued on July 29, 1994

Founder and publisher is Pirogov Russian National Research Medical University (Moscow, Russia)

The journal is distributed under the terms of Creative Commons Attribution 4.0 International License www.creativecommons.org



Approved for print 31.08.2022
Circulation: 100 copies. Printed by Print.Formula
www.print-formula.ru

ВЕСТНИК РОССИЙСКОГО ГОСУДАРСТВЕННОГО МЕДИЦИНСКОГО УНИВЕРСИТЕТА

НАУЧНЫЙ МЕДИЦИНСКИЙ ЖУРНАЛ РНИМУ ИМ. Н. И. ПИРОГОВА

ГЛАВНЫЙ РЕДАКТОР Денис Ребриков, д. б. н., профессор

ЗАМЕСТИТЕЛЬ ГЛАВНОГО РЕДАКТОРА Александр Эттингер, д. м. н., профессор

РЕДАКТОРЫ Валентина Гейдебрехт, Надежда Тихомирова

ТЕХНИЧЕСКИЙ РЕДАКТОР Евгений Лукьянов

ПЕРЕВОДЧИКИ Наталия Усман

ДИЗАЙН И ВЕРСТКА Марины Дорониной

РЕДАКЦИОННАЯ КОЛЛЕГИЯ

В. И. Аверин, д. м. н., профессор (Минск, Белоруссия)
Н. Н. Алипов, д. м. н., профессор (Москва, Россия)
В. В. Белоусов, д. б. н., профессор (Москва, Россия)
М. Р. Богомилский, член-корр. РАН, д. м. н., профессор (Москва, Россия)
В. К. Боженко, д. м. н., к. б. н., профессор (Москва, Россия)
Н. А. Былова, к. м. н., доцент (Москва, Россия)
Р. Р. Гайнетдинов, к. м. н. (Санкт-Петербург, Россия)
Г. Е. Гендлин, д. м. н., профессор (Москва, Россия)
Е. К. Гинтер, академик РАН, д. б. н. (Москва, Россия)
Л. Р. Горбачева, д. б. н., профессор (Москва, Россия)
И. Г. Гордеев, д. м. н., профессор (Москва, Россия)
А. В. Гудков, PhD, DSc (Буффало, США)
Н. В. Гуляева, д. б. н., профессор (Москва, Россия)
Е. И. Гусев, академик РАН, д. м. н., профессор (Москва, Россия)
В. Н. Даниленко, д. б. н., профессор (Москва, Россия)
Т. В. Зарубина, д. м. н., профессор (Москва, Россия)
И. И. Затевахин, академик РАН, д. м. н., профессор (Москва, Россия)
В. Е. Каган, профессор (Питтсбург, США)
Ю. Г. Кжышковска, д. б. н., профессор (Гейдельберг, Германия)
Б. А. Кобринский, д. м. н., профессор (Москва, Россия)
А. В. Козлов, MD PhD (Вена, Австрия)
Ю. В. Котелевцев, к. х. н. (Москва, Россия)
М. А. Лебедев, PhD (Дарем, США)
Н. Е. Мантурова, д. м. н. (Москва, Россия)
О. Ю. Милушкина, д. м. н., доцент (Москва, Россия)
З. Б. Митупов, д. м. н., профессор (Москва, Россия)
С. А. Мошковский, д. б. н., профессор (Москва, Россия)
Д. Б. Мунблит, MSc, PhD (Лондон, Великобритания)

В. В. Негребский, д. х. н., профессор (Москва, Россия)
А. А. Новиков, д. б. н. (Москва, Россия)
Ю. П. Пивоваров, д. м. н., академик РАН, профессор (Москва, Россия)
Н. В. Полунина, член-корр. РАН, д. м. н., профессор (Москва, Россия)
Г. В. Порядин, член-корр. РАН, д. м. н., профессор (Москва, Россия)
А. Ю. Разумовский, член-корр., профессор (Москва, Россия)
О. Ю. Реброва, д. м. н. (Москва, Россия)
А. С. Рудой, д. м. н., профессор (Минск, Белоруссия)
А. К. Рылова, д. м. н., профессор (Москва, Россия)
Г. М. Савельева, академик РАН, д. м. н., профессор (Москва, Россия)
В. Ф. Семглазов, член-корр. РАН, д. м. н., профессор (Санкт-Петербург, Россия)
Н. А. Скоблина, д. м. н., профессор (Москва, Россия)
Т. А. Славянская, д. м. н., профессор (Москва, Россия)
В. М. Смирнов, д. б. н., профессор (Москва, Россия)
А. Спаллоне, д. м. н., профессор (Рим, Италия)
В. И. Стародубов, академик РАН, д. м. н., профессор (Москва, Россия)
В. А. Степанов, член-корр. РАН, д. б. н., профессор (Томск, Россия)
С. В. Сучков, д. м. н., профессор (Москва, Россия)
Х. П. Тахчиди, академик РАН, д. м. н., профессор (Москва, Россия)
Г. Е. Труфанов, д. м. н., профессор (Санкт-Петербург, Россия)
О. О. Фаворова, д. б. н., профессор (Москва, Россия)
М. Л. Филипенко, к. б. н. (Новосибирск, Россия)
Р. Н. Хазипов, д. м. н. (Марсель, Франция)
М. А. Чундокова, д. м. н., профессор (Москва, Россия)
Н. Л. Шимановский, член-корр. РАН, д. м. н., профессор (Москва, Россия)
Л. Н. Шишкина, д. б. н. (Новосибирск, Россия)
Р. И. Якубовская, д. б. н., профессор (Москва, Россия)

ПОДАЧА РУКОПИСЕЙ <http://vestnikrgmu.ru/login>

ПЕРЕПИСКА С РЕДАКЦИЕЙ editor@vestnikrgmu.ru

СОТРУДНИЧЕСТВО manager@vestnikrgmu.ru

АДРЕС РЕДАКЦИИ ул. Островитянова, д. 1, г. Москва, 117997

Журнал включен в Scopus. CiteScore 2021: 0,5

Журнал включен в WoS. JCR 2021: 0,5

Индекс Хирша (h²) журнала по оценке Google Scholar: 8

Scopus[®]

SCImago Journal & Country Rank 2020: 0,14

SJR
Scimago Journal & Country Rank

WEB OF SCIENCE[™]

Журнал включен в Перечень 31.01.2020 (№ 507)



**ВЫСШАЯ
АТТЕСТАЦИОННАЯ
КОМИССИЯ (ВАК)**

Google
scholar

Здесь находится открытый архив журнала

CYBERLENINKA

DOI выпуска: 10.24075/vrgmu.2022-04

Свидетельство о регистрации средства массовой информации № 012769 от 29 июля 1994 г.

Учредитель и издатель — Российский национальный исследовательский медицинский университет имени Н. И. Пирогова (Москва, Россия)

Журнал распространяется по лицензии Creative Commons Attribution 4.0 International www.creativecommons.org



Подписано в печать 31.08.2022

Тираж 100 экз. Отпечатано в типографии Print.Formula
www.print-formula.ru

REVIEW**5****Recent advances in diagnostics of neonatal hypoxic ischemic encephalopathy**

Starodubtseva NL, Eldarov ChM, Kirtbaya AR, Balashova EN, Gryzunova AS, Ionov OV, Zubkov VV, Silachev DN

Новейшие достижения в диагностике гипоксической ишемической энцефалопатии новорожденных

Н. Л. Стародубцева, Ч. М. Эльдаров, А. Р. Киртбая, Е. Н. Балашова, А. С. Грызунова, О. В. Ионов, В. В. Зубков, Д. Н. Силачев

ORIGINAL RESEARCH**17****Content of CD4⁺ cells expressing CD39/CD73 ectonucleotidases in children with inflammatory bowel diseases**

Radygina TV, Petrichuk SV, Kuptsova DG, Potapov AS, Illarionov AS, Anushenko AO, Kurbatova OV, Semikina EL

Содержание CD4⁺-клеток с экспрессией эктонуклеотидаз CD39/CD73 у детей с воспалительными заболеваниями кишечника

Т. В. Радыгина, С. В. Петричук, Д. Г. Купцова, А. С. Потапов, А. С. Илларионов, А. О. Анушенко, О. В. Курбатова, Е. Л. Семикина

ORIGINAL RESEARCH**24****Androgen levels in blood and follicular fluid of IVF patients with diminished ovarian reserve**

Gavisova AA, Shevtsova MA, Kindysheva SV, Starodubtseva NL, Frankevich VE, Nazarenko TA, Dolgushina NV

Уровень андрогенов в крови и фолликулярной жидкости у женщин с бесплодием и сниженным овариальным резервом в программах ВРТ

А. А. Гависова, М. А. Шевцова, С. В. Киндышева, Н. Л. Стародубцева, В. Е. Франкевич, Т. А. Назаренко, Н. В. Долгушина

ORIGINAL RESEARCH**31****Experience of Stanford neuromodulation therapy in patients with treatment-resistant depression**

Poydasheva AG, Bakulin IS, Sinitsyn DO, Zabirowa AH, Suponeva NA, Maslennikov NV, Tsukarzi EE, Mosolov SN, Piradov MA

Опыт применения Стэнфордской нейромодулирующей терапии у пациентов с терапевтически резистентной депрессией

А. Г. Пойдашева, И. С. Бакулин, Д. О. Синицын, А. Х. Забиrowa, Н. А. Супонева, Н. В. Маслеников, Э. Э. Цукарзи, С. Н. Мосолов, М. А. Пирадов

ORIGINAL RESEARCH**38****Systemic inflammation markers of diet-induced metabolic syndrome in rat model**

Biriulina JG, Voronkova OV, Ivanov VV, Buyko EE, Shcherbakova MM, Chernyshov NA, Motlokhova EA

Маркеры системного воспаления у крыс в модели диет-индуцированного метаболического синдрома

Ю. Г. Бирулина, О. В. Воронкова, В. В. Иванов, Е. Е. Буйко, М. М. Щербакoва, Н. А. Чернышов, Е. А. Мотлохова

ORIGINAL RESEARCH**44****EPOR/CD131-mediated attenuation of rotenone-induced retinal degeneration is associated with upregulation of autophagy genes**

Soldatov VO, Pokrovsky MV, Puchenkova OA, Zhunusov NS, Krayushkina AM, Grechina AV, Soldatova MO, Lapin KN, Bushueva OYu

EPOR/CD131-опосредованная ретинопротекция при ротенон-индуцированной нейротоксичности связана с увеличением экспрессии генов аутофагии

В. О. Солдатов, М. В. Покровский, О. А. Пученкова, Н. С. Жунусов, А. М. Краюшкина, А. В. Гречина, М. О. Солдатова, К. Н. Лапин, О. Ю. Бушуева

ORIGINAL RESEARCH**51****Prognostic significance of oral fluid fluoride measurement in acute pericoronitis**

Vagner VD, Sarf EA, Belskaya LV, Korshunov AS, Kuryatnikov KN, Bondar AA, Meloyan AD, Maksimenko KA, Kasiy MN

Прогностическая значимость определения фторид-ионов в ротовой жидкости при остром перикороните

В. Д. Вагнер, Е. А. Сарф, Л. В. Бельская, А. С. Коршунов, К. Н. Курятников, А. А. Бондарь, А. Д. Мелоян, К. А. Максименко, М. Н. Касий

***In silico* algorithm for optimization of pharmacokinetic studies of [25Mg²⁺]porphyrin-fullerene nanoparticles**

Fursov VV, Zinchenko DI, Namestnikova DD, Kuznetsov DA

***In silico*-моделирование в оптимизации алгоритмов фармакокинетических исследований [25Mg²⁺] порфирин-фуллереновых наночастиц**

В. В. Фурсов, Д. И. Зинченко, Д. Д. Наместникова, Д. А. Кузнецов

RECENT ADVANCES IN DIAGNOSTICS OF NEONATAL HYPOXIC ISCHEMIC ENCEPHALOPATHY

Starodubtseva NL, Eldarov ChM, Kirtbaya AR, Balashova EN, Gryzunova AS, Ionov OV, Zubkov VV, Silachev DN 

Kulakov National Medical Research Center for Obstetrics, Gynecology and Perinatology, Moscow, Russia

The prognosis in neonatal hypoxic ischemic encephalopathy (HIE) depends on early differential diagnosis for justified administration of emergency therapeutic hypothermia. The moment of therapy initiation directly affects the long-term neurological outcome: the earlier the commencement, the better the prognosis. This review analyzes recent advances in systems biology that facilitate early differential diagnosis of HIE as a pivotal complement to clinical indicators. We discuss the possibilities of clinical translation for proteomic, metabolomic and extracellular vesicle patterns characteristic of HIE and correlations with severity and prognosis. Identification and use of selective biomarkers of brain damage in neonates during the first hours of life is hindered by systemic effects of hypoxia. Chromatography–mass spectrometry blood tests allow analyzing hundreds and thousands of metabolites in a small biological sample to identify characteristic signatures of brain damage. Clinical use of advanced analytical techniques will facilitate the accurate and timely diagnosis of HIE for enhanced management.

Keywords: neonatal hypoxic ischemic encephalopathy, diagnostics, mass-spectrometry, proteomics, metabolomics, lipidomics

Funding: the study was supported by the Russian Science Foundation grant number 22-15-00454; <https://rscf.ru/project/22-15-00454/>

Author contribution: Starodubtseva NL, Eldarov ChM, Kirtbaya AR, Balashova EN, Gryzunova AS, Ionov OV, Zubkov VV and Silachev DN — literature analysis, manuscript writing and editing.

✉ **Correspondence should be addressed:** Denis N. Silachev
Akademika Oparina, 4, Moscow, 117997, Russia; d_silachev@oparina4.ru

Received: 06.07.2022 **Accepted:** 20.07.2022 **Published online:** 29.07.2022

DOI: 10.24075/brsmu.2022.038

НОВЕЙШИЕ ДОСТИЖЕНИЯ В ДИАГНОСТИКЕ ГИПОКСИЧЕСКОЙ ИШЕМИЧЕСКОЙ ЭНЦЕФАЛОПАТИИ НОВОРОЖДЕННЫХ

Н. Л. Стародубцева, Ч. М. Эльдаров, А. Р. Киртбая, Е. Н. Балашова, А. С. Грызунова, О. В. Ионов, В. В. Зубков, Д. Н. Силачев 

Национальный медицинский исследовательский центр акушерства, гинекологии и перинатологии имени В. И. Кулакова, Москва, Россия

Основной проблемой при гипоксической ишемической энцефалопатии новорожденных (ГИЭ) является ранняя дифференциальная диагностика, прогнозирование и классификация заболевания, от результатов которой напрямую зависит дальнейший метод терапии, в частности, назначение терапевтической гипотермии. Существует прямая зависимость времени начала терапевтической гипотермии и долгосрочного неврологического исхода: чем раньше начата терапевтическая гипотермия, тем лучше прогноз для пациента. В обзоре проанализированы последние достижения в области системной биологии, направленные на раннюю дифференциальную диагностику ГИЭ в дополнение к клиническим: применение протеомных и метаболомных биомаркеров, а также внеклеточных везикул, для которых установлена связь с тяжестью ГИЭ и прогнозом исхода. Выявление селективных маркеров повреждения головного мозга у новорожденных в первые часы жизни затруднено из-за системного влияния гипоксии на весь организм. Особый интерес представляют метаболомные исследования крови новорожденных с использованием хромато-масс-спектрометрии, позволяющие анализировать сотни метаболитов на небольшом количестве биологического образца и определять паттерны, соответствующие повреждению мозга, что будет способствовать более точной и своевременной постановке диагноза ГИЭ для назначения терапевтической гипотермии.

Ключевые слова: гипоксическая ишемическая энцефалопатия новорожденных, диагностика, масс-спектрометрия, протеомика, метаболомика, липидомика

Финансирование: исследование выполнено за счет гранта Российского научного фонда № 22-15-00454, <https://rscf.ru/project/22-15-00454/>

Вклад авторов: Н. Л. Стародубцева, Ч. М. Эльдаров, А. Р. Киртбая, Е. Н. Балашова, А. С. Грызунова, О. В. Ионов, В. В. Зубков, Д. Н. Силачев — анализ литературных данных, написание и редактирование рукописи.

✉ **Для корреспонденции:** Денис Николаевич Силачев
ул. Академика Опарина, д. 4, г. Москва, 117997, Россия; d_silachev@oparina4.ru

Статья получена: 06.07.2022 **Статья принята к печати:** 20.07.2022 **Опубликована онлайн:** 29.07.2022

DOI: 10.24075/vrgmu.2022.038

Neonatal hypoxic ischemic encephalopathy

Neonatal hypoxic ischemic encephalopathy (HIE) is one of the leading causes of neonatal mortality and disability. Among premature babies (gestational age < 28 weeks) HIE occurs in about 4–48 cases per 1000 pregnancies, and the incidence strongly correlates with a decrease in gestational age [1–4]. HIE accounts for 6–9% of all neonatal deaths and 21–23% of term infant deaths. According to the literature, up to 10% of neonates with HIE die after birth and 25% develop severe neurological disorders: cerebral palsy, seizures, mental retardation, cognitive impairment and epilepsy [5–9].

Clinical outcomes in infants with this pathology depend on its correct prediction, detection and classification as a basis for the choice of strategy. Among infants with signs of perinatal asphyxia, about 20% are at risk for HIE of varying severity,

of which 40–50% will be at risk of disability, including mental retardation, epileptic seizures, visual and hearing impairments and possibly death [10].

Therapeutic hypothermia (TH) is a proven, effective treatment for HIE that improves survival and long-term prognosis [11, 12]. Current recommendations for the use of TH include infants with moderate to severe HIE starting from 37 weeks of gestation and exclude infants with mild HIE. Still, 75% of neonatal centers in UK perform TH in infants with mild HIE, according to a national survey [13]. The prospective research on infants with mild encephalopathy (PRIME) project revealed early emergent electroencephalography (EEG) changes, seizures, pathological signs in brain MRI or neurological symptoms in 52% of infants with mild HIE at discharge [14]; a follow-up examination in 19 months on average revealed disability in 16% and Bayley-III scores below 85 in 40% of the cases. It was noted that in

children with mild HIE receiving no TH, cognitive outcomes were similar to those in children with HIE of moderate severity and no TH. A systematic follow-up in infants with mild HIE revealed neurodevelopmental pathological sequelae in 25% of the cases ($n = 341$) [15–17].

Clinical diagnosis and prognosis of HIE

The early and accurate assessment of HIE severity remains one of the most challenging tasks in neonatal care. Neonatology uses a variety of clinical methods to assess the morphological and functional state of the nervous system in order to predict long-term outcomes, such as neuroimaging and neurophysiological techniques, and their combinations [18–22]. However, the currently available instrumental assessments for the risks of brain damage in neonates have inherent limitations that prevent using them during the first hours of life; hence the uncertainty about the severity of ongoing brain damage and concomitant neurological risks during the early postnatal period [23, 24].

The available clinical assessment tools for HIE include amplitude-integrated EEG, neuroimaging and cerebral blood flow scans [22, 24–27]. A number of studies have shown that about 80% of EEG seizures in neonates are unrelated to clinical status and thus cannot be identified without constant EEG monitoring, even by experienced clinicians. Moreover, there is no straightforward correlation between HIE severity and the incidence of seizure activity revealed clinically or by EEG [28–30].

The amplitude-integrated background EEG patterns in HIE strongly correlate with neurological outcome [31]. However, their prognostic value depends on the duration of background pattern changes with regard to HIE, whereas time limit for the prevention of adverse outcomes in infants receiving TH constitutes 48–72 h of life [27]. Qualitative assessment of brain damage by MRI during the first 48 hours of life is prone to underestimation [32–34].

Various risk factors have been shown to undermine the benefits of TH in newborns with asphyxia, including HIE severity, delayed commencement of the treatment, hypo- and hyperglycemia, seizures, hyperoxia and hypocapnia during the therapy, as well as certain comorbidities. A well-known risk factor for poor neurological outcome in neonates is perinatal sepsis; besides, TH has a negligible neuroprotective effect in the inflammation-sensitized hypoxic-ischemic encephalopathy [35–39].

HIE is rarely caused by metabolic imbalances [40]. Congenital metabolic disorders manifest in neonatal period after normal delivery with no signs of perinatal asphyxia. The newborns develop neurological symptoms and signs of multiple organ failure, which may clinically resemble HIE. A detailed family history to establish risk factors such as parental consanguinity or infant death in the anamnesis is essential, as most congenital metabolic disorders have an autosomal recessive pattern of inheritance. All neonates at risk for congenital metabolic disorders should be examined accordingly, as these patients may decisively benefit from specific therapies rather than hypothermia.

Another category of genetically determined neurological disorders mimicking HIE are neonatal myopathies and encephalopathies. Neonates with congenital centronuclear myopathy present with muscular hypotension associated with respiratory failure and early lethal outcome, which may also mimic HIE [41]. The widespread use of whole-genome sequencing methods has revealed a number of new pathological variants, e.g. in *GNAO1*, associated with functional defects of the central nervous system and clinical phenotypes similar to

HIE [42, 43]. Thus, TH has been effective only in some patients with clinical signs of HIE. The early differential diagnosis of HIE in neonates can be facilitated by analysis of blood levels for a variety of metabolites using advanced analytical techniques, notably chromatography–mass spectrometry. This method allows identification of hundreds of metabolites within a few hours, which fits the time window for a decision on TH.

New approaches in HIE diagnostics: proteomic studies

Recent years have been marked by a constantly growing interest in systems biology — a science that integrates several levels of information to achieve a more comprehensive knowledge of a biological system. Genomics, transcriptomics, proteomics and metabolomics are the pillars of systems biology, forming a group of the so-called 'omics'-sciences. The ongoing boom in 'omics'-sciences is a consequence of recent breakthroughs in instrumental technologies, particularly in the fields of chromatography, mass spectrometry and sequencing. Technologies used to create the 'omics'-platforms are analytical approaches for obtaining information about molecules of various order that make up a biological sample: nucleic acids, proteins and metabolites. These methods allow simultaneous recording of quantitative and qualitative content for thousands of compounds, thus creating a unique 'fingerprint' of the current state of the body. The 'omics'-sciences are mutually complementing: genomics reveals the potential, transcriptomic shows the intention, proteomics tells what is going on and metabolomics reflects the influence of external and internal environments on the genetically determined biochemical landscape. As genes and proteins provide the basis for cellular activities, big shifts in physiological status mostly occur at the level of metabolites. In the applied perspective, metabolome is probably the best sensor for pathophysiological status of cells, tissues, organs and the body [44].

Research on biomarkers of various diseases, including those with high social impact, constitutes a booming field at the intersection of genomics, proteomics, metabolomics and instrumental analytics including nuclear magnetic resonance (NMR), mass spectrometry (MS), high performance liquid chromatography coupled with mass spectrometry (HPLC-MS/MS) and enzyme immunoassay (ELISA). This is reflected by a soaring number of publications, symposia and special sections at industry conferences focused on this issue.

It should be noted that opportunities of clinical investigation during the neonatal period are tightly limited. Among neonatal biological samples suitable for the study of molecular marker dynamics those collected non-invasively (urine, stools) or low-invasively (blood, dried blood spots) are highly preferable for medical reasons. Leftovers from routine clinical tests can be used straightforwardly for advanced analysis without additional contacts with the patient.

Several studies featuring quests for biomarkers in neonatal blood, urine and cerebrospinal fluid (CSF) samples have been published, representing various pathologies including HIE [45]. It should be noted that CSF collection is highly invasive. True enough, CSF may contain neural markers including glial fibrillary acidic protein (GFAP) and S100B, but not during the first critical 6 h after birth, although these markers can be of significant value for the prognosis of already developed HIE [46]. The use of urine has been considered as well, notably for the measurements of lactate-creatinine ratio in suspected HIE; however, the infants with congenital neonatal asphyxia usually present with delayed onset of urination because of the concomitant kidney damage, which makes urine a hardly

suitable substrate for clinical diagnosis of HIE on a routine basis [47].

Accordingly, the major efforts are focused on the use of biomarkers circulating with the blood, mostly of peptide nature, as well as neuronal exosomes and inflammatory cytokines and metabolites. The latest advances in metabolomics, proteomics and transcriptomics shift the focus towards complex molecular patterns instead of individual biological compounds. The much sought-for patterns should clearly distinguish HIE against the background of concomitant damage to kidney, myocardium, etc., inevitable in perinatal asphyxia. So far, the available 'omics' data for the initial stage of brain injury in HIE (hypoxic phase during the first 6 h after birth) have been clinically irrelevant.

The search for 'omics' patterns is complicated, firstly, by the nature of pathological process in HIE. The hypoxic conditions switch brain cells to anaerobic metabolism, to which they are not fit (especially neurons). Under conditions of stress, excitotoxicity and metabolic waste accumulation, the energy resources quickly become depleted and the cells die massively by necrosis thereby seeding the inflammatory reaction. The ischemic/hypoxic phase is followed by reperfusion/reoxygenation phase marked by reactive oxygen species production, initiation of apoptosis cascades and inflammation. The final and permanent phase of chronic inflammation aggravates the excitotoxicity, oxidative metabolism impairment and protease and caspase activation, eventually leading to organic brain injury and impaired functionalities [48]. The associated dynamic changes in molecular and biochemical cascades are mirrored by corresponding profiles in blood plasma; noteworthy, many relevant candidate markers (compounds with characteristic disease-related dynamics) 'miss' the time window of the emergency decision making (within 6 h after birth). For instance, blood levels of the above-mentioned GFAP and S100B, as well as neuron-specific enolase and myelin basic protein, rise 12–24 h after birth i.e. clearly beyond the 6 h limit [49–51]. Clinically, HIE is difficult to differentiate from neonatal sepsis or congenital metabolic disorders; moreover, sepsis may accompany HIE, modifying its clinical presentation. It is important to emphasize that erroneous administration of HT due to diagnostic inaccuracy can be harmful to patients with non-ischemic encephalopathies [52]. This additional constraint underscores the demand for reliable markers of neonatal brain damage associated specifically with the ischemic/hypoxic genesis of the condition.

Another obstacle in molecular diagnostics of HIE is marker specificity with regard to neuronal damage. By assumption, such markers should be mostly proteins essential for structural integrity of nervous tissue; accordingly, upon violation of the blood brain barrier such markers penetrate to CSF first and then to the blood [53]. Very often, though, the cues are blurred by collateral processes, e.g. inflammatory, triggered by asphyxia. For instance, in cord blood of full-term newborns with severe HIE ($n = 25$) the brain-type creatine phosphokinase (BT-CC) levels were increased several-fold compared with matching healthy controls over the first 6 h and 24 h of life [54]. Of note, BT-CC is not a brain damage-specific enzyme, but is expressed in most tissues and its elevated levels may result from damage to other organs in asphyxia [55]. Another candidate molecule, ubiquitin C-terminal hydrolase L1, is a neuron-specific cytoplasmic marker of apoptosis. Blood tests for this protein carried out in 50 newborns (37 weeks of gestation on average) revealed significant increase within 24 h of life specifically in moderate and severe HIE, despite a negligible correlation of its levels with subsequent MRI changes recorded on day 5 and in 1 year follow-up [56]. Yet another study focused on neurofilament light chain protein (NFL)

showing increased blood levels in newborns with moderate and severe HIE receiving HT. The initial measurement was made at 18 h, when the temperature inside HT chamber reached its target level. Despite strong correlation of NFL blood dynamics with MRI scans revealed in the study, no data for the first 6 h of life were available, and apparently NFL should be regarded as a late prognostic marker non-applicable for the early diagnosis required for the emergency treatment [57].

The violation of the blood-brain barrier integrity promotes endothelial cell activation with induced secretion of non-specific angiogenic markers, notably VEGF. Apart from endothelial cells, VEGF can also be produced by astrocytes and microglia. However, the evidence on its increased plasma levels in HIE is contradictory [58] and the molecule is not specific for brain tissues [59]. A similar situation is observed for adrenomedullin and secretoneurin, produced by the brain but also by the endocrine and neuroendocrine systems, with the expression significantly enhanced by hypoxia [60, 61].

Inflammation markers can also have diagnostic significance, as different types of immune cells and inflammatory factors participate in primary and secondary reactions to ischemic damage, including regeneration. A number of cytokines (TNF α , interleukins IL1 β , IL6, IL8, IL10, etc.) show significantly increased serum levels in both term and preterm babies with neonatal asphyxia [62]. In a study enrolling 20 newborns with asphyxia, 36 weeks of gestation on average, plasma levels of pro-inflammatory cytokines (notably IL6 and IL8) were significantly increased within 6–24 h of life and correlated with HIE severity [63]. At the same time, it should be remembered that hypoxia-ischemia-associated inflammatory processes affect all systems of the body, especially in preterm babies. In fact, the inflammatory reaction can be triggered by the labor itself and subsequently amplified under conditions of HIE [64]. A study enrolling newborns at 35 weeks of gestation with HIE, receiving HT (33 °C for 72 h, commenced within 6 h of life) or not, revealed an important role of IL6, IL1 β , IL8, TNF α and IL10 in HIE and correlation of their levels with the outcome; importantly, these levels cannot be attributed specifically to brain damage. In cases of successful HT, the IL6, IL8 and IL10 levels decreased significantly by 36 h of life [65]. Yet another study assessed the cytokine profiles in newborns (36 weeks of gestation) with pronounced HIE, receiving HT (33.5 °C for 72 h) starting from within 6 h of life. Blood samples collected 24 h and 72 h after birth revealed sustainably elevated cytokine levels for IL6 only [51].

Overall, the above-mentioned studies indicate low prognostic capacity and questionable feasibility of using individual molecular and biochemical markers for clinical purposes in HIE. Hopefully, the use of 'omics' technologies to reveal complex disease-specific patterns of biomolecules will be more helpful; in this regard mass spectrometry holds great promise as a universal tool for high-throughput analysis of various biological compounds in one sample, including proteins, lipids and metabolites.

Studies considering proteomic analysis of biological fluids collected from neonates with HIE are still rare [66, 67]. One of them (2020) enrolled newborns with HIE (gestational age 37 weeks; $n = 12$ including four pts of each grade — mild, moderate and severe) and matching controls ($n = 16$). Blood samples (3 mL) were collected before HT, within 5–7 h of life. The blood was tested by quantitative mass spectrometry using an isobaric label for relative quantification (iTRAQ). Subsequent bioinformatic analysis showed that blood levels of certain proteins differed between HIE patients and controls in a severity-dependent manner; a set of 133 unique candidate proteins were identified, 14 of them showing elevated blood levels. Most of the differentially represented proteins were involved

in cell damage responses or acute/chronic inflammation, or incorporated in the membranes of extracellular organelles and exosomes. However, only two candidate markers, haptoglobin and S100A8, were subsequently confirmed by Western blot and PCR as differentially represented. The S100A8 protein is involved in several important pathways, including inflammation and the regulation of calcium homeostasis, through interactions with S100A9 [68]. The S100A8/A9 complex inhibits pro-inflammatory cytokine production thus suppressing excessive inflammation [69], whereas haptoglobin is an antioxidant protein which binds free hemoglobin thereby protecting the brain from reactive oxygen species upon hemorrhage; haptoglobin is also expressed in the liver [70]. So far, this is the only published proteomic analysis of blood samples collected from neonates with HIE [67].

Yet another published attempt of proteomic/peptidomic analysis (2020) involved CSF samples collected from newborns with HIE ($n = 4$; 38–39 weeks of gestation at birth, Apgar score < 5) within 24 h of. The iTRAQ mass spectrometry revealed differential representation of 34 peptides belonging to a total of 25 proteins compared with the control. Bioinformatic analysis implicated many of these proteins in chromatin compaction processes within the nucleus. The most prominent reduction was shown by a heat shock protein 90 α peptide involved in cell death program through formation of pores in the membrane, as confirmed by functional *in vitro* assay. The experiments on PC12 cell line demonstrated that the studied heat shock protein 90 α peptide indeed protects the cells from pyroptosis induced by a 6 h glucose-oxygen deprivation [66]. These results illustrate the utility of animal and cell experimental models in the search for brain damage-associated specific patterns for clinical translation. The approach enables differentiation of the clinical picture of brain tissue damage from other complications and dysfunctions associated with asphyxia.

Experimental models for brain damage marker identification

In vitro and *in vivo* experimental models help to identify specific proteomic and metabolomic patterns in HIE by means of reducing the system's complexity. The newly identified molecular patterns of brain damage can be used in clinical data interpretation and analysis. One study modeled hypoxic ischemia in mice on postnatal day 7; the experiments involved ligation of carotid artery and 92% N₂ / 8% O₂ chamber for 30 min, followed by mass spectrometry analysis of brain tissue 24 h post-intervention. The results indicate significantly reduced expression of collapsin response mediator proteins known to be involved in axon pathfinding and neuronal outgrowth in general [71]. Another team conducted metabolomics studies in newborn pigs. The animals underwent ligation of the left jugular vein and right carotid artery and were placed under hypoxic conditions to model asphyxia (12–36 h of life). Blood samples collected at three time points (before the procedure, immediately after hypoxia and 120 min after hypoxia during the reoxygenation phase) were analyzed by liquid chromatography–time-of-flight mass spectrometry. The results indicate substantial increase in biochemical markers of anaerobic metabolic pathways including cytidine and uridine derivatives, free fatty acids and choline. The authors suggest using these compounds as early diagnostic markers of HIE in neonates [72]. Several published *in vitro* studies used cell cultures as model systems to identify candidate markers of brain cell damage. In one study, murine hippocampal cell line HT22 underwent 17.5 h of hypoxia in the presence of 0.69 mM glucose. Proteomic analysis by HPLC–tandem mass spectrometry revealed a set of 105 unique proteins expressed differentially by treated cells compared with the control (normoxia).

As shown by subsequent processing, the majority of these proteins were targets of HIF-1 α induced by hypoxia; although the factor per se escaped proteomic detection, its increased expression was revealed by western blot analysis. The induction of HIF-1 α targets triggered glycolysis and antioxidant systems while blocking inflammatory reactions [73]. Another study modeled the acidosis-induced cell damage in neuronal cultures by 24 h incubation at pH = 6.2. Subsequent proteomic analysis revealed a set of 69 unique proteins related to cell death, impaired synaptic plasticity and oxidative stress [74]. Such studies demonstrate the suitability of cell models for identification of specific proteomic markers of neuronal damage for the purposes of differential diagnostics.

Metabolomic approaches in HIE diagnosis and prognosis

Metabolomic profiling of the blood can be a highly sensitive diagnostic and prognostic tool for neonatal conditions including congenital metabolic disorders, sepsis and HIE. Neonatal sepsis is invariably accompanied by changes in glucose and lactate metabolism, reflecting a shift from the mitochondrial oxidative phosphorylation to glycolysis and pentose phosphate pathway, as well as oxidative stress and fatty acid oxidation [75]. Several candidate metabolites have been also proposed as markers for the early diagnosis of HIE.

It should be emphasized that HIE severity and dynamics depend on gestational age at birth. Accordingly, metabolomic and proteomic profiles of the disease are likely to be gestational age-dependent both qualitatively and quantitatively [76, 77]. In term and preterm babies, metabolomic profiles behave differently. For instance, markers of tyrosine metabolism, tryptophan/phenylalanine biosynthesis, urea cycle and arginine/proline metabolism in the urine significantly correlate with gestational age [78].

Contemporary advances in MS and NMR have enabled metabolomics analysis for HIE with simultaneous recording of spectra for hundreds of metabolites, which is an absolute prerequisite given the dynamic character and complexity of the pathogenic process in HIE. In accordance with the nature of pathology, the metabolomic tests are focused on the signs of hypoxia and metabolic impairments. The strategies can be roughly defined as targeted (i.e. analysis of a small number of particular metabolites), semi-targeted (analysis of a large panel of metabolites), and non-targeted (whole-metabolome). About a dozen of studies describing urine and blood metabolome dynamics in neonates with HIE have been published so far; the urine samples were studied by MS and NMR.

One study (2018) analyzed urine samples from newborns with HIE ($n = 10$; 38 weeks of gestation at birth, Apgar score 5–7). The urine was collected 6 h, 48 h (during HT), 72 h (after HT) and 1 month after birth. A NMR study revealed significantly increased urine levels of lactate, myoinositol and betaine along with significantly decreased urine levels of the Krebs cycle intermediates (citrate, α -ketoglutarate, succinate), acetone, dimethylamine, glutamine, pyruvate, N-acetyl groups, arginine and acetate in lethal cases compared with matching healthy controls [79]. Another study (2017) used HPLC-MS/MS for metabolomic analysis of urine samples from newborns with HIE ($n = 13$; 36 weeks of gestation at birth on average, Apgar score 2–3). The urine was collected 12 h and on days 3 and 9 after birth. The results indicate significantly decreased levels of certain amino acids (the branched leucine and isoleucine and aromatic phenylalanine, tyrosine and tryptophan), kynurenine and hippuric acid along with increased acylcarnitine levels in HIE compared with matching healthy controls [80].

Metabolomic studies on neonatal blood samples collected from patients with HIE have been attempted as well. One

study applied non-targeted metabolomic analysis of cord blood collected from newborns (gestational age 36 weeks, Apgar score 6) diagnosed with neonatal asphyxia with or without signs of HIE. The samples were collected within 20 min after delivery of the placenta during labor. The HIE and non-developed HIE subgroups revealed statistically significant differences in cord blood levels of melatonin, leucine, kynurenine and 3-hydroxydodecanoic acid. HIE severity markers were also identified, including D-erythrose phosphate, acetone, 3-oxotetradecanoic acid and methylglutaryl carnitine. Bioinformatic analysis has shown that HIE disrupts about 50 and 75% of tryptophan and pyrimidine metabolic pathways, respectively [81]. A recent study (2021) applied gas chromatography with time-of-flight mass spectrometry in a similar setting. The study enrolled newborns with moderate and severe HIE ($n = 24$; gestational age 35 weeks, Apgar score < 7) and matching healthy controls ($n = 24$). The samples (2 mL of blood from femoral artery) were collected immediately after birth in order to obtain plasma for metabolomic analysis. A set of 52 metabolites detected in the blood of newborns with HIE clearly differentiated the patients from the control group. These metabolites have been affiliated to pathways of amino acid metabolism, energy metabolism, neurotransmitter biosynthesis, pyrimidine metabolism, HIF regulation by oxygen and G protein-coupled receptor (GPCR) signaling. Fourteen compounds showed high predictive value for HIE, including alanine, glutamic acid, glutamine, L-malic acid, succinic acid, pyruvic acid and taurine. In addition, α -ketoglutaric acid and hydroxylamine revealed high predictive value between moderate and severe forms of HIE, with the area under ROC curve being 0.729 [82].

Metabolomic patterns revealed in these studies are consistent with the impaired energy metabolism and mitochondrial damage initiated in HIE. The most typically observed changes involved energy metabolites indicating a shift towards anaerobic metabolism (elevated lactate levels) and Krebs cycle disruption. The accumulation of lactate and Krebs cycle intermediates (citrate, alpha-keto-glutarate, succinate and fumarate) are explained by ATP depletion and respiratory chain dysfunction. In newborns with pronounced (moderate to severe) HIE, elevated succinate levels may also correlate with severity [83]. We should also note that a number of studies have repeatedly emphasized that even after 48 h of intensive care with HT, newborns with successfully treated HIE have altered metabolic features distinguishing them from healthy peers [84]. The altered glutamine levels reflect its being a precursor for glutamate, the main excitatory mediator during perinatal brain injury [85]. Hypoxanthine, which promotes formation of the detrimental reactive oxygen species upon interaction with xanthine oxidase, is often mentioned in such studies; a characteristic increase in hypoxanthine levels is considered the main clinical biochemical feature of asphyxia [86].

Metabolomic analysis revealed an important role of lipids in perinatal asphyxia. Choline revealed the most prominent HIE-related changes (elevated levels) among lipid metabolites [83]. Choline and its derivatives are essential for the structural integrity of cell membranes and signaling (phospholipids), neurotransmission (acetylcholine synthesis), lipid transport (lipoproteins) and methyl group metabolism (homocysteine reduction) [87]. Blood levels of inositol, the main precursor in the synthesis of phosphorylated signaling compounds, increase significantly in newborns after perinatal asphyxia, but these changes are not specific for nervous system damage [46, 77]. Overall, the search for markers of neuronal damage by metabolomic analysis can be assumed the most effective and appropriate vector for the field of early diagnosis in HIE.

Extracellular vesicles in HIE diagnostics

The targeted analysis of extracellular vesicles produced by neurons in HIE should be mentioned as a promising alternative. Extracellular vesicles (EVs) are specialized 'containers' of cellular origin consisting of cytoplasm enclosed in phospholipid membrane [88]. EVs have been shown to participate in a variety of biological processes including immune regulation, inflammation modulation, cell-to-cell communication, angiogenesis, etc. EVs released by neurons play important roles in their functional maintenance and development [89]. Neuronal EVs have been shown to increase in number under conditions of traumatic brain injury or stroke [90, 91]. EVs hold promise as diagnostic markers in many fields of medicine; their cell type-specific transmembrane proteins can be used as tags for EV sorting and subsequent analysis of particular classes. Neuronal EVs exhibit adhesion molecules, as well as receptors and ligands for specific recognition by target cells, and are probably involved in synaptogenesis. Their cytoplasmic content is protected from degradation, which makes them storable and generally adds to their value as a diagnostic/prognostic substrate [92–94].

Few clinical studies published so far describe the use of neuronal EVs as brain damage markers in HIE. One study (2015) enrolled 14 newborns (36 weeks of gestation, Apgar score 2–5) diagnosed with HIE and receiving HT starting from within 6 h of life. Blood samples (500 μ L) were collected 8, 10 and 14 h after commencement of the therapy. The study used an original protocol for neuronal EV isolation: 100 μ L of blood plasma were treated with commercial reagent for exosome precipitation (EXOQ; System Biosciences, Inc.; Mountainview, CA) and the total yield of exosomes was incubated with biotinylated antibodies to contactin-2 — a neuron-specific adhesion molecule. The exosome-Ab complexes were subsequently precipitated with streptavidin to yield a pure fraction of neuronal EVs. Although EV concentrations in the isolates are not specified in the article, they should have been low, providing for measurements of four markers only: synaptopodin, synaptophysin, neuronal enolase and mitochondrial cytochrome-C-oxidase. Of those, only synaptopodin proved to be of diagnostic value; at that, its dynamics reflects secondary damage arising after 6 h of life [95]. It should be noted that such modification of EVs renders them unsuitable for MS-based metabolomic assay. Moreover, very low yields of EVs will hardly afford reliable measurements above the noise threshold. Another study by the same team (2021) enrolled 26 newborns with HIE (39 weeks of gestation, Apgar score 5); the venous blood samples were collected at 0–6, 12, 24, 48 and 96 h of life. Neuronal EVs were isolated by the same method and analyzed by enzyme immunoassay for a different set of neuronal markers including synaptopodin, neutrophil gelatinase-associated lipocalin (NGAL) and neuropentraxin-2 [96]. NGAL levels have been shown to correlate with severity and outcomes in hemorrhagic stroke, while also being a marker of kidney damage [97, 98]. Neuropentraxin-2 binds α -amino-3-hydroxy-5-methyl-4-isoxazolepropionic acid (AMPA) glutamate receptors at excitatory synaptic terminals [99]. Similarly with the previous study, synaptopodin revealed significant prognostic value and correlated with MRI data in cases of mild damage, whereas in more severe cases its prognostic value was non-significant and the sensitivity dropped from 40% to 18% within 0–12 h window. Prognostic value of NGAL (with regard to MRI data) was significant in cases of moderate and high severity, but within a 12–48 h window, and no inverse correlation between synaptopodin and NGAL levels was identified [96]. The utility of this approach for clinical diagnostic purposes remains questionable due to the extremely low yields of neuronal EVs.

Thus, proteomic and metabolomic approaches can be applied in differential diagnosis of HIE at early stages of pathogenesis. However, the clinical utility of corresponding brain damage-specific molecular patterns is undermined by the thick background of concomitant damage to other organs during systemic exposure to hypoxia.

CONCLUSION

The continued high rates of neonatal HIE morbidity and mortality necessitate the use of advanced methods to verify the etiology and distinguish it from clinically similar conditions, e.g. early

neonatal sepsis and certain congenital metabolic disorders, for a timely decision-making on therapeutic hypothermia. The moment of therapy initiation directly affects the long-term neurological outcome: the earlier the commencement, the better the prognosis. The early differential diagnosis of HIE in neonates may involve detection of changes in the metabolite composition of the blood by means of chromatography–mass spectrometry focusing on candidate compounds with the highest diagnostic potential in HIE. The much anticipated translation of 'omics'-based tests, tissue culture models and extracellular vesicle assays into practice will enhance the differentiation of HIE from clinically similar neonatal conditions.

References

- Manuck TA, Rice MM, Bailit JL, Grobman WA, Reddy UM, Wapner RJ, et al. Preterm neonatal morbidity and mortality by gestational age: a contemporary cohort. *Am J Obstet Gynecol*. 2016 [cited 2022 Jun 28]; 215 (1): 103.e1–103.e14. Available from: <https://pubmed.ncbi.nlm.nih.gov/26772790/>.
- Thornberg E, Thiringer K, Odeback A, Milsom I. Birth asphyxia: incidence, clinical course and outcome in a Swedish population. *Acta Paediatrica*. 1995 [cited 2022 Jun 28]; 84 (8): 927–32. Available from: <https://pubmed.ncbi.nlm.nih.gov/7488819/>.
- Thorngren-Jerneck K, Herbst A. Low 5-minute Apgar score: a population-based register study of 1 million term births. *Obstet Gynecol*. 2001 [cited 2022 Jun 28]; 98 (1): 65–70. Available from: <https://pubmed.ncbi.nlm.nih.gov/11430958/>.
- Volpe JJ. Neonatal encephalopathy: an inadequate term for hypoxic-ischemic encephalopathy. *Ann Neurol*. 2012 [cited 2022 Jun 28]; 72 (2): 156–66. Available from: <https://pubmed.ncbi.nlm.nih.gov/22926849/>.
- Lawn J, Shibuya K, Stein C. No cry at birth: global estimates of intrapartum stillbirths and intrapartum-related neonatal deaths. *Bull World Health Organ*. 2005 [cited 2022 Jun 28]; 83 (6): 409. Available from: <https://pmc/articles/PMC2626256/?report=abstract>.
- Hoehn T, Hansmann G, Bühner C, Simbruner G, Gunn AJ, Yager J, et al. Therapeutic hypothermia in neonates. Review of current clinical data, ILCOR recommendations and suggestions for implementation in neonatal intensive care units. *Resuscitation*. 2008 [cited 2022 Jun 28]; 78 (1): 7–12. Available from: <https://pubmed.ncbi.nlm.nih.gov/18554560/>.
- Okerefor A, Allsop J, Counsell SJ, Fitzpatrick J, Azzopardi D, Rutherford MA, et al. Patterns of brain injury in neonates exposed to perinatal sentinel events. *Pediatrics*. 2008 [cited 2022 Jun 28]; 121 (5): 906–14. Available from: <https://pubmed.ncbi.nlm.nih.gov/18450893/>.
- Long M, Brandon DH. Induced hypothermia for neonates with hypoxic-ischemic encephalopathy. *J Obstet Gynecol neonatal Nurs JOGNN*. 2007 [cited 2022 Jun 28]; 36 (3): 293–8. Available from: <https://pubmed.ncbi.nlm.nih.gov/17489937/>.
- Pierrat V, Haouari N, Liska A, Thomas D, Subtil D, Truffert P. Prevalence, causes, and outcome at 2 years of age of newborn encephalopathy: population based study. *Arch Dis Child Fetal Neonatal Ed*. 2005 [cited 2022 Jun 28]; 90(3). Available from: <https://pubmed.ncbi.nlm.nih.gov/15846019/>.
- Lee ACC, Kozuki N, Blencowe H, Vos T, Bahalim A, Darmstadt GL, et al. Intrapartum-related neonatal encephalopathy incidence and impairment at regional and global levels for 2010 with trends from 1990. *Pediatr Res*. 2013 [cited 2022 Jun 28]; 74 Suppl 1(Suppl 1): 50–72. Available from: <https://pubmed.ncbi.nlm.nih.gov/24366463/>.
- Wang LS, Cheng GQ, Zhou WH, Sun JQ, Cao Y, Shao XM. Meta-analysis of mild hypothermia for gestational age over 35-week newborns with hypoxic-ischemic encephalopathy. *Natl Med J China*. 2012 [cited 2022 Jun 28]; 92 (20): 1400–4. Available from: <https://pubmed.ncbi.nlm.nih.gov/22883198/>.
- Edwards AD, Brocklehurst P, Gunn AJ, Halliday H, Juszczak E, Levene M, et al. Neurological outcomes at 18 months of age after moderate hypothermia for perinatal hypoxic ischaemic encephalopathy: synthesis and meta-analysis of trial data. *BMJ*. 2010 [cited 2022 Jun 28]; 340 (7743): 409. Available from: <https://pubmed.ncbi.nlm.nih.gov/20144981/>.
- Oliveira V, Singhvi DP, Montaldo P, Lally PJ, Mendoza J, Manerker S, et al. Therapeutic hypothermia in mild neonatal encephalopathy: a national survey of practice in the UK. *Arch Dis Child Fetal Neonatal Ed*. 2018 [cited 2022 Jun 28]; 103 (4): F1–3. Available from: <https://pubmed.ncbi.nlm.nih.gov/28942433/>.
- Prempunpong C, Chalalak LF, Garfinkle J, Shah B, Kalra V, Rollins N, et al. Prospective research on infants with mild encephalopathy: The PRIME study. *Journal of Perinatology. J Perinatol*. 2018 [cited 2022 Jun 28]; 38: 80–5. Available from: <https://pubmed.ncbi.nlm.nih.gov/29095433/>.
- Chalalak LF, Nguyen KA, Prempunpong C, Heyne R, Thayyil S, Shankaran S, et al. Prospective research in infants with mild encephalopathy identified in the first six hours of life: neurodevelopmental outcomes at 18–22 months. *Pediatr Res*. 2018 [cited 2022 Jun 28]; 84 (6): 861–8. Available from: <https://pubmed.ncbi.nlm.nih.gov/30250303/>.
- Murray DM, O'Connor CM, Anthony Ryan C, Korotchikova I, Boylan GB. Early EEG Grade and Outcome at 5 Years After Mild Neonatal Hypoxic Ischemic Encephalopathy. *Pediatrics*. 2016 [cited 2022 Jun 28]; 138 (4). Available from: <https://pubmed.ncbi.nlm.nih.gov/27650049/>.
- Conway JM, Walsh BH, Boylan GB, Murray DM. Mild hypoxic ischaemic encephalopathy and long term neurodevelopmental outcome — A systematic review. *Early Hum Dev*. 2018 [cited 2022 Jun 28]; 120: 80–7. Available from: <https://pubmed.ncbi.nlm.nih.gov/29496329/>.
- Nanavati T, Seemaladinne N, Regier M, Yossuck P, Pergami P. Can We Predict Functional Outcome in Neonates with Hypoxic Ischemic Encephalopathy by the Combination of Neuroimaging and Electroencephalography? *Pediatr Neonatol*. 2015 [cited 2022 Jun 28]; 56 (5): 307–16. Available from: <https://pubmed.ncbi.nlm.nih.gov/25862075/>.
- Polat M, Şimşek A, Tansuğ N, Sezer RG, Özkol M, Başpınar P, et al. Prediction of neurodevelopmental outcome in term neonates with hypoxic-ischemic encephalopathy. *Eur J Paediatr Neurol*. 2013 [cited 2022 Jun 28]; 17 (3): 288–93. Available from: <https://pubmed.ncbi.nlm.nih.gov/23231917/>.
- Shellhaas RA, Kushwaha JS, Plegue MA, Selewski DT, Barks JDE. An Evaluation of Cerebral and Systemic Predictors of 18-Month Outcomes for Neonates With Hypoxic Ischemic Encephalopathy. *J Child Neurol*. 2015 [cited 2022 Jun 28]; 30 (11): 1526–31. Available from: <https://pubmed.ncbi.nlm.nih.gov/25724376/>.
- Chang T, Du Plessis A. Neurodiagnostic techniques in neonatal critical care. *Curr Neurol Neurosci Rep*. 2012 [cited 2022 Jun 29]; 12 (2): 145–52. Available from: <https://pubmed.ncbi.nlm.nih.gov/22318538/>.
- Van Laerhoven H, De Haan TR, Offringa M, Post B, Van Der Lee JH. Prognostic tests in term neonates with hypoxic-ischemic

- encephalopathy: a systematic review. *Pediatrics*. 2013 [cited 2022 Jun 29]; 131 (1): 88–98. Available from: <https://pubmed.ncbi.nlm.nih.gov/23248219/>.
23. Rasmussen LA, Cascio MA, Ferrand A, Shevell M, Racine E. The complexity of physicians' understanding and management of prognostic uncertainty in neonatal hypoxic-ischemic encephalopathy. *J Perinatol*. 2019 [cited 2022 Jun 29]; 39 (2): 278–85. Available from: <https://pubmed.ncbi.nlm.nih.gov/30568164/>.
 24. Natarajan N, Pardo AC. Challenges in neurologic prognostication after neonatal brain injury. *Semin Perinatol*. 2017 [cited 2022 Jun 29]; 41 (2): 117–23. Available from: <https://pubmed.ncbi.nlm.nih.gov/28139254/>.
 25. Merchant N, Azzopardi D. Early predictors of outcome in infants treated with hypothermia for hypoxic-ischaemic encephalopathy. *Dev Med Child Neurol*. 2015 [cited 2022 Jun 29]; 57 (S3): 8–16. Available from: <https://pubmed.ncbi.nlm.nih.gov/25800487/>.
 26. Merhar SL, Chau V. Neuroimaging and Other Neurodiagnostic Tests in Neonatal Encephalopathy. *Clin Perinatol*. 2016 [cited 2022 Jun 29]; 43 (3): 511–27. Available from: <https://pubmed.ncbi.nlm.nih.gov/27524451/>.
 27. Del Río R, Ochoa C, Alarcon A, Arnáez J, Blanco D, García-Alix A. Amplitude integrated electroencephalogram as a prognostic tool in neonates with hypoxic-ischemic encephalopathy: A systematic review. *PLoS One*. 2016 [cited 2022 Jun 29]; 11 (11). Available from: <https://pubmed.ncbi.nlm.nih.gov/27802300/>.
 28. Mizrahi EM. Neonatal seizures and neonatal epileptic syndromes. *Neurol Clin*. 2001 [cited 2022 Jun 29]; 19 (2): 427–63. Available from: <https://pubmed.ncbi.nlm.nih.gov/11358751/>.
 29. Murray DM, Boylan GB, Ali I, Ryan CA, Murphy BP, Connolly S. Defining the gap between electrographic seizure burden, clinical expression and staff recognition of neonatal seizures. *Arch Dis Child Fetal Neonatal Ed*. 2008 [cited 2022 Jun 29]; 93 (3). Available from: <https://pubmed.ncbi.nlm.nih.gov/17626147/>.
 30. Clancy RR, Legido A, Lewis D. Occult neonatal seizures. *Epilepsia*. 1988 [cited 2022 Jun 29]; 29 (3): 256–61. Available from: <https://pubmed.ncbi.nlm.nih.gov/3371282/>.
 31. Weeke LC, Boylan GB, Pressler RM, Hallberg B, Blennow M, Toet MC, et al. Role of EEG background activity, seizure burden and MRI in predicting neurodevelopmental outcome in full-term infants with hypoxic-ischaemic encephalopathy in the era of therapeutic hypothermia. *Eur J Paediatr Neurol*. 2016 [cited 2022 Jun 28]; 20 (6): 855–64. Available from: <https://pubmed.ncbi.nlm.nih.gov/27370316/>.
 32. Gunn AJ, Wyatt JS, Whitelaw A, Barks J, Azzopardi D, Ballard R, et al. Therapeutic hypothermia changes the prognostic value of clinical evaluation of neonatal encephalopathy. *J Pediatr*. 2008 [cited 2022 Jun 29]; 152 (1). Available from: <https://pubmed.ncbi.nlm.nih.gov/18154900/>.
 33. Boudes E, Tan X, Saint-Martin C, Shevell M, Wintermark P. MRI obtained during versus after hypothermia in asphyxiated newborns. *Arch Dis Child Fetal Neonatal Ed*. 2015 [cited 2022 Jun 29]; 100 (3): F238–42. Available from: <https://pubmed.ncbi.nlm.nih.gov/25605620/>.
 34. Bonifacio SL, deVries LS, Groenendaal F. Impact of hypothermia on predictors of poor outcome: how do we decide to redirect care? *Semin Fetal Neonatal Med*. 2015 [cited 2022 Jun 29]; 20 (2): 122–7. Available from: <https://pubmed.ncbi.nlm.nih.gov/25577654/>.
 35. Thoresen M, Tooley J, Liu X, Jary S, Fleming P, Luyt K, et al. Time is brain: starting therapeutic hypothermia within three hours after birth improves motor outcome in asphyxiated newborns. *Neonatology*. 2013 [cited 2022 Jun 29]; 104 (3): 228–33. Available from: <https://pubmed.ncbi.nlm.nih.gov/24030160/>.
 36. Basu SK, Kaiser JR, Guffey D, Minard CG, Guillet R, Gunn AJ. Hypoglycaemia and hyperglycaemia are associated with unfavourable outcome in infants with hypoxic ischaemic encephalopathy: A post hoc analysis of the CoolCap Study. *Arch Dis Child Fetal Neonatal Ed*. 2016 [cited 2022 Jun 29]; 101 (2): F149–55. Available from: <https://pubmed.ncbi.nlm.nih.gov/26283669/>.
 37. Shah DK, Wusthoff CJ, Clarke P, Wyatt JS, Ramaiah SM, Dias RJ, et al. Electrographic seizures are associated with brain injury in newborns undergoing therapeutic hypothermia. *Arch Dis Child Fetal Neonatal Ed*. 2014 [cited 2022 Jun 29]; 99 (3). Available from: <https://pubmed.ncbi.nlm.nih.gov/24443407/>.
 38. Sabir H, Jary S, Tooley J, Liu X, Thoresen M. Increased inspired oxygen in the first hours of life is associated with adverse outcome in newborns treated for perinatal asphyxia with therapeutic hypothermia. *J Pediatr*. 2012 [cited 2022 Jun 29]; 161 (3): 409–16. Available from: <https://pubmed.ncbi.nlm.nih.gov/22521111/>.
 39. Osredkar D, Thoresen M, Maes E, Flatebø T, Elstad M, Sabir H. Hypothermia is not neuroprotective after infection-sensitized neonatal hypoxic-ischemic brain injury. *Resuscitation*. 2014 [cited 2022 Jun 29]; 85 (4): 567–72. Available from: <https://pubmed.ncbi.nlm.nih.gov/24361672/>.
 40. Uziel G, Ghezzi D, Zeviani M. Infantile mitochondrial encephalopathy. *Seminars in Fetal and Neonatal Medicine*. *Semin Fetal Neonatal Med*. 2011 [cited 2022 Jun 29]; 16: 205–15. Available from: <https://pubmed.ncbi.nlm.nih.gov/21620787/>.
 41. Bruyland M, Liebaers I, Sacre L, Vandeplass Y, De Meirleir L, Martin JJ. Neonatal myotubular myopathy with a probable X-linked inheritance: observations on a new family with a review of the literature. *J Neurol*. 1984 [cited 2022 Jun 29]; 231 (4): 220–2. Available from: <https://pubmed.ncbi.nlm.nih.gov/6512577/>.
 42. Danti FR, Galosi S, Romani M, Montomoli M, Carss KJ, Lucy Raymond F, et al. GNAO1 encephalopathy: Broadening the phenotype and evaluating treatment and outcome. *Neurol Genet*. 2017 [cited 2022 Jul 4]; 3 (2). Available from: <https://pubmed.ncbi.nlm.nih.gov/28357411/>.
 43. Solis GP, Kozhanova TV, Koval A, Zhilina SS, Mescheryakova TI, Abramov AA, et al. Pediatric Encephalopathy: Clinical, Biochemical and Cellular Insights into the Role of Gln52 of GNAO1 and GNAI1 for the Dominant Disease. *Cells*. 2021 [cited 2022 Jul 4]; 10 (10). Available from: <https://pubmed.ncbi.nlm.nih.gov/34685729/>.
 44. Cuzzolin L, Zaccaron A, Fanos V. Unlicensed and off-label uses of drugs in paediatrics: a review of the literature. *Fundam Clin Pharmacol*. 2003 [cited 2022 Jun 30]; 17 (1): 125–31. Available from: <https://pubmed.ncbi.nlm.nih.gov/12588640/>.
 45. Robertson NJ, Thayil S, B. Cady E, Raivich G. Magnetic resonance spectroscopy biomarkers in term perinatal asphyxial encephalopathy: from neuropathological correlates to future clinical applications. *Curr Pediatr Rev*. 2014 [cited 2022 Jun 30]; 10 (1): 37–47. Available from: <https://pubmed.ncbi.nlm.nih.gov/25055862/>.
 46. Massaro AN, Chang T, Kadom N, Tsuchida T, Scafidi J, Glass P, et al. Biomarkers of brain injury in neonatal encephalopathy treated with hypothermia. *J Pediatr*. 2012 [cited 2022 Jun 30]; 161 (3): 434–40. Available from: <https://pubmed.ncbi.nlm.nih.gov/22494878/>.
 47. Jones R, Heep A, Odd D. Biochemical and clinical predictors of hypoxic-ischemic encephalopathy after perinatal asphyxia. *J Matern Fetal Neonatal Med*. 2018 [cited 2022 Jun 30]; 31 (6): 791–6. Available from: <https://pubmed.ncbi.nlm.nih.gov/28274150/>.
 48. Fatemi A, Wilson MA, Johnston M V. Hypoxic-Ischemic Encephalopathy in the Term Infant [Internet]. *Clinics in Perinatology*. *Clin Perinatol*. 2009 [cited 2022 Jun 30]; 36: 835–58. Available from: <https://pubmed.ncbi.nlm.nih.gov/19944838/>.
 49. Ennen CS, Huisman TAGM, Savage WJ, Northington FJ, Jennings JM, Everett AD, et al. Glial fibrillary acidic protein as a biomarker for neonatal hypoxic-ischemic encephalopathy treated with whole-body cooling. *Am J Obstet Gynecol*. 2011 [cited 2022 Jun 30]; 205 (3): 251.e1-251.e7. Available from: <https://pubmed.ncbi.nlm.nih.gov/21784396/>.
 50. Kim HJ, Tsao JW, Stanfill AG. The current state of biomarkers of mild traumatic brain injury. *JCI insight*. 2018 [cited 2022 Jun 30]; 3 (1). Available from: <https://pubmed.ncbi.nlm.nih.gov/29321373/>.
 51. Orrock JE, Panchapakesan K, Vezina G, Chang T, Harris K, Wang Y, et al. Association of brain injury and neonatal cytokine response during therapeutic hypothermia in newborns with hypoxic-ischemic encephalopathy. *Pediatr Res*. Available from: <https://pubmed.ncbi.nlm.nih.gov/26717001/>.
 52. Tann CJ, Martinello KA, Sadoo S, Lawn JE, Seale AC, Vega-Poblete M, et al. Neonatal Encephalopathy With Group B Streptococcal Disease Worldwide: Systematic Review, Investigator Group Datasets, and Meta-analysis. *Clin Infect Dis*. 2017 [cited 2022 Jun 30]; 65 (suppl_2): S173–89. Available from:

- <https://pubmed.ncbi.nlm.nih.gov/29117330/>.
53. Murray DM. Biomarkers in neonatal hypoxic-ischemic encephalopathy-Review of the literature to date and future directions for research. *Handb Clin Neurol*. 2019 [cited 2022 Jun 30]; 162: 281–93. Available from: <https://pubmed.ncbi.nlm.nih.gov/31324315/>.
 54. Alkholy UM, Abdalmonem N, Zaki A, Ali YF, Mohamed SA, Abdelsalam NI, et al. Early predictors of brain damage in full-term newborns with hypoxic ischemic encephalopathy. *Neuropsychiatr Dis Treat*. 2017 [cited 2022 Jun 30]; 13: 2133–9. Available from: <https://pubmed.ncbi.nlm.nih.gov/28860770/>.
 55. Douglas-Escobar M, Weiss MD. Biomarkers of brain injury in the premature infant. *Front Neurol*; 2013 [cited 2022 Jun 30]; 3 JAN. Available from: <https://pubmed.ncbi.nlm.nih.gov/23346073/>.
 56. Massaro AN, Wu YW, Bammler TK, Comstock B, Mathur A, McKinstry RC, et al. Plasma Biomarkers of Brain Injury in Neonatal Hypoxic-Ischemic Encephalopathy. *J Pediatr*. 2018 [cited 2022 Jun 30]; 194: 67–75.e1. Available from: <https://pubmed.ncbi.nlm.nih.gov/29478510/>.
 57. Shah DK, Ponnusamy V, Evanson J, Kapellou O, Ekitidou G, Gupta N, et al. Raised plasma neurofilament light protein levels are associated with abnormal MRI outcomes in newborns undergoing therapeutic hypothermia. *Front Neurol*. 2018 [cited 2022 Jun 30]; 9 (MAR). Available from: <https://pubmed.ncbi.nlm.nih.gov/29556208/>.
 58. Sweetman DU, Onwuneme C, Watson WR, Murphy JFA, Molloy EJ. Perinatal Asphyxia and Erythropoietin and VEGF: Serial Serum and Cerebrospinal Fluid Responses. *Neonatology*. 2017 [cited 2022 Jul 4]; 111 (3): 253–9. Available from: <https://pubmed.ncbi.nlm.nih.gov/27902983/>.
 59. Lv H, Wang Q, Wu S, Yang L, Ren P, Yang Y, et al. Neonatal hypoxic ischemic encephalopathy-related biomarkers in serum and cerebrospinal fluid. *Clin Chim Acta*. 2015 [cited 2022 Jul 4]; 450: 282–97. Available from: <https://pubmed.ncbi.nlm.nih.gov/26320853/>.
 60. Hasslacher J, Lehner GF, Harler U, Beer R, Ulmer H, Kirchmair R, et al. Secretoneurin as a marker for hypoxic brain injury after cardiopulmonary resuscitation. *Intensive Care Med*. 2014 [cited 2022 Jul 4]; 40 (10): 1518–27. Available from: <https://pubmed.ncbi.nlm.nih.gov/25138227/>.
 61. Risso FM, Sannia A, Gavilanes DAW, Vles HJ, Colivicchi M, Ricotti A, et al. Biomarkers of brain damage in preterm infants. *J Matern Fetal Neonatal Med*. 2012 [cited 2022 Jul 4]; 25 (SUPPL.4): 93–6. Available from: <https://pubmed.ncbi.nlm.nih.gov/22958034/>.
 62. Chaparro-Huerta V, Flores-Soto ME, Merin Sigala ME, Barrera de León JC, Lemus-Varela M de L, Torres-Mendoza BM de G, et al. Proinflammatory Cytokines, Enolase and S-100 as Early Biochemical Indicators of Hypoxic-Ischemic Encephalopathy Following Perinatal Asphyxia in Newborns. *Pediatr Neonatol*. 2017 [cited 2022 Jul 4]; 58 (1): 70–6. Available from: <https://pubmed.ncbi.nlm.nih.gov/27522459/>.
 63. Chalak LF, Sánchez PJ, Adams-Huet B, Laptook AR, Heyne RJ, Rosenfeld CR. Biomarkers for severity of neonatal hypoxic-ischemic encephalopathy and outcomes in newborns receiving hypothermia therapy. *J Pediatr*. 2014 [cited 2022 Jul 4]; 164 (3). Available from: <https://pubmed.ncbi.nlm.nih.gov/24332821/>.
 64. Chiesa C, Pellegrini G, Panero A, De Luca T, Assumma M, Signore F, et al. Umbilical cord interleukin-6 levels are elevated in term neonates with perinatal asphyxia. *Eur J Clin Invest*. 2003 [cited 2022 Jul 4]; 33 (4): 352–8. Available from: <https://pubmed.ncbi.nlm.nih.gov/12662167/>.
 65. Jenkins DD, Rollins LG, Perkel JK, Wagner CL, Katikaneni LP, Bass WT, et al. Serum cytokines in a clinical trial of hypothermia for neonatal hypoxic-ischemic encephalopathy. *J Cereb Blood Flow Metab*. 2012 [cited 2022 Jul 4]; 32 (10): 1888–96. Available from: <https://pubmed.ncbi.nlm.nih.gov/22805873/>.
 66. Hou X, Yuan Z, Wang X, Cheng R, Zhou X, Qiu J. Peptidome analysis of cerebrospinal fluid in neonates with hypoxic-ischemic brain damage. *Mol Brain*. 2020 [cited 2022 Jul 4]; 13 (1). Available from: <https://pubmed.ncbi.nlm.nih.gov/33008433/>.
 67. Zhu Y, Yun Y, Jin M, Li G, Li H, Miao P, et al. Identification of novel biomarkers for neonatal hypoxic-ischemic encephalopathy using iTRAQ. *Ital J Pediatr*. 2020 [cited 2022 Jul 4]; 46 (1). Available from: <https://pubmed.ncbi.nlm.nih.gov/32448169/>.
 68. Viemann D, Strey A, Janning A, Jurk K, Klimmek K, Vogl T, et al. Myeloid-related proteins 8 and 14 induce a specific inflammatory response in human microvascular endothelial cells. *Blood*. 2005 [cited 2022 Jul 4]; 105 (7): 2955–62. Available from: <https://pubmed.ncbi.nlm.nih.gov/15598812/>.
 69. Ehrchen JM, Sunderkötter C, Foell D, Vogl T, Roth J. The endogenous Toll-like receptor 4 agonist S100A8/S100A9 (calprotectin) as innate amplifier of infection, autoimmunity, and cancer. *J Leukoc Biol*. 2009 [cited 2022 Jul 4]; 86 (3): 557–66. Available from: <https://pubmed.ncbi.nlm.nih.gov/19451397/>.
 70. Zhao X, Song S, Sun G, Strong R, Zhang J, Grotta JC, et al. Neuroprotective role of haptoglobin after intracerebral hemorrhage. *J Neurosci*. 2009 [cited 2022 Jul 4]; 29 (50): 15819–27. Available from: <https://pubmed.ncbi.nlm.nih.gov/20016097/>.
 71. Zhou Y, Bhatia I, Cai Z, He QY, Cheung PT, Chiu JF. Proteomic analysis of neonatal mouse brain: Evidence for hypoxia- and ischemia-induced dephosphorylation of collapsin response mediator proteins. *J Proteome Res*. 2008 [cited 2022 Jul 4]; 7 (6): 2507–15. Available from: <https://pubmed.ncbi.nlm.nih.gov/18471005/>.
 72. Solberg R, Kuligowski J, Pankratov L, Escobar J, Quintás G, Lliso I, et al. Changes of the plasma metabolome of newly born piglets subjected to postnatal hypoxia and resuscitation with air. *Pediatr Res*. 2016 [cited 2022 Jul 4]; 80 (2): 284–92. Available from: <https://pubmed.ncbi.nlm.nih.gov/27055187/>.
 73. Li H, Kittur FS, Hung CY, Li PA, Ge X, Sane DC, et al. Quantitative Proteomics Reveals the Beneficial Effects of Low Glucose on Neuronal Cell Survival in an in vitro Ischemic Penumbra Model. *Front Cell Neurosci*. 2020 [cited 2022 Jul 4]; 14. Available from: <https://pubmed.ncbi.nlm.nih.gov/33033473/>.
 74. Shi Y, Cai EL, Yang C, Ye CY, Zeng P, Wang XM, et al. Protection of melatonin against acidosis-induced neuronal injuries. *J Cell Mol Med*. 2020 [cited 2022 Jul 4]; 24 (12): 6928–42. Available from: <https://pubmed.ncbi.nlm.nih.gov/32364678/>.
 75. Bjerkhaug AU, Granslo HN, Klingenberg C. Metabolic responses in neonatal sepsis-A systematic review of human metabolomic studies. *Acta Paediatr*. 2021 [cited 2022 Jun 29]; 110 (8): 2316–25. Available from: <https://pubmed.ncbi.nlm.nih.gov/33851423/>.
 76. Beckstrom AC, Ricca RL, Gow KW, McAdams RM. Persistent posterior pneumomediastinum in a neonate. *Pediatr Int*. 2012 [cited 2022 Jul 4]; 54 (3): 441–2. Available from: <https://pubmed.ncbi.nlm.nih.gov/22631580/>.
 77. Nicholson JK, Lindon JC. Systems biology: Metabonomics. *Nature*. 2008 [cited 2022 Jul 4]; 455 (7216): 1054–6. Available from: <https://pubmed.ncbi.nlm.nih.gov/18948945/>.
 78. Atzori L, Antonucci R, Barberini L, Griffin JL, Fanos V. Metabonomics: a new tool for the neonatologist. *J Matern Fetal Neonatal Med*. 2009 [cited 2022 Jul 4]; 22 (SUPPL. 3): 50–3. Available from: <https://pubmed.ncbi.nlm.nih.gov/19701858/>.
 79. Locci E, Noto A, Puddu M, Pomerio G, Demontis R, Dalmazzo C, et al. A longitudinal 1H-NMR metabolomics analysis of urine from newborns with hypoxic-ischemic encephalopathy undergoing hypothermia therapy. *Clinical and medical legal insights. PLoS One*. 2018 [cited 2022 Jul 4]; 13 (4). Available from: <https://pubmed.ncbi.nlm.nih.gov/29668681/>.
 80. Sarafidis K, Efstathiou N, Begou O, Soubasi V, Agakidou E, Gika E, et al. Urine metabolomic profile in neonates with hypoxic-ischemic encephalopathy. *Hippokratia*. 2017 [cited 2022 Jul 4]; 21 (2): 80. Available from: <https://pubmed.ncbi.nlm.nih.gov/3239088/>.
 81. Denihan NM, Kirwan JA, Walsh BH, Dunn WB, Broadhurst DI, Boylan GB, et al. Untargeted metabolomic analysis and pathway discovery in perinatal asphyxia and hypoxic-ischaemic encephalopathy. *J Cereb Blood Flow Metab*. 2019 [cited 2022 Jul 4]; 39 (1): 147–62. Available from: <https://pubmed.ncbi.nlm.nih.gov/3239088/>.
 82. Jia Y, Jia X, Xu H, Gao L, Wei C, Li Y, et al. Blood Plasma Metabolic Profile of Newborns with Hypoxic-Ischaemic Encephalopathy by GC-MS. *Biomed Res Int*. 2021 [cited 2022 Jul 4]; 2021. Available from: <https://pubmed.ncbi.nlm.nih.gov/34258280/>.
 83. Reinke SN, Walsh BH, Boylan GB, Sykes BD, Kenny LC, Murray DM, et al. 1H NMR derived metabolomic profile of neonatal asphyxia in umbilical cord serum: implications for hypoxic ischemic encephalopathy. *J Proteome Res*. 2013 [cited 2022 Jul 4];

- 12 (9): 4230–9. Available from: <https://pubmed.ncbi.nlm.nih.gov/23931672/>.
84. Longini M, Giglio S, Perrone S, Vivi A, Tassini M, Fanos V, et al. Proton nuclear magnetic resonance spectroscopy of urine samples in preterm asphyctic newborn: a metabolomic approach. *Clin Chim Acta*. 2015 [cited 2022 Jul 4]; 444: 250–6. Available from: <https://pubmed.ncbi.nlm.nih.gov/25727514/>.
 85. Johnston M V. Excitotoxicity in perinatal brain injury. *Brain Pathol*. 2005 [cited 2022 Jul 4]; 15 (3): 234–40. Available from: <https://pubmed.ncbi.nlm.nih.gov/16196390/>.
 86. Pietz J, Guttentberg N, Gluck L. Hypoxanthine: a marker for asphyxia. *Obstet Gynecol*. 1988 [cited 2022 Jul 4]; 72 (5): 762–6. Available from: <https://pubmed.ncbi.nlm.nih.gov/3140152/>.
 87. Penry JT, Manore MM. Choline: An important micronutrient for maximal endurance-exercise performance? *Int J Sport Nutr Exerc Metab*. 2008 [cited 2022 Jul 4]; 18: 191–203. Available from: <https://pubmed.ncbi.nlm.nih.gov/18458362/>.
 88. Raposo G, Stoorvogel W. Extracellular vesicles: exosomes, microvesicles, and friends. *J Cell Biol*. 2013 [cited 2022 Jul 4]; 200 (4): 373–83. Available from: <https://pubmed.ncbi.nlm.nih.gov/23420871/>.
 89. Chivet M, Hemming F, Pernet-Gallay K, Fraboulet S, Sadoul R. Emerging role of neuronal exosomes in the central nervous system. *Front Physiol*. 2012 [cited 2022 Jul 4]; 3. Available from: <https://pubmed.ncbi.nlm.nih.gov/22654762/>.
 90. Chiva-Blanch G, Suades R, Crespo J, Peña E, Padró T, Jiménez-Xarrié E, et al. Microparticle Shedding from Neural Progenitor Cells and Vascular Compartment Cells Is Increased in Ischemic Stroke. *PLoS One*. 2016 [cited 2022 Jul 4]; 11 (1). Available from: <https://pubmed.ncbi.nlm.nih.gov/26815842/>.
 91. Patz S, Trattinig C, Grünbacher G, Ebner B, Güllly C, Novak A, et al. More than cell dust: microparticles isolated from cerebrospinal fluid of brain injured patients are messengers carrying mRNAs, miRNAs, and proteins. *J Neurotrauma*. 2013 [cited 2022 Jul 4]; 30 (14): 1232–42. Available from: <https://pubmed.ncbi.nlm.nih.gov/23360174/>.
 92. Goetzl EJ, Boxer A, Schwartz JB, Abner EL, Petersen RC, Miller BL, et al. Low neural exosomal levels of cellular survival factors in Alzheimer's disease. *Ann Clin Transl Neurol*. 2015 [cited 2022 Jul 4]; 2 (7): 769–73. Available from: <https://pubmed.ncbi.nlm.nih.gov/26273689/>.
 93. Goetzl EJ, Boxer A, Schwartz JB, Abner EL, Petersen RC, Miller BL, et al. Altered lysosomal proteins in neural-derived plasma exosomes in preclinical Alzheimer disease. *Neurology*. 2015 [cited 2022 Jul 4]; 85 (1): 40–7. Available from: <https://pubmed.ncbi.nlm.nih.gov/26062630/>.
 94. Silachev DN, Goryunov KV, Plotnikov EY, Shevtsova YA, Babenko VA, Burov AA, et al. Urinary extracellular vesicles as markers for kidney diseases. *Pediatrics n.a. G.N. Speransky*. 2020 [cited 2022 Jul 4]; 99 (5): 154–63. Available from: <https://pediatricsjournal.ru/archive?show=378§ion=6017>. Russian.
 95. Goetzl L, Merabova N, Darbinian N, Martirosyan D, Poletto E, Fugarolas K, et al. Diagnostic Potential of Neural Exosome Cargo as Biomarkers for Acute Brain Injury. *Ann Clin Transl Neurol*. 2018 [cited 2022 Jul 4]; 5 (1): 4–10. Available from: <https://pubmed.ncbi.nlm.nih.gov/29376087/>.
 96. Pineles B, Mani A, Sura L, Rossignol C, Albayram M, Weiss MD, et al. Neuronal exosome proteins: novel biomarkers for predicting neonatal response to therapeutic hypothermia. *Arch Dis Child Fetal Neonatal Ed*. 2022 [cited 2022 Jul 4]; 107 (1): F60–4. Available from: <https://pubmed.ncbi.nlm.nih.gov/34021027/>.
 97. Chen S, Chen XC, Lou XH, Qian SQ, Ruan ZW. Determination of serum neutrophil gelatinase-associated lipocalin as a prognostic biomarker of acute spontaneous intracerebral hemorrhage. *Clin Chim Acta*. 2019 [cited 2022 Jul 4]; 492: 72–7. Available from: <https://pubmed.ncbi.nlm.nih.gov/30771300/>.
 98. Plotnikov EY, Silachev DN, Pavlenko TA, Pavlova VS, Kryukov DS, Zubkov VV, et al. Acute kidney injury in newborns. From experiment to clinic. *Neonatologiya*. 2017; (4): 58–63. Russian.
 99. Xu D, Hopf C, Reddy R, Cho RW, Guo L, Lanahan A, et al. Narp and NP1 form heterocomplexes that function in developmental and activity-dependent synaptic plasticity. *Neuron*. 2003 [cited 2022 Jul 4]; 39 (3): 513–28. Available from: <https://pubmed.ncbi.nlm.nih.gov/12895424/>.

Литература

1. Manuck TA, Rice MM, Bailit JL, Grobman WA, Reddy UM, Wapner RJ, et al. Preterm neonatal morbidity and mortality by gestational age: a contemporary cohort. *Am J Obstet Gynecol*. 2016 [cited 2022 Jun 28]; 215 (1): 103.e1–103.e14. Available from: <https://pubmed.ncbi.nlm.nih.gov/26772790/>.
2. Thornberg E, Thiringer K, Odeback A, Milsom I. Birth asphyxia: incidence, clinical course and outcome in a Swedish population. *Acta Paediatrica*. 1995 [cited 2022 Jun 28]; 84 (8): 927–32. Available from: <https://pubmed.ncbi.nlm.nih.gov/7488819/>.
3. Thorngren-Jerneck K, Herbst A. Low 5-minute Apgar score: a population-based register study of 1 million term births. *Obstet Gynecol*. 2001 [cited 2022 Jun 28]; 98 (1): 65–70. Available from: <https://pubmed.ncbi.nlm.nih.gov/11430958/>.
4. Volpe JJ. Neonatal encephalopathy: an inadequate term for hypoxic-ischemic encephalopathy. *Ann Neurol*. 2012 [cited 2022 Jun 28]; 72 (2): 156–66. Available from: <https://pubmed.ncbi.nlm.nih.gov/22926849/>.
5. Lawn J, Shibuya K, Stein C. No cry at birth: global estimates of intrapartum stillbirths and intrapartum-related neonatal deaths. *Bull World Health Organ*. 2005 [cited 2022 Jun 28]; 83 (6): 409. Available from: <https://pmc/articles/PMC2626256/?report=abstract>.
6. Hoehn T, Hansmann G, Bührer C, Simbruner G, Gunn AJ, Yäger J, et al. Therapeutic hypothermia in neonates. Review of current clinical data, ILCOR recommendations and suggestions for implementation in neonatal intensive care units. *Resuscitation*. 2008 [cited 2022 Jun 28]; 78 (1): 7–12. Available from: <https://pubmed.ncbi.nlm.nih.gov/18554560/>.
7. Okereafor A, Allsop J, Counsell SJ, Fitzpatrick J, Azzopardi D, Rutherford MA, et al. Patterns of brain injury in neonates exposed to perinatal sentinel events. *Pediatrics*. 2008 [cited 2022 Jun 28]; 121 (5): 906–14. Available from: <https://pubmed.ncbi.nlm.nih.gov/18450893/>.
8. Long M, Brandon DH. Induced hypothermia for neonates with hypoxic-ischemic encephalopathy. *J Obstet Gynecol neonatal Nurs JOGNN*. 2007 [cited 2022 Jun 28]; 36 (3): 293–8. Available from: <https://pubmed.ncbi.nlm.nih.gov/17489937/>.
9. Pierrat V, Haouari N, Liska A, Thomas D, Subtil D, Truffert P. Prevalence, causes, and outcome at 2 years of age of newborn encephalopathy: population based study. *Arch Dis Child Fetal Neonatal Ed*. 2005 [cited 2022 Jun 28]; 90(3). Available from: <https://pubmed.ncbi.nlm.nih.gov/15846019/>.
10. Lee ACC, Kozuki N, Blencowe H, Vos T, Bahalim A, Darmstadt GL, et al. Intrapartum-related neonatal encephalopathy incidence and impairment at regional and global levels for 2010 with trends from 1990. *Pediatr Res*. 2013 [cited 2022 Jun 28]; 74 Suppl 1(Suppl 1): 50–72. Available from: <https://pubmed.ncbi.nlm.nih.gov/24366463/>.
11. Wang LS, Cheng GQ, Zhou WH, Sun JQ, Cao Y, Shao XM. Meta-analysis of mild hypothermia for gestational age over 35-week newborns with hypoxic-ischemic encephalopathy. *Natl Med J China*. 2012 [cited 2022 Jun 28]; 92 (20): 1400–4. Available from: <https://pubmed.ncbi.nlm.nih.gov/22883198/>.
12. Edwards AD, Brocklehurst P, Gunn AJ, Halliday H, Juszczak E, Levene M, et al. Neurological outcomes at 18 months of age after moderate hypothermia for perinatal hypoxic ischaemic encephalopathy: synthesis and meta-analysis of trial data. *BMJ*. 2010 [cited 2022 Jun 28]; 340 (7743): 409. Available from: <https://pubmed.ncbi.nlm.nih.gov/20144981/>.
13. Oliveira V, Singhvi DP, Montaldo P, Lally PJ, Mendoza J, Manerker S, et al. Therapeutic hypothermia in mild neonatal encephalopathy: a national survey of practice in the UK. *Arch Dis Child Fetal Neonatal Ed*. 2018 [cited 2022 Jun 28]; 103 (4): F1–3. Available from: <https://pubmed.ncbi.nlm.nih.gov/28942433/>.
14. Prempunpong C, Chalak LF, Garfinkle J, Shah B, Kalra V, Rollins N,

- et al. Prospective research on infants with mild encephalopathy: The PRIME study. *Journal of Perinatology*. J Perinatol. 2018 [cited 2022 Jun 28]; 38: 80–5. Available from: <https://pubmed.ncbi.nlm.nih.gov/29095433/>.
15. Chalak LF, Nguyen KA, Prempunpong C, Heyne R, Thayil S, Shankaran S, et al. Prospective research in infants with mild encephalopathy identified in the first six hours of life: neurodevelopmental outcomes at 18–22 months. *Pediatr Res*. 2018 [cited 2022 Jun 28]; 84 (6): 861–8. Available from: <https://pubmed.ncbi.nlm.nih.gov/30250303/>.
 16. Murray DM, O'Connor CM, Anthony Ryan C, Korotchikova I, Boylan GB. Early EEG Grade and Outcome at 5 Years After Mild Neonatal Hypoxic Ischemic Encephalopathy. *Pediatrics*. 2016 [cited 2022 Jun 28]; 138 (4). Available from: <https://pubmed.ncbi.nlm.nih.gov/27650049/>.
 17. Conway JM, Walsh BH, Boylan GB, Murray DM. Mild hypoxic ischaemic encephalopathy and long term neurodevelopmental outcome — A systematic review. *Early Hum Dev*. 2018 [cited 2022 Jun 28]; 120: 80–7. Available from: <https://pubmed.ncbi.nlm.nih.gov/29496329/>.
 18. Nanavati T, Seemaladinne N, Regier M, Yossuck P, Pergami P. Can We Predict Functional Outcome in Neonates with Hypoxic Ischemic Encephalopathy by the Combination of Neuroimaging and Electroencephalography? *Pediatr Neonatol*. 2015 [cited 2022 Jun 28]; 56 (5): 307–16. Available from: <https://pubmed.ncbi.nlm.nih.gov/25862075/>.
 19. Polat M, Şimşek A, Tansuğ N, Sezer RG, Özkol M, Başpınar P, et al. Prediction of neurodevelopmental outcome in term neonates with hypoxic-ischemic encephalopathy. *Eur J Paediatr Neurol*. 2013 [cited 2022 Jun 28]; 17 (3): 288–93. Available from: <https://pubmed.ncbi.nlm.nih.gov/23231917/>.
 20. Shellhaas RA, Kushwaha JS, Plegue MA, Selewski DT, Barks JDE. An Evaluation of Cerebral and Systemic Predictors of 18-Month Outcomes for Neonates With Hypoxic Ischemic Encephalopathy. *J Child Neurol*. 2015 [cited 2022 Jun 28]; 30 (11): 1526–31. Available from: <https://pubmed.ncbi.nlm.nih.gov/25724376/>.
 21. Chang T, Du Plessis A. Neurodiagnostic techniques in neonatal critical care. *Curr Neurol Neurosci Rep*. 2012 [cited 2022 Jun 29]; 12 (2): 145–52. Available from: <https://pubmed.ncbi.nlm.nih.gov/22318538/>.
 22. Van Laerhoven H, De Haan TR, Offringa M, Post B, Van Der Lee JH. Prognostic tests in term neonates with hypoxic-ischemic encephalopathy: a systematic review. *Pediatrics*. 2013 [cited 2022 Jun 29]; 131 (1): 88–98. Available from: <https://pubmed.ncbi.nlm.nih.gov/23248219/>.
 23. Rasmussen LA, Cascio MA, Ferrand A, Shevell M, Racine E. The complexity of physicians' understanding and management of prognostic uncertainty in neonatal hypoxic-ischemic encephalopathy. *J Perinatol*. 2019 [cited 2022 Jun 29]; 39 (2): 278–85. Available from: <https://pubmed.ncbi.nlm.nih.gov/30568164/>.
 24. Natarajan N, Pardo AC. Challenges in neurologic prognostication after neonatal brain injury. *Semin Perinatol*. 2017 [cited 2022 Jun 29]; 41 (2): 117–23. Available from: <https://pubmed.ncbi.nlm.nih.gov/28139254/>.
 25. Merchant N, Azzopardi D. Early predictors of outcome in infants treated with hypothermia for hypoxic-ischaemic encephalopathy. *Dev Med Child Neurol*. 2015 [cited 2022 Jun 29]; 57 (S3): 8–16. Available from: <https://pubmed.ncbi.nlm.nih.gov/25800487/>.
 26. Merhar SL, Chau V. Neuroimaging and Other Neurodiagnostic Tests in Neonatal Encephalopathy. *Clin Perinatol*. 2016 [cited 2022 Jun 29]; 43 (3): 511–27. Available from: <https://pubmed.ncbi.nlm.nih.gov/27524451/>.
 27. Del Río R, Ochoa C, Alarcon A, Arnáez J, Blanco D, García-Alix A. Amplitude integrated electroencephalogram as a prognostic tool in neonates with hypoxic-ischemic encephalopathy: A systematic review. *PLoS One*. 2016 [cited 2022 Jun 29]; 11 (11). Available from: <https://pubmed.ncbi.nlm.nih.gov/27802300/>.
 28. Mizrahi EM. Neonatal seizures and neonatal epileptic syndromes. *Neurol Clin*. 2001 [cited 2022 Jun 29]; 19 (2): 427–63. Available from: <https://pubmed.ncbi.nlm.nih.gov/11358751/>.
 29. Murray DM, Boylan GB, Ali I, Ryan CA, Murphy BP, Connolly S. Defining the gap between electrographic seizure burden, clinical expression and staff recognition of neonatal seizures. *Arch Dis Child Fetal Neonatal Ed*. 2008 [cited 2022 Jun 29]; 93 (3). Available from: <https://pubmed.ncbi.nlm.nih.gov/17626147/>.
 30. Clancy RR, Legido A, Lewis D. Occult neonatal seizures. *Epilepsia*. 1988 [cited 2022 Jun 29]; 29 (3): 256–61. Available from: <https://pubmed.ncbi.nlm.nih.gov/3371282/>.
 31. Weeke LC, Boylan GB, Pressler RM, Hallberg B, Blennow M, Toet MC, et al. Role of EEG background activity, seizure burden and MRI in predicting neurodevelopmental outcome in full-term infants with hypoxic-ischaemic encephalopathy in the era of therapeutic hypothermia. *Eur J Paediatr Neurol*. 2016 [cited 2022 Jun 28]; 20 (6): 855–64. Available from: <https://pubmed.ncbi.nlm.nih.gov/27370316/>.
 32. Gunn AJ, Wyatt JS, Whitelaw A, Barks J, Azzopardi D, Ballard R, et al. Therapeutic hypothermia changes the prognostic value of clinical evaluation of neonatal encephalopathy. *J Pediatr*. 2008 [cited 2022 Jun 29]; 152 (1). Available from: <https://pubmed.ncbi.nlm.nih.gov/18154900/>.
 33. Boudes E, Tan X, Saint-Martin C, Shevell M, Wintermark P. MRI obtained during versus after hypothermia in asphyxiated newborns. *Arch Dis Child Fetal Neonatal Ed*. 2015 [cited 2022 Jun 29]; 100 (3): F238–42. Available from: <https://pubmed.ncbi.nlm.nih.gov/25605620/>.
 34. Bonifacio SL, deVries LS, Groenendaal F. Impact of hypothermia on predictors of poor outcome: how do we decide to redirect care? *Semin Fetal Neonatal Med*. 2015 [cited 2022 Jun 29]; 20 (2): 122–7. Available from: <https://pubmed.ncbi.nlm.nih.gov/25577654/>.
 35. Thoresen M, Tooley J, Liu X, Jary S, Fleming P, Luyt K, et al. Time is brain: starting therapeutic hypothermia within three hours after birth improves motor outcome in asphyxiated newborns. *Neonatology*. 2013 [cited 2022 Jun 29]; 104 (3): 228–33. Available from: <https://pubmed.ncbi.nlm.nih.gov/24030160/>.
 36. Basu SK, Kaiser JR, Guffey D, Minard CG, Guillet R, Gunn AJ. Hypoglycaemia and hyperglycaemia are associated with unfavourable outcome in infants with hypoxic ischaemic encephalopathy: A post hoc analysis of the CoolCap Study. *Arch Dis Child Fetal Neonatal Ed*. 2016 [cited 2022 Jun 29]; 101 (2): F149–55. Available from: <https://pubmed.ncbi.nlm.nih.gov/26283669/>.
 37. Shah DK, Wusthoff CJ, Clarke P, Wyatt JS, Ramaiah SM, Dias RJ, et al. Electrographic seizures are associated with brain injury in newborns undergoing therapeutic hypothermia. *Arch Dis Child Fetal Neonatal Ed*. 2014 [cited 2022 Jun 29]; 99 (3). Available from: <https://pubmed.ncbi.nlm.nih.gov/24443407/>.
 38. Sabir H, Jary S, Tooley J, Liu X, Thoresen M. Increased inspired oxygen in the first hours of life is associated with adverse outcome in newborns treated for perinatal asphyxia with therapeutic hypothermia. *J Pediatr*. 2012 [cited 2022 Jun 29]; 161 (3): 409–16. Available from: <https://pubmed.ncbi.nlm.nih.gov/22521111/>.
 39. Osredkar D, Thoresen M, Maes E, Flatebø T, Elstad M, Sabir H. Hypothermia is not neuroprotective after infection-sensitized neonatal hypoxic-ischemic brain injury. *Resuscitation*. 2014 [cited 2022 Jun 29]; 85 (4): 567–72. Available from: <https://pubmed.ncbi.nlm.nih.gov/24361672/>.
 40. Uziel G, Ghezzi D, Zeviani M. Infantile mitochondrial encephalopathy. *Seminars in Fetal and Neonatal Medicine*. *Semin Fetal Neonatal Med*. 2011 [cited 2022 Jun 29]; 16: 205–15. Available from: <https://pubmed.ncbi.nlm.nih.gov/21620787/>.
 41. Bruylant M, Liebaers I, Sacre L, Vandeplas Y, De Meirleir L, Martin JJ. Neonatal myotubular myopathy with a probable X-linked inheritance: observations on a new family with a review of the literature. *J Neurol*. 1984 [cited 2022 Jun 29]; 231 (4): 220–2. Available from: <https://pubmed.ncbi.nlm.nih.gov/6512577/>.
 42. Danti FR, Galosi S, Romani M, Montomoli M, Carss KJ, Lucy Raymond F, et al. GNAO1 encephalopathy: Broadening the phenotype and evaluating treatment and outcome. *Neurol Genet*. 2017 [cited 2022 Jul 4]; 3 (2). Available from: <https://pubmed.ncbi.nlm.nih.gov/28357411/>.
 43. Solis GP, Kozhanova TV, Koval A, Zhilina SS, Mescheryakova TI, Abramov AA, et al. Pediatric Encephalopathy: Clinical, Biochemical and Cellular Insights into the Role of Gln52 of GNAO1 and GNAI1 for the Dominant Disease. *Cells*. 2021 [cited 2022 Jul 4]; 10 (10).

- Available from: <https://pubmed.ncbi.nlm.nih.gov/34685729/>.
44. Cuzzolin L, Zaccaron A, Fanos V. Unlicensed and off-label uses of drugs in paediatrics: a review of the literature. *Fundam Clin Pharmacol*. 2003 [cited 2022 Jun 30]; 17 (1): 125–31. Available from: <https://pubmed.ncbi.nlm.nih.gov/12588640/>.
 45. Robertson NJ, Thayil S, B. Cady E, Raivich G. Magnetic resonance spectroscopy biomarkers in term perinatal asphyxial encephalopathy: from neuropathological correlates to future clinical applications. *Curr Pediatr Rev*. 2014 [cited 2022 Jun 30]; 10 (1): 37–47. Available from: <https://pubmed.ncbi.nlm.nih.gov/25055862/>.
 46. Massaro AN, Chang T, Kadom N, Tsuchida T, Scafidi J, Glass P, et al. Biomarkers of brain injury in neonatal encephalopathy treated with hypothermia. *J Pediatr*. 2012 [cited 2022 Jun 30]; 161 (3): 434–40. Available from: <https://pubmed.ncbi.nlm.nih.gov/22494878/>.
 47. Jones R, Heep A, Odd D. Biochemical and clinical predictors of hypoxic-ischemic encephalopathy after perinatal asphyxia. *J Matern Fetal Neonatal Med*. 2018 [cited 2022 Jun 30]; 31 (6): 791–6. Available from: <https://pubmed.ncbi.nlm.nih.gov/28274150/>.
 48. Fatemi A, Wilson MA, Johnston M V. Hypoxic-Ischemic Encephalopathy in the Term Infant [Internet]. *Clinics in Perinatology*. Clin Perinatol. 2009 [cited 2022 Jun 30]; 36: 835–58. Available from: <https://pubmed.ncbi.nlm.nih.gov/19944838/>.
 49. Ennen CS, Huisman TAGM, Savage WJ, Northington FJ, Jennings JM, Everett AD, et al. Glial fibrillary acidic protein as a biomarker for neonatal hypoxic-ischemic encephalopathy treated with whole-body cooling. *Am J Obstet Gynecol*. 2011 [cited 2022 Jun 30]; 205 (3): 251.e1–251.e7. Available from: <https://pubmed.ncbi.nlm.nih.gov/21784396/>.
 50. Kim HJ, Tsao JW, Stanfill AG. The current state of biomarkers of mild traumatic brain injury. *JCI insight*. 2018 [cited 2022 Jun 30]; 3 (1). Available from: <https://pubmed.ncbi.nlm.nih.gov/29321373/>.
 51. Orrock JE, Panchapakesan K, Vezina G, Chang T, Harris K, Wang Y, et al. Association of brain injury and neonatal cytokine response during therapeutic hypothermia in newborns with hypoxic-ischemic encephalopathy. *Pediatr Res*. Available from: <https://pubmed.ncbi.nlm.nih.gov/26717001/>.
 52. Tann CJ, Martinello KA, Sadoo S, Lawn JE, Seale AC, Vega-Poblete M, et al. Neonatal Encephalopathy With Group B Streptococcal Disease Worldwide: Systematic Review, Investigator Group Datasets, and Meta-analysis. *Clin Infect Dis*. 2017 [cited 2022 Jun 30]; 65 (suppl_2): S173–89. Available from: <https://pubmed.ncbi.nlm.nih.gov/29117330/>.
 53. Murray DM. Biomarkers in neonatal hypoxic-ischemic encephalopathy-Review of the literature to date and future directions for research. *Handb Clin Neurol*. 2019 [cited 2022 Jun 30]; 162: 281–93. Available from: <https://pubmed.ncbi.nlm.nih.gov/31324315/>.
 54. Alkholi UM, Abdalmonem N, Zaki A, Ali YF, Mohamed SA, Abdelsalam NI, et al. Early predictors of brain damage in full-term newborns with hypoxic ischemic encephalopathy. *Neuropsychiatr Dis Treat*. 2017 [cited 2022 Jun 30]; 13: 2133–9. Available from: <https://pubmed.ncbi.nlm.nih.gov/28860770/>.
 55. Douglas-Escobar M, Weiss MD. Biomarkers of brain injury in the premature infant. *Front Neurol*; 2013 [cited 2022 Jun 30]; 3 JAN. Available from: <https://pubmed.ncbi.nlm.nih.gov/23346073/>.
 56. Massaro AN, Wu YW, Bammler TK, Comstock B, Mathur A, McKinstry RC, et al. Plasma Biomarkers of Brain Injury in Neonatal Hypoxic-Ischemic Encephalopathy. *J Pediatr*. 2018 [cited 2022 Jun 30]; 194: 67–75.e1. Available from: <https://pubmed.ncbi.nlm.nih.gov/29478510/>.
 57. Shah DK, Ponnusamy V, Evanson J, Kapellou O, Ekitzidou G, Gupta N, et al. Raised plasma neurofilament light protein levels are associated with abnormal MRI outcomes in newborns undergoing therapeutic hypothermia. *Front Neurol*. 2018 [cited 2022 Jun 30]; 9 (MAR). Available from: <https://pubmed.ncbi.nlm.nih.gov/29556208/>.
 58. Sweetman DU, Onwuneme C, Watson WR, Murphy JFA, Molloy EJ. Perinatal Asphyxia and Erythropoietin and VEGF: Serial Serum and Cerebrospinal Fluid Responses. *Neonatology*. 2017 [cited 2022 Jul 4]; 111 (3): 253–9. Available from: <https://pubmed.ncbi.nlm.nih.gov/27902983/>.
 59. Lv H, Wang Q, Wu S, Yang L, Ren P, Yang Y, et al. Neonatal hypoxic ischemic encephalopathy-related biomarkers in serum and cerebrospinal fluid. *Clin Chim Acta*. 2015 [cited 2022 Jul 4]; 450: 282–97. Available from: <https://pubmed.ncbi.nlm.nih.gov/26320853/>.
 60. Hasslacher J, Lehner GF, Harler U, Beer R, Ulmer H, Kirchmair R, et al. Secretoneurin as a marker for hypoxic brain injury after cardiopulmonary resuscitation. *Intensive Care Med*. 2014 [cited 2022 Jul 4]; 40 (10): 1518–27. Available from: <https://pubmed.ncbi.nlm.nih.gov/25138227/>.
 61. Rizzo FM, Sannia A, Gavilanes DAW, Vles HJ, Colivicchi M, Ricotti A, et al. Biomarkers of brain damage in preterm infants. *J Matern Fetal Neonatal Med*. 2012 [cited 2022 Jul 4]; 25 (SUPPL.4): 93–6. Available from: <https://pubmed.ncbi.nlm.nih.gov/22958034/>.
 62. Chaparro-Huerta V, Flores-Soto ME, Merin Sigala ME, Barrera de León JC, Lemus-Varela M de L, Torres-Mendoza BM de G, et al. Proinflammatory Cytokines, Enolase and S-100 as Early Biochemical Indicators of Hypoxic-Ischemic Encephalopathy Following Perinatal Asphyxia in Newborns. *Pediatr Neonatol*. 2017 [cited 2022 Jul 4]; 58 (1): 70–6. Available from: <https://pubmed.ncbi.nlm.nih.gov/27522459/>.
 63. Chalak LF, Sánchez PJ, Adams-Huet B, Luptook AR, Heyne RJ, Rosenfeld CR. Biomarkers for severity of neonatal hypoxic-ischemic encephalopathy and outcomes in newborns receiving hypothermia therapy. *J Pediatr*. 2014 [cited 2022 Jul 4]; 164 (3). Available from: <https://pubmed.ncbi.nlm.nih.gov/24332821/>.
 64. Chiesa C, Pellegrini G, Panero A, De Luca T, Assumma M, Signore F, et al. Umbilical cord interleukin-6 levels are elevated in term neonates with perinatal asphyxia. *Eur J Clin Invest*. 2003 [cited 2022 Jul 4]; 33 (4): 352–8. Available from: <https://pubmed.ncbi.nlm.nih.gov/12662167/>.
 65. Jenkins DD, Rollins LG, Perkel JK, Wagner CL, Katikaneni LP, Bass WT, et al. Serum cytokines in a clinical trial of hypothermia for neonatal hypoxic-ischemic encephalopathy. *J Cereb Blood Flow Metab*. 2012 [cited 2022 Jul 4]; 32 (10): 1888–96. Available from: <https://pubmed.ncbi.nlm.nih.gov/22805873/>.
 66. Hou X, Yuan Z, Wang X, Cheng R, Zhou X, Qiu J. Peptidome analysis of cerebrospinal fluid in neonates with hypoxic-ischemic brain damage. *Mol Brain*. 2020 [cited 2022 Jul 4]; 13 (1). Available from: <https://pubmed.ncbi.nlm.nih.gov/33008433/>.
 67. Zhu Y, Yun Y, Jin M, Li G, Li H, Miao P, et al. Identification of novel biomarkers for neonatal hypoxic-ischemic encephalopathy using iTRAQ. *Ital J Pediatr*. 2020 [cited 2022 Jul 4]; 46 (1). Available from: <https://pubmed.ncbi.nlm.nih.gov/32448169/>.
 68. Viemann D, Strey A, Janning A, Jurk K, Klimmek K, Vogl T, et al. Myeloid-related proteins 8 and 14 induce a specific inflammatory response in human microvascular endothelial cells. *Blood*. 2005 [cited 2022 Jul 4]; 105 (7): 2955–62. Available from: <https://pubmed.ncbi.nlm.nih.gov/15598812/>.
 69. Ehrchen JM, Sunderkötter C, Foell D, Vogl T, Roth J. The endogenous Toll-like receptor 4 agonist S100A8/S100A9 (calprotectin) as innate amplifier of infection, autoimmunity, and cancer. *J Leukoc Biol*. 2009 [cited 2022 Jul 4]; 86 (3): 557–66. Available from: <https://pubmed.ncbi.nlm.nih.gov/19451397/>.
 70. Zhao X, Song S, Sun G, Strong R, Zhang J, Grotta JC, et al. Neuroprotective role of haptoglobin after intracerebral hemorrhage. *J Neurosci*. 2009 [cited 2022 Jul 4]; 29 (50): 15819–27. Available from: <https://pubmed.ncbi.nlm.nih.gov/20016097/>.
 71. Zhou Y, Bhatia I, Cai Z, He QY, Cheung PT, Chiu JF. Proteomic analysis of neonatal mouse brain: Evidence for hypoxia- and ischemia-induced dephosphorylation of collapsin response mediator proteins. *J Proteome Res*. 2008 [cited 2022 Jul 4]; 7 (6): 2507–15. Available from: <https://pubmed.ncbi.nlm.nih.gov/18471005/>.
 72. Solberg R, Kuligowski J, Pankratov L, Escobar J, Quintás G, Lliso I, et al. Changes of the plasma metabolome of newly born piglets subjected to postnatal hypoxia and resuscitation with air. *Pediatr Res*. 2016 [cited 2022 Jul 4]; 80 (2): 284–92. Available from: <https://pubmed.ncbi.nlm.nih.gov/27055187/>.
 73. Li H, Kittur FS, Hung CY, Li PA, Ge X, Sane DC, et al. Quantitative Proteomics Reveals the Beneficial Effects of Low Glucose on Neuronal Cell Survival in an in vitro Ischemic Penumbra Model. *Front Cell Neurosci*. 2020 [cited 2022 Jul 4]; 14. Available from: <https://pubmed.ncbi.nlm.nih.gov/33033473/>.

74. Shi Y, Cai EL, Yang C, Ye CY, Zeng P, Wang XM, et al. Protection of melatonin against acidosis-induced neuronal injuries. *J Cell Mol Med*. 2020 [cited 2022 Jul 4]; 24 (12): 6928–42. Available from: <https://pubmed.ncbi.nlm.nih.gov/32364678/>.
75. Bjerkhaug AU, Granslo HN, Klingenberg C. Metabolic responses in neonatal sepsis-A systematic review of human metabolomic studies. *Acta Paediatr*. 2021 [cited 2022 Jun 29]; 110 (8): 2316–25. Available from: <https://pubmed.ncbi.nlm.nih.gov/33851423/>.
76. Beckstrom AC, Ricca RL, Gow KW, McAdams RM. Persistent posterior pneumomediastinum in a neonate. *Pediatr Int*. 2012 [cited 2022 Jul 4]; 54 (3): 441–2. Available from: <https://pubmed.ncbi.nlm.nih.gov/22631580/>.
77. Nicholson JK, Lindon JC. Systems biology: Metabonomics. *Nature*. 2008 [cited 2022 Jul 4]; 455 (7216): 1054–6. Available from: <https://pubmed.ncbi.nlm.nih.gov/18948945/>.
78. Atzori L, Antonucci R, Barberini L, Griffin JL, Fanos V. Metabonomics: a new tool for the neonatologist. *J Matern Fetal Neonatal Med*. 2009 [cited 2022 Jul 4]; 22 (SUPPL. 3): 50–3. Available from: <https://pubmed.ncbi.nlm.nih.gov/19701858/>.
79. Locci E, Noto A, Puddu M, Pomero G, Demontis R, Dalmazzo C, et al. A longitudinal 1H-NMR metabolomics analysis of urine from newborns with hypoxic-ischemic encephalopathy undergoing hypothermia therapy. *Clinical and medical legal insights. PLoS One*. 2018 [cited 2022 Jul 4]; 13 (4). Available from: <https://pubmed.ncbi.nlm.nih.gov/29668681/>.
80. Sarafidis K, Efstathiou N, Begou O, Soubasi V, Agakidou E, Gika E, et al. Urine metabolomic profile in neonates with hypoxic-ischemic encephalopa-thy. *Hippokratia*. 2017 [cited 2022 Jul 4]; 21 (2): 80. Available from: <https://pubmed.ncbi.nlm.nih.gov/29668681/>.
81. Denihan NM, Kirwan JA, Walsh BH, Dunn WB, Broadhurst DI, Boylan GB, et al. Untargeted metabolomic analysis and pathway discovery in perinatal asphyxia and hypoxic-ischaemic encephalopathy. *J Cereb Blood Flow Metab*. 2019 [cited 2022 Jul 4]; 39 (1): 147–62. Available from: <https://pubmed.ncbi.nlm.nih.gov/3116688/>.
82. Jia Y, Jia X, Xu H, Gao L, Wei C, Li Y, et al. Blood Plasma Metabolic Profile of Newborns with Hypoxic-Ischaemic Encephalopathy by GC-MS. *Biomed Res Int*. 2021 [cited 2022 Jul 4]; 2021. Available from: <https://pubmed.ncbi.nlm.nih.gov/34258280/>.
83. Reinke SN, Walsh BH, Boylan GB, Sykes BD, Kenny LC, Murray DM, et al. 1H NMR derived metabolomic profile of neonatal asphyxia in umbilical cord serum: implications for hypoxic ischemic encephalopathy. *J Proteome Res*. 2013 [cited 2022 Jul 4]; 12 (9): 4230–9. Available from: <https://pubmed.ncbi.nlm.nih.gov/23931672/>.
84. Longini M, Giglio S, Perrone S, Vivi A, Tassini M, Fanos V, et al. Proton nuclear magnetic resonance spectroscopy of urine samples in preterm asphyctic newborn: a metabolomic approach. *Clin Chim Acta*. 2015 [cited 2022 Jul 4]; 444: 250–6. Available from: <https://pubmed.ncbi.nlm.nih.gov/25727514/>.
85. Johnston M V. Excitotoxicity in perinatal brain injury. *Brain Pathol*. 2005 [cited 2022 Jul 4]; 15 (3): 234–40. Available from: <https://pubmed.ncbi.nlm.nih.gov/16196390/>.
86. Pietz J, Guttenberg N, Gluck L. Hypoxanthine: a marker for asphyxia. *Obstet Gynecol*. 1988 [cited 2022 Jul 4]; 72 (5): 762–6. Available from: <https://pubmed.ncbi.nlm.nih.gov/3140152/>.
87. Penry JT, Manore MM. Choline: An important micronutrient for maximal endurance-exercise performance? *Int J Sport Nutr Exerc Metab*. 2008 [cited 2022 Jul 4]; 18: 191–203. Available from: <https://pubmed.ncbi.nlm.nih.gov/18458362/>.
88. Raposo G, Stoorvogel W. Extracellular vesicles: exosomes, microvesicles, and friends. *J Cell Biol*. 2013 [cited 2022 Jul 4]; 200 (4): 373–83. Available from: <https://pubmed.ncbi.nlm.nih.gov/23420871/>.
89. Chivet M, Hemming F, Pernet-Gallay K, Fraboulet S, Sadoul R. Emerging role of neuronal exosomes in the central nervous system. *Front Physiol*. 2012 [cited 2022 Jul 4]; 3. Available from: <https://pubmed.ncbi.nlm.nih.gov/22654762/>.
90. Chiva-Blanch G, Suades R, Crespo J, Peña E, Padró T, Jiménez-Xarrié E, et al. Microparticle Shedding from Neural Progenitor Cells and Vascular Compartment Cells Is Increased in Ischemic Stroke. *PLoS One*. 2016 [cited 2022 Jul 4]; 11 (1). Available from: <https://pubmed.ncbi.nlm.nih.gov/26815842/>.
91. Patz S, Trattng C, Grünbacher G, Ebner B, Güllly C, Novak A, et al. More than cell dust: microparticles isolated from cerebrospinal fluid of brain injured patients are messengers carrying mRNAs, miRNAs, and proteins. *J Neurotrauma*. 2013 [cited 2022 Jul 4]; 30 (14): 1232–42. Available from: <https://pubmed.ncbi.nlm.nih.gov/23360174/>.
92. Goetzl EJ, Boxer A, Schwartz JB, Abner EL, Petersen RC, Miller BL, et al. Low neural exosomal levels of cellular survival factors in Alzheimer's disease. *Ann Clin Transl Neurol*. 2015 [cited 2022 Jul 4]; 2 (7): 769–73. Available from: <https://pubmed.ncbi.nlm.nih.gov/26273689/>.
93. Goetzl EJ, Boxer A, Schwartz JB, Abner EL, Petersen RC, Miller BL, et al. Altered lysosomal proteins in neural-derived plasma exosomes in preclinical Alzheimer disease. *Neurology*. 2015 [cited 2022 Jul 4]; 85 (1): 40–7. Available from: <https://pubmed.ncbi.nlm.nih.gov/26062630/>.
94. Силачев Д. Н., Горюнов К. В., Плотников Е. Ю., Швецова Ю. А., Бабенко В. А., Буров А. А., et al. Внеклеточные везикулы мочи как диагностический маркер почечных патологий. «Педиатрия» имени Г. Н. Сперанского. 2020 [cited 2022 Jul 4]; 99 (5): 154–63. Available from: <https://pediatrajournal.ru/archive?show=378§ion=6017>.
95. Goetzl L, Merabova N, Darbinian N, Martirosyan D, Poletto E, Fugarolas K, et al. Diagnostic Potential of Neural Exosome Cargo as Biomarkers for Acute Brain Injury. *Ann Clin Transl Neurol*. 2018 [cited 2022 Jul 4]; 5 (1): 4–10. Available from: <https://pubmed.ncbi.nlm.nih.gov/29376087/>.
96. Pineles B, Mani A, Sura L, Rossignol C, Albayram M, Weiss MD, et al. Neuronal exosome proteins: novel biomarkers for predicting neonatal response to therapeutic hypothermia. *Arch Dis Child Fetal Neonatal Ed*. 2022 [cited 2022 Jul 4]; 107 (1): F60–4. Available from: <https://pubmed.ncbi.nlm.nih.gov/34021027/>.
97. Chen S, Chen XC, Lou XH, Qian SQ, Ruan ZW. Determination of serum neutrophil gelatinase-associated lipocalin as a prognostic biomarker of acute spontaneous intracerebral hemorrhage. *Clin Chim Acta*. 2019 [cited 2022 Jul 4]; 492: 72–7. Available from: <https://pubmed.ncbi.nlm.nih.gov/30771300/>.
98. Плотников Е. Ю., Силачев Д. Н., Павленко Т. А., Павлова В. С., Крючко Д. С., Зубков ВВ, et al. Острое повреждение почек у новорожденных. От эксперимента к клинике. *Неонатология*. 2017; (4): 58–63.
99. Xu D, Hopf C, Reddy R, Cho RW, Guo L, Lanahan A, et al. Narp and NP1 form heterocomplexes that function in developmental and activity-dependent synaptic plasticity. *Neuron*. 2003 [cited 2022 Jul 4]; 39 (3): 513–28. Available from: <https://pubmed.ncbi.nlm.nih.gov/12895424/>.

CONTENT OF CD4⁺ CELLS EXPRESSING CD39/CD73 ECTONUCLEOTIDASES IN CHILDREN WITH INFLAMMATORY BOWEL DISEASES

Radygina TV¹ ✉, Petrichuk SV¹, Kuptsova DG¹, Potapov AS^{1,2}, Illarionov AS², Anushenko AO¹, Kurbatova OV¹, Semikina EL^{1,2}

¹ National Medical Research Center for Children's Health, Moscow, Russia

² Sechenov First Moscow State Medical University, Moscow, Russia

The regulation of TNF inhibitor therapy-associated immune responses in inflammatory bowel diseases (IBD) in children remains an urgent problem. The study aimed at analyzing the expression of CD39/CD73 endonucleotidases by different subsets of peripheral blood T cells in children with IBD including Crohn's disease ($n = 34$) and ulcerative colitis ($n = 33$) having received TNF inhibitors in comparison with conditionally healthy children ($n = 45$). Lymphocyte subsets including regulatory T cells (Treg, CD4⁺CD127^{low}CD25^{high}), activated T cells (Tact, CD4⁺CD25⁺CD127^{high}) and Th17 cells (CD4⁺CD161⁺CD3⁺) were studied by flow cytometry. The results are presented as medians (Me) and quartiles (Q₂₅–Q₇₅). In children with IBD the highest and the lowest relative counts of CD39⁺ cells were found in Treg and Tact subsets — 31% (15–38) and 4% (1–7), respectively. The highest relative counts of CD73⁺ cells were found in Tact — 13% (8–21). The CD39 and CD73 expression ratio in patients with IBD, and in the control group as well, depended on particular subset. CD39 expression in Treg, Tact and Th17 of patients with IBD was not age-dependent. Patients with acute Crohn's disease revealed decreased expression of CD39 in Treg compared with the control group (12% (9–23) vs 35% (28–39), respectively; $p = 10^{-6}$). Patients with Crohn's disease in remission revealed increased expression of CD39 in Treg compared with the acute of the disease (31% (27–40) vs 12% (9–23); $p = 9.4 \times 10^{-5}$). Patients with Crohn's disease in remission revealed no significant differences with the control group apart from reduced expression of CD73 by Treg in Crohn's disease. The results indicate significant association of CD39 and CD73 expression levels in particular subsets of CD4⁺ cells with the phase of the disease (acute vs remission) and, accordingly, with the anti-TNF regimen efficacy.

Keywords: lymphocyte subsets, CD4⁺ subsets, Treg, Th17, Tact, CD39, CD73, children, inflammatory bowel diseases

Funding: the study was carried out on state assignment of the Ministry of Health of Russia, number AAAA-A19-119013090093-2.

Acknowledgement: the authors thank all patients for participation and acknowledge the Gastroenterology Department with Hepatology Group of the National Medical Research Center for Children's Health and its collaboration.

Compliance with ethical standards: the study was approved by the Ethics Committee of the National Medical Research Center for Children's Health, Moscow (protocol № 6 dated June 11, 2019). The informed consent was submitted by all study participants.

✉ **Correspondence should be addressed:** Tatiana V. Radygina
Lomonosovsky prospekt, 2/1, Moscow, 119296, Russia; tvradigina@mail.ru

Received: 22.06.2022 **Accepted:** 16.07.2022 **Published online:** 30.07.2022

DOI: 10.24075/brsmu.2022.039

СОДЕРЖАНИЕ CD4⁺-КЛЕТОК С ЭКСПРЕССИЕЙ ЭКТОНУКЛЕОТИДАЗ CD39/CD73 У ДЕТЕЙ С ВОСПАЛИТЕЛЬНЫМИ ЗАБОЛЕВАНИЯМИ КИШЕЧНИКА

Т. В. Радыгина¹ ✉, С. В. Петричук¹, Д. Г. Купцова¹, А. С. Потапов^{1,2}, А. С. Илларионов², А. О. Анушенко¹, О. В. Курбатова¹, Е. Л. Семикина^{1,2}

¹ Национальный медицинский исследовательский центр здоровья детей, Москва, Россия

² Первый московский государственный медицинский университет имени И. М. Сеченова (Сеченовский Университет), Москва, Россия

Изучение регуляции иммунного ответа на фоне терапии блокаторами TNF при воспалительных заболеваниях кишечника (ВЗК) у детей остается актуальной проблемой. Целью исследования было изучить экспрессию CD39/CD73 в субпопуляциях лимфоцитов (регуляторных Т-клеток (Treg) — CD4⁺CD127^{low}CD25^{high}; активированных Т-клеток (Tact) — CD4⁺CD25⁺CD127^{high}; Th17-лимфоцитов — CD4⁺CD161⁺CD3⁺) периферической крови у детей с ВЗК (с болезнью Крона (БК), $n = 34$; с язвенным колитом — $n = 33$), принимавших блокаторы TNF, и у 45 условно здоровых детей. Результаты представлены в виде медианы (Me) и квартилей (Q₂₅–Q₇₅). С помощью многоцветной цитометрии показано, что у детей с ВЗК наибольшее количество CD39⁺ выявлено в популяции Treg — 31% (15–38), наименьшее — в Tact 4% (1–7), а наибольшее количество CD73⁺ — в Tact 13% (8–21). Соотношение экспрессии CD39 и CD73 у пациентов с ВЗК, так же как и в группе сравнения, зависело от популяции клеток. Экспрессия CD39 в Treg, Tact и Th17 у пациентов с ВЗК не зависела от возраста ребенка. В группе детей с БК в обострении относительно группы сравнения получено снижение экспрессии CD39 в Treg (12% (9–23) против 35% (28–39), $p = 0,000001$). У детей в ремиссии БК экспрессия CD39 в Treg достоверно выше, чем при обострении (31% (27–40) против 12% (9–23); $p = 0,000094$). Между группой пациентов в ремиссии и группой сравнения достоверных различий выявлено не было, за исключением снижения экспрессии CD73 в Treg при БК. Полученные результаты показывают, что экспрессия CD39 и CD73 в популяциях CD4⁺-лимфоцитов в значительной степени связана с течением заболевания, с обострением или ремиссией, и, соответственно, с эффективностью проводимой анти-TNF-терапии.

Ключевые слова: популяции лимфоцитов, CD4⁺-лимфоциты, Treg, Th17, Tact, CD39, CD73, ВЗК, дети

Финансирование: исследование проведено в рамках государственного задания Минздрава России, № AAAA-A19-119013090093-2.

Благодарности: авторы выражают благодарность всем пациентам, участвовавшим в исследовании, а также признательность за сотрудничество коллегам из гастроэнтерологического отделения с гепатологической группой национального медицинского исследовательского центра здоровья детей.

Соблюдение этических стандартов: исследование одобрено этическим комитетом ФГАУ «НМИЦ здоровья детей» МЗ РФ (протокол № 6 от 11 июня 2019 г.). Для всех участников исследования было получено информированное согласие родителей в соответствии с принципами Хельсинкской декларации.

✉ **Для корреспонденции:** Татьяна Вячеславовна Радыгина
Ломоносовский проспект, д. 2/1, г. Москва, 119296, Россия; tvradigina@mail.ru

Статья получена: 22.06.2022 **Статья принята к печати:** 16.07.2022 **Опубликована онлайн:** 30.07.2022

DOI: 10.24075/vrgmu.2022.039

Advanced understanding of pathogenic processes in the inflammatory bowel diseases (IBD) together with the search for new approaches in predicting patient's responses to therapy is an urgent pediatric problem. The prevalence of IBD in Russia

is 5.1 : 100,000 [1]. The 30% increase in the incidence of IBD among children observed over the past decade and the emergence of severe forms of the disease in early childhood are of particular concern to pediatricians [2, 3]. The onset of IBD has

been associated with a combination of several adverse factors including genetic predisposition, immune system dysfunction, abnormal gut microbiota and the harmful environmental factor exposure [4]. Among those, immune dysregulations are considered the most impactful. In particular, the dynamics of certain subsets of T lymphocytes including T helper 17 cells (Th17) and regulatory T cells (Treg) correlates with the severity of pathological process and therapy efficacy in IBD [5, 6]. As naïve T cells differentiate into Th1, Th2, Th17 and Treg cells under the action of specific combinations of cytokines produced by antigen-presenting cells, Th17 and Treg use a common TGFβ-mediated signaling pathway. In the presence of IL6, IL21 and TGFβ, naïve CD4⁺ T cells differentiate into Th17, whereas in the absence of pro-inflammatory cytokines they differentiate into Treg cells. Abnormal balance between Th17 and Treg leads to autoimmune disorders including IBD [7, 8].

The past decade was marked by intensive research on the purinergic system and its immediate involvement in immune functionalities. The purinergic signaling hypothesis was proposed by Geoffrey Burnstock back in 1972 [9]. Its modern understanding implicates the extracellular adenosine triphosphoric acid (eATP) as a pro-inflammatory mediator participating in the regulation of cell metabolism, cell migration, cell proliferation and apoptosis through signaling pathways triggered by P2Y and P2X receptors [10, 11]. The ectonucleotidase enzymes CD39 (a.k.a. ecto-nucleoside

triphosphate diphosphohydrolase 1, E-NTPDase1) and CD73 (a.k.a. ecto-5'-nucleotidase, Ecto5'NTase) enable sequential dephosphorylation of ATP to adenosine which exerts anti-inflammatory properties [11]. A quantitative imbalance between eATP and adenosine may trigger inflammation [12]. The CD39 ectonucleotidase plays an important regulatory role in bowel inflammation: high expression of CD39 in circulating Tregs correlates with clinical and endoscopic remission in patients with IBD [13, 14]. It has been also demonstrated that single nucleotide polymorphisms associated with decreased expression of CD39 increase the risks of Crohn's disease [15].

Ectonucleotidases are expressed by different lymphocyte subsets including Treg and Th17 cells. About 90% of the Foxp3⁺ Treg cells exhibit CD39 on their surface [16] and the non-uniformity of Treg cells in terms of CD39 expression is relevant. Although both CD4⁺CD25^{high}CD39⁺ and CD4⁺CD25^{high}CD39⁻ Treg cells suppress proliferation and IFNγ production by effector T cells in multiple sclerosis [17], Treg cells with CD4⁺CD25^{high}FoxP3⁺CD39⁺ phenotype suppress IL17 production, while CD4⁺CD25^{high}CD39⁻ Treg cells produce IL17 [17]. Importantly, Th17 cell subsets are also non-uniform in terms of CD39 expression and apart from the majority of pro-inflammatory Th17 there is a minor pool of suppressor Th17 lymphocytes (supTh17) expressing high levels of CD39 and facilitating adenosine production. These supTh17 cells are found in peripheral blood and lamina propria of the intestinal

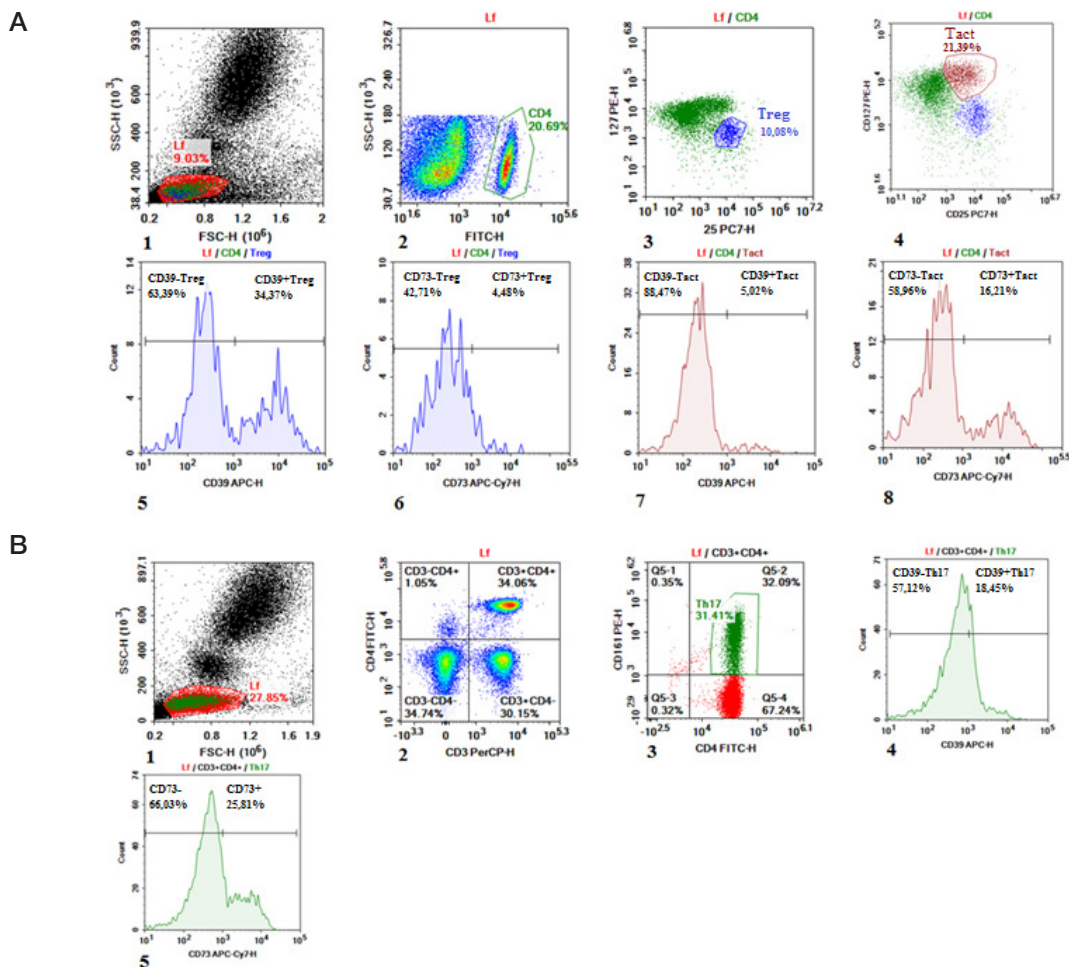


Fig. 1. Stepwise gating strategies for Treg, Tact and Th17 expressing CD39 and CD73. **A.** Stepwise gating for Treg and Tact: 1 — discrimination of the 'lymphoid' region based on forward scatter (FSC) and side scatter (SSC) parameters; 2 — discrimination of CD4-positive lymphocytes; 3 — discrimination of Treg as CD4⁺CD127^{low}CD25^{high}; 4 — discrimination of Tact as CD4⁺CD25⁺CD127^{high}; 5 — determination of CD39⁺ Treg; 6 — determination of CD73⁺ Treg; 7 — determination of CD39⁺ Tact; 8 — determination of CD73⁺ Tact. **B.** Stepwise gating for Th17: 1 — discrimination of the 'lymphoid' region based on forward scatter (FSC) and side scatter (SSC) parameters; 2 — discrimination of CD3⁺CD4⁺ double-positive set; 3 — discrimination of Th17 subset; 4 — determination of CD39⁺ Th17; 5 — determination of CD73⁺ Th17

Table 1. Relative counts of CD39 and CD73 ectonucleotidase-expressing cells (positivity rates) in CD4⁺ T lymphocyte subsets of patients with IBD and comparison group

Enzyme Indicators	Patients with IBD (n = 67)				Comparison group (n = 45)				p
	CD39		CD73		CD39		CD73		
	Me (Q _{0.25} -Q _{0.75})	Min-Max							
Treg, %	31.2 (14.8-37.8)	6-58	5.0 (3.0-8.3)	0-15	35 (27.8-39.4)	19-49	8.1 (6.9-12.2)	2-39	p ₃₉ = 0.023 p ₇₃ = 0.000
Tact, %	3.9 (1.1-6.7)	0-14	12.9 (8.0-21.1)	2-30	5 (4.4-7.4)	3-11	17.6 (11.9-21.5)	8-35	p ₃₉ = 0.001 p ₇₃ = 0.021
Th17, %	10.4 (5.2-16.8)	0-29	7.7 (4.7-11.4)	1-26	9.6 (8.6-12.1)	6-24	10.2 (7.3-14.4)	3-33	p ₃₉ = 0.771 p ₇₃ = 0.007

Note: p₃₉ — levels of significance for the differences in CD39 positivity rates between IBD and comparison group; p₇₃ — levels of significance for the differences in CD73 positivity rates between IBD and comparison group

mucosa in healthy individuals and their numbers are reduced significantly in Crohn's disease, which indicates their relevance to the bowel inflammation control [18, 19]. Noteworthy, the majority of studies on the abnormal purinergic signaling in IBD enrolled adult patients [12-14].

In this regard, we aimed at a pilot quantitative evaluation of CD39/CD73 ectonucleotidase-expressing cells in CD4⁺ lymphocyte subsets of children with IBD compared with healthy controls.

METHODS

The study enrolled 67 pediatric patients with IBD (34 pts with Crohn's disease and 33 pts with ulcerative colitis) aged 3.4-18 years and having received TNF inhibitor therapy. The patients were assigned to four groups in accordance with the course (phase) of the disease: group 1 — acute Crohn's disease (n = 18), group 2 — Crohn's disease in remission (n = 16), group 3 — acute ulcerative colitis (n = 22), group 4 — ulcerative colitis in remission (n = 11). The assignment was based on the Pediatric Crohn's Disease Activity Index (PCDAI) for Crohn's disease (≤ 10 — remission, > 10 — acute) and the Pediatric Ulcerative Colitis Activity Index (PUCAI) for ulcerative colitis (≤ 10 — remission, > 10 — acute). The comparison group (group 5, n = 45) enrolled conditionally healthy children aged 3.7-17.5 years. Inclusion criteria for group 5 were as follows: all standard clinical and biochemical laboratory indicators within reference values;

no acute or aggravating chronic conditions; no traumatic injury; no history of autoimmune, oncological or mental diseases. Venous blood samples for immunological tests were collected from cubital vein, fasting, in BDVacutainer® tubes with K2EDTA as an anticoagulant. Erythrocytes were lysed with BD FACS™ Lysing Solution (BD Biosciences; USA) for 10-12 min at room temperature in the dark. Immunophenotyping of lymphocytes for Th17, Treg and Tact subset markers and CD39/CD73 cell surface enzymes was carried out by laser flow cytometry (Novocyte, ACEA Biosciences; USA) using monoclonal antibodies conjugated with different fluorochromes: CD4-FITC (cat. A07750, Beckman Coulter; USA), CD127-PE (cat. IM 10980U, Beckman Coulter), CD25-PC7 (cat. A52882, Beckman Coulter), CD161-PE (cat. IM 3450, Beckman Coulter), CD3-PC5 (cat. A07749, Beckman Coulter), CD39-APC-Cy7 (Clone A1, cat. RT2241130, Sony Biotechnology; USA), CD73-APC-Cy7 (Clone AD2, cat. RT2320110, Sony Biotechnology). The measurements of CD39- and CD73-expressing fractions in Treg (CD4⁺CD127^{low}CD25^{high}), Tact (CD4⁺CD25⁺CD127^{high}) and Th17 (CD4⁺CD161⁺CD3⁺) subsets were carried out using a stepwise gating procedure (Fig. 1).

Statistical processing of the data was carried out in Statistica 10.0 (StatSoft; USA). The descriptive statistics for quantitative variables are given in the median (lower and upper quartiles) — Me (Q_{0.25}-Q_{0.75}), minimum/maximum (Min/Max) format. Between-the-group differences were evaluated for significance using the nonparametric Mann-Whitney U test.

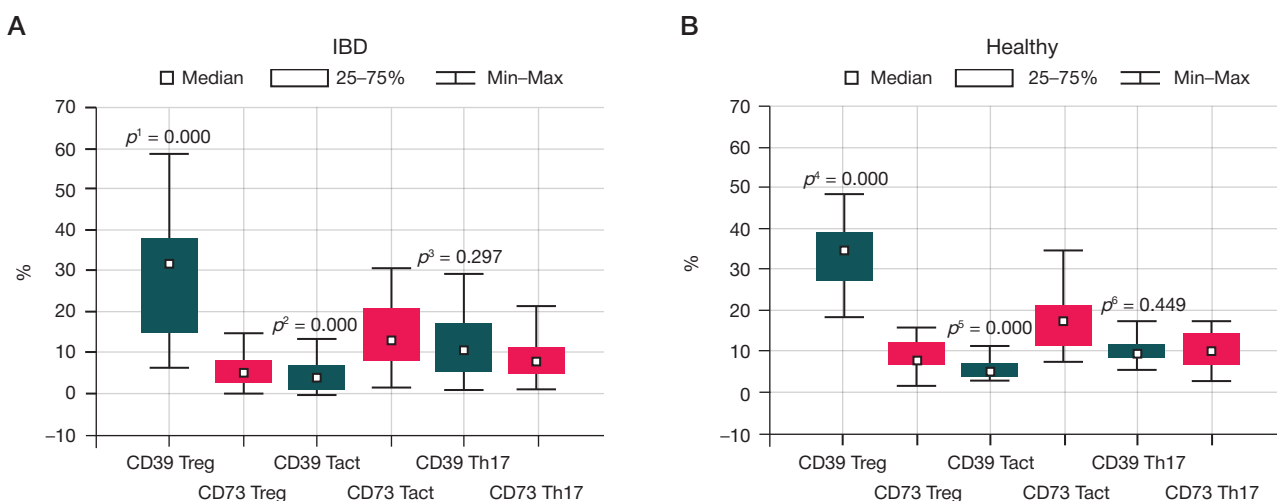


Fig. 2. Proportions of cells expressing CD39 and CD73 among CD4⁺ lymphocytes in patients with IBD and healthy individuals (comparison group). **A.** p¹ — level of significance for the difference between CD39⁺ Treg and CD73⁺ Treg; p² — level of significance for the difference between CD39⁺ Tact and CD73⁺ Tact; p³ — level of significance for the difference between CD39⁺ Th17 and CD73⁺ Th17. **B.** p⁴ — level of significance for the difference between CD39⁺ Treg and CD73⁺ Treg; p⁵ — level of significance for the difference between CD39⁺ Tact and CD73⁺ Tact; p⁶ — level of significance for the difference between CD39⁺ Th17 and CD73⁺ Th17

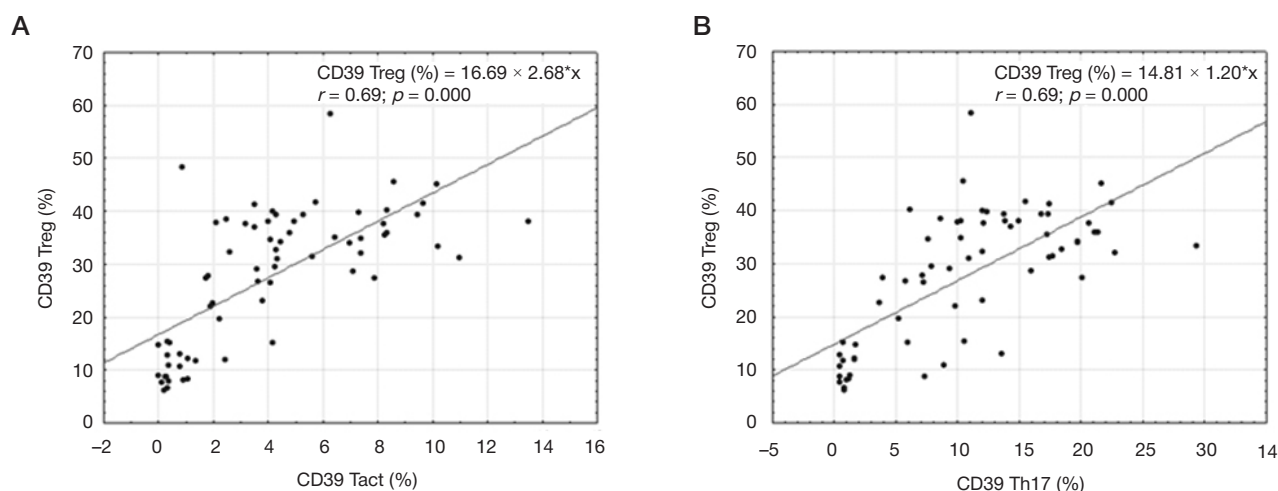


Fig. 3. Correlations of CD39+ content in Treg vs Tact and Th17 (respectively, A and B) in pediatric patients with IBD

The distributions were compared by Pearson's chi-square test (χ^2). The differences were considered statistically significant at $p < 0.05$.

RESULTS

CD39 and CD73 positivity rates in IBD vs healthy controls

The flow cytometry assay of CD39 and CD73 positivity for different subsets of CD4+ T cells in pediatric patients with IBD revealed the highest content of CD39+ cells among Treg (6–58% of Treg) and the lowest content of CD39+ cells among Tact (0–14% of Tact). By contrast, CD73 positivity was the highest in Tact (2–30% of Tact, Table 1). The comparison group showed similar subset-specific positivity ratios (Table 1).

Indeed, Treg expressed CD39 at significantly higher rates than CD73 ($p = 0.000$) and Tact expressed CD39 at significantly lower rates than CD73 ($p = 0.000$) (Fig. 2A). In Th17 lymphocytes, positivity rates for the two markers were similar (Table 1; Fig. 2B).

Patients with IBD revealed significantly reduced CD39 and CD73 positivity rates in Treg and Tact compared with the controls (Table 1). As for Th17, CD73 positivity rates were significantly reduced in IBD, whereas CD39 positivity rates in IBD and the controls were similar.

The correlation analysis revealed significant positive correlations between CD39+ Treg and CD39+ Tact ($r = 0.69$; $p = 0.000$; Fig. 3A) and CD39+ Treg and CD39+ Th17 ($r = 0.69$; $p = 0.000$; Fig. 3B) in patients with IBD. Similar trends were observed for CD73: CD73+ Treg correlated with CD73+ Tact ($r = 0.45$; $p = 0.000$) and CD73+ Treg correlated with CD73+ Th17 ($r = 0.46$; $p = 0.000$).

Table 2. Relative counts of CD39 and CD73 ectonucleotidase-expressing cells (positivity rates) in CD4+ T lymphocyte subsets of patients with Crohn's disease and ulcerative colitis at different stages and the comparison group

	CD acute	CD remission	UC acute	UC remission	Healthy children	CD	UC
Indicator	Group 1 (n = 18) Me (Q _{0.25} -Q _{0.75})	Group 2 (n = 16) Me (Q _{0.25} -Q _{0.75})	Group 3 (n = 22) Me (Q _{0.25} -Q _{0.75})	Group 4 (n = 11) Me (Q _{0.25} -Q _{0.75})	Group 5 (n = 45) Me (Q _{0.25} -Q _{0.75})	p_{12}	p_{34}
CD39 Treg, %	12.48 (8.64-22.53)	30.71 (26.62-39.56)	32.77 (14.60-39.19)	35.51 (33.91-37.70)	35 (27.8-39.4)	0	0.355
p	0	0.556	0.198	0.627			
CD73 Treg, %	3.90 (3.25-5.91)	5.87 (2.50-8.86)	4.80 (3.20-7.00)	5.45 (1.97-12.68)	8.1 (6.9-12.2)	0.606	0.836
p	0	0.022	0.001	0.072			
CD39 Tact, %	0.59 (0.30-3.20)	4.18 (2.92-7.35)	4.08 (1.36-6.05)	7.00 (2.50-8.28)	5 (4.4-7.4)	0.001	0.204
p	0	0.158	0.025	0.76			
CD73 Tact, %	11.50 (8.04-15.18)	13.07 (8.26-23.47)	13.10 (8.00-18.23)	16.28 (8.78-21.60)	17.6 (11.9-21.5)	0.423	0.585
p	0.014	0.325	0.066	0.427			
CD39 Th17, %	3.71 (0.71-12.10)	9.60 (8.54-10.3)	14.08 (1.72-17.31)	17.26 (8.60-20.64)	9.6 (8.6-12.1)	0.092	0.462
p	0.014	0.486	0.062	0.059			
CD73 Th17, %	6.30 (4.32-10.20)	8.22 (3.50-16.54)	6.50 (5.40-9.05)	8.30 (3.00-18.70)	10.2 (7.3-14.4)	0.224	0.418
p	0.008	0.489	0.002	0.569			

Note: p_{12} — levels of significance for the differences in CD39/CD73 positivity rates between groups 1 and 2; p_{34} — levels of significance for the differences in CD39/CD73 positivity rates between groups 3 and 4; p — levels of significance for the differences in CD39/CD73 positivity rates in Crohn's disease, ulcerative colitis and comparison groups; CD — Crohn's disease; UC — ulcerative colitis

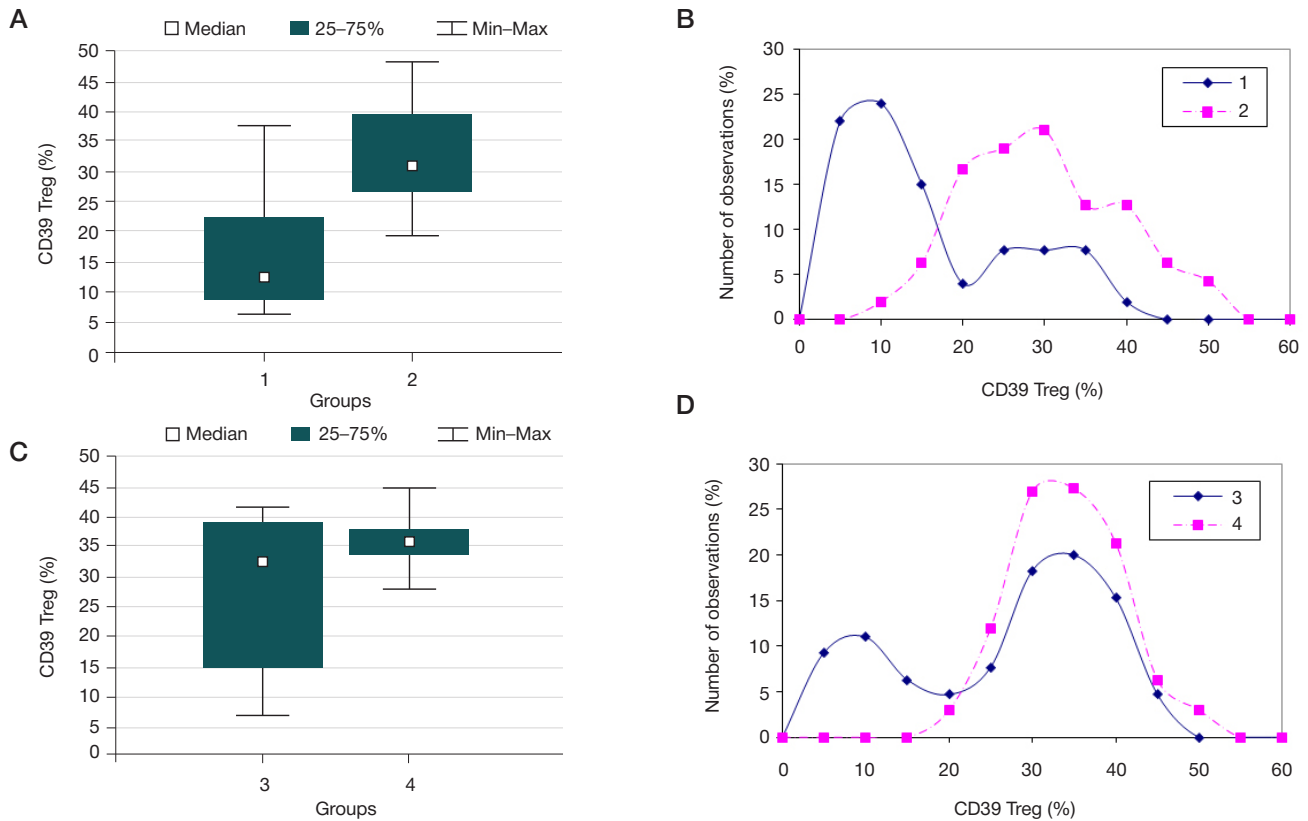


Fig. 4. CD39⁺ Treg content distributions for Crohn's disease groups 1 and 2 (respectively, A and B) and ulcerative colitis groups 3 and 4 (respectively, C and D)

The data indicate that CD39 positivity rates in Treg, Tact and Th17 in patients with IBD are age-independent. For the comparison group, we observed an inverse correlation of CD39 positivity rate in Th17 with the age ($r = -0.39$; $p = 0.009$). Of note, patients with IBD and conditionally healthy children (comparison group) were of matching age ($p = 0.435$).

By contrast, CD73 positivity rates in Th17 tended to increase with the age in patients with IBD and healthy controls similarly ($r = 0.43$; $p = 0.000$).

The time since diagnosis in patients with IBD varied widely within 5 months to 7.7 years, and the therapy lasted 2–288 weeks. We identified no correlations of CD39/CD73 positivity rates with the time lapse since diagnosis or on therapy.

CD39/CD73 expression in CD4⁺ cells in groups of children with acute IBD and remission

We further compared CD39 and CD73 positivity rates of CD4⁺ lymphocyte subpopulations in patients with Crohn's disease and ulcerative colitis acute disease (groups 1 and 3) or remission (groups 2 and 4) mutually or against the conditionally healthy children (group 5, comparison group) (Table 2). Patients with Crohn's disease revealed significantly reduced CD39 positivity rates among Treg and Tact in group 1 (acute) compared with group 2 (remission). Moreover, group 1 (Crohn's disease, acute) revealed significantly decreased CD39 and CD73 positivity rates in Treg, Tact and Th17 subsets compared with group 5 (healthy children) (Table 2). Comparison of patients with Crohn's disease in remission (group 2) and conditionally healthy children (group 5) revealed no significant differences for the studied markers apart from reduced CD73 positivity rates in Treg (Table 2).

Patients with acute ulcerative colitis (group 3) revealed significantly reduced CD39 positivity rates in Tact, as well as significantly reduced CD73 positivity rates in Treg and Th17, compared with conditionally healthy children (group 5) (Table 2).

Comparison of patients with ulcerative colitis in remission (group 4) and group 5 revealed no significant differences for the studied markers.

In addition, significant differences in CD39⁺ Treg index were revealed among patients with Crohn's disease depending on the phase (group 1 vs group 2) (Fig. 4A). The lack of corresponding differences in the same index for ulcerative colitis (group 3 vs group 4) may be related to its broad variation in these groups (Fig. 4C). The plots in Figs. 4B and 4D show the CD39⁺ Treg index distribution densities for patients with Crohn's disease (groups 1 and 2) and ulcerative colitis (groups 3 and 4), with both high and low values identified in each group. The plots reveal a clear threshold value of 20% to differentiate between the phases of Crohn's disease on the basis of CD39⁺ Treg index. Thus, 78% of group 1 had CD39⁺ Treg index within 20% (Fig. 4C), whereas in group 2 (remission) the index exceeded 20% in 82% of the patients (Fig. 4C). In the ulcerative colitis groups 3 and 4, the CD39⁺ Treg index exceeded 20% in, respectively, 67% and 100% of the cases (Fig. 4D).

DISCUSSION

A study enrolling adult healthy donors revealed a broad variation of CD39 positivity rates in Treg (2–60%) affecting the ability of these cells to hydrolyze ATP [20]. Treg cells expressing higher levels of CD39 hydrolyze ATP more efficiently. Here we show that in healthy children CD39⁺ Treg indexes vary within 19–49%. Our estimates of the content of ectonucleotidase-expressing cells among CD4⁺ lymphocyte subsets in pediatric IBD treated with TNF blockers revealed higher CD39⁺ indexes during remission consistently with published evidence [13].

Administration of anti-TNF regimens in adult patients has been previously shown to promote CD39 expression in Treg [21]. In our setting, a group of patients with Crohn's disease (acute) had significantly lower CD39⁺ Treg index compared with the

same disease in remission. A comparison between patients with Crohn's disease (acute) and ulcerative colitis (acute) revealed higher incidence of reduced CD39 expression by Treg among the former.

One study dealing with altered functional activity of CD39 in Treg in autoimmune hepatitis revealed reduced levels of ATP hydrolysis and adenosine formation [22]. By inference, a similar reduction in the ATP hydrolysis efficiency can be assumed in IBD on the basis of reduced CD39 positivity. Occasional presentation of elevated CD39⁺ Treg indexes in acute Crohn's disease can be related to modest effects of anti-TNF therapy in counteracting the disease. The increased relative counts of Tregs exhibiting CD39 ectonucleotidase on their surface under these conditions are likely to be compensatory and reflect insufficient activity of the enzyme.

Our results also indicate significantly reduced counts of supTh17 lymphocytes, endowed with immunosuppressive properties, in pediatric patients with Crohn's disease (acute) compared with conditionally healthy children. In this regard, supTh17 can be considered as a candidate sensor subset for transitions from acute disease to remission and vice versa. Of note, in children with and without IBD this population dwindles with the age. It can be assumed that the age-related decline of supTh17 contributes to increased risks of pronounced inflammatory reactions.

CD73 plays an important role in the intestinal homeostasis [23–25] and its dysfunction leads to damaging inflammatory processes in the colon as demonstrated using a knockout

mouse model [26]. Here we show a reduction in CD73 positivity rates among Treg, Tact and Th17 in children with IBD compared with conditionally healthy peers. CD73 is known to exert its enzymatic activity (AMP conversion to adenosine) as a membrane-anchored protein but also in soluble form [27]. It is possible therefore that a comprehensive assessment of the patient's condition using this marker should also involve the activity of its soluble form, which reportedly correlates with the inflammation severity [28].

CONCLUSIONS

The results indicate that the content of cells expressing CD39/CD73 ectonucleotidases among CD4⁺ cells depends on the subset (Treg, Tact or Th17) and phase of the disease (acute or remission), the latter being dependent on the success of anti-TNF therapy. Most of the children in remission present with high numbers of CD4⁺ lymphocytes expressing ectonucleotidase, which helps reducing the inflammation by converting ATP to adenosine. At the same time, high content of CD39-expressing cells among the studied subsets may also accompany the acute stage of the disease, which is probably related to diverse activities of the enzyme. We believe that further elucidation of the functional activity of CD39 and CD73 ectonucleotidases complemented by other quantitative indicators can be informative for understanding and predicting the efficacy of anti-TNF regimens in IBD.

References

- Burisch J, Pedersen N, Cukovic-Cavka S, et al. East-West gradient in the incidence of inflammatory bowel disease in Europe: the ECCOEpiCom inception cohort. *Gut*. 2014; 63 (4): 588–97.
- Benchimol EI, Guttman A, Griffiths AM, et al. Increasing incidence of paediatric inflammatory bowel disease in Ontario, Canada: evidence from health administrative data. *Gut*. 2009; 58: 1490–7.
- Papamichael K, Gils A, Rutgeerts P, Levesque BG, Vermeire S, Sandborn WJ, et al. Role for therapeutic drug monitoring during induction therapy with TNF antagonists in IBD: evolution in the definition and management of primary nonresponse. *Inflamm. Bowel Dis*. 2015; 21: 182–97.
- Kniazev OV, Shkurko TV, Kagrananova AV, Veselov AV, Nikonov EL. Epidemiology of inflammatory bowel disease. State of the problem (review). *Russian Journal of Evidence-Based Gastroenterology*. 2020; 9 (2): 66–73. Russian.
- Yan JB, Luo MM, Chen ZY, He BH. The function and role of the Th17/Treg cell balance in Inflammatory bowel disease. *J Immunol Res*. 2020; 2020: 8813558. DOI: 10.1155/2020/8813558.
- Petrichuk SV, Miroshkina LV, Semikina EL, Toptygina AP, Potapov AS, Tsimbalova EG, et al. Indicators of the lymphocyte subsets as efficiency predictors of therapy with inhibitors of TNF α in children with inflammatory bowel disease. *Medical Immunology*. 2018; 20 (5): 721–30. <https://doi.org/10.15789/1563-0625-2018-5-721-730>. Russian.
- Bettelli E, Carrier Y, Gao W, Korn T, Strom T. B, Oukka M, et al. Reciprocal developmental pathways for the generation of pathogenic effector TH17 and regulatory T cells. *Nature*. 2006; 441 (7090): 235–8.
- Lee GR. The balance of Th17 versus Treg cells in autoimmunity. *Int J Mol Sci*. 2018. 19: 730. Available from: <https://doi.org/10.3390/ijms19030730>.
- Burnstock G. Purinergic nerves. *Pharmacological Reviews*. 1972; 24 (3): 509–81.
- Kukulski F, et al. Impact of ectoenzymes on p2 and p1 receptor signaling. *Adv Pharmacol*. 2011; 61: 263–99. PubMed: 21586362.
- Virgilio FD, Sarti AC, Silva RC. Purinergic signaling, DAMPs, and inflammation. *American Journal of Physiology-Cell Physiology*. 2020; 318 (5): 832–5. Available from: <https://doi.org/10.1152/ajpcell.00053.2020>.
- Faas MM, Sáez T, de Vos P. Extracellular ATP and adenosine: the yin and yang in immune responses? *Mol Aspects Med*. 2017; 55: 9–19. DOI: 10.1016/j.mam.2017.01.002.
- Vuerich M, Mukherjee S, Robson SC, Longhi MS. Control of gut inflammation by modulation of purinergic signaling. *Front Immunol*. 2020; 11: 1882. DOI: 10.3389/fimmu.2020.01882.
- Gibson DJ, Elliott L, McDermott E, Tosetto M, Keegan D, Byrne K, et al. Heightened expression of CD39 by regulatory T lymphocytes is associated with therapeutic remission in Inflammatory Bowel Disease. *Inflamm Bowel Dis*. 2015; 21: 2806–14.
- Friedman DJ, Kunzli BM, A-Rahim YI, Sevigny J, Berberat PO, Enyoji K, et al. From the cover: CD39 deletion exacerbates experimental murine colitis and human polymorphisms increase susceptibility to inflammatory bowel disease. *Proc Natl Acad Sci USA*. 2009; 106: 16788–93.
- Zeng J, Ning Z, Wang Y, Xiong H. Implications of CD39 in immune-related diseases. *Int Immunopharmacol*. 2020; 89 (Pt A): 107055. DOI: 10.1016/j.intimp.2020.107055.
- Fletcher JM, Lonergan R, Costelloe L, Kinsella K, Moran B, O'Farrelly C, et al. CD39Foxp3 regulatory T Cells suppress pathogenic Th17 cells and are impaired in multiple sclerosis. *The Journal of Immunology*. 2009; 183: 7602–10.
- Longhi MS, Moss A, Bai A, Wu Y, Huang H, Cheifetz A, et al. Characterization of human CD39⁺ Th17 cells with suppressor activity and modulation in inflammatory bowel disease. *PLoS ONE*. 2014; 9: e87956. DOI: 10.1371/journal.pone.0087956.
- Fernández D, Flores-Santibáñez F, Neira J, Osorio-Barrios F, Tejón G, Nuñez S, et al. Purinergic signaling as a regulator of Th17 cell plasticity. *PLoS ONE*. 2016; 11: e0157889. DOI: 10.1371/journal.pone.0157889.
- Borsellino G, Kleinewietfeld M, Di Mitri D, Sternjak A, Diamantini A, Giometto R, et al. Expression of ectonucleotidase CD39 by Foxp3⁺-Treg cells: Hydrolysis of extracellular ATP and immune suppression. *Blood*. 2007; 110 (4): 1225–32.
- Gibson DJ, Elliott L, McDermott E, Tosetto M, Keegan D, Byrne K, et al. Heightened expression of CD39 by regulatory T lymphocytes

- is associated with therapeutic remission in inflammatory bowel disease. *Inflamm Bowel Dis.* 2015; 21: 2806–14. DOI: 10.1097/MIB.0000000000000566.
22. Grant Ch R, Liberal R, Holder BS, Cardone J, Ma Y, Robson SC, et al. Dysfunctional CD39(POS) regulatory T cells and aberrant control of T-helper type 17 cells in autoimmune hepatitis. *Hepatology.* 2014; 59 (3): 1007–15. DOI: 10.1002/hep.26583.
 23. Louis NA, Robinson AM, MacManus CF, Karhausen J, Scully M, Colgan SP. Control of IFN-alphaA by CD73: implications for mucosal inflammation. *J Immunol.* 2000; 180: 4246–55. DOI: 10.4049/jimmunol.180.6.4246.
 24. Sotnikov I, Louis NA. CD73-dependent regulation of interferon alpha and interleukin-10 in the inflamed mucosa. *Sci World J.* 2010; 10: 2167–80. DOI: 10.1100/tsw.2010.203
 25. Colgan SP, Eitzschig HK, Eckle T, Thompson LF. Physiological roles for ecto-5'-nucleotidase (CD73). *Purinergic Signal.* 2006; 351–60. DOI: 10.1007/s11302-005-5302-5.
 26. Bynoe MS, Waickman AT, Mahamed DA, Mueller C, Mills JH, Czopik A. CD73 is critical for the resolution of murine colonic inflammation. *BioMed Research International.* 2012, Article ID 260983, 13 pages, 2012. Available from: <https://doi.org/10.1155/2012/260983>.
 27. Schneider E, Rissiek A, Winzer R, Puig B, Rissiek B, Haag F, et al. Generation and function of non-cell-bound CD73 in inflammation. *Frontiers in Immunology.* 2019; 10, article 1729. DOI: 10.3389/fimmu.2019.01729.
 28. Maksimow M, Lea K, Nieminen A, Kylänpää L, Aalto K, et al. Early prediction of persistent organ failure by soluble CD73 in patients with acute pancreatitis. *Critical Care Medicine.* 2014; 42 (12): 2556–64. DOI: 10.1097/CCM.0000000000000550.

Литература

1. Burisch J, Pedersen N, Cukovic-Cavka S, et al. East-West gradient in the incidence of inflammatory bowel disease in Europe: the ECCO-EpiCom inception cohort. *Gut.* 2014; 63 (4): 588–97.
2. Benchimol El, Guttman A, Griffiths AM, et al. Increasing incidence of paediatric inflammatory bowel disease in Ontario, Canada: evidence from health administrative data. *Gut.* 2009; 58: 1490–7.
3. Papamichael K, Gils A, Rutgeerts P, Levesque BG, Vermeire S, Sandborn WJ, et al. Role for therapeutic drug monitoring during induction therapy with TNF antagonists in IBD: evolution in the definition and management of primary nonresponse. *Inflamm. Bowel Dis.* 2015; 21: 182–97.
4. Князев О. В., Шкурко Т. В., Каграманова А. В., Веселов А. В., Никонов Е. Л. Эпидемиология воспалительных заболеваний кишечника. Современное состояние проблемы. Докладная гастроэнтерология. 2020; 9 (2): 66–73. Доступно по ссылке: <https://doi.org/10.17116/dokgastro2020902166>.
5. Yan JB, Luo MM, Chen ZY, He BH. The function and role of the Th17/Treg cell balance in inflammatory bowel disease. *J Immunol Res.* 2020; 2020: 8813558. DOI: 10.1155/2020/8813558.
6. Петричук С. В., Мирошкина Л. В., Семкина Е. Л., Топтыгина А. П., Потапов А. С., Цимбалова Е. Г. и др. Показатели популяционного состава лимфоцитов как предикторы эффективности терапии ингибитором TNF α у детей с воспалительными заболеваниями кишечника. Медицинская иммунология. 2018; 20 (5): 721–30. Доступно по ссылке: <https://doi.org/10.15789/1563-0625-2018-5-721-730>.
7. Bettelli E, Carrier Y, Gao W, Korn T, Strom T. B, Oukka M, et al. Reciprocal developmental pathways for the generation of pathogenic effector TH17 and regulatory T cells. *Nature.* 2006; 441 (7090): 235–8.
8. Lee GR. The balance of Th17 versus Treg cells in autoimmunity. *Int J Mol Sci.* 2018. 19: 730. Available from: <https://doi.org/10.3390/ijms19030730>.
9. Burnstock G. Purinergic nerves. *Pharmacological Reviews.* 1972; 24 (3): 509–81.
10. Kukulski F, et al. Impact of ectoenzymes on p2 and p1 receptor signaling. *Adv Pharmacol.* 2011; 61: 263–99. PubMed: 21586362.
11. Virgilio FD, Sarti AC, Silva RC. Purinergic signaling, DAMPs, and inflammation. *American Journal of Physiology-Cell Physiology.* 2020; 318 (5): 832–5. Available from: <https://doi.org/10.1152/ajpcell.00053.2020>.
12. Faas MM, Sáez T, de Vos P. Extracellular ATP and adenosine: the yin and yang in immune responses? *Mol Aspects Med.* 2017; 55: 9–19. DOI: 10.1016/j.mam.2017.01.002.
13. Vuerich M, Mukherjee S, Robson SC, Longhi MS. Control of gut inflammation by modulation of purinergic signaling. *Front Immunol.* 2020; 11: 1882. DOI: 10.3389/fimmu.2020.01882.
14. Gibson DJ, Elliott L, McDermott E, Tosetto M, Keegan D, Byrne K, et al. Heightened expression of CD39 by regulatory T lymphocytes is associated with therapeutic remission in Inflammatory Bowel Disease. *Inflamm Bowel Dis.* 2015; 21: 2806–14.
15. Friedman DJ, Kunzli BM, A-Rahim YI, Sevigny J, Berberat PO, Enjyoji K, et al. From the cover: CD39 deletion exacerbates experimental murine colitis and human polymorphisms increase susceptibility to inflammatory bowel disease. *Proc Natl Acad Sci USA.* 2009; 106: 16788–93.
16. Zeng J, Ning Z, Wang Y, Xiong H. Implications of CD39 in immune-related diseases. *Int Immunopharmacol.* 2020; 89 (Pt A): 107055. DOI: 10.1016/j.intimp.2020.107055.
17. Fletcher JM, Lonergan R, Costelloe L, Kinsella K, Moran B, O'Farrelly C, et al. CD39/Foxp3 regulatory T Cells suppress pathogenic Th17 cells and are impaired in multiple sclerosis. *The Journal of Immunology.* 2009; 183: 7602–10.
18. Longhi MS, Moss A, Bai A, Wu Y, Huang H, Cheifetz A, et al. Characterization of human CD39+ Th17 cells with suppressor activity and modulation in inflammatory bowel disease. *PLoS ONE.* 2014; 9: e87956. DOI: 10.1371/journal.pone.0087956.
19. Fernández D, Flores-Santibáñez F, Neira J, Osorio-Barrios F, Tejón G, Nuñez S, et al. Purinergic signaling as a regulator of Th17 cell plasticity. *PLoS ONE.* 2016; 11: e0157889. DOI: 10.1371/journal.pone.0157889.
20. Borsellino G, Kleinewietfeld M, Di Mitri D, Sternjak A, Diamantini A, Giometto R, et al. Expression of ectonucleotidase CD39 by Foxp3+Treg cells: Hydrolysis of extracellular ATP and immune suppression. *Blood.* 2007; 110 (4): 1225–32.
21. Gibson DJ, Elliott L, McDermott E, Tosetto M, Keegan D, Byrne K, et al. Heightened expression of CD39 by regulatory T lymphocytes is associated with therapeutic remission in inflammatory bowel disease. *Inflamm Bowel Dis.* 2015; 21: 2806–14. DOI: 10.1097/MIB.0000000000000566.
22. Grant Ch R, Liberal R, Holder BS, Cardone J, Ma Y, Robson SC, et al. Dysfunctional CD39(POS) regulatory T cells and aberrant control of T-helper type 17 cells in autoimmune hepatitis. *Hepatology.* 2014; 59 (3): 1007–15. DOI: 10.1002/hep.26583.
23. Louis NA, Robinson AM, MacManus CF, Karhausen J, Scully M, Colgan SP. Control of IFN-alphaA by CD73: implications for mucosal inflammation. *J Immunol.* 2000; 180: 4246–55. DOI: 10.4049/jimmunol.180.6.4246.
24. Sotnikov I, Louis NA. CD73-dependent regulation of interferon alpha and interleukin-10 in the inflamed mucosa. *Sci World J.* 2010; 10: 2167–80. DOI: 10.1100/tsw.2010.203
25. Colgan SP, Eitzschig HK, Eckle T, Thompson LF. Physiological roles for ecto-5'-nucleotidase (CD73). *Purinergic Signal.* 2006; 351–60. DOI: 10.1007/s11302-005-5302-5.
26. Bynoe MS, Waickman AT, Mahamed DA, Mueller C, Mills JH, Czopik A. CD73 is critical for the resolution of murine colonic inflammation. *BioMed Research International.* 2012, Article ID 260983, 13 pages, 2012. Available from: <https://doi.org/10.1155/2012/260983>.
27. Schneider E, Rissiek A, Winzer R, Puig B, Rissiek B, Haag F, et al. Generation and function of non-cell-bound CD73 in inflammation. *Frontiers in Immunology.* 2019; 10, article 1729. DOI: 10.3389/fimmu.2019.01729.
28. Maksimow M, Lea K, Nieminen A, Kylänpää L, Aalto K, et al. Early prediction of persistent organ failure by soluble CD73 in patients with acute pancreatitis. *Critical Care Medicine.* 2014; 42 (12): 2556–64. DOI: 10.1097/CCM.0000000000000550.

ANDROGEN LEVELS IN BLOOD AND FOLLICULAR FLUID OF IVF PATIENTS WITH DIMINISHED OVARIAN RESERVE

Gavisova AA [✉], Shevtsova MA, Kindysheva SV, Starodubtseva NL, Frankevich VE, Nazarenko TA, Dolgushina NV

Kulakov national medical research center for obstetrics, gynecology and perinatology, Moscow, Russia

Androgen concentrations in follicular fluid samples collected from patients undergoing in vitro fertilization (IVF) may provide useful clinical indicators. This study aimed to analyze possible associations of the androgen levels in follicular fluid and blood plasma in patients with diminished ovarian reserve (POR) in IVF programs. Cross-sectional study with a parallel group design, conducted in 2019–2021, enrolled 300 patients with infertility, aged 18–42 years, applying for assisted reproduction involving IVF/intracytoplasmic sperm injection and embryo transfer. The androgen profiles of blood plasma and follicular fluid were determined by liquid chromatography with tandem mass spectrometry (LC-MS/MS). Androgen concentrations in blood plasma and follicular fluid, particularly those of dehydroepiandrosterone (DHEA-S), androstenedione and total testosterone, significantly correlated. The results implicate androgen levels in blood plasma and follicular fluid as early markers of POR in patients with infertility.

Keywords: androgens, androgen deficiency, testosterone, dehydroepiandrosterone, androstenedione, reproductive age, infertility, assisted reproductive technologies, LC-MS/MS, follicular fluid

Author contribution: Gavisova AA, Dolgushina NV — study concept and design; Gavisova AA, Shevtsova MA — analysis, manuscript writing; Kindysheva SV — laboratory tests, statistical analysis; Starodubtseva NL, Nazarenko TA, Frankevich VE, Dolgushina NV — manuscript editing.

Compliance with ethical standards: the study was approved by the ethical review board at the Kulakov National Medical Research Center for Obstetrics, Gynecology and Perinatology (protocol № 140 of 15 December 2014). The informed consent was submitted by all study participants.

✉ **Correspondence should be addressed:** Alla A. Gavisova
Akademika Oparina, 4, Moscow, 117997; gaviialla@ya.ru

Received: 29.07.2022 **Accepted:** 13.08.2022 **Published online:** 19.08.2022

DOI: 10.24075/brsmu.2022.041

УРОВЕНЬ АНДРОГЕНОВ В КРОВИ И Фолликулярной жидкости у женщин с бесплодием и сниженным овариальным резервом в программах ВРТ

А. А. Гависова [✉], М. А. Шевцова, С. В. Киндышева, Н. Л. Стародубцева, В. Е. Франкевич, Т. А. Назаренко, Н. В. Долгушина

Национальный медицинский исследовательский центр акушерства, гинекологии и перинатологии имени В. И. Кулакова, Москва, Россия

Концентрация андрогенов в образцах фолликулярной жидкости у пациенток в программах вспомогательных репродуктивных технологий (ВРТ) может быть связана с процессами оогенеза и эмбриогенеза. Целью исследования было проанализировать связь уровня андрогенов в плазме крови и фолликулярной жидкости у пациенток с бесплодием и сниженным овариальным резервом яичников в программах ВРТ. Проведено одномоментное исследование в параллельных группах 300 пациенток 18–42 лет с бесплодием с 2019 по 2021 гг., обратившихся для проведения программы ЭКО/ИКСИ и ПЭ. Определяли андрогенный профиль в плазме крови и фолликулярной жидкости методом масс-спектрометрии жидкостной хроматографии и тандемной масс-спектрометрии (ВЭЖХ-МС/МС). Полученные результаты показали, что андрогены в плазме крови и фолликулярной жидкости, а именно уровни ДГЭА-С, андростендиона и общего тестостерона, могут быть ранними маркерами снижения овариального резерва (СОР) у женщин с бесплодием. Статистически значимая корреляционная связь между уровнями андрогенов в крови и фолликулярной жидкости свидетельствует об их вкладе в формирование снижения овариального резерва. Таким образом, при сниженном овариальном резерве выявлено снижение концентрации андрогенов в плазме крови и в фолликулярной жидкости, что свидетельствует о роли андрогенов в процессах фолликулогенеза, таких как тестостерон и андростендион.

Ключевые слова: андрогены, андрогенный дефицит, тестостерон, дегидроэпиандростерон, андростендион, репродуктивный возраст, бесплодие, ВРТ, ВЭЖХ-МС/МС, фолликулярная жидкость

Вклад авторов: А. А. Гависова, Н. В. Долгушина — концепция и дизайн исследования; А. А. Гависова, М. А. Шевцова — сбор и обработка материала, обзор литературы, написание статьи; С. В. Киндышева — лабораторная постановка и статистическая обработка материала; Н. Л. Стародубцева В. Е. Франкевич, Т. А. Назаренко, Н. В. Долгушина — редактирование.

Соблюдение этических стандартов: исследование одобрено этическим комитетом ФГБУ «НМИЦ Акушерства гинекологии и перинатологии им. В. И. Кулакова» (протокол № 2 от 07 февраля 2019 г.); все участники подписали добровольное информированное согласие на участие в исследовании.

✉ **Для корреспонденции:** Алла Анатольевна Гависова
ул. Академика Опарина, д. 4, г. Москва, 117997; gaviialla@ya.ru

Статья получена: 29.07.2022 **Статья принята к печати:** 13.08.2022 **Опубликована онлайн:** 19.08.2022

DOI: 10.24075/vrgmu.2022.041

Poor ovarian reserve (POR) in patients with infertility has been associated with low rates of success in the assisted reproductive technology (ART) programs. The age-dependent and/or POR-related declines in androgen levels indirectly suggest their special relevance to folliculogenesis and successful ART outcomes.

Despite the overall diversity of androgens, only two of them, testosterone and dihydrotestosterone, exert high biological activity. The relationship between systemic and local androgen levels (as measured in plasma and follicular fluid, respectively)

is an up-to-date prognostic factor of success in ART programs, especially in patients with DOR. Still, it is not clear which androgen and in which biological medium can be the highest prognostic value with regard to reproductive success in patients with DOR.

The role of follicular fluid (FF) as a biological medium surrounding the oocyte, participating in metabolic processes within the follicle, and ultimately the medium for the conclusive steps in oogenesis, is a major focus of clinical research on both hypo- and hyperandrogenic conditions [1–3]. The

endocrine environment, particularly the anti-Müllerian hormone concentration (AMH), in FF has been associated with the yields of mature follicles and implantation potential of the embryos [4–6]. These biological phenomena depend on complex dynamic interactions between the oocyte and its microenvironment composed of FF and other structural components of the follicle.

At an advanced reproductive age, serum levels of both AMH and testosterone decrease concomitantly with the decline in folliculogenesis [7]. Several studies addressed hormonal profiles in blood serum and FF with regard to patient's age in natural IVF cycles. A decrease in FF testosterone levels was observed in patients aged 40–45 years compared with 20–25-year-olds [8].

Comparative measurements of testosterone in serum and FF may have certain diagnostic value as well. For instance, the age-related decrease in serum testosterone levels can be unaccompanied by a similar decrease in FF testosterone levels specifically in patients with poor response in natural cycle [9]. Obviously, more comprehensive efforts are needed to validate the possible correlation of endocrine status between blood and FF for clinical significance in patients with infertility and POR.

Previous studies used immunochemical methods to measure steroid levels in FF. Such methods have a major disadvantage of low specificity due to the cross-reactions with structurally related compounds [10–12]. The methods of liquid chromatography (LC) and mass-spectrometry (MS) are more specific [13] and allow simultaneous quantitative measurements of several steroids [14, 15].

This study aimed to assess for possible correlations of blood and FF androgen levels with POR in IVF programs.

METHODS

The cross-sectional study with a parallel group design enrolled 300 reproductive age patients with infertility, aged 18–42 years, applying for ART program at FSBI «National Medical Research Medical Center For Obstetrics, Gynecology and Perinatology named after Academician V. I. Kulakov» Ministry Of Healthcare of the Russian Federation in 2019–2021. Blood samples were collected from all patients on day 2–3 of menstrual cycle. Inclusion criteria: age 18–42 years; a history of infertility; written informed consent for the study. Exclusion criteria: surgical menopause; hysterectomy; adrenal failure; hormone-producing tumors; obesity (BMI ≥ 30 kg/m²); body mass deficiency (BMI ≤ 18 kg/m²); AIDS and other immunodeficiency,

immunoinflammatory rheumatic diseases, immunomodulatory therapy, glucocorticoids, oncological diseases.

The patients were assigned into groups depending on age: group 1 — 149 young reproductive age (18–35 year-olds), group 2 — 151 patients of advanced reproductive age (35–42 year-olds).

In accordance with the Patient-Oriented Strategies Encompassing Individualized Oocyte Number (POSEIDON) the patients were assigned into subgroups depending on ovarian reserve: subgroup 0 — normal ovarian reserve (76 early reproductive age pts and 69 advanced reproductive age pts; anti-Müllerian hormone (AMH) ≥ 1.2 ng/mL, antral follicle count (AFC) ≥ 5), subgroup 1 — POR (73 young reproductive age pts and 82 advanced reproductive age pts; AMH < 1.2 ng/mL, AFC < 5). The block-scheme is given in Fig. 1.

Individual histories collected for the study included age; mother's age at menopause; a history of internal genital surgeries/traumas; a history of inflammations/infections genital diseases; a history of endometriosis/adhesive diseases; a history of IVF cycles (number); obstetric anamnesis.

Folliculogenesis was monitored by ultrasound scans. The IVF program was carried out in accordance with the standard, using a gonadotropin-releasing hormone (GnRH) antagonist-based protocol with urinary or recombinant gonadotropins, or a combination of both, as inducers of folliculogenesis. The daily doses of gonadotropins were determined individually depending on the ovarian reserve status, but not less than 225 IU a day; human chorionic gonadotropin was used as an ovulation trigger. Biological samples (blood, follicular fluid from the first follicle) were collected upon transvaginal ovarian puncture.

Concentrations of hormones (testosterone, dehydroepiandrosterone (DHEA), dehydroepiandrosterone-sulfate (DHEA-S), androstenedione, dihydrotestosterone, progesterone, hydroxyprogesterone, pregnenolone, hydroxypregnenolone and cortisol) were quantified by tandem mass-spectrometry using Steroid Hormones in Serum LC-MS/MS Analysis Kit (JASEM; Türkiye) as analytical standards. The kit contained four calibrating mixtures of 16 steroid hormones, two-level quality control samples and internal standards. The mobile phases A and B contained 0.01% formic acid in Milli-Q water and acetonitrile, respectively. Methyl tert-butyl ether (MTBE, $\geq 99.5\%$, HPLC grade, Fisher Chemical; USA), methanol (99.9%, HPLC Basic, Scharlau; Spain), acetonitrile (99.9%, HPLC Gradient grade, Fisher Chemical; USA) and formic acid

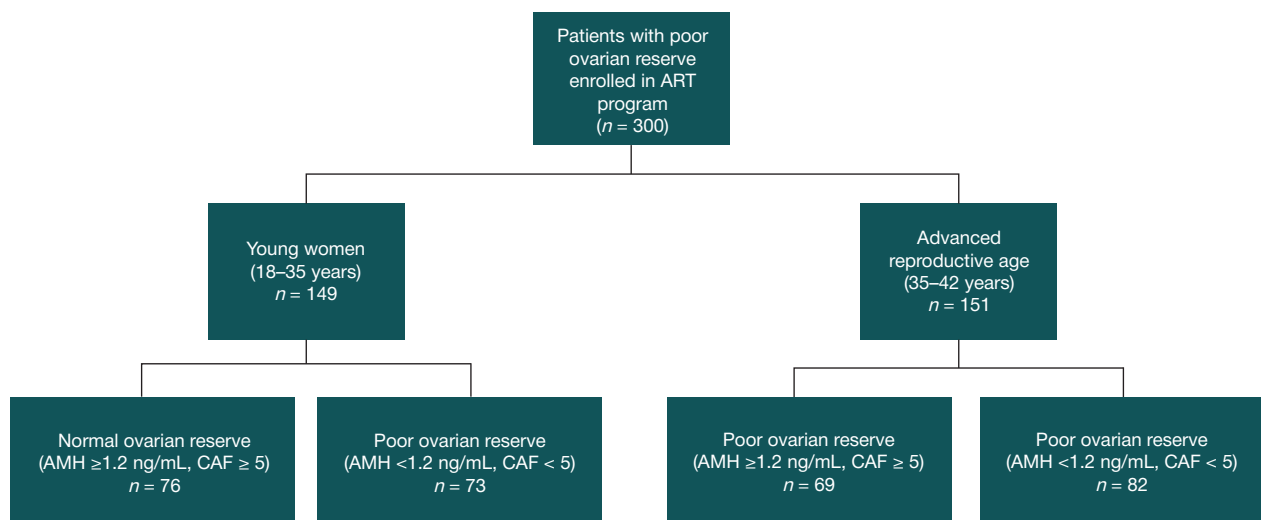


Fig. 1. Block-scheme of the study

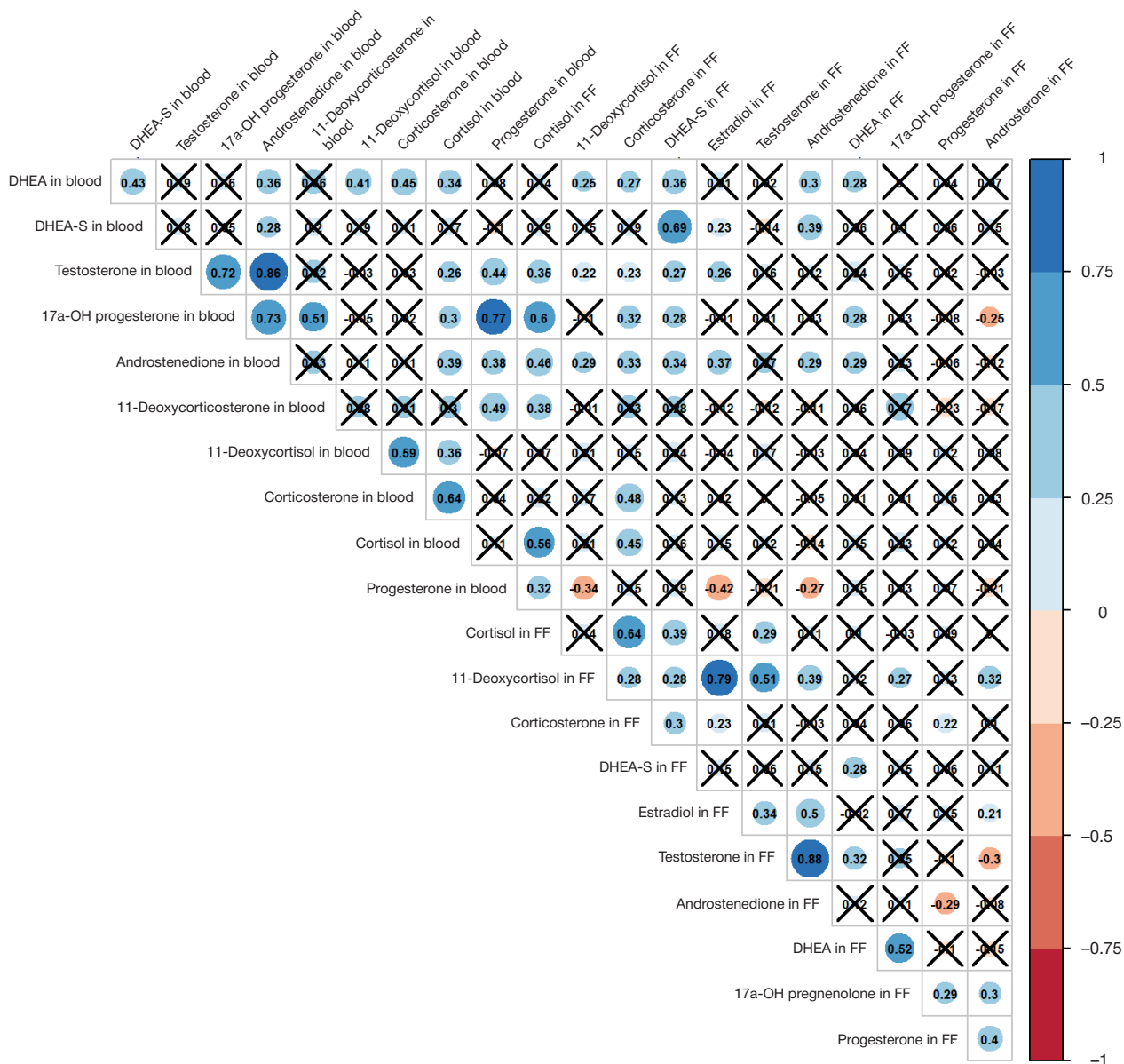


Fig. 2. Correlation coefficients for hormone concentrations in plasma vs follicular fluid as measured by LC-MS/MS in patients with infertility and diminished ovarian reserve

(98%, Sigma-Aldrich; USA) were used in phase preparation and sample preparation procedures. The hormones were separated in a 100 mm Poroshel 120 EC-C18 column (Agilent; USA) with 2.1 mm inner diameter and 2.7 μm particle size.

During the sample preparation procedure, a mixture of 460 μL sample with 25 μL internal standard was double-extracted with 1 mL MTBE followed by retrieval of the supernatant (800 μL) in a clean Eppendorf tube for drying under flowing nitrogen gas at 50 °C. The dry residue was dissolved in 100 μL of 50% MeOH and transferred into a vial with an insert for LC-MS/MS measurements.

The samples were run in a LC-MS/MS system consisting of an AB Sciex QTRAP 5500 quadrupole mass-spectrometry detector with an electrospray ionization source and an Agilent 1260 Infinity liquid chromatograph (Agilent; USA) equipped with a high-pressure pump, column thermostat and an automated sampling unit for 108 vials.

Statistical analysis

Statistical analysis was carried out using scripts in R [16]. Correlation analysis was used to determine a possible

relationship between variables. Statistical significance of correlations for analytical measurements was assessed using a nonparametric Spearman's test. In cases of missing numerical values, the correlation coefficient was calculated for all available complete pairs of measurements for each pair of variables individually. Statistical significance of correlations for the questionnaire data was assessed by nonparametric Kendall's test. The quantitative data were described by medians (Me) with lower and upper quartiles in a Me (Q₁; Q₃) format.

RESULTS

The mean age of participants was 37.3 ± 2.4 years. The body mass index (BMI) tended to increase with age: in advanced reproductive age patients with POR, it reached 24.6 ± 5.4 though remained statistically similar to BMI in other groups.

The reproductive histories typically included unsuccessful IVF cycles/cryo protocols, which ended in a negative result at the stage of hormone pregnancy test. The infertility duration increased significantly with age and ovarian reserve decrease, amounting to 7.2 ± 2.4 years in the group of advanced reproductive age patients with POR, 65.4% of whom had

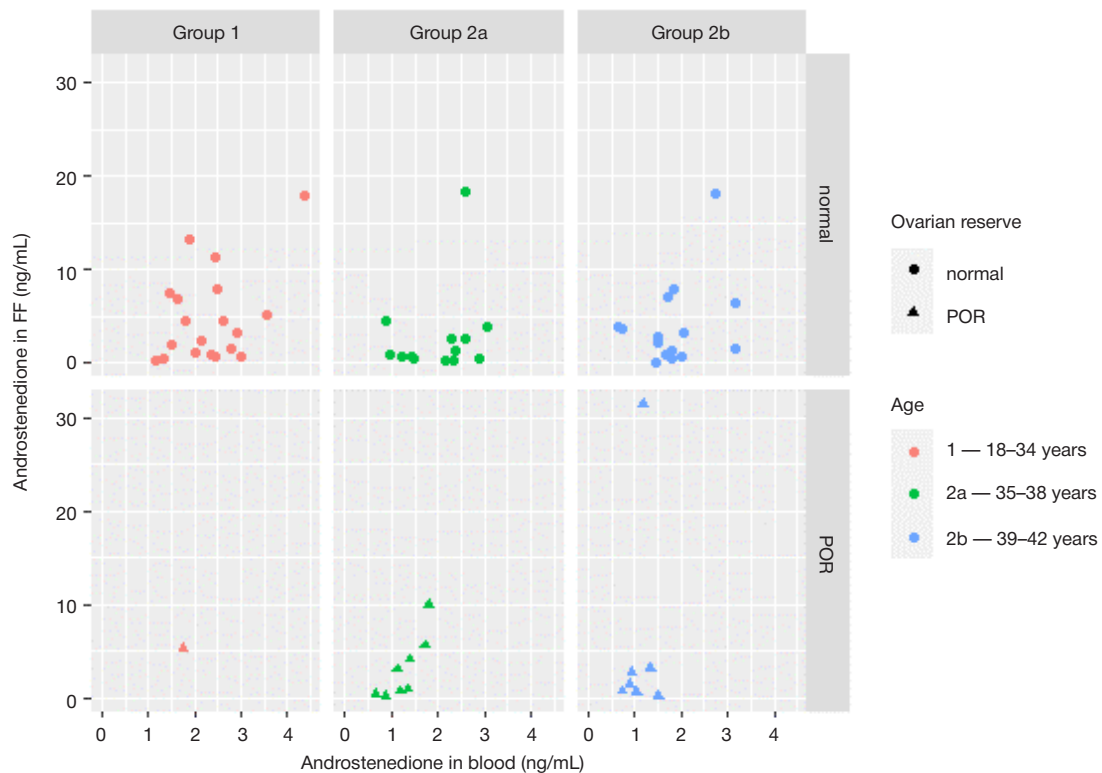


Fig. 3. The concentrations of androstenedione in follicular fluid (FF) and blood plasma per groups: younger than 35 years (group 1), aged 35–38 years (group 2a) and older than 39 years (group 2b), with ovarian reserves diminished (subgroup 1) or normal (subgroup 0)

primary infertility. The ART cycle number showed a similar tendency amounting to 2.3 ± 0.9 in the advanced reproductive age patients with POR.

The analytical data on hormone concentrations in blood plasma and follicular fluid collected on the day of oocyte aspiration were subject to correlation analysis. For many of the studied hormones (DHEA-S, total testosterone, 17-OH progesterone, androstenedione), concentrations in plasma and follicular fluid correlated (Fig. 2). Blood vs FF levels of the same hormone revealed weak association for androstenedione (correlation coefficient 0.29) and moderate association for DHEA-S (correlation coefficient 0.69). Strong correlations between androstenedione and testosterone levels in blood (correlation coefficient 0.86) and FF (correlation coefficient 0.88) confirm the pathogenetic link between POR and androgen levels as dependent\connected factors of folliculogenesis.

Concentrations of androstenedione and DHEA-S in blood and FF were comparatively analyzed in patients of different age groups with regard to ovarian reserve. For a detailed assessment of age-dependent dynamics in ovarian function by measuring DHEA-S and androstenedione in blood and FF, patients of group 2 (35–42 years) were stratified as 35–38-year-olds (subgroup 2a) and 39–42-year-olds (subgroup 2b).

Comparative analysis of blood and FF concentrations revealed a POR-related decrease for androstenedione (Fig. 3) and DHEA-S (Fig. 4) in both biological media. A strong agreement between blood and FF levels of DHEA-S across the groups (Fig. 5) adds to its prospective clinical value as a marker of androgenic activity and androstenedione precursor.

DISCUSSION

This study involved comparative measurement of androgens as estrogen precursors using the sensitive and highly specific LC-MS/MS method [9, 15] in blood and FF samples collected during IVF cycles. The results indicate significant association

of POR with 'ovarian androgen deficiency' defined as selective decrease in androgen output from thecal cells. Such effects can be regarded as early signs of the age-related androgen deficiency. We also revealed a correlation between androgen levels in blood and FF, the latter being the essential medium for oocyte growth and maturation. A decrease in concentration of androstenedione as a precursor for testosterone in FF was significant, as well as a similar decrease for DHEA-S as a precursor for androstenedione and a marker of androgenic activity in FF. Moreover, FF concentrations positively correlated with blood levels for each of these hormones.

The known ovarian reserve markers, notably AMH and AFC, often misrepresent the real clinical picture and embryological parameters in both early and late reproductive age patients. These markers only loosely correlate with the mature oocyte numbers, fertilization efficacy and blastulation frequency [15, 17, 18], as well as with androgen levels and their receptor concentrations and activities. FF, which constitutes the microenvironment for oocyte growth and maturation, becomes available as a biological sample during follicular puncture in IVF programs. FF provides a useful substrate for biochemical tests gaining information on the course of oogenesis.

For instance, in patients with polycystic ovarian syndrome (PCOS) have higher testosterone concentrations in mature follicles compared to women with normal ovarian reserve, whereas ovarian stimulation in such patients only slightly enhances the FF testosterone levels, as compared with natural cycles [10].

In a prospective cohort study of endogenous steroid concentrations determined by liquid chromatography and mass spectrometry in the follicular fluid, a significant androgen in the follicular fluid was identified, which was androstenedione [9].

In one study, focusing on intrafollicular concentrations of estradiol, progesterone, 17-hydroxyprogesterone, androstenedione and testosterone during periovulatory period, FF was collected on the day of the ovulation trigger injection

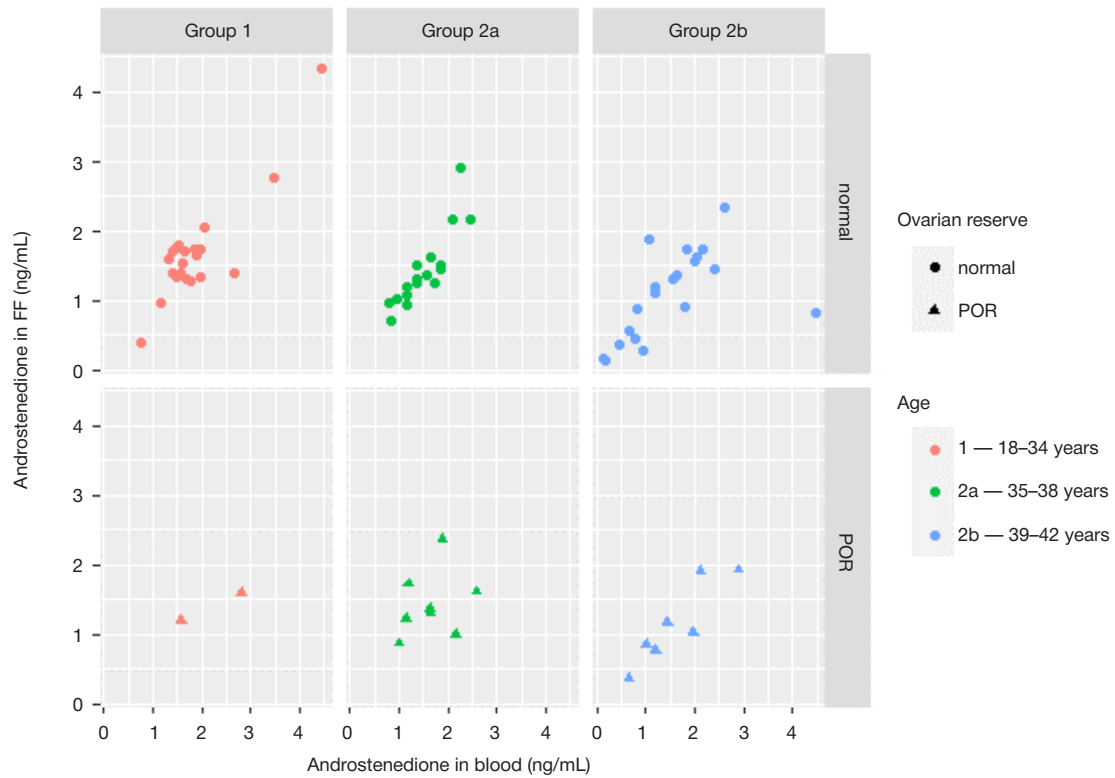


Fig. 4. The DHEA-S levels in follicular fluid (FF) and blood plasma per groups: younger than 35 years (group 1), aged 35–38 years (group 2a) and older than 39 years (group 2b), with poor ovarian reserves (subgroup 1) or normal (subgroup 0)

and then 12, 17, 32 and 36 h post-injection [17]. The analytical measurements revealed dynamic changes for estradiol and testosterone, whereas androstenedione levels in both blood and FF remained stable over the entire periovulatory period. Nevertheless, consistently with our findings, correlation analysis revealed a positive association between androstenedione and testosterone levels in FF. Considering that total blood levels of testosterone in women are low and their reliable measurement is problematic, the correlating levels of androstenedione and total testosterone in both plasma and FF implicate androstenedione as a candidate marker of POR in reproductive age women with infertility.

A statistically significant increase in FF androgen levels against the background of menotropins as ovarian stimulators

has been reported as well [18]; however, our data provide no support for this association.

Yet another study focused on androgen concentrations in blood serum and FF in patients with poor ovarian response, assigned into four groups according to POSEIDON criteria. Despite the lack of significant differences in blood levels of testosterone, androstenedione and DHEA-S between patients with normal ovarian reserve (controls) and POSEIDON group 1, significantly decreased blood levels of hormones were revealed in POSEIDON group 3 compared with the controls. At that, FF concentrations of DHEA-S in group 3 were significantly lower, whereas FF concentrations of testosterone, androstenedione, estradiol and sex steroid-binding globulin (SSBG) were similar in

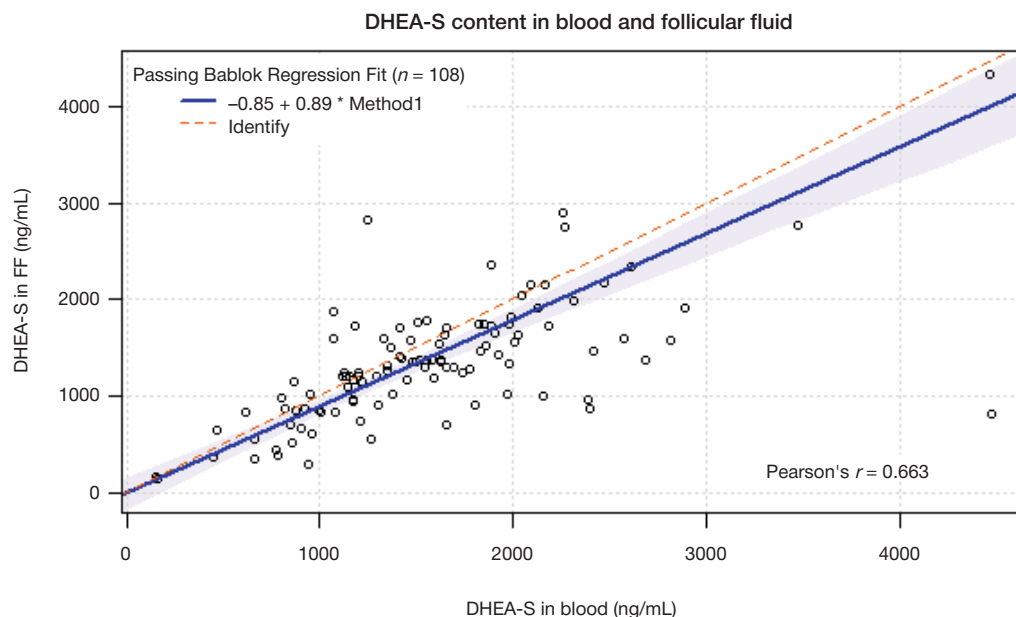


Fig. 5. The correlation and linear regression analyses of DHEA-S concentrations in follicular fluid (FF) vs blood plasma for all data points

all groups. In patients older than 35 years, serum testosterone levels were significantly lower independently of the ovarian reserve status (POSEIDON groups 2 and 4). The study also demonstrated a positive correlation between serum and FF concentrations for DHEA-S [19]. Our own data confirm the overall tendency of correlating hormone levels in blood and FF.

CONCLUSIONS

The presented data indicate that with a diminished ovarian reserve there is a selective decrease in androgen levels in the follicular fluid, which confirms the hypothesis about the contribution of androgens and the role of their deficiency. The findings of the correlation between total testosterone

and androstenedione not only in the blood plasma but also in the follicular fluid indicate the diagnostic value of these androgens as early markers of androgen deficiency formation in women with infertility with decreased ovarian reserve. The use of LC-MS/MS to determine androgen levels in women with infertility in an IVF program may be predictive of the relationship between testosterone and androstenedione concentrations in plasma and follicular fluid as an oocyte microenvironment. The discussion about the possibility of predicting the outcomes of ART on the basis of androgen levels requires more in-depth research due to the growing clinical need to improve the effectiveness of IVF and to predict their outcomes at the stage of analysis of follicular fluid composition.

References

- Hill MJ, Levens ED, Levy G, Ryan ME, Csokmay JM, DeCheme AH, et al. The use of recombinant luteinizing hormone in patients undergoing assisted reproductive techniques with advanced reproductive age: a systematic review and meta-analysis. *Fertil Steril.* 2012; 97 (5): 1108–14.
- Luo S, Li S, Li X, Qin L, Jin S. Effect of pretreatment with transdermal testosterone on poor ovarian responders undergoing IVF/ICSI: a meta-analysis. *Exp Ther Med.* 2014; 8 (1): 187–94.
- Von Wolff M, Kollmann Z, Flück CE, Stute P, Marti U, Weiss B, et al. Gonadotrophin stimulation for in vitro fertilization significantly alters the hormone milieu in follicular fluid: a comparative study between natural cycle IVF and conventional IVF. *Hum Reprod.* 2014; 29 (5): 1049–57.
- Fanchin R, Mendez Lozano DH, Frydman N, Gougeon A, di Clemente N, Frydman R, et al. Anti-Müllerian hormone concentrations in the follicular fluid of the preovulatory follicle are predictive of the implantation potential of the ensuing embryo obtained by in vitro fertilization. *J Clin Endocrinol Metab.* 2007; 92 (5): 1796–802.
- Pabuuccu R, Kaya C, Çağlar GS, Oztas E, Satiroglu H. Follicular-fluid anti-Mullerian hormone concentrations are predictive of assisted reproduction outcome in PCOS patients. *Reprod Biomed Online.* 2009; 19 (5): 631–37.
- Takahashi C, Fujito A, Kazuka M, Sugiyama R, Ito H, Isaka K. Anti-Müllerian hormone substance from follicular fluid is positively associated with success in oocyte fertilization during in vitro fertilization. *Fertil Steril.* 2008; 89 (3): 586–91.
- Van Disseldorp J, Faddy MJ, Themmen AP, de Jong FH, Peeters PH, van der Schouw YT. Relationship of serum antimüllerian hormone concentration to age at menopause. *J Clin Endocrinol Metab.* 2008; 93 (6): 2129–34.
- Barbieri RL, Sluss PM, Powers RD, McShane PM, Vitonis A, Ginsburg E, et al. Association of body mass index, age, and cigarette smoking with serum testosterone levels in cycling women undergoing in vitro fertilization. *Fertil Steril.* 2005; 83 (2): 302–8.
- Kushnir M, Naessen T, Wanggren K, Hreinsson J, Rockwood AL, Meikle AW. Exploratory study of the association of steroid profiles in stimulated ovarian follicular fluid with outcomes of IVF treatment. *J Steroid Biochem Mol Biol.* 2016; 162: 126–33.
- Kim J, Lee J, Chang H, Jee BC, Chang SS, Kim SH. Anti-Mullerian hormone levels in the follicular fluid of the preovulatory follicle: a predictor for oocyte fertilization and quality of embryo. *J Korean Med Sci.* 2014; 29 (9): 1266–70.
- Wen X, Li D, Tozer A, Suzanna MD, Ray KI. Estradiol, progesterone, testosterone profiles in human follicular fluid and cultured granulosa cells from luteinized pre-ovulatory follicles. *Reprod Biol Endocrinol.* 2010; 8: 117.
- Handelsman D. Mass spectrometry, immunoassay and valid steroid measurements in reproductive medicine and science. *Hum Reprod.* 2017; 32 (6): 1–4.
- Yang Z, Zhou W, Zhou C, Zhou Y, Liu X, Ding G, et al. Steroid metabolome profiling of follicular fluid in normo- and hyperandrogenic women with polycystic ovary syndrome. *J Steroid Biochem Mol Biol Epub.* 2021; 206: 105806.
- Bongrani A, Plotton I, Mellouk N, Ramé C, Guerif F, Froment P, et al. High androgen concentrations in follicular fluid of polycystic ovary syndrome women. *Reprod Biol Endocrinol.* 2022; 20 (1): 88.
- Harwood DT, Handelsman DJ. Development and validation of a sensitive liquid chromatography-tandem mass spectrometry assay to simultaneously measure androgens and estrogens in serum without derivatization. *Clin Chim Acta.* 2009; 409 (1–2): 78–84.
- Jonas Schäler, Georg Thaller, Dirk Hinrichs. A language and environment for statistical computing. R Foundation for Statistical Computing, Vienna, Austria, 2018. R Studio: Integrated Development for R. R Studio, Inc., Boston MA.
- Poulsen LC, Englund ALM, Andersen AS, Bøtkjær JA, Mamsen LS, Damdimopoulou P, et al. Follicular hormone dynamics during the midcycle surge of gonadotropins in women undergoing fertility treatment. *Mol Hum Reprod.* 2020; 26 (4): 256–68.
- Burduli AG, Kitsilovskaya NA, Sukhova YV, Vedikhina IA, Ivanets TY, Chagovets VV, Starodubtseva NL, Frankevich VE. Follicular fluid and assisted reproductive technology programs outcomes (literature review). *Gynecology.* 2019; 21 (6): 36–40. Russian.
- Fuentes A, Sequeira K, Tapia-Pizarro A, Muñoz A, Salinas A, Céspedes P, et al. Androgens profile in blood serum and follicular fluid of women with poor ovarian response during controlled ovarian stimulation reveals differences amongst POSEIDON stratification groups: a pilot study. *Front Endocrinol (Lausanne).* 2019; 10: 458.

Литература

- Hill MJ, Levens ED, Levy G, Ryan ME, Csokmay JM, DeCheme AH, et al. The use of recombinant luteinizing hormone in patients undergoing assisted reproductive techniques with advanced reproductive age: a systematic review and meta-analysis. *Fertil Steril.* 2012; 97 (5): 1108–14.
- Luo S, Li S, Li X, Qin L, Jin S. Effect of pretreatment with transdermal testosterone on poor ovarian responders undergoing IVF/ICSI: a meta-analysis. *Exp Ther Med.* 2014; 8 (1): 187–94.
- Von Wolff M, Kollmann Z, Flück CE, Stute P, Marti U, Weiss B, et al. Gonadotrophin stimulation for in vitro fertilization significantly alters the hormone milieu in follicular fluid: a comparative study between natural cycle IVF and conventional IVF. *Hum Reprod.*

- 2014; 29 (5): 1049–57.
4. Fanchin R, Mendez Lozano DH, Frydman N, Gougeon A, di Clemente N, Frydman R, et al. Anti-Müllerian hormone concentrations in the follicular fluid of the preovulatory follicle are predictive of the implantation potential of the ensuing embryo obtained by in vitro fertilization. *J Clin Endocrinol Metab.* 2007; 92 (5): 1796–802.
 5. Pabuccu R, Kaya C, Çağlar GS, Oztas E, Satiroglu H. Follicular-fluid anti-Mullerian hormone concentrations are predictive of assisted reproduction outcome in PCOS patients. *Reprod Biomed Online.* 2009; 19 (5): 631–37.
 6. Takahashi C, Fujito A, Kazuka M, Sugiyama R, Ito H, Isaka K. Anti-Müllerian hormone substance from follicular fluid is positively associated with success in oocyte fertilization during in vitro fertilization. *Fertil Steril.* 2008; 89 (3): 586–91.
 7. Van Disseldorp J, Faddy MJ, Themmen AP, de Jong FH, Peeters PH, van der Schouw YT. Relationship of serum antimüllerian hormone concentration to age at menopause. *J Clin Endocrinol Metab.* 2008; 93 (6): 2129–34.
 8. Barbieri RL, Sluss PM, Powers RD, McShane PM, Vitonis A, Ginsburg E, et al. Association of body mass index, age, and cigarette smoking with serum testosterone levels in cycling women undergoing in vitro fertilization. *Fertil Steril.* 2005; 83 (2): 302–8.
 9. Kushnir M, Naessen T, Wanggren K, Hreinsson J, Rockwood AL, Meikle AW. Exploratory study of the association of steroid profiles in stimulated ovarian follicular fluid with outcomes of IVF treatment. *J Steroid Biochem Mol Biol.* 2016; 162: 126–33.
 10. Kim J, Lee J, Chang H, Jee BC, Chang SS, Kim SH. Anti-Mullerian hormone levels in the follicular fluid of the preovulatory follicle: a predictor for oocyte fertilization and quality of embryo. *J Korean Med Sci.* 2014; 29 (9): 1266–70.
 11. Wen X, Li D, Tozer A, Suzanna MD, Ray KI. Estradiol, progesterone, testosterone profiles in human follicular fluid and cultured granulosa cells from luteinized pre-ovulatory follicles. *Reprod Biol Endocrinol.* 2010; 8: 117.
 12. Handelsman D. Mass spectrometry, immunoassay and valid steroid measurements in reproductive medicine and science. *Hum Reprod.* 2017; 32 (6): 1–4.
 13. Yang Z, Zhou W, Zhou C, Zhou Y, Liu X, Ding G, et al. Steroid metabolome profiling of follicular fluid in normo- and hyperandrogenic women with polycystic ovary syndrome. *J Steroid Biochem Mol Biol Epub.* 2021; 206: 105806.
 14. Bongrani A, Plotton I, Mellouk N, Ramé C, Guerif F, Froment P, et al. High androgen concentrations in follicular fluid of polycystic ovary syndrome women. *Reprod Biol Endocrinol.* 2022; 20 (1): 88.
 15. Harwood DT, Handelsman DJ. Development and validation of a sensitive liquid chromatography-tandem mass spectrometry assay to simultaneously measure androgens and estrogens in serum without derivatization. *Clin Chim Acta.* 2009; 409 (1–2): 78–84.
 16. Jonas Schäler, Georg Thaller, Dirk Hinrichs. A language and environment for statistical computing. R Foundation for Statistical Computing, Vienna, Austria, 2018. R Studio: Integrated Development for R. R Studio, Inc., Boston MA.
 17. Poulsen LC, Englund ALM, Andersen AS, Bøtkjær JA, Mamsen LS, Damdimopoulou P, et al. Follicular hormone dynamics during the midcycle surge of gonadotropins in women undergoing fertility treatment. *Mol Hum Reprod.* 2020; 26 (4): 256–68.
 18. Бурдули А. Г., Кициловская Н. А., Сухова Ю. В., Ведицина И. А., Иванец Т. Ю. и др. Фолликулярная жидкость и исходы программ вспомогательных репродуктивных технологий (обзор литературы). *Гинекология.* 2019; 21 (6): 36–40.
 19. Fuentes A, Sequeira K, Tapia-Pizarro A, Muñoz A, Salinas A, Céspedes P. et al. Androgens profile in blood serum and follicular fluid of women with poor ovarian response during controlled ovarian stimulation reveals differences amongst POSEIDON stratification groups: a pilot study. *Front Endocrinol (Lausanne).* 2019; 10: 458.

EXPERIENCE OF STANFORD NEUROMODULATION THERAPY IN PATIENTS WITH TREATMENT-RESISTANT DEPRESSION

Poydasheva AG¹✉, Bakulin IS¹, Sinitsyn DO¹, Zabirowa AH¹, Suponeva NA¹, Maslenikov NV², Tsukarzi EE², Mosolov SN^{2,3}, Piradov MA¹

¹ Research Center of Neurology, Moscow, Russia

² Moscow Research Institute of Psychiatry, Moscow, Russia

³ Russian Medical Academy of Continuous Professional Education, Moscow, Russia

Stanford neuromodulation therapy (SNT) is the state-of-the-art magnetic stimulation protocol that has been developed for management of treatment-resistant depression (TRD). The study was aimed to assess the possibility of SNT implementation in clinical practice and to define the protocol safety and efficacy in patients with TRD being an episode of the recurrent depressive disorder or bipolar disorder at the independent center. The study involved six patients (among them three women aged 21–66) with TRD associated with recurrent depression and type 1 or 2 bipolar disorder. The patients received intermittent theta-burst stimulation in accordance with the SNT protocol for five days: applying 10 triple blocks of stimulation daily at intervals of 1 hr between the blocks to the selected stimulation site showing maximum negative functional connectivity with subgenual cingulate cortex within the left dorsolateral prefrontal cortex. The Montgomery–Asberg Depression Rating Scale (MADRS) was used for clinical assessment of the effects, the follow-up period was three months. The improvement of depressive symptoms to the levels characteristic of remission immediately after the SNT completion was observed in five patients (MADRS score ≤ 10). After three months, two patients still had remission, the condition of three patients met the criteria of mild depressive episode, and one female patient withdrew from the study due to logistical difficulties. No serious adverse events were reported. The findings confirm safety and potentially high efficacy of SNT, including in patients with type 1 and 2 bipolar disorders.

Keywords: treatment-resistant depression, bipolar disorder, transcranial magnetic stimulation, theta-burst stimulation

Author contribution: Poydasheva AG, Bakulin IS, Mosolov SN — study planning and design; Poydasheva AG, Zabirowa AH — literature review; Poydasheva AG, Sinitsyn DO, Maslenikov NV, Tsukarzi EE — data acquisition and analysis; all authors — data interpretation; Poydasheva AG, Sinitsyn DO — manuscript writing; all authors — manuscript editing.

Compliance with ethical standards: the research protocol was approved by the Ethics Committee at the Research Center of Neurology (protocol № 11-1/21 of 22 December 2021); the study was conducted in accordance with the principles of the Declaration of Helsinki; the informed consent was submitted by all study participants.

✉ **Correspondence should be addressed:** Alexandra G. Poydasheva
Volokolamskoe shosse, 80, Moscow, 125367, Russia; poydasheva@neurology.ru

Received: 08.08.2022 **Accepted:** 22.08.2022 **Published online:** 30.08.2022

DOI: 10.24075/brsmu.2022.044

ОПЫТ ПРИМЕНЕНИЯ СТЭНФОРДСКОЙ НЕЙРОМОДУЛИРУЮЩЕЙ ТЕРАПИИ У ПАЦИЕНТОВ С ТЕРАПЕВТИЧЕСКИ РЕЗИСТЕНТНОЙ ДЕПРЕССИЕЙ

А. Г. Пойдашева¹✉, И. С. Бакулин¹, Д. О. Синицын¹, А. Х. Забиrowa¹, Н. А. Супонева¹, Н. В. Масленников², Э. Э. Цукарзи², С. Н. Мосолов^{2,3}, М. А. Пирадов¹

¹ Научный центр неврологии, Москва, Россия

² Московский научно-исследовательский институт психиатрии, Москва, Россия

³ Российская медицинская академия непрерывного профессионального образования, Москва, Россия

Стэнфордская нейромодулирующая терапия (SNT) — новейший протокол магнитной стимуляции, разработанный для лечения терапевтически резистентных депрессий (ТРД). Целью исследования было оценить возможности реализации SNT в клинической практике, определить безопасность и эффективность протокола в независимом центре у пациентов с ТРД в рамках рекуррентной депрессивной и биполярного расстройств. В исследование вошли шесть пациентов (из них три женщины в возрасте 21–66 лет) с ТРД в рамках рекуррентной депрессии и биполярного расстройства 1-го и 2-го типов. В течение пяти дней пациентам проводили стимуляцию интермиттирующими тета-вспышками по протоколу SNT: ежедневно по 10 тройных блоков стимуляции с интервалом 1 ч между соседними блоками и выбором зоны стимуляции с максимальной негативной функциональной связностью с субгенуальной поясной корой в пределах левой дорсолатеральной префронтальной коры. Для клинической оценки эффекта применяли шкалу Монтгомери–Асберг, длительность периода наблюдения составила три месяца. У пяти пациентов сразу после окончания SNT отмечено снижение выраженности депрессии до уровня ремиссии (≤ 10 баллов по MADRS). Через три месяца два пациента оставались в ремиссии, у троих состояние соответствовало легкому депрессивному эпизоду, одна пациентка выбыла из исследования из-за логистических трудностей. Серьезных нежелательных явлений не зарегистрировано. Полученные результаты подтверждают безопасность и потенциально высокую эффективность SNT в том числе при биполярных расстройствах 1-го и 2-го типов.

Ключевые слова: терапевтически резистентная депрессия, биполярное аффективное расстройство, транскраниальная магнитная стимуляция, стимуляция тета-вспышками

Вклад авторов: А. Г. Пойдашева, И. С. Бакулин, С. Н. Мосолов — планирование и дизайн исследования; А. Г. Пойдашева, А. Х. Забиrowa — анализ литературы; А. Г. Пойдашева, Д. О. Синицын, Н. В. Масленников, Э. Э. Цукарзи — сбор и анализ данных; все авторы — интерпретация данных; А. Г. Пойдашева, Д. О. Синицын — написание статьи; все авторы — редактирование статьи.

Соблюдение этических стандартов: протокол исследования одобрен этическим комитетом ФГБНУ НЦН (протокол № 11-1/21 от 22 декабря 2021 г.); исследование проведено в соответствии с принципами Хельсинкской декларации; все пациенты подписывали добровольное информированное согласие.

✉ **Для корреспонденции:** Александра Георгиевна Пойдашева
Волоколамское шоссе, д. 80, Москва, 125367, Россия; poydasheva@neurology.ru

Статья получена: 08.08.2022 **Статья принята к печати:** 22.08.2022 **Опубликована онлайн:** 30.08.2022

DOI: 10.24075/vrgmu.2022.044

High prevalence of treatment-resistant depressive (TRD) determines the relevance of developing new effective non-drug approaches to treatment of this condition [1–3]. The noninvasive brain stimulation techniques, such as repetitive transcranial magnetic stimulation (rTMS), can be considered the non-pharmacological methods most widely used in clinical practice. According to the existing concepts, the long-term effects of stimulation result from induction of processes similar to the processes underlying synaptic plasticity, and are mediated by NMDA and AMPA receptors [4]. Along with modulation of synaptic plasticity, the impact of rTMS on neurogenesis and neurotransmitter secretion, together with physical effects of electromagnetic fields, continue to be discussed [4, 5].

Large double-blind controlled trials provided strong evidence of the efficiency of using non-invasive stimulation methods in treatment of depression [6, 7]. According to current guidelines, high levels of evidence for the effects of using rTMS and theta-burst stimulation (TBS) in treatment of TRD were reached [8]. The U. S. Food and Drug Administration (FDA) approved two protocols for management of TRD: high-frequency (10 Hz) rTMS applied to the left dorsolateral prefrontal cortex (DLPFC) in 2008, and intermittent theta-burst stimulation (iTBS) of the left DLPFC in 2018 [9]. However, despite a rather strong evidence to support the use of the listed above stimulation protocols in patients with TRD, pronounced variability of the effects is the main constraint on greater use of the protocols. Thus, according to two largest meta-analyses, the patients who respond to therapy with rTMS constitute 25–55%, and clinical remission can be achieved only in 16–30% of cases [10, 11]. Increasing the efficiency of stimulation and reducing the effect variability are the major challenges faced by researchers.

Several approaches to increasing the efficiency are currently being developed. Personalized target selection and the use of so-called accelerated protocols could be considered the most promising and well understood in the context of TRD. A personalized approach to the stimulation target selection was proposed in 2012 that was based on the analysis of functional connectivity (FC) between the subgenual cingulate (Sg) and left DLPFC [12]. The approach is based on the data on the altered functional connectivity of Sg in patients with depression [13], as well as on the relationship between the clinical effects of rTMS and FC between the stimulated site and Sg [12]. However, when comparing the effectiveness of rTMS using personalized and standard approaches, heterogenous results were obtained [14, 15]. Protocols, that include several sessions of stimulation per day aimed at achieving the total numbers of pulses significantly above the standard values, are called accelerated protocols. According to recent meta-analysis that includes studies involving accelerated protocols, the use of such protocols has a moderate effect and still does not solve the problem of high variability [16].

Finally, the protocol combining target selection based on the analysis of FC and extremely large number of pulses (18,000 pulses per day vs. 3000 and 600 pulses per day in standard rTMS and TBS protocols) was developed in 2019, called Stanford neuromodulation therapy (SNT) [17]. According to the pilot data of the open-label trial, 90% of patients, who received SNT, achieved remission (defined as the Montgomery–Asberg Depression Rating Scale score below 11), which was well above the effectiveness of the previously used protocols [17]. In 2022, the same group published the results of the double-blind controlled trial that showed significant effects of SNT compared to sham stimulation, confirmed safety and a very high proportion of responders and remitters [18].

But so far the findings have not been confirmed by other research groups. Furthermore, the patients diagnosed with

major depressive disorder (major depression) were included in the original study, while no studies of safety and efficacy of SNT in patients with depressive episode associated with bipolar disorder were performed.

Thus, the pilot study was aimed to assess the possibility of the SNT protocol implementation in clinical practice and to acquire data on the protocol safety and efficacy at the independent center, particularly in the new cohort of patients with bipolar disorder.

METHODS

Patients

The patients were recruited at the Moscow Research Institute of Psychiatry, the branch of V.P. Serbsky Federal Medical Research Center for Psychiatry and Narcology, and SNT was performed at the Institute of Neurorehabilitation, Research Center of Neurology, in 2022.

Inclusion criteria: ongoing mild-to-moderate drug-resistant depressive episode associated with recurrent depressive disorder or bipolar disorder; age 18–70 years; no contraindications to MRI and TMS; no severe general medical condition that requires maintenance of vital functions using the life-support devices; no severe cognitive impairment or other nervous system disease. Drug resistance was defined based on the absence of clinical effects after two or more courses of treatment with antidepressants of various groups used in adequate doses for at least 4 weeks [19, 20]. Some patients continued to receive the unchanged doses of antidepressant, antipsychotic, and anxiolytic medications. Exclusion criteria: serious adverse events (SAEs) during TBS, such as epileptic seizure, syncope, intense headache; onset of severe general medical condition or mental disorder, nervous system disease after the study enrollment, as well as pacemaker insertion, cardiac catheterization, brain surgery that requires metal objects retained in the cranial cavity, getting pregnant, or refusal to participate further in the study.

Prior to stimulation with the use of the Neuron-Spectrum-4/P (Neurosoft; Russia) and actiCHamp Plus 64 (BP-100-2511) (Brain Products GmbH; Germany) systems the patients underwent screening EEG aimed at detecting epileptiform discharges. The patients, who showed epileptiform discharges, were excluded from the study.

Identification of stimulation target

To perform target localization for stimulation, all patients underwent neuroimaging on the Magnetom Prisma 3T system (SIEMENS; Germany) that included two sequences: T1-weighted images were acquired at isotropic resolution for further multiplanar reconstruction (MPR) aimed at obtaining structural data (TR 2200 ms, 1 mm slice thickness, number of slices 176), and multiplanar gradient echo mode (ep2d_bold_moco: TR 2200 ms, 36 slices in the axial plane) was used for assessment of functional connectivity. The targets for stimulation were determined for each patients based on assessment of the resting-state functional MRI data. Neuroimaging data were preprocessed in the CONN functional connectivity toolbox (Functional Connectivity SPM Toolbox 2017, McGovern Institute for Brain Research, Massachusetts Institute of Technology, Cambridge, USA; <http://www.nitrc.org/projects/conn>), ver. 17f, and SPM12 (Functional Imaging Laboratory, Wellcome Department of Imaging Neuroscience, Institute of Neurology, London, UK; <http://www.fil.ion.ucl.ac.uk/>

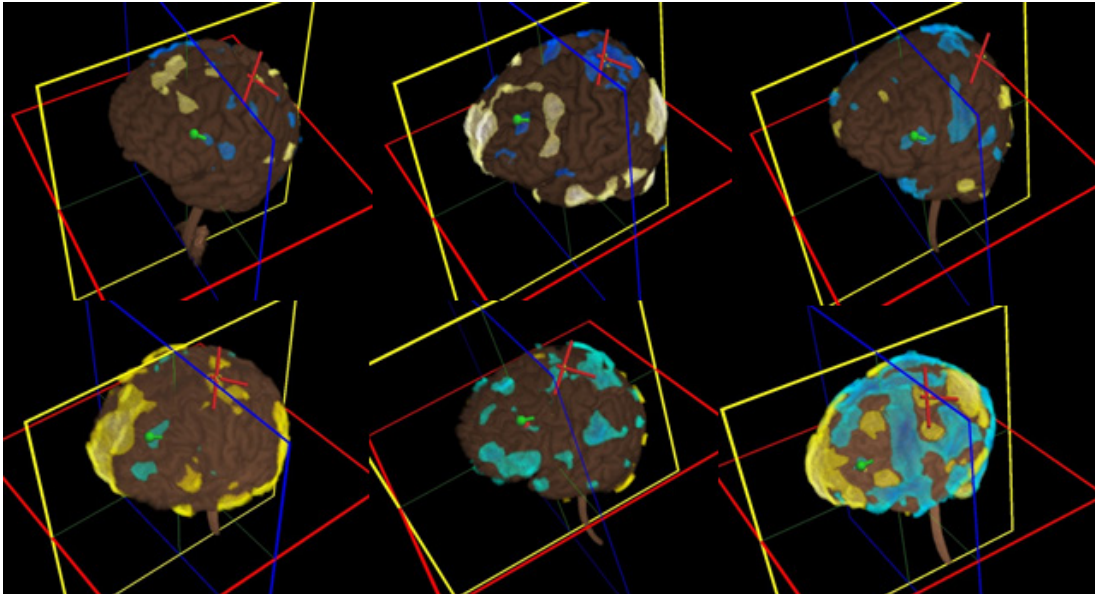


Fig. 1. Visualization of the functional connectivity (FC) analysis data and target selection in patients. Color shows FC values between the subgenual cingulate and the visualized cortical areas. The target is marked with a green tag

spm/software). Preprocessing consisted of the earlier reported standard steps [15]. After preprocessing, the maps showing FC of subgenual cingulate with all other brain regions were created individually for each patient using the same software package, the region was selected within anatomical limits of left DLPFC that showed maximum negative FC (Fig. 1). A 10-mm diameter sphere generated around the subgenual part of the cingulate gyrus (Sg) (a point with MNI coordinates (6, 16, -10)) was used as a seed region.

Stimulation protocol

Intermittent theta-burst stimulation was performed with the MagPro X100 MagOption system (Tonica Elektronik A/S; Denmark), equipped with the liquid-cooled figure-eight coil, in combination with the Localite TMS Navigator navigation system (Localite GmbH; Germany) and Axilum Robotics TMS-Cobot robotic device (Axilum Robotics; France). The stimulus intensity was 120% resting motor threshold defined by recording motor evoked potentials (MEPs) of the right first dorsal interosseous muscle in accordance with the Rossini–Rothwell algorithm.

Stimulation was performed for five consecutive weekdays. Every day, the patients were through 10 sessions of intermittent theta-burst stimulation with a 1-hr interval between sessions. Each session included three standard blocks of theta-burst stimulation (600 pulses/block). Thus, the patient received a total of 18,000 pulses during the day, and 90,000 pulses during the entire course (Fig. 2).

Clinical assessment

The Montgomery-Asberg Depression Rating Scale (MADRS) was used to assess the clinical effects of SNT [21]. Assessment was performed at five different time points: prior to stimulation, immediately after stimulation, 1, 2 and 3 months after stimulation. The MADRS scores reduced by more than 50% from baseline were considered a clinically significant response, while the scores of 10 points and lower were considered a remission [22]. Furthermore, TRD was staged by Maudsley Staging Method (MSM) in all patients prior to the study [23]. The original questionnaires were used to assess safety, tolerability and adverse events (AEs): AEs reported during stimulation and

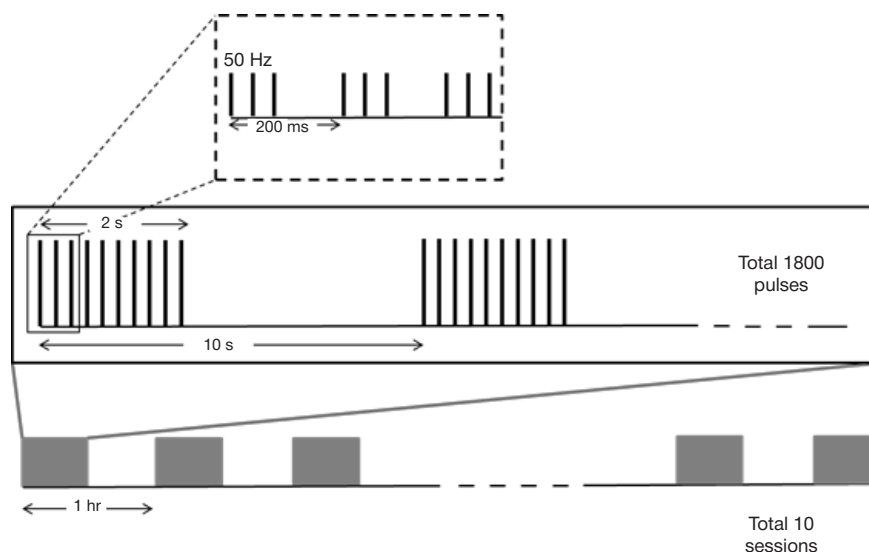


Fig. 2. Scheme of the Stanford Neuromodulation Therapy (SNT) protocol

Table. Clinical and demographic data of the patients enrolled

№	Sex	Age	Diagnosis (ICD-10 code)	MADRS score	MSM score	Disease duration, years	Number of episodes
1	м	36	F33.1	19	10	13	8
2	м	29	F33.1	14	7	13	7
3	м	66	F31.8	19	10	47	10
4	ф	31	F31.3	19	6	15	10
5	ф	21	F31.8	21	7	5	4
6	ф	58	F31.3	27	6	34	12

Note: MADRS — Montgomery–Asberg Depression Rating Scale; MSM — Maudsley Staging Method.

AEs reported within 24 hrs after stimulation were analyzed separately.

RESULTS

The study involved six patients (three women and three men) aged 21–66 with the ongoing mild-to-moderate drug-resistant depression associated with recurrent depressive disorder (two patients), bipolar disorder type 1 (two patients) and 2 (two patients) (Table). The disease duration was 5–47 years, and the number of episodes per patient was at least four.

The improvement of depressive symptoms to the levels characteristic of remission (MADRS score 10 or lower) immediately after the end of therapy (day 6) was observed in five patients out of six (Fig. 3). The MADRS score of the sixth patient remained unchanged immediately after the end of the course. One of the female patients withdrew from the study at the assessment stage immediately after the stimulation completion. Thus, the data acquired from five patients were available for investigation of the clinical effect stability. Assessment performed within a month showed that one patient still had remission (diagnosis code F31.8), while the scores of other four patients met the criteria of mild depressive episode (diagnosis code F33.1 in two patients, and F31.3 in two female patients). Two months later the condition of three patients met the criteria of remission (diagnosis codes F31.8, F33.1, F31.3), and the condition of two patients was considered a mild depressive episode (diagnosis codes F33.1, F31.3). Assessment of scores, that were compared to baselines, in four patients out of five met the criteria of the clinically significant response to therapy (reduction by more than 50% from baseline). After three months, two patients still had remission (diagnosis codes F33.1, F31.3), and the

condition of three patients met the criteria of mild depressive episode (diagnosis codes F31.8, F33.1, F31.3). Two patients met the criteria of the clinically significant response to therapy compared to baselines. It is interesting to note that no long-term effects were observed in the only patient who showed no response to therapy immediately after the end of stimulation (diagnosis code F33.1).

No serious AEs were reported, such as epileptic seizure, syncope, or intense headache. Two patients reported mild headache (pain intensity with the Numerical Pain Rating Scale score below 3 points), that resolved spontaneously within 2–3 hrs without supplementary medication, after the end of the first block of stimulation (in the evening of the first day). These patients had no headache on other days. Furthermore, one female patient complained of the increase in anxiety, mood change, and sleeping disorder after the first block of stimulation. However, agitation resolved by the next morning. Later, mood changes and insomnia did not bother this patient. Phase inversion was reported in none of the patients with bipolar disorder.

DISCUSSION

The pilot study showed safety and good tolerability of the new SNT protocol in patients with depressive episodes associated with both recurrent depression and bipolar disorder. Inclusion of patients with bipolar disorder distinguishes our study from other research. The identified AEs were mild, never required prescribing supplementary medication and never resulted in rejection of procedures or refusal to participate in the study.

The findings showed that the proportion of patients, whose symptoms of depression met the criteria of remission immediately after the end of stimulation, was 83%. Heterogeneous data

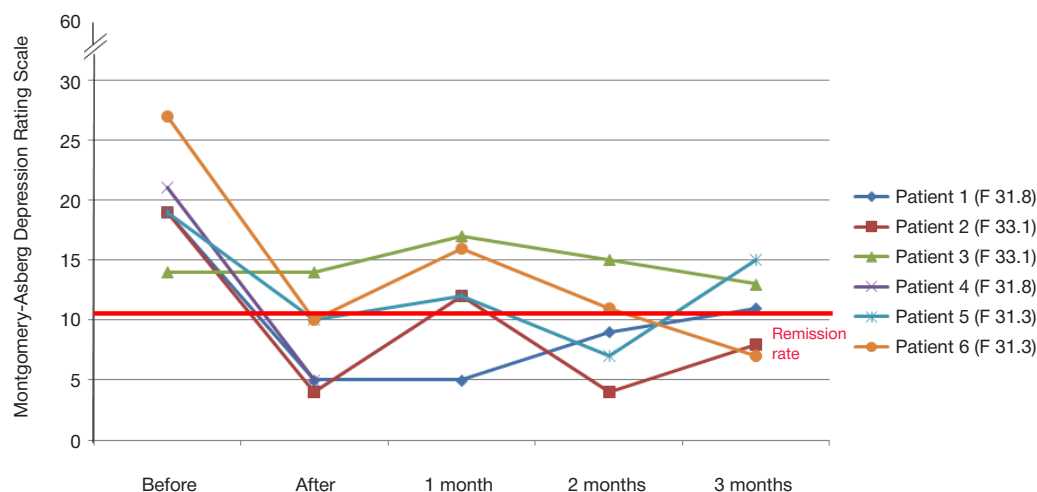


Fig. 3. Dynamics of depressive symptoms: individual data

were obtained when assessing durability of response: in 75% of patients, who showed clinically significant effects of SNT immediately after the end of stimulation, the effects persisted for two months, and in a third of patients the effects persisted for at least three months. The pilot data obtained suggest that SNT efficacy in patients with recurrent depression is high, it is well above the efficacy of the FDA-approved protocols, which is in line with the data provided by the designers of SNT. Furthermore, reduced depressive symptom severity is reported in patients with bipolar disorder, which brings up to date conducting the double-blind controlled trials of SNT efficacy in this cohort of patients as well.

To date, there is no clear concept whether higher efficacy of SNT compared to FDA-approved protocols results from more precise target selection, larger number of pulses per session or course, the combination of these factors, or other mechanisms. Despite the fact that some researchers have shown the effectiveness of the target selection algorithm based on the analysis of FC with Sg compared to sham stimulation [24], no increase in the efficacy of stimulation has been found when using the algorithm involving standard target selection [15]. Thus, it seems unlikely that precise target selection is the only contributor to the increased efficacy. Talking about accelerated protocols, it is important to note heterogeneity of the currently available results: the early studies showed encouraging results [25], however, further larger trials, that involved the use of both high-frequency rTMS and theta-burst stimulation, generated negative results [26, 27]. However, direct comparison of the protocols, used in the two latter studies, with SNT is not quite correct since the total number of pulses used in SNT is several times larger than the number of those used in the studied accelerated protocols. Moreover, not only the total number of pulses, but also, for instance, the duration of single block of stimulation or the time between blocks can contribute significantly to the effect size. These issues are particularly relevant in the context of metaplasticity concept, which has been actively developed in recent years [28]. According to the concept of metaplasticity, prior activity determines the threshold for induction of the activity-dependent plasticity, not only the values and duration of the neuroplastic changes induced, but also the direction of neuroplasticity. Thus, in the context of SNT, each preceding block of stimulation can promote changes induced by subsequent block through the mechanism of additive metaplasticity. It is important to note that the discussed potential mechanisms of increasing the efficacy of SNT compared to approved protocols are hypothetical and

require testing in the studies that involve controlling each of the mentioned factors separately.

When performing clinical testing of the SNT protocol, we have identified a number of factors that restrict widespread introduction of the method into practice. First, these factors include high labor costs of the protocol: each patient needs 10 sessions of stimulation provided at intervals of 1 hr daily for five days. This requires special organisation of both the employee work mode and the patient mode. The total working hours of both staff and patients are 11 hrs per day. Moreover, when used for SNT, the transcranial magnetic stimulation device throughput is significantly limited: only three patients can be treated with the same device at the same time. Implementation of the protocol requires high-tech equipment (TMS device equipped with the neuronavigation system and high-field MRI scanner) and staff members involved in analysis of neuroimaging data and working with the neuronavigation system. These factors negate affordability of the technique in general. It seems promising to study the efficacy of protocols that are partially compliant with SNT (for example, with respect of multiplicity and number of pulses, but without precise target selection), the use of which given their efficacy would significantly increase the method affordability.

The study limitations are as follows: small number of patients enrolled, no controls, and moderate severity of the patients' affective disorders. However, it is important to note that the study was aimed to assess the possibility of the SNT protocol implementation in clinical practice, as well as to provide independent confirmation of its safety and efficacy, particularly in the new cohort of patients with bipolar disorder. The findings show SNT feasibility and the perspective for further investigation of the method efficacy and safety, including the potential of blind controlled trials within the larger cohorts of patients.

CONCLUSIONS

The results of clinical testing performed in a small sample of patients show that Stanford neuromodulation therapy is a safe and potentially highly efficient method for management of treatment-resistant depression. However, the labor costs of the method are high. Further research, that would potentially allow to expand the spectrum of indications for SNT and increase affordability of the method, seems to be a promising area in the field of non-invasive brain stimulation in patients with affective disorders resistant to psychopharmacotherapy.

References

- Maksimova NM, Rusaev VYu, Uzbekov MG. Nejrobiologicheskie mexanizmy razvitiya rezistentnyx depressij. *Social'naya i klinicheskaya psixiatriya*. 2021; 31 (4): 71–79. Russian.
- Voineskos D, Daskalakis ZJ, Blumberger DM. Management of Treatment-Resistant Depression: Challenges and Strategies. *Neuropsychiatr Dis Treat*. 2020; 16: 221–34.
- Mosolov SN, Alfimov PV, Kostyukova EG. Sovremennye metody preodoleniya terapevticheskoy rezistentnosti pri rekurrentnoj depressii. V knige: S. N. Mosolov, redaktor. *Biologicheskie metody terapii psicheskix rasstrojstv*. M., 2012; s. 438–73. Russian.
- Miron JP, Jodoin VD, Lespérance P, Blumberger DM. Repetitive transcranial magnetic stimulation for major depressive disorder: basic principles and future directions. *Ther Adv Psychopharmacol*. 2021; 11: 20451253211042696.
- Chervyakov AV, Chernyavsky AY, Sinitsyn DO, Piradov MA. Possible Mechanisms Underlying the Therapeutic Effects of Transcranial Magnetic Stimulation. *Front Hum Neurosci*. 2015; 9: 303.
- O'Reardon JP, Solvason HB, Janicak PG, Sampson S, Isenberg KE, Nahas Z, et al. Efficacy and safety of transcranial magnetic stimulation in the acute treatment of major depression: a multisite randomized controlled trial. *Biol Psychiatry*. 2007; 62 (11): 1208–16.
- Blumberger DM, Vila-Rodriguez F, Thorpe KE, Feffer K, Noda Y, Giacobbe P, et al. Effectiveness of theta burst versus high-frequency repetitive transcranial magnetic stimulation in patients with depression (THREE-D): a randomised non-inferiority trial. *Lancet*. 2018; 391 (10131): 1683–92.
- Lefaucheur JP, Aleman A, Baeken C, Benninger DH, Brunelin J, Di Lazzaro V, et al. Evidence-based guidelines on the therapeutic use of repetitive transcranial magnetic stimulation (rTMS): An

- update (2014–2018). *Clin Neurophysiol.* 2020; 131 (2): 474–528.
9. Boes AD, Kelly MS, Trapp NT, Stern AP, Press DZ, Pascual-Leone A. Noninvasive Brain Stimulation: Challenges and Opportunities for a New Clinical Specialty. *J Neuropsychiatry Clin Neurosci.* 2018; 30 (3): 173–79.
 10. Berlim MT, van den Eynde F, Tovar-Perdomo S, Daskalakis ZJ. Response, remission and drop-out rates following high-frequency repetitive transcranial magnetic stimulation (rTMS) for treating major depression: a systematic review and meta-analysis of randomized, double-blind and sham-controlled trials. *Psychol Med.* 2014; 44 (2): 225–39.
 11. Sehatzadeh S, Daskalakis ZJ, Yap B, Tu HA, Palimaka S, Bowen JM, et al. Unilateral and bilateral repetitive transcranial magnetic stimulation for treatment-resistant depression: a meta-analysis of randomized controlled trials over 2 decades. *J Psychiatry Neurosci.* 2019; 44 (3): 151–63.
 12. Fox MD, Buckner RL, White MP, Greicius MD, Pascual-Leone A. Efficacy of transcranial magnetic stimulation targets for depression is related to intrinsic functional connectivity with the subgenual cingulate. *Biol Psychiatry.* 2012; 72 (7): 595–603.
 13. Drevets WC, Price JL, Furey ML. Brain structural and functional abnormalities in mood disorders: implications for neurocircuitry models of depression. *Brain Struct Funct.* 2008; 213 (1–2): 93–118.
 14. Antonovich BA, Maforova LA, Cukarzi EhEh, Mosolov SN. Neĭronnye seti sostoyaniya pokoya pri depressiyax i perspektivy primeneniya personificirovannoj TMS. *Sovremennaya terapiya psixicheskix rasstrojstv.* 2019; 3: 2–11. Russian.
 15. Poydasheva AG, Sinitsyn DO, Bakulin IS, Suponeva NA, Maslenikov NV, Tsukarzi EE. i dr. Opredelenie misheni dlya transkraniĭnoĭ magnitnoĭ stimulyacii u pacientov s rezistentnym k farmakoterapii depressivnym ehpizodom na osnove individual'nyx parametrov funkcional'noĭ magnitno-rezonansnoĭ tomografii pokoya (pilotnoe slepoe kontroliruemoe issledovanie. *Nevrologiya, nejropsixiatriya, psixosomatika.* 2019; 11 (4): 44–50. Russian.
 16. Sonmez AI, Camsari DD, Nandakumar AL, Voort JLV, Kung S, Lewis CP, et al. Accelerated TMS for Depression: A systematic review and meta-analysis. *Psychiatry Res.* 2019; 273: 770–81.
 17. Cole EJ, Stimpson KH, Bentzley BS, Gulser M, Cherian K, Tischler C, et al. Stanford Accelerated Intelligent Neuromodulation Therapy for Treatment-Resistant Depression. *Am J Psychiatry.* 2020; 177 (8): 716–26.
 18. Cole EJ, Phillips AL, Bentzley BS, Stimpson KH, Nejad R, Barnak F, et al. Stanford Neuromodulation Therapy (SNT): A Double-Blind Randomized Controlled Trial. *Am J Psychiatry.* 2022; 179 (2): 132–41.
 19. Axapkin RV, Bukreeva ND, Vazagaeva TI, Kostyukova EG, Mazo GEh, Mosolov SN. Depressivnyĭ ehpizod, rekurrentnoe depressivnoe rasstrojstvo. *Klinicheskie rekomendacii. Vzroslye. Ehlektronnoe izdanie.* 2021. Dostupno po ssylke: https://cr.minzdrav.gov.ru/recomend/301_2. Russian.
 20. Mosolov SN, Kostyukova EG, Ladyzhenskij MYa. Algoritm biologicheskoy terapii ostrogo ehpizoda rekurrentnogo depressivnogo rasstrojstva. *Sovremennaya terapiya psixicheskix rasstrojstv.* 2016; 3: 27–40. Russian.
 21. Montgomery SA, Asberg M. A new depression scale designed to be sensitive to change. *Br J Psychiatry.* 1979; 134: 382–9.
 22. Hawley CJ, Gale TM, Sivakumaran T; Hertfordshire Neuroscience Research group. Defining remission by cut off score on the MADRS: selecting the optimal value. *J Affect Disord.* 2002; 72 (2): 177–84.
 23. Fekadu A, Wooderson SC, Markopoulou K, Cleare AJ. The Maudsley Staging Method for treatment-resistant depression: prediction of longer-term outcome and persistence of symptoms. *J Clin Psychiatry.* 2009; 70 (7): 952–7.
 24. Siddiqi SH, Taylor SF, Cooke D, Pascual-Leone A, George MS, Fox MD. Distinct Symptom-Specific Treatment Targets for Circuit-Based Neuromodulation. *Am J Psychiatry.* 2020; 177 (5): 435–46.
 25. Loo CK, Mitchell PB, McFarquhar TF, Malhi GS, Sachdev PS. A sham-controlled trial of the efficacy and safety of twice-daily rTMS in major depression. *Psychol Med.* 2007; 37 (3): 341–9.
 26. Blumberger DM, Vila-Rodriguez F, Wang W, Knyahnytska Y, Butterfield M, Noda Y, et al. A randomized sham controlled comparison of once vs twice-daily intermittent theta burst stimulation in depression: A Canadian rTMS treatment and biomarker network in depression (CARTBIND) study. *Brain Stimul.* 2021; 14 (6): 1447–55.
 27. Fitzgerald PB, Hoy KE, Elliot D, Susan McQueen RN, Wambeek LE, Daskalakis ZJ. Accelerated repetitive transcranial magnetic stimulation in the treatment of depression. *Neuropsychopharmacology.* 2018; 43 (7): 1565–72.
 28. Abraham WC, Bear MF. Metaplasticity: the plasticity of synaptic plasticity. *Trends Neurosci.* 1996; 19 (4): 126–30.

Литература

1. Максимова Н. М., Русяев В. Ю., Узбеков М. Г. Нейробиологические механизмы развития резистентных депрессий. *Социальная и клиническая психиатрия.* 2021; 31 (4): 71–79.
2. Voineskos D, Daskalakis ZJ, Blumberger DM. Management of Treatment-Resistant Depression: Challenges and Strategies. *Neuropsychiatr Dis Treat.* 2020; 16: 221–34.
3. Мосолов С. Н., Алфимов П. В., Костюкова Е. Г. Современные методы преодоления терапевтической резистентности при рекуррентной депрессии. В книге: С. Н. Мосолов, редактор. Биологические методы терапии психических расстройств. М., 2012; с. 438–73.
4. Miron JP, Jodoin VD, Lespérance P, Blumberger DM. Repetitive transcranial magnetic stimulation for major depressive disorder: basic principles and future directions. *Ther Adv Psychopharmacol.* 2021; 11: 20451253211042696.
5. Chervyakov AV, Chernyavsky AY, Sinitsyn DO, Piradov MA. Possible Mechanisms Underlying the Therapeutic Effects of Transcranial Magnetic Stimulation. *Front Hum Neurosci.* 2015; 9: 303.
6. O'Reardon JP, Solvason HB, Janicak PG, Sampson S, Isenberg KE, Nahas Z, et al. Efficacy and safety of transcranial magnetic stimulation in the acute treatment of major depression: a multisite randomized controlled trial. *Biol Psychiatry.* 2007; 62 (11): 1208–16.
7. Blumberger DM, Vila-Rodriguez F, Thorpe KE, Feffer K, Noda Y, Giacobbe P, et al. Effectiveness of theta burst versus high-frequency repetitive transcranial magnetic stimulation in patients with depression (THREE-D): a randomised non-inferiority trial. *Lancet.* 2018; 391 (10131): 1683–92.
8. Lefaucheur JP, Aleman A, Baeken C, Benninger DH, Brunelin J, Di Lazzaro V, et al. Evidence-based guidelines on the therapeutic use of repetitive transcranial magnetic stimulation (rTMS): An update (2014–2018). *Clin Neurophysiol.* 2020; 131 (2): 474–528.
9. Boes AD, Kelly MS, Trapp NT, Stern AP, Press DZ, Pascual-Leone A. Noninvasive Brain Stimulation: Challenges and Opportunities for a New Clinical Specialty. *J Neuropsychiatry Clin Neurosci.* 2018; 30 (3): 173–79.
10. Berlim MT, van den Eynde F, Tovar-Perdomo S, Daskalakis ZJ. Response, remission and drop-out rates following high-frequency repetitive transcranial magnetic stimulation (rTMS) for treating major depression: a systematic review and meta-analysis of randomized, double-blind and sham-controlled trials. *Psychol Med.* 2014; 44 (2): 225–39.
11. Sehatzadeh S, Daskalakis ZJ, Yap B, Tu HA, Palimaka S, Bowen JM, et al. Unilateral and bilateral repetitive transcranial magnetic stimulation for treatment-resistant depression: a meta-analysis of randomized controlled trials over 2 decades. *J Psychiatry Neurosci.* 2019; 44 (3): 151–63.
12. Fox MD, Buckner RL, White MP, Greicius MD, Pascual-Leone A. Efficacy of transcranial magnetic stimulation targets for depression is related to intrinsic functional connectivity with the subgenual cingulate. *Biol Psychiatry.* 2012; 72 (7): 595–603.
13. Drevets WC, Price JL, Furey ML. Brain structural and functional abnormalities in mood disorders: implications for neurocircuitry

- models of depression. *Brain Struct Funct.* 2008; 213 (1–2): 93–118.
14. Антонович Б. А., Майорова Л. А., Цукарзи Э. Э., Мосолов С. Н. Нейронные сети состояния покоя при депрессиях и перспективы применения персонифицированной ТМС. Современная терапия психических расстройств. 2019; 3: 2–11.
 15. Пойдашева А. Г., Сеницын Д. О., Бакулин И. С., Супонева Н. А., Маслеников Н. В., Цукарзи Э. Э. и др. Определение мишени для транскраниальной магнитной стимуляции у пациентов с резистентным к фармакотерапии депрессивным эпизодом на основе индивидуальных параметров функциональной магнитно-резонансной томографии покоя (пилотное слепое контролируемое исследование). *Неврология, нейропсихиатрия, психосоматика.* 2019; 11 (4): 44–50.
 16. Sonmez AI, Camsari DD, Nandakumar AL, Voort JLV, Kung S, Lewis CP, et al. Accelerated TMS for Depression: A systematic review and meta-analysis. *Psychiatry Res.* 2019; 273: 770–81.
 17. Cole EJ, Stimpson KH, Bentzley BS, Gulser M, Cherian K, Tischler C, et al. Stanford Accelerated Intelligent Neuromodulation Therapy for Treatment-Resistant Depression. *Am J Psychiatry.* 2020; 177 (8): 716–26.
 18. Cole EJ, Phillips AL, Bentzley BS, Stimpson KH, Nejad R, Barmak F, et al. Stanford Neuromodulation Therapy (SNT): A Double-Blind Randomized Controlled Trial. *Am J Psychiatry.* 2022; 179 (2): 132–41.
 19. Ахапкин Р. В., Букреева Н. Д., Вазагаева Т. И., Костюкова Е. Г., Мазо Г. Э., Мосолов С. Н. Депрессивный эпизод, рекуррентное депрессивное расстройство. Клинические рекомендации. Взрослые. Электронное издание. 2021. Доступно по ссылке: https://cr.minzdrav.gov.ru/recomend/301_2.
 20. Мосолов С. Н., Костюкова Е. Г., Ладыженский М. Я. Алгоритм биологической терапии острого эпизода рекуррентного депрессивного расстройства. Современная терапия психических расстройств. 2016; 3: 27–40.
 21. Montgomery SA, Asberg M. A new depression scale designed to be sensitive to change. *Br J Psychiatry.* 1979; 134: 382–9.
 22. Hawley CJ, Gale TM, Sivakumaran T; Hertfordshire Neuroscience Research group. Defining remission by cut off score on the MADRS: selecting the optimal value. *J Affect Disord.* 2002; 72 (2): 177–84.
 23. Fekadu A, Wooderson SC, Markopoulou K, Cleare AJ. The Maudsley Staging Method for treatment-resistant depression: prediction of longer-term outcome and persistence of symptoms. *J Clin Psychiatry.* 2009; 70 (7): 952–7.
 24. Siddiqi SH, Taylor SF, Cooke D, Pascual-Leone A, George MS, Fox MD. Distinct Symptom-Specific Treatment Targets for Circuit-Based Neuromodulation. *Am J Psychiatry.* 2020; 177 (5): 435–46.
 25. Loo CK, Mitchell PB, McFarquhar TF, Malhi GS, Sachdev PS. A sham-controlled trial of the efficacy and safety of twice-daily rTMS in major depression. *Psychol Med.* 2007; 37 (3): 341–9.
 26. Blumberger DM, Vila-Rodriguez F, Wang W, Knyahnytska Y, Butterfield M, Noda Y, et al. A randomized sham controlled comparison of once vs twice-daily intermittent theta burst stimulation in depression: A Canadian rTMS treatment and biomarker network in depression (CARTBIND) study. *Brain Stimul.* 2021; 14 (6): 1447–55.
 27. Fitzgerald PB, Hoy KE, Elliot D, Susan McQueen RN, Wambeek LE, Daskalakis ZJ. Accelerated repetitive transcranial magnetic stimulation in the treatment of depression. *Neuropsychopharmacology.* 2018; 43 (7): 1565–72.
 28. Abraham WC, Bear MF. Metaplasticity: the plasticity of synaptic plasticity. *Trends Neurosci.* 1996; 19 (4): 126–30.

SYSTEMIC INFLAMMATION MARKERS OF DIET-INDUCED METABOLIC SYNDROME IN RAT MODEL

Birulina JG , Voronkova OV, Ivanov VV, Buyko EE, Shcherbakova MM, Chernyshov NA, Motlokhova EA

Siberian State Medical University, Tomsk, Russia

Chronic systemic inflammation is essential in many chronic non-infectious diseases, including type 2 diabetes, obesity and metabolic syndrome (MS). This study aimed at characterization of systemic inflammatory reaction as a component of diet-induced MS in rat model. Thirty-three male Wistar rats were distributed into two groups designated 'control' ($n = 15$) and 'experimental (MS)' ($n = 18$). The groups were fed, respectively, regular and high-fat/high-carbohydrate diets for 12 weeks. The intensity of systemic inflammatory process against the background of metabolic impairments was assessed by total and differential counts of white blood cells and serum levels of total protein, C-reactive protein, cytokines (IL6, IL10 and TNF α), insulin and leptin. We also assessed the production of reactive oxygen species in adipose tissue samples. The experiment revealed signs of systemic inflammation in MS as compared to control, including reactive leukocytosis, hyperproteinemia and increased serum levels of C-reactive protein (2.6-fold; $p = 0.001$), IL10 (3.7-fold; $p = 0.029$) and TNF α (4.2-fold; $p = 0.035$). The observed changes were accompanied by elevated metabolic activity of visceral adipose tissue, indicated by hyperleptinemia and increased free radical oxidation intensity. Pairwise positive correlations of serum levels were revealed for leptin and insulin ($r = 0.701$; $p = 0.001$) and leptin and IL10 ($r = 0.523$; $p = 0.012$). Thus, high-fat/high-carbohydrate diet promoted metabolic impairments concomitantly with early signs of systemic inflammation characteristic of MS and obesity.

Keywords: metabolic syndrome, insulin resistance, obesity, inflammation, C-reactive protein, IL10, TNF α

Funding: the study was supported by the Russian Science Foundation, Grant № 22-25-20039, <https://rscf.ru/project/22-25-20039/> and funds of the Tomsk Region Administration.

Author contribution: Birulina JG, Voronkova OV — concept and design, manuscript writing; Ivanov VV, Buyko EE — metabolic syndrome modeling, biochemical blood tests; Shcherbakova MM — blood cytokine assay; Chernyshov NA — literature analysis, hemogram tests; Motlokhova EA — statistical analysis.

Compliance with ethical standards: the study was approved by Ethical Review Board at SibSMU (Protocol № 8201 of 27 March 2020) and carried out in compliance with humanity principles stated in the 86/609 EEC Directive and the Declaration of Helsinki.

 **Correspondence should be addressed:** Julia G. Birulina
Moskovsky Trakt, 2, str. 7, Tomsk, 634050, Russia; birulina20@yandex.ru

Received: 11.08.2022 **Accepted:** 25.08.2022 **Published online:** 30.08.2022

DOI: 10.24075/brsmu.2022.043

МАРКЕРЫ СИСТЕМОГО ВОСПАЛЕНИЯ У КРЫС В МОДЕЛИ ДИЕТ-ИНДУЦИРОВАННОГО МЕТАБОЛИЧЕСКОГО СИНДРОМА

Ю. Г. Бирулина , О. В. Воронкова, В. В. Иванов, Е. Е. Буйко, М. М. Щербакова, Н. А. Чернышов, Е. А. Мотлохова

Сибирский государственный медицинский университет, Томск, Россия

Системное воспаление лежит в основе патогенеза многих хронических неинфекционных заболеваний, в том числе таких, как сахарный диабет 2-го типа, ожирение, метаболический синдром (МС). Целью работы было оценить изменения параметров системной воспалительной реакции у крыс в модели диет-индуцированного МС. Исследование выполнено на 33 крысах-самцах Wistar, распределенных на контрольную и экспериментальную группы. Крысы контрольной группы ($n = 15$) находились на стандартной диете. Крысы экспериментальной группы ($n = 18$) в течение 12 недель находились на высокожировой и высокоуглеводной диете. Для оценки интенсивности воспалительного процесса на фоне метаболических нарушений определяли общее количество и морфологический состав лейкоцитов крови, концентрацию общего белка, С-реактивного белка, концентрацию цитокинов IL6, IL10, TNF α , инсулина и лептина. В образцах жировой ткани оценивали уровень продукции активных форм кислорода. В результате проведенного эксперимента у крыс с МС были зарегистрированы общие признаки воспаления: реактивный лейкоцитоз, гиперпротеинемия, повышение концентрации С-реактивного белка в 2,6 раза ($p = 0,001$), IL10 — в 3,7 раза ($p = 0,029$), TNF α — в 4,2 раза ($p = 0,035$). Выявленные изменения происходили на фоне повышения метаболической активности висцеральной жировой ткани, о чем свидетельствовали гиперлептинемия и высокая интенсивность процессов свободнорадикального окисления. Были обнаружены положительные корреляционные взаимосвязи между уровнями лептина и инсулина в крови ($r = 0,701$; $p = 0,001$), а также между сывороточной концентрацией лептина и IL10 ($r = 0,523$; $p = 0,012$). Таким образом, высокожировая и высокоуглеводная диета наряду с метаболическими нарушениями позволяет воспроизвести ранние признаки системного воспаления, характерные для МС и ожирения.

Ключевые слова: метаболический синдром, инсулинорезистентность, ожирение, воспаление, С-реактивный белок, IL10, TNF α

Финансирование: исследование выполнено за счет гранта Российского научного фонда № 22-25-20039, <https://rscf.ru/project/22-25-20039/> и средств Администрации Томской области.

Вклад авторов: Ю. Г. Бирулина, О. В. Воронкова — разработка концепции и дизайна, написание рукописи; В. В. Иванов, Е. Е. Буйко — моделирование метаболического синдрома на животных, выполнение анализа биохимических показателей крови; М. М. Щербакова — исследование цитокинов крови, Н. А. Чернышов — анализ литературы, исследование гемограммы; Е. А. Мотлохова — статистическая обработка результатов.

Соблюдение этических стандартов: исследование одобрено этическим комитетом СибГМУ (протокол № 8201 от 27 марта 2020 г.). Исследование выполнено с соблюдением принципов гуманности, изложенных в директивах Европейского сообщества (86/609/ЕЕС) и Хельсинкской декларации.

 **Для корреспонденции:** Юлия Георгиевна Бирулина
ул. Московский тракт, д. 2, строение 7, г. Томск, 634050, Россия; birulina20@yandex.ru

Статья получена: 11.08.2022 **Статья принята к печати:** 25.08.2022 **Опубликована онлайн:** 30.08.2022

DOI: 10.24075/vrgmu.2022.043

Chronic systemic inflammation is essential in many multifactorial non-infectious diseases, including such alimentary-dependent conditions as type 2 diabetes, obesity and metabolic syndrome (MS). The low-grade chronic inflammation of adipose tissue is

a key contributor to the insulin resistance development [1]. Metabolic impairments (hyperglycemia, hyperinsulinemia, dyslipidemia) confer pro-inflammatory properties to cellular elements in adipose tissue, with macrophage functionalities

switching from anti-inflammatory M2 to pro-inflammatory M1. Together with hypertrophied adipose cells, the M1-polarized resident macrophages produce vast quantities of adipokines (leptin, resistin, etc.), pro-inflammatory cytokines (IL6, TNF α , IL1 β , etc.) and chemokines (MCP-1, MIF, CCL-2, etc.), which stimulate infiltration of adipose tissue with recruited monocytic macrophages arriving from circulation [1, 2] thus supporting perpetuation of the inflammatory process and potentiating insulin resistance.

Although subclinical chronic inflammation in patients with MS is a well-known fact, no clinical-laboratory criteria for the basic phenomena of chronic systemic inflammation, (including subtypes, stages, compensatory reactions, maladaptation and damage) have been established. Experimental animal models provide an essential tool for the analysis of early and delayed manifestations of systemic inflammatory reactions as well as their specific mechanisms in diseases that affect multiple parameters of homeostasis [3].

One of the common principles used for in vivo modeling of the obesity-associated MS involves combined high-fat, high-carbohydrate (HFHC) diets fed *ad libitum* [4, 5]. Such diets provide sustainable models of metabolic impairments (insulin resistance, hyperglycemia, dyslipidemia, etc.) etiopathogenetically similar to alimentary-constitutional obesity in humans. At the same time, it has been noted that in only 60–80% of animal models the diet-induced obesity eventually conveys a spectrum of metabolic impairments fully corresponding to MS [6, 7]. Accordingly, MS modeling should involve identification and analysis of additional parameters potentially useful as valid biomarkers of pathogenesis in MS and associated conditions including chronic systemic inflammation.

This study aimed at characterization of systemic inflammatory reaction as a component of diet-induced MS in rat model.

METHODS

Experimental MS was modeled in male Wistar rats (33 animals, body weight 280.5 \times 36.1 g, age 6 weeks at the start of the experiment). The rats obtained from Goldberg Research Institute of Pharmacology and Regenerative Medicine (Tomsk, Russia) and randomized into control and experimental groups (15 and 18 animals, respectively) were housed in polypropylene cages (1612 cm² floor area), three individuals per cage at 20–26 °C, 40–70% relative humidity and 12:12 light cycle. The animals were included in the study based on the following criteria: lack of explicit health problems; body weight deviation from the average value within 10%. The control group animals received a standard 24 : 6 : 44% protein-fat-carbohydrate diet (Delta Feeds chow; BioPro, Russia) with *ad libitum* access to food and water. The experimental (MS) group animals received a HFHC diet of the standard chow (66%) mixed with rendered lard (17%), fructose (17%) and cholesterol (0.25%; Sigma, USA) to a 16 : 21 : 54% protein-fat-carbohydrate ratio and replacement of drinking water with a 20% fructose solution. The experiment lasted 12 weeks.

Consistency of the model with established criteria for MS was tested as described previously [5, 8]. The recorded parameters were as follows: systemic arterial pressure ("Systola" system for non-invasive measurement of blood pressure in rodents; Neurobotics, Russia), body weight (Pioneer PX224 analytical balance; OHAUS, China), weight fractions of visceral adipose tissue and the liver (g per 100 g body weight) and biochemical indicators including serum glucose fasting, oral glucose tolerance test by spectrophotometry using enzymatic

kits (Chronolab; Spain), triacylglycerol (TAG), total cholesterol (TC) and low-density (LDL-C), very low-density (VLDL-C) and high-density (HDL-C) lipoproteins levels (Architect c4000 clinical chemistry analyzer; Abbot, USA).

The animals were withdrawn from the experiment by CO₂ asphyxia. The blood was collected from the heart into two test tubes: with a clotting activator for serum production and subsequent biochemical and enzyme immunoassay and with an anticoagulant for WBC quantitation.

The inflammatory process intensity was assessed by total and differential white blood cell (WBC) quantitation using BC-2800 Vet automatic hematology analyzer (Mindray; China), Bradford total protein assay and high-sensitivity C-reactive protein test (Rat CRP ELISA Kit; Elabscience Biotechnology, China).

Immunsorbent assay was used to assess serum levels of IL6, IL10 and TNF α (corresponding kits by Bender MedSystems GmbH, Austria), insulin (Insulin Rat ELISA Kit; Thermo Fisher Scientific, USA) and leptin (Leptin Rat ELISA Kit; Thermo Fisher Scientific, USA). The homeostatic model for assessing insulin resistance (HOMA-IR) was calculated by the formula:

$$[\text{serum insulin}] \times [\text{serum glucose}] / 22.5$$

The intensity of local inflammatory process in fat tissue was accessed through reactive oxygen species (ROS) production rate measured with the 2,3-dihydrodichlorofluorescein diacetate (DHCF-DA) assay, by incubation of 50 mg fragments of visceral fat tissue in 10 μ M DHCF-DA for 60 min. The fluorescence was measured at an excitation wavelength of 530 nm and an emission wavelength of 485 nm using a microplate reader (Infinite 200 Pro M-plex; Tecan, Switzerland) [9].

Statistical analysis was carried out in SPSS Statistics 23 (IBM; USA). Data complying with the normal distribution law are presented as means and standard deviations, M \pm SD, non-complying — as medians and interquartile ranges, Me (Q₂₅; Q₇₅). Between-the-group comparisons were made by Student's t-test or Mann-Whitney U test. The differences were considered significant at $p < 0.05$. Statistical relationships between quantitative indicators were assessed by calculating Spearman rank correlation coefficient or Pearson correlation coefficient for pairs.

RESULTS

The 12-week HFHC diet promoted physiological and laboratory manifestations of metabolic impairments in animals of experimental group (MS). The analysis of morphometric/physiological/biochemical indicators revealed arterial hypertension, increased body weight and increased relative weights of the liver and visceral adipose tissue in animals with modeled MS compared to control group. Biochemical tests revealed impaired glucose tolerance (increased area under curve for glucose concentration on time, AUC_{0–120}), fasting hyperglycemia and altered lipid spectrum indicators including increased serum levels of TAG, TC, LDL-C and VLDL-C specifically in animals with modeled MS (Table 1). These findings characterize the model as consistent and suitable for the analysis of accessory criteria in MS.

Serum insulin levels were used as insulin resistance indicator in experimental MS. In animals with modeled MS, serum insulin levels were increased more than two-fold compared with control group, and HOMA-IR was 1.3 \times 0.4. Animals with modeled MS also presented with elevated serum levels of the adipose tissue hormone leptin, which exceeded control values 1.5-fold on average (Table 1).

The analysis of free radical oxidation rates in visceral fat tissue revealed ROS production increased significantly to

Table 1. Physiological parameters and biochemical markers of metabolic syndrome in rats

Parameter	Group		<i>p</i>
	Control, <i>n</i> = 15	Experimental, <i>n</i> = 18	
Body weight, g	433.32 ± 39.4	489.1 ± 47.9	0.01
Systolic blood pressure, mm Hg	130.4 ± 9.5	145.1 ± 8.7	0.01
Diastolic blood pressure, mm Hg	86.5 ± 9.3	101.4 ± 12.2	0.028
Adipose tissue/body weight ratio	2.2 ± 0.22.2 ± 0.2	4.3 ± 0.64.3 ± 0.6	0.001
Liver/body weight ratio	3.1 ± 0.43.1 ± 0.4	4.2 ± 0.54.2 ± 0.5	0.001
Glucose fasting, mmol/L	4.9 ± 0.5	7.6 ± 0.4	0.001
AUC _{0–120} , mmol/L × 120 minAUC _{0–120} , mmol/L × 120 min	752.2 ± 50.4	940.9 ± 55.8	0.001
TC, mmol/L	1.7 ± 0.2	2.3 ± 0.3	0.001
HDL-C, mmol/L	0.6 ± 0.1	0.4 ± 0.1	0.003
LDL-C, mmol/L	0.9 ± 0.2	1.4 ± 0.4	0.02
VLDL-C, mmol/L	0.3 ± 0.1	0.5 ± 0.1	0.03
TAG, mmol/L	0.7 ± 0.2	1.7 ± 0.5	0.001
Insulin, pmol/L	11.2 ± 0.8	24.2 ± 5.6	0.001
HOMA-IR	0.4 ± 0.1	1.3 ± 0.4	0.004
Leptin, ng/mL	3.1 ± 0.3	4.5 ± 0.1	0.01
Total protein, g/L	52.7 ± 3.4	66.7 ± 3.8	0.015
C-reactive protein, ng/mL	4.0 ± 0.4	10.5 ± 1.3	0.001

Note: The data are given as M ± SD; AUC_{0–120} is the area under curve of glucose concentration on time (glucose tolerance test); *p*-values characterize experimental vs control group comparisons.

2.5 conventional units — more than two-fold compared with control group (1.2 conventional units, *p* = 0.008).

Biochemical tests revealed serum levels of total protein and C-reactive protein elevated, respectively, 1.3-fold and 2.6-fold in experimental MS compared with control values (Table 1).

The analysis also revealed significant increase in total WBC counts, as well as total and differential blood granulocyte counts, in animals with experimental MS (Table 2).

Serum levels of IL10 and TNFα in rats with HFHC diet-induced metabolic impairments exceeded the corresponding control values, respectively, 3.7- and 4.2-fold on average (Table 3). A similar trend observed for IL6 proved statistically non-significant.

DISCUSSION

Two basic methodologies for MS modeling in small rodents have been established in experimental medical biology: (1) animal strains genetically predisposed to diabetes/obesity/cardiovascular diseases and (2) imbalanced diets with modified nutrient ratio (rich in fats and sugars) [4, 10]. Both approaches result in the excessive accumulation of visceral fat as a key pathogenic factor mediating the profound metabolic impairments.

Despite the widespread use of HFHC diets as a basis for MS modeling, certain methodological complications have been recognized as hampering verification of the efficacy. For example, the developing visceral obesity cannot be monitored in medical terms, as routine biometric screenings (body mass indexing, waist measurements, etc.) are not extrapolatable to rodents. Several studies demonstrate that such hallmarks of MS as hypertension, dyslipoproteinemia and hyperglycemia are only partly reproducible in animals [11, 12]. In some cases, these limitations are due to insufficient duration of the diet, as well as age- and sex-related differences, genetic distinctions of particular strains of experimental animals, systematic errors in nutrition formula/regimen, etc.

The rates of metabolic activity of fat tissue can provide useful indicators for MS verification in laboratory animals. The leptin/ghrelin ratio has been shown to correlate with changes in body, splenic and fat weights in Wistar rats with experimental dyslipidemia and altered levels of inflammation-regulating cytokines (MCP-1, M-CSF, IL18 and RANTES) which identifies these criteria as prospective biomarkers of direction and severity of metabolic impairments in obesity and MS [13].

Chronic inflammation of fat tissue, a strong pathogenic factor in MS, develops on the background of insulin resistance coupled to hyperglycemia and dyslipoproteinemia [1, 2]. The highly active signaling substances (adipokines, pro-inflammatory cytokines) produced by adipose and stromal cells facilitate macrophage infiltration thus supporting the maintenance of local inflammatory response [14].

Our analysis of metabolic activity of cellular elements in the visceral fat of rats after a 12-week HFHC diet reveals augmentation of free-radical reactions with a 2-fold increase in the spontaneous ROS production levels compared with control group.

The high secretory activity of adipose cells in animals with modeled MS is also indicated by elevated blood levels of leptin showing an average 1.5-fold increase compared with control group (Table 1). At that, serum levels of leptin and insulin revealed a moderate positive correlation (*r* = 0.701; *p* = 0.001).

Leptin is predominantly produced by adipose cells of white fat tissue, and its blood levels correlate with the visceral fat volume. Under physiological conditions, leptin inhibits insulin production by the pancreas [15]. The MS-associated hyperleptinemia observed by us in this study is most probably of compensatory nature, reflecting insulin resistance and the elevated blood levels of insulin. Incidentally, such metabolic impairments as hyperglycemia and dyslipoproteinemia have been associated with decreased expression of leptin receptors on cells, promoting resistance [16, 17].

Based on its structure, leptin can be classified as pro-inflammatory adipokine. Leptin participates in chemotaxis

Table 2. Hematological parameters for experimental and control groups

Parameter	Group		<i>p</i>
	Control, <i>n</i> = 15	Experimental, <i>n</i> = 18	
Leukocytes, 10 ⁹ /L	9.9 (9.4; 10.9)	13.7 (11.4; 15.0)	0.001
Lymphocytes, 10 ⁹ /L	7.6 (5.9; 8.3)	7.1 (6.4; 8.5)	0.84
Monocytes, 10 ⁹ /L	0.4 (0.2; 0.4)	0.5 (0.3; 0.4)	0.166
Granulocytes, 10 ⁹ /L	2.5 (1.7; 3.6)	3.9 (3.2; 4.4)	0.003
Lymphocytes, %	65.3 (64.2; 67.6)	64.2 (62.7; 66.2)	0.343
Monocytes, %	3.4 (3.0; 3.6)	3.5 (3.1; 4.0)	0.1
Granulocytes, %	28.2 (25.9; 31.3)	33.2 (31.5; 34.2)	0.001

Note: The data are given as Me (Q₂₅; Q₇₅); *p*-values characterize experimental vs control group comparisons.

Table 3. Blood cytokine levels for experimental and control groups

Parameter	Group		<i>p</i>
	Control, <i>n</i> = 15	Experimental, <i>n</i> = 18	
IL6, pg/mL	5.5 (2.3; 6.3)	7.8 (4.7; 14.1)	0.152
IL10, pg/mL	11.8 (6.0; 23.8)	43.3 (21.9; 54.7)	0.029
TNF α , pg/mL	2.6 (2.6; 5.2)	10.8 (6.4; 11.7)	0.035

Note: The data are given as Me (Q₂₅; Q₇₅); *p*-values characterize experimental vs control group comparisons.

regulation and neutrophil activation, T cell differentiation and NK cell pool maintenance. At the humoral level, leptin stimulates production of TNF α and IL6. Increased secretion of leptin by adipose cells attracts macrophages and facilitates their transfer to adipose tissue by stimulating angiogenesis [18].

The metabolic conditions relevant for activation of cellular elements in fat tissue (notably the levels of glucose, insulin and fatty acids) have been shown to determine its cytokine repertoire. For example, high concentrations of free fatty acids can activate TLR4 receptors on macrophages, indirectly triggering expression of genes responsible for the inflammatory mediator synthesis [2, 14]. This leads to formation of the 'vicious circle' in the adipose tissue inflammation pathogenesis, as systemic effects of certain pro-inflammatory cytokines include fatty acid synthesis activation and increase in their blood levels through suppression of adiponectin secretion and regulation of production for other cytokines.

In this study, we recorded a statistically significant increase in serum levels of TNF α and IL10 in rats with experimentally induced MS compared to control animals (Table 3).

At early stages of inflammation, the balance between defensive-adaptive and pathological inflammatory reactions is ensured by anti-inflammatory cytokines (IL10, IL13, TGF β , etc.), which limit tissue damage by inhibiting expression of major histocompatibility complex class II and other costimulatory molecules on immunocompetent cells [19]. This probably explains the elevated serum levels of anti-inflammatory IL10 in experimental group animals with MS against the background of metabolic impairments. Such inference is indirectly supported by a moderate positive correlation between IL10 and leptin levels ($r = 0.523$; $p = 0.012$).

Of note, progression of MS and obesity may be accompanied by a decrease in production of anti-inflammatory cytokines and hormones (ghrelin, adiponectin) by fat tissue, which enhances the mononuclear cell infiltration of fat tissue and aggravates the inflammation [20, 21]. As a rule, this is a low-grade inflammation, given that the anti-inflammatory resistance factors are capable of prolonged deterrence of the generalized process and prevent the deployment of secondary damage against the background of chronic systemic alterations. Accordingly, compared with acute inflammatory conditions, chronic inflammation is accompanied by modest shifts in systemic indicators.

In this study we assessed the dynamics of systemic manifestations of the inflammatory process confined to visceral fat tissue. Apart from the altered cytokine levels, animals with MS showed significant increases in total WBC and differential granulocyte counts, as well as serum levels of total and C-reactive protein compared to control animals.

Many inflammatory conditions are accompanied by elevated production of acute phase proteins, chiefly by hepatocytes. Under pathological conditions, white adipose cells are also capable of producing high amounts of C-reactive protein, which exacerbates the glucose metabolism impairment and aggravates insulin resistance [22, 23].

Reactive leukocytosis can be attributed to particular components in MS pathogenesis. High-fat diets have been shown to induce myeloid hyperplasia in animal models, especially with regard to neutrophil cellular patterns [24]. Several studies enrolling patients with glucose intolerance and obesity revealed a positive correlation between antropometric/physiological/biochemical indicators (body mass index, arterial hypertension, hyperinsulinemia, dyslipoproteinemia) and increased WBC counts [25–27]. A possible role of leptin in MS-associated leukocytosis has been highlighted: leptin and its receptors have been implicated in hemopoiesis-stimulating signaling in the red bone marrow [25].

Glycation end-products, ROS and pro-inflammatory cytokines exert similar effects on hemopoietic cells and mature leukocytes. Pro-inflammatory cytokines are important inducers of leukocytosis, particularly neutrophilic, by multiple mechanisms including demargination of intravascular neutrophils and facilitation of granulocytopenia and neutrophil exit in the bone marrow [28, 29].

CONCLUSIONS

The experiment revealed signs of systemic inflammation, including reactive leukocytosis, hyperproteinemia and elevated serum levels of C-reactive protein and cytokines TNF α and IL10, alongside the visceral obesity and impaired lipid/carbohydrate metabolism (hyperinsulinemia, hyperglycemia, dyslipoproteinemia) in rats with modeled MS. The observed immunological changes were accompanied by increased metabolic activity of visceral fat tissue, indicated by hyperleptinemia and increased free radical

oxidation rates. Serum levels of leptin positively correlated with serum levels of both insulin and IL10. Thus, apart from metabolic impairments, the 12-week experimental exposure to a HFHC diet reproducibly modeled the early signs of systemic inflammation

characteristic of MS and obesity. Such diet-induced MS models can be considered a convenient tool for studying the early and delayed MS complications mediated by pathogenetic factors of chronic systemic inflammation.

References

- Kryukov NN, Ginzburg MM, Kiseleva EV. Sovremennyy vzglyad na rol' asepticeskogo vospaleniya zhirovoj tkani v geneze ozhireniya i metabolicheskogo sindroma. *Arterial'naya gipertenziya*. 2013; 19 (4): 305–10. Russian.
- McCracken E, Monaghan M, Sreenivasan S. Pathophysiology of the metabolic syndrome. *Clin Dermatol*. 2018; 36 (1): 14–20.
- Makarova MN, Makarov VG. Diet-inducirovannyye modeli metabolicheskix narushenij. *Ehksperimental'nyj metabolicheskij sindrom. Laboratornye zhivotnye dlya nauchnyx issledovanij*. 2018; 1. Dostupno po sсылке: <https://labanimalsjournal.ru/ru/2618723x-2018-01-08>. Russian.
- Kravchuk EN, Galagudza MM. Ehksperimental'nye modeli metabolicheskogo sindroma. *Arterial'naya gipertenziya*. 2014; 20 (5): 377–83. Russian.
- Birulina YuG, Ivanov VV, Buyko EE, Trubacheva OA, Petrova IV, Grechishnikova AYU, i dr. Vliyanie vysokozhirovoj i vysokouglevodnoj diety na kletki krovi krys. *Byulleten' sibirskoj mediciny*. 2021; 20 (3): 6–12. Russian.
- Chernysheva MB, Tsvetkov IS, Diatropov ME, Makarova OV. Morfologicheskie izmeneniya vnutrennix organov i metabolicheskie narusheniya pri ehksperimental'nom alimentarnom ozhirenii. *Klinicheskaya i ehksperimental'naya morfologiya*. 2016; 1 (17): 44–51. Russian.
- Henning RJ. Obesity and obesity-induced inflammatory disease contribute to atherosclerosis: a review of the pathophysiology and treatment of obesity. *Am J Cardiovasc Dis*. 2021; 11 (4): 504–29.
- Birulina YuG, Ivanov VV, Buyko EE, Bykov VV, Nosarev AV, Kovalev IV, Smaglij LV, Gusakova SV, avtory. Sposob modelirovaniya diet-inducirovannogo metabolicheskogo sindroma. FGBOU VO SibGMU Minzdrava Rossii, patentoobladatel'. Patent RF # #2740007 ot 30.12.2020. Russian
- Liu L, Zou P, Zheng L, Linarelli LE, Amarell S, Passaro A, et al. Tamoxifen reduces fat mass by boosting reactive oxygen species. *Cell Death Dis*. 201; 6 (1): e1586.
- Bayrasheva VK, Pchelina IYu, Egorova AEh, Vasilkova ON, Korniyushin OV. Ehksperimental'nye modeli alimentarnogo ozhireniya u krys. *Juvenis Scientia*. 2019; 9–10: 8–13. Russian.
- Lucero D, Olano C, Bursztyn M, Morales C, Stranges A, Friedman S, et al. Supplementation with n-3, n-6, n-9 fatty acids in an insulin resistance animal model: Does it improve VLDL quality? *Food Funct*. 2017; 8 (5): 2053–61.
- Kwitek AE. Rat models of metabolic syndrome. *Methods Mol Biol*. 2019; 2018: 269–85.
- Riger NA, Shipelin VA, Apryatina SA, Gmshinski IV. Immunologicheskije markery alimentarno-inducirovannoj giperlipidemii u krys linii Vistar. *Voprosy pitaniya*. 2019; 88 (3): 44–52. Russian.
- Romantsova TI, Sych YuP. Immunometabolizm i metavospalenie pri ozhirenii. *Ozhirenie i metabolizm*. 2019; 16 (4): 3–17. Russian.
- Ghadge AA, Khaire AA. Leptin as a predictive marker for metabolic syndrome. *Cytokine*. 2019; 121: 154735.
- Gonzalez-Carter D, Goode AE, Fiammengo R, Dunlop IE, Dexter DT, Porter AE. Inhibition of Leptin-ObR Interaction Does not Prevent Leptin Translocation Across a Human Blood-Brain Barrier Model. *J Neuroendocrinol*. 2016; 28 (6). Available from: <https://onlinelibrary.wiley.com/doi/10.1111/jne.12392>.
- Kiernan K, MacIver NJ. The Role of the Adipokine Leptin in Immune Cell Function in Health and Disease. *Front Immunol*. 2021; 11: 622468.
- Frühbeck G, Catalán V, Rodríguez A, et al. Normalization of adiponectin concentrations by leptin replacement in ob/ob mice is accompanied by reductions in systemic oxidative stress and inflammation. *Scientific Reports*. 2017; 7 (1): 2752.
- Lee B-C, Lee J. Cellular and molecular players in adipose tissue inflammation in the development of obesity-induced insulin resistance. *Biochimica et Biophysica Acta (BBA) — Molecular Basis of Disease*. 2014; 1842 (3): 446–62.
- Tanyanskiy DA, Denisenko AD. Vliyanie adiponektina na obmen uglevodov, lipidov i lipoproteinov: analiz signal'nyx mexanizmov. *Ozhirenie i metabolizm*. 2021; 18 (2): 103–11. Russian.
- Ritchie IR, Dyck DJ. Rapid loss of adiponectin-stimulated fatty acid oxidation in skeletal muscle of rats fed a high fat diet is not due to altered muscle redox state. *PLoS One*. 2012; 7 (12): e52193.
- Memoli B, Procino A, Calabrò P, Esposito P, Grandaliano G, Pertosa G, et al. Inflammation may modulate IL6 and C-reactive protein gene expression in the adipose tissue: the role of IL6 cell membrane receptor. *Am J Physiol Endocrinol Metab*. 2007; 293: E1030–E1035.
- Kaneko H, Anzai T, Nagai T, Anzai A, Takahashi T, Mano Y, et al. Human C-reactive protein exacerbates metabolic disorders in association with adipose tissue remodeling. *Cardiovasc Res*. 2011; 1: 546–55.
- do Carmo LS, Rogero MM, Paredes-Gamero EJ, Nogueira-Pedro A, Xavier JG, Cortezet M, et al. A high-fat diet increases interleukin-3 and granulocyte colony-stimulating factor production by bone marrow cells and triggers bone marrow hyperplasia and neutrophilia in Wistar rats. *Exp Biol Med (Maywood)*. 2013; 238 (4): 375–84.
- Purdy JC, Shatzel JJ. The hematologic consequences of obesity. *Eur J Haematol*. 2021; 106 (3): 306–19.
- Farhangi MA, Keshavarz SA, Eshraghian M, Ostadrahimi A, Saboor-Yaraghi AA. White blood cell count in women: relation to inflammatory biomarkers, haematological profiles, visceral adiposity, and other cardiovascular risk factors. *J Health Popul Nutr*. 2013; 31 (1): 58–64.
- Herishanu Y, Rogowski O, Polliack A, Marilus R. Leukocytosis in obese individuals: possible link in patients with unexplained persistent neutrophilia. *European journal of haematology*. 2006; 76 (6): 516–20.
- Pini M, Rhodes DH, Fantuzzi G. Hematological and acute-phase responses to diet-induced obesity in IL6 KO mice. *Cytokine*. 2011; 56 (3): 708–16.
- Netzer N, Gatterer H, Faulhaber M, Burtscher M, Pramsohler S, Pesta D. Hypoxia, oxidative stress and fat. *Biomolecules*. 2015; 5: 1143–50.

Литература

- Крюков Н. Н., Гинзбург М. М., Киселева Е. В. Современный взгляд на роль асептического воспаления жировой ткани в генезе ожирения и метаболического синдрома. *Артериальная гипертензия*. 2013; 19 (4): 305–310.
- McCracken E, Monaghan M, Sreenivasan S. Pathophysiology of the metabolic syndrome. *Clin Dermatol*. 2018; 36 (1): 14–20.
- Макарова М. Н., Макаров В. Г. Диет-индуцированные модели метаболических нарушений. Экспериментальный метаболический синдром. *Лабораторные животные для научных исследований*. 2018; 1. Доступно по ссылке: <https://labanimalsjournal.ru/ru/2618723x-2018-01-08>.
- Кравчук, Е. Н., Галагудза, М. М. Экспериментальные модели

- метаболического синдрома. Артериальная гипертензия. 2014; 20 (5); 377–83.
5. Бирулина Ю. Г., Иванов В. В., Буйко Е. Е., Трубачева О. А., Петрова И. В., Гречишников А. Ю. и др. Влияние высокожировой и высокоуглеводной диеты на клетки крови крыс. Бюллетень сибирской медицины. 2021; 20 (3): 6–12.
 6. Чернышева М. Б., Цветков И. С., Диатроптов М. Е., Макарова О. В. Морфологические изменения внутренних органов и метаболические нарушения при экспериментальном алиментарном ожирении. Клиническая и экспериментальная морфология. 2016; 1 (17): 44–51.
 7. Henning RJ. Obesity and obesity-induced inflammatory disease contribute to atherosclerosis: a review of the pathophysiology and treatment of obesity. *Am J Cardiovasc Dis.* 2021; 11 (4): 504–29.
 8. Бирулина Ю. Г., Иванов В. В., Буйко Е. Е., Быков В. В., Носарев А. В., Ковалев И. В., Смаглий Л. В., Гусакова С. В., авторы. Способ моделирования диет-индуцированного метаболического синдрома. ФГБОУ ВО СибГМУ Минздрава России, патентообладатель. Патент РФ № №2740007 от 30.12.2020.
 9. Liu L, Zou P, Zheng L, Linarelli LE, Amarell S, Passaro A, et. al. Tamoxifen reduces fat mass by boosting reactive oxygen species. *Cell Death Dis.* 2011; 6 (1): e1586.
 10. Байрашева В. К., Пчелин И. Ю., Егорова А. Э., Василькова О. Н., Корнюшин О. В. Экспериментальные модели алиментарного ожирения у крыс. *Juvenis Scientia.* 2019; 9–10: 8–13.
 11. Lucero D, Olano C, Bursztyn M, Morales C, Stranges A, Friedman S, et al. Supplementation with n-3, n-6, n-9 fatty acids in an insulin resistance animal model: Does it improve VLDL quality? *Food Funct.* 2017; 8 (5): 2053–61.
 12. Kwitek AE. Rat models of metabolic syndrome. *Methods Mol Biol.* 2019; 2018: 269–85.
 13. Ригер Н. А., Шипелин В. А., Апрятин С. А., Гмошинский И. В. Иммунологические маркеры алиментарно-индуцированной гиперлипидемии у крыс линии Вистар. *Вопросы питания.* 2019; 88 (3): 44–52.
 14. Романцова Т. И., Сыч Ю. П. Иммунометаболизм и метавоспаление при ожирении. *Ожирение и метаболизм.* 2019; 16 (4): 3–17.
 15. Ghadge AA, Khaire AA. Leptin as a predictive marker for metabolic syndrome. *Cytokine.* 2019; 121: 154735.
 16. Gonzalez-Carter D, Goode AE, Fiammengo R, Dunlop IE, Dexter DT, Porter AE. Inhibition of Leptin-ObR Interaction Does not Prevent Leptin Translocation Across a Human Blood-Brain Barrier Model. *J Neuroendocrinol.* 2016; 28 (6). Available from: <https://onlinelibrary.wiley.com/doi/10.1111/jne.12392>.
 17. Kiernan K, MacIver NJ. The Role of the Adipokine Leptin in Immune Cell Function in Health and Disease. *Front Immunol.* 2021; 11: 622468.
 18. Frühbeck G, Catalán V, Rodríguez A, et al. Normalization of adiponectin concentrations by leptin replacement in ob/ob mice is accompanied by reductions in systemic oxidative stress and inflammation. *Scientific Reports.* 2017; 7 (1): 2752.
 19. Lee B-C, Lee J. Cellular and molecular players in adipose tissue inflammation in the development of obesity-induced insulin resistance. *Biochimica et Biophysica Acta (BBA) — Molecular Basis of Disease.* 2014; 1842 (3): 446–62.
 20. Тянянский Д. А., Денисенко А. Д. Влияние адипонектина на обмен углеводов, липидов и липопротеинов: анализ сигнальных механизмов. *Ожирение и метаболизм.* 2021; 18 (2): 103–11.
 21. Ritchie IR, Dyck DJ. Rapid loss of adiponectin-stimulated fatty acid oxidation in skeletal muscle of rats fed a high fat diet is not due to altered muscle redox state. *PLoS One.* 2012; 7 (12): e52193.
 22. Memoli B, Procino A, Calabrò P, Esposito P, Grandaliano G, Pertosa G, et al. Inflammation may modulate IL6 and C-reactive protein gene expression in the adipose tissue: the role of IL6 cell membrane receptor. *Am J Physiol Endocrinol Metab.* 2007; 293: E1030–E1035.
 23. Kaneko H, Anzai T, Nagai T, Anzai A, Takahashi T, Mano Y, et al. Human C-reactive protein exacerbates metabolic disorders in association with adipose tissue remodeling. *Cardiovasc Res.* 2011; 1: 546–55.
 24. do Carmo LS, Rogero MM, Paredes-Gamero EJ, Nogueira-Pedro A, Xavier JG, Cortezet M, et al. A high-fat diet increases interleukin-3 and granulocyte colony-stimulating factor production by bone marrow cells and triggers bone marrow hyperplasia and neutrophilia in Wistar rats. *Exp Biol Med (Maywood).* 2013; 238 (4): 375–84.
 25. Purdy JC, Shatzel JJ. The hematologic consequences of obesity. *Eur J Haematol.* 2021; 106 (3): 306–19.
 26. Farhangi MA, Keshavarz SA, Eshraghian M, Ostadrahimi A, Saboor-Yaraghi AA. White blood cell count in women: relation to inflammatory biomarkers, haematological profiles, visceral adiposity, and other cardiovascular risk factors. *J Health Popul Nutr.* 2013; 31 (1): 58–64.
 27. Herishanu Y, Rogowski O, Polliack A, Marilus R. Leukocytosis in obese individuals: possible link in patients with unexplained persistent neutrophilia. *European journal of haematology.* 2006; 76 (6): 516–20.
 28. Pini M, Rhodes DH, Fantuzzi G. Hematological and acute-phase responses to diet-induced obesity in IL6 KO mice. *Cytokine.* 2011; 56 (3): 708–16.
 29. Netzer N, Gatterer H, Faulhaber M, Burtscher M, Pramsohler S, Pesta D. Hypoxia, oxidative stress and fat. *Biomolecules.* 2015; 5: 1143–50.

EPOR/CD131-MEDIATED ATTENUATION OF ROTENONE-INDUCED RETINAL DEGENERATION IS ASSOCIATED WITH UPREGULATION OF AUTOPHAGY GENES

Soldatov VO¹✉, Pokrovsky MV¹, Puchenkova OA¹, Zhunusov NS¹, Krayushkina AM¹, Grechina AV², Soldatova MO³, Lapin KN⁴, Bushueva OYu³

¹ Belgorod State National Research University, Belgorod, Russia

² Sechenov First Moscow State Medical University, Moscow, Russia

³ Kursk State Medical University, Kursk, Russia

⁴ Federal Research and Clinical Center for Resuscitation and Rehabilitation, Moscow, Russia

Mitochondrial dysfunction is a key driver of neurodegeneration. This study aimed to evaluate the protective potential of EPOR/CD131 (heterodimeric erythropoietin receptor) stimulation in the neurodegeneration caused by rotenone-induced mitochondrial dysfunction. The effects of erythropoietin (EPO) and an EPO mimetic peptide pHBSF were assessed using *in vivo* and *in vitro* models. Single injections of 10 µg/kg EPO or 5 µg/kg pHBSF significantly alleviated the degeneration of ganglion cells of the retina in a rotenone-induced retinopathy in rats ($p < 0.05$). Consistently, *in vitro* exposure of rotenone-treated murine primary neuroglial cultures to 500 nM EPO or pHBSF significantly rescued the survival of the cells ($p < 0.005$). The observed enhancement of LC3A, ATG7, Beclin-1, Parkin and BNIP3 mRNA expression by EPOR/CD131 agonists implicates the autophagy and mitophagy activation as a plausible mitoprotective mechanism.

Keywords: mitochondrial dysfunction, rotenone-induced retinopathy, EPOR/CD131 receptors, erythropoietin, pHBSF

Funding: State Assignment "Laboratory for Genome Editing in Biomedicine and Veterinary FZWG-2021-0016".

Author contribution: Soldatov VO — concept and design of the study, writing of the manuscript; Pokrovsky MV, Lapin KN — consulting on the concept and design of the study; Puchenkova OA — collection of samples for histological examination and target gene expression analysis; Puchenkova OA, Zhunusov NS — modeling of the rotenone-induced retinal degeneration; Zhunusov NS, Krayushkina AM — *in vitro* assay of rotenone cytoprotective activity; Grechina AV — morphological study; Bushueva OYu, Soldatova MO — RNA extraction, quantitative PCR assay.

Compliance with ethical standards: the study was approved by the ethical committee of the Belgorod State National Research University (Protocol № 06-07/21 of 15 July 2021); all procedures were performed in accordance with the Regulations on Laboratory Practice in the Russian Federation of 2003, in compliance with the 86/609 EEC Directive and ARRIVE guidelines.

✉ **Correspondence should be addressed:** Vladislav O. Soldatov
Pobedy, 85, Belgorod, 308015, Russia; pharmsoldatov@gmail.com

Received: 11.07.2022 **Accepted:** 01.08.2022 **Published online:** 12.08.2022

DOI: 10.24075/brsmu.2022.040

EPOR/CD131-ОПОСРЕДОВАННАЯ РЕТИНОПРОТЕКЦИЯ ПРИ РОТЕНОН-ИНДУЦИРОВАННОЙ НЕЙРОТОКСИЧНОСТИ СВЯЗАНА С УВЕЛИЧЕНИЕМ ЭКСПРЕССИИ ГЕНОВ АУТОФАГИИ

В. О. Солдатов¹✉, М. В. Покровский¹, О. А. Пученкова¹, Н. С. Жунусов¹, А. М. Краюшкина¹, А. В. Гречина², М. О. Солдатова³, К. Н. Лапин⁴, О. Ю. Бушуева³

¹ Белгородский государственный национальный исследовательский университет, Белгород, Россия

² Первый московский государственный медицинский университет имени И. М. Сеченова, Москва, Россия

³ Курский государственный медицинский университет, Курск, Россия

⁴ Федеральный научно-клинический центр реаниматологии и реабилитологии, Москва, Россия

Митохондриальная дисфункция является ключевым драйвером развития нейродегенерации. Целью исследования было оценить протективный потенциал стимуляции EPOR/CD131, гетеродимерного рецептора эритропоэтина (EPO), при нейродегенерации, вызванной нарушением функции митохондрий. В качестве агонистов EPOR/CD131 были использованы EPO или pHBSF, эффективность которых оценивали в условиях *in vivo* и *in vitro*. В модели ротенон-индуцированной ретинопатии однократная инъекция 10 мкг/кг EPO или 5 мкг/кг pHBSF привела к значительному снижению дегенерации ганглионарных клеток сетчатки ($p < 0,05$). Кроме того, инкубация в 500 нМ растворах EPO и pHBSF резко увеличила выживаемость первичной мышшиной нейроглиальной культуры, обработанной ротенонем ($p < 0,005$). Примечательно, что применение агонистов EPOR/CD131 привело к увеличению экспрессии мРНК LC3A, ATG7, Beclin-1, Паркина и BNIP3, что свидетельствует об активации аутофагии и митофагии как потенциальном механизме митопротективного действия.

Ключевые слова: митохондриальная дисфункция, ротенон-индуцированная ретинопатия, рецептор EPOR/CD131, эритропоэтин, pHBSF

Финансирование: государственное задание «Лаборатория геномного редактирования для биомедицины и ветеринарии FZWG-2021-0016».

Вклад авторов: В. О. Солдатов — идея и дизайн эксперимента, написание статьи; М. В. Покровский, А. В. Дейкин — консультация по идее и дизайну исследования; О. А. Пученкова — моделирование ротенон-индуцированной ретинопатии, забор материала для гистологического исследования и анализа экспрессии целевых генов; Н. С. Жунусов — моделирование ротенон-индуцированной ретинопатии, исследование цитопротективной активности ротенона *in vitro*; А. М. Краюшкина — исследование цитопротективной активности ротенона *in vitro*; А. В. Гречина — проведение морфологических исследований; О. Ю. Бушуева — выделение РНК, проведение количественной ПЦР; М. О. Солдатова — выделение РНК, проведение количественной ПЦР.

Соблюдение этических стандартов: исследование одобрено этическим комитетом Белгородского государственного национального исследовательского университета (протокол № 06-07/21 от 15 июля 2021 г.). Все процедуры выполняли согласно Положению о лабораторной практике в РФ 2003 г. с соблюдением требований Директивы Европейского сообщества (86/609 EC) и рекомендаций руководства ARRIVE.

✉ **Для корреспонденции:** Владислав Олегович Солдатов
ул. Победы, д. 85, г. Белгород, 308015, Россия; pharmsoldatov@gmail.com

Статья получена: 11.07.2022 **Статья принята к печати:** 01.08.2022 **Опубликована онлайн:** 12.08.2022

DOI: 10.24075/vrgmu.2022.040

Despite the remarkable advances in our understanding of brain pathophysiology, the progress in handling neurodegenerative disorders remains modest. With the continued increase in human lifespan, the social and medical burden of neurodegenerative disorders is growing ever so fast [1], while etiologic approaches in their management are missing and the available pathogenetic and symptomatic options are of limited efficacy with regard to outcomes. Obviously, this situation dictates the urgent need for new neuroprotection strategies. In ophthalmology, neurodegeneration is of special relevance, as many retinal abnormalities have strong neurodegenerative component [2].

Mitochondrial dysfunctions are often considered as one of the key pathophysiological links in the context of neuronal degeneration [3]. Rather than being a passive indicator, mitochondrial defects have been shown to drive neurodegeneration [4]. Considering the vital importance of the oxidative energy metabolism in nervous tissue, the maintenance of healthy mitochondrial pools is essential for its functioning. Mitophagy is the key cellular mechanism ensuring the timely elimination of defective mitochondria [5]. The term 'mitophagy', introduced by Lemasters [6], stands for selective degradation of unfit mitochondria by macroautophagy [7] involving two major pathways known as PINK1/Parkin-mediated and receptor-mediated autophagy [8].

The timely elimination of defective mitochondria alleviates the oxidative stress and boosts the energy metabolism efficiency [9]. Accordingly, mitophagy stimulation can be considered an efficient neuroprotective strategy. Moreover, the overall fitness of autophagy mechanisms prevents the overloading of neurons with misfolded proteins and counteracts the accumulation of dysfunctional bulk protein aggregates — the common pathomorphological substratum in neurodegeneration [10].

Pharmacological activation of EPOR/CD131, the heterodimeric erythropoietin (EPO) receptor, is a promising

neuroprotection strategy apparently related to the enhancement of mitochondrial function and autophagy [11]. The neuroprotective capacity of EPOR/CD131 agonists [12–14] and their stimulating effect on autophagy [15] have been demonstrated previously. This study aimed to evaluate the neuroprotective capacity of EPO and its peptide analog pHBSP in experimental neuronal damage.

METHODS

Rotenone toxicity was chosen as a model background for the assessment of mitotropic effects *in vivo* and *in vitro*. Pesticide rotenone interrupts the mitochondrial respiratory chain by blocking the electron transfer complex I. The action of rotenone can induce cellular changes characteristic of mitochondrial dysfunctions and neurodegeneration [16].

Animals

The experiments involved 24 male rats purchased from 'Stolbovaya' breeding facilities (Moscow region, Russia) and 3 female CD-1 mice (purchased from Pushchino facilities; Moscow region, Russia) with 24 newborn pups. The animals were housed in rooms with artificial lighting (12/12 h mode) at 21–23 °C, 38–50% humidity and *ad libitum* access to food and water.

The rotenone-induced retinal degeneration model

To induce retinal degeneration 18 male rats (age 20 weeks, body weight 250–275 g) were intravitreally injected by 5 µL of 0.4 mM rotenone in 5% DMSO in Dulbecco's phosphate-buffered saline (D-PBS) (2 nmol/eye) under local novocainamide anesthesia [17].

Table. Primers used in qPCR target gene expression assay

Gene (encoded protein)	Primer sequence	Product length (b.p.)
Retinal degeneration marker		
<i>Nefl</i> (NEFL)	F: 5'-GGAGTACCAGGACCTCCTCA-3'	102
	R: 5'-CTGGTGAAACTGAGCCTGGT-3'	
Autophagy/mitophagy regulating genes		
<i>Becn1</i> (Beclin 1)	F: 5'-CAGCTGGACACTCAGCTCAA-3'	99
	R: 5'-CTGTTCACTGTCGCCCTCAT-3'	
<i>Map1lc3a</i> (LC3A)	F: 5'-TTGGTCAAGATCATCCGGCG-3'	104
	R: 5'-TCAGCGATGGGTGTGGATAC-3'	
<i>Atg7</i> (ATG7)	F: 5'-TCCTGGCCAAGGTGTTAACT	104
	R: 5'-ACTCATGTCCAGATCTCAGC-3'	
<i>Prkn</i> (Паркин)	F: 5'-TGCCATTGAAAAGAATGGAGG-3'	95
	R: 5'-GTTCCACTCACAGCCACAGT-3'	
<i>Bnip3</i> (BNIP3)	F: 5'-AACAGCACTCTGTCTGAGGA-3'	100
	R: 5'-GCCGACTTGACCAATCCCA-3'	
Inflammatory response genes		
<i>Il1b</i> (IL1b)	F: 5'-GGCTGACAGACCCCAAAAGA-3'	101
	R: 5'-TGTCGAGATGCTGCTGTGAG-3'	
<i>Il6</i> (IL6)	F: 5'-CTCATTCTGTCTCGAGCCAC-3'	105
	R: 5'-AGAAGGCAACTGGCTGGAAG-3'	
Housekeeping gene		
<i>Actb</i> (B-actin)	F: 5'-CCACCCGCGAGTACAACC-3'	95
	R: 5'-GACGACGAGCGCAGCGATA-3'	

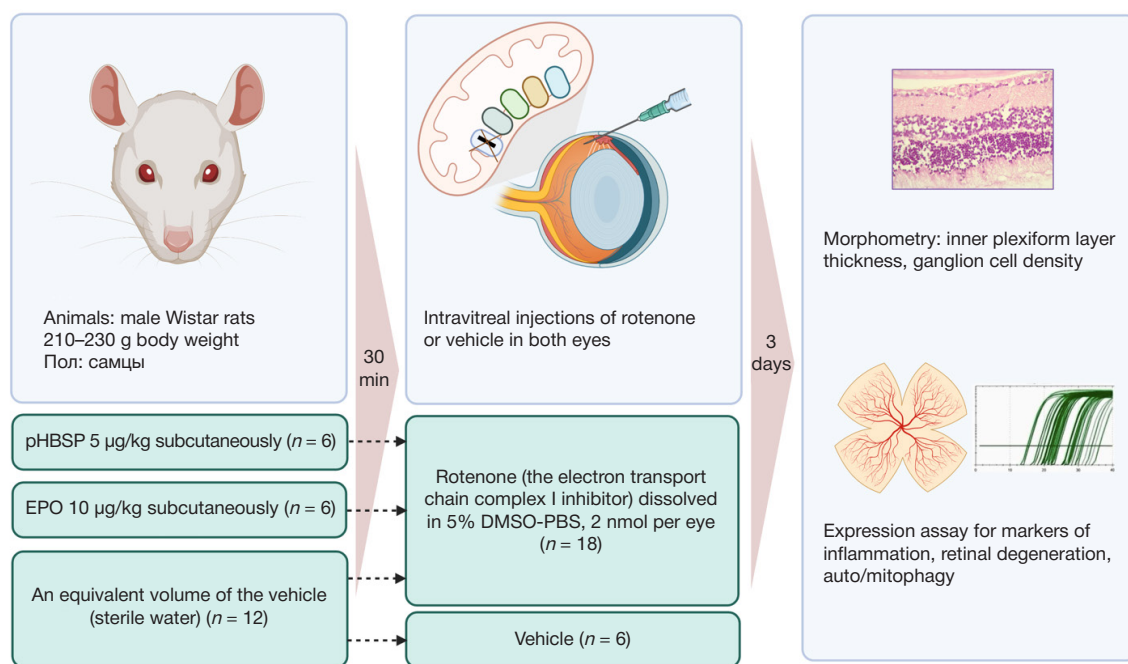


Fig. 1. A scheme of *in vivo* experiments to assess retinoprotective effects of EPOR/CD131 agonists in rotenone-induced retinopathy

The animals were distributed into three equal groups:

- 1) 'control' (sterile water subcutaneously + rotenone intraorbitally);
- 2) 'pHBSP' (pHBSP 5 µg/kg subcutaneously + rotenone intraorbitally);
- 3) 'EPO' (EPO 10 µg/kg subcutaneously + rotenone intraorbitally).

Additionally, the group of 'intact' animals ($n = 6$; matching by age and weight) received identical injections of the vehicle instead of rotenone.

The studied agents (EPO and pHBSP) were injected subcutaneously 30 min before the rotenone administration; the 'control' and 'intact' animals received similar injections of sterile water instead of the agents. On day 3, the eyes were enucleated for histomorphological examination and gene expression analysis (Fig. 1).

Morphological study

The eyeballs were embedded in paraffin after fixation in buffered formalin (pH about 7.0) with 0.002% picric acid followed by gentle aspiration of the vitreous humor and its replacement with molten wax as described previously [18]. All sections were standardized for the area (1 mm above the blind spot) and thickness (7 µm) to enable a proper comparison. The slides were stained by standard protocols [19] for morphometric examination including the inner plexiform layer (IPL) thickness measurements and the nuclei counts per 100 µm of ganglion cell layer.

Quantitative polymerase chain reaction (qPCR) assay

Extraction of the total RNA and reverse transcription were carried out as previously described [20]. The expression of target genes was analyzed by qPCR in a CFX96 real-time PCR thermal cycler (BioRad; USA) using the commercial SYBR® Green Master Mix (Bio-Rad Laboratories, Inc.; USA) and oligonucleotide primers (Evrogen; Russia).

The primers were designed using Primer-BLAST tool (NCBI) with the following stipulations: 1) melting temperature 59–61 °C;

- 2) each primer must span an exon-exon junction or the two primers must fall into different exons; 3) forward and reverse primers in a pair must not form auto- and cross-dimers; 4) the size of PCR product must be 95–107 b.p. (Table).

Processing of the raw qPCR data was carried out using the delta-delta Ct method. Following the amplification, ΔCt value (the difference in threshold cycles between the reference housekeeping gene and threshold cycle for the gene of interest) was calculated for each sample in the Bio-Rad CFX Manager software (Bio-Rad; USA).

The data were transformed by formula (1) [21]:

$$2E \Delta\Delta Ct = \Delta Ct - \Delta Ct_{\text{cont}} \quad (1)$$

where ΔCt is the cycle at which the logarithmic curve of the SYBR Green fluorescence intensity reaches the threshold level (threshold cycle) when running the reaction with housekeeping gene as a reference target;

ΔCt_{contr} is the difference in threshold cycles between the gene of interest and the reference gene.

Cytoprotective effects of pHBSP against rotenone toxicity *in vitro*

The cultures were obtained from brain tissues of CD1 mice collected on postnatal day 1. The animal was decapitated and the head was transferred to a Petri dish placed on ice. The dissection of the skull from skin and fascia was carried out under ice cooling. The brain was extracted and placed in a Petri dish with chilled PBS. The hippocampus, cortex and midbrain portions were dissected under a Leica binocular (magnification $\times 10$) on a cooled glass slide placed in a Petri dish.

The tissues were collected in a tube, washed with D-PBS, trypsinized, and seeded at 20,000 cells in poly-D-lysine-treated plates with Neurobasal medium (PanEco; Russia). After 16–18 h, half of the medium was replaced with Neurobasal™ Plus (Thermo Fisher; USA). The cultures were examined microscopically every 2 days and half of the medium was replaced with a fresh portion; the cultures were maintained like this for 10 days. Rotenone to a final concentration of 2.5 µM

was added to the wells 24 h prior to cell viability assay. After 20 h exposure to rotenone, a putative cytoprotectant (pHBSP or EPO) was added to the suspension in a final concentration of 50 nM or 500 nM. The viability was accessed after staining with [3-(4,5-dimethylthiazol-2-yl)-2,5-diphenyltetrazolium bromide] (MTT) in an automated Cell Counter with cell viability analyzer function (Corning; USA) using CytoSmart software (Axion; the Netherlands).

Statistics

The normality of distributions was challenged by Shapiro–Wilk test. Normally distributed data are presented as M ± SD; for distributions other than normal the data are presented as Me [Q1; Q3]. Statistical processing and visualization of the data were carried out in GraphPad Prism 9.2.0 (Graphpad Software Inc; USA). Significance of the differences was accessed by one-way ANOVA with Kruskal–Wallis test and post-hoc Dunn's test with Benjamini–Hochberg procedure. The heat maps involved statistically unprocessed data.

RESULTS

Cytoprotective effects *in vivo*

The intravitreal injections of rotenone led to specific morphological changes in the retina: its overall thinning, a decrease in IPL thickness and a decrease in ganglion cell numbers. The IPL thickness decreased from 41.92 μm [38.74; 43.70] in the vehicle injection group to 23.59 μm [21.37; 25.62] in the rotenone injection group, whereas the nuclei counts per 100 μm of the ganglion cell layer (GCL) decreased from 8.22 [7.75; 8.83] to 4.78 [4.42; 4.67]. These changes are indicative of ganglion cell degeneration revealing a rotenone-induced neurodegenerative process. The gene expression assay revealed elevated mRNA levels for *Il6* and *Il1b* and reduced expression of the retinal ganglion cell marker *Nefl* additionally confirming the retinal damage.

Both pHBSP and EPO significantly alleviated the rotenone-induced degenerative changes as assessed histologically (Figs. 2A–C) or by gene expression measurements (Fig. 2D). Of note, the effects of pHBSP in reducing retinal degeneration were stronger compared with EPO. The IPL thickness and the nuclei counts per 100 μm of GCL in rats receiving pHBSP constituted 34.34 [31.52; 36.02] and 6.89 [7.00; 7.33], respectively.

Moreover, rats receiving pHBSP or EPO on the background of rotenone had elevated expression levels of the mitophagy/autophagy markers *Map1lc3a*, *Atg7*, *Becn1*, *Prkn* and *Bnip3* in the retina compared with rotenone only (Fig. 2D). Both agents demonstrated similar cytoprotective activity as assessed through the elevated expression of *Nefl* and autophagy protein-encoding genes, and their suppressive effects on the pro-inflammatory cytokine expression were comparable as well.

Thus, single subcutaneous systemic administration of 5 μg/kg pHBSP or 10 μg/kg EPO promoted a reduction in the degree of retinal degeneration induced by intravitreal injections of rotenone. The EPOR/CD131 stimulation-mediated retinoprotective effects are likely to involve a decrease in pro-inflammatory component and an increase in mitophagy, as indicated by a decrease in the expression of inflammation markers and an increase in the expression of auto/mitophagy markers.

Cytoprotective effects *in vitro*

The 24 h incubation of the primary neuroglial cultures in 2.5 μM rotenone killed over 50% of the cells, as reflected by a

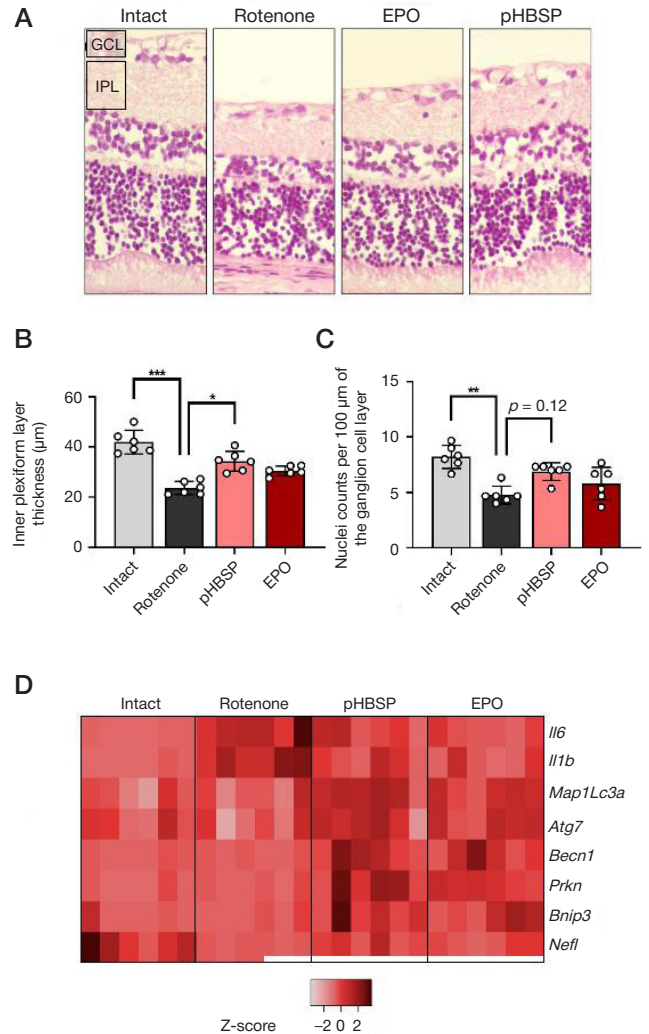


Fig. 2. The therapeutic effect of pHBSP and EPO in the rotenone-induced retinopathy in rats. **A.** Representative histological images of the retina. **B.** The inner plexiform layer thickness measurements. **C.** Nuclei counts in the ganglion cell layer. **D.** Normalized heat map of gene expression levels for inflammation (*Il6*, *Il1b*), autophagy (*Map1Lc3a*, *Atg7*), mitophagy (*Becn1*, *Prkn*, *Bnip3*) and retinal degeneration (*Nefl*) markers. GCL — ganglion cell layer; IPL — inner plexiform layer; * — $p < 0.05$; ** — $p < 0.005$; *** — $p < 0.0005$ (Kruskal–Wallis test, post-hoc Dunn's test).

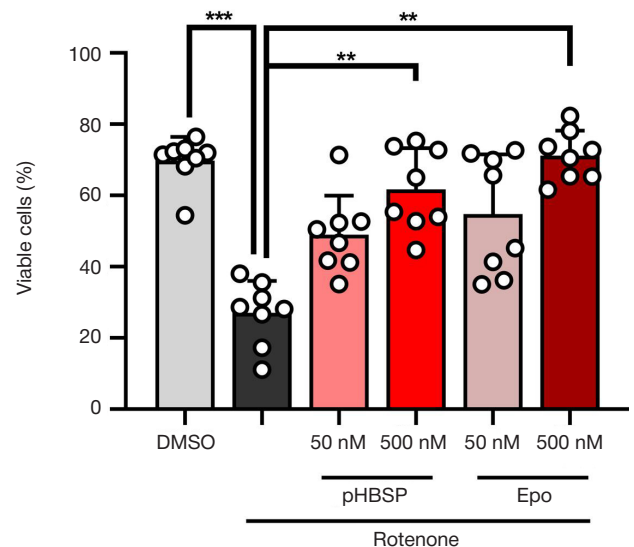


Fig. 3. Cytoprotective effects of pHBSP and EPO on the primary neuroglial cultures treated with 2.5 μM rotenone. ** — $p < 0.005$; *** — $p < 0.0005$ (Dunn's test)

69.80 ± 6.62% to 27.06 ± 8.98% decrease in viability observed in the 'rotenone-only' cultures (Fig. 3). The use of EPOR/CD131-binding agents at 500 nM concentrations significantly rescued the viability of rotenone-treated cultures to 61.73 ± 11.56% ($p < 0.005$) and 71.20 ± 6.97% ($p < 0.005$) for pHBSP and EPO, respectively. At concentrations reduced to 50 nM, both agents showed a similar rescuing tendency, albeit the effects lacked statistical significance.

DISCUSSION

The functional state of mitochondria is considered one of the main factors defining cellular homeostasis. Tissues with the top energy demands, such as the brain and the retina, show the highest sensitivity to mitochondrial abnormalities [2].

In this study, we demonstrate that EPOR/CD131 stimulation can improve the functional state of neuronal cells of the retina *in vivo* and the survival of primary neuroglial cultures *in vitro* under conditions of chemically induced mitochondrial dysfunction. As the neurotoxic effect of rotenone is associated with the respiratory chain disruption in mitochondria, the observed beneficial effects of EPOR/CD131 agonists are most likely due to their mitoprotective action. This assumption is consistent with the previously reported beneficial influence of EPO on mitochondrial function [22]. The results of gene expression analysis support the view of auto- and mitophagy stimulation as a potential mechanism of mitoprotective effects exerted by EPOR/CD131 agonists, indicated by increased mRNA expression levels for LC3A, ATG7, Beclin-1, Prkn and

BNIP3. These results also agree with our previous research on the effects of pHBSP on the autophagy gene expression under conditions of ethanol-induced neurodegeneration in rats [23]. Although we provided no quantitative or semi-quantitative assessment of the autophagy protein phosphorylation levels, some of the identified factors had been already recognized as neuroprotective mediators in mitochondrial dysfunctions [16, 24, 25]. In addition, there is a line of evidence showing a connection of the positive effects of pHBSP with autophagy stimulation. For example, the hepatoprotective activity of pHBSP is accompanied by elevated expression of LC3II, LC3I, and Beclin 1, while being sensitive to autophagy inhibition [15]. Consistently, autophagy has been identified as one of major links mediating the neuroprotective effects of EPO [26].

CONCLUSIONS

Thus, both erythropoietin and pHBSP, a selective peptide agonist of EPOR/CD131, reveal pronounced neuroprotective activity during the rotenone-induced damage. The data implicate the autophagy/mitophagy stimulation as a likely mechanism of the observed pharmacological effects. The use of EPOR/CD131 agonists is a promising direction for the treatment of neurodegenerative processes in the central nervous system and retina. Further studies using specific models of particular neurodegenerative disorders, such as Parkinson's and Alzheimer's diseases or amyotrophic lateral sclerosis, may help to determine the clinical prospects of pHBSP administration.

References

- Logroscino G, Urso D, Savica R. Descriptive epidemiology of neurodegenerative diseases: What are the critical questions? *Neuroepidemiology*. 2022 Jun 21. Online ahead of print. PMID: 35728570.
- Soldatov VO, Kukharsky MS, Belykh AE, Sobolev AM, Deykin AV. Retinal Damage in Amyotrophic Lateral Sclerosis: Underlying Mechanisms. *Eye Brain*. 2021; 13: 131–146. PMID: 34012311.
- Angelova PR, Esteras N, Abramov AY. Mitochondria and lipid peroxidation in the mechanism of neurodegeneration: Finding ways for prevention. *Med Res Rev*. 2021; 41 (2): 770–784. PMID: 32656815.
- Ludtmann MHR, Abramov AY. Mitochondrial calcium imbalance in Parkinson's disease. *Neurosci Lett*. 2018; 663: 86–90. PMID: 28838811.
- Lou G, Palikaras K, Lautrup S, Scheibye-Knudsen M, Tavernarakis N, Fang EF. Mitophagy and Neuroprotection. *Trends Mol Med*. 2020; 26 (1): 8–20. PMID: 31375365.
- Lemasters JJ. Selective mitochondrial autophagy, or mitophagy, as a targeted defense against oxidative stress, mitochondrial dysfunction, and aging. *Rejuvenation Res*. 2005; 8 (1): 3–5. doi: 10.1089/rej.2005.8.3.
- Palikaras K, Lionaki E, Tavernarakis N. Mechanisms of mitophagy in cellular homeostasis, physiology and pathology. *Nat. Cell Biol*. 2018; 20 (9): 1013–1022. doi: 10.1038/s41556-018-0176-2.
- Zuo Z, Jing K, Wu H, Wang S, Ye L, Li Z, Yang C, Pan Q, Liu WJ, Liu HF. Mechanisms and Functions of Mitophagy and Potential Roles in Renal Disease. *Front Physiol*. 2020; 11: 935. PMID: 32903665.
- Moreau K, Luo S, Rubinsztein DC. Cytoprotective roles for autophagy. *Curr Opin Cell Biol*. 2010; 22 (2): 206–211. PMID: 20045304.
- Cai Q, Ganesan D. Regulation of neuronal autophagy and the implications in neurodegenerative diseases. *Neurobiol Dis*. 2022; 162: 105582. PMID: 34890791.
- Senousy MA, Hanafy ME, Shehata N, Rizk SM. Erythropoietin and Bacillus Calmette-Guérin Vaccination Mitigate 3-Nitropropionic Acid-Induced Huntington-like Disease in Rats by Modulating the PI3K/Akt/mTOR/P70S6K Pathway and Enhancing the Autophagy. *ACS Chem Neurosci*. 2022; 13(6): 721–732. PMID: 35226456.
- Nichol A, French C, Little L, Haddad S, Presneill J, Arabi Y, Bailey M, Cooper DJ, Duranteau J, Huet O, Mak A, McArthur C, Pettilä V, Skrifvars M, Vallance S, Varma D, Wills J, Bellomo R. EPO-TBI Investigators; ANZICS Clinical Trials Group. Erythropoietin in traumatic brain injury (EPO-TBI): a double-blind randomised controlled trial. *Lancet*. 2015; 386 (10012): 2499–2506. PMID: 26452709.
- Hemani S, Lane O, Agarwal S, Yu SP, Woodbury A. Systematic Review of Erythropoietin (EPO) for Neuroprotection in Human Studies. *Neurochem Res*. 2021; 46 (4): 732–739. PMID: 33521906.
- Robertson CS, Garcia R, Gaddam SS, Grill RJ, Cerami Hand C, Tian TS, Hannay HJ. Treatment of mild traumatic brain injury with an erythropoietin-mimetic peptide. *J Neurotrauma*. 2013; 30 (9): 765–74. PMID: 22827443.
- Tan R, Tian H, Yang B, Zhang Bo, Dai C, Han Z, Wang M, Li Y, Wei L, Chen D, Wang G, Yang H, He F, Chen Z. Autophagy and Akt in the protective effect of erythropoietin helix B surface peptide against hepatic ischaemia/reperfusion injury in mice. *Sci Rep*. 2018; 8 (1): 14703.
- Filomeni G, Graziani I, De Zio D, Dini L, Centonze D, Rotilio G, Ciriolo MR. Neuroprotection of kaempferol by autophagy in models of rotenone-mediated acute toxicity: possible implications for Parkinson's disease. *Neurobiol Aging*. 2012; 33 (4): 767–85. PMID: 20594614.
- Sasaoka M, Ota T, Kageyama M. Rotenone-induced inner retinal degeneration via presynaptic activation of voltage-dependent sodium and L-type calcium channels in rats. *Sci Rep*. 2020; 10: 969. <https://doi.org/10.1038/s41598-020-57638-y>.
- Benjamin AB, Ahenkorah J, Bismarck AH, Esther D, Addai FK. Improved method of producing satisfactory sections of whole

- eyeball by routine histology. *Microscopy Research and Technique*. 2014; 77 (2): 138–142. PMID: 24249388.
19. Goldberg MF, McLeod S, Tso M, Packo K, Edwards M, Bhutto IA, Baldeosingh, Eberhart C, Weber BHF, Luttly GA. Ocular Histopathology and Immunohistochemical Analysis in the Oldest Known Individual with Autosomal Dominant Vitreoretinopathology. *Ophthalmology Retina*. 2018; 2 (4): 360–378. PMID: 29774302.
 20. Kubekina MV, Silaeva YYu, Bruter AV, Korshunova DS, Ilchuk LA, Okulova YD, Soldatova MO, Seryogina E, Kolesnik IM, Ukolova PA, Korokin MV, Deykin AV. Transgenic mice Cre-dependently expressing mutant polymerase-gamma: novel test-system for pharmacological study of mitoprotective drugs. *Research Results in Pharmacology*. 2021; 7 (3): 33–39.
 21. Livak KJ. Analysis of relative gene expression data using real-time quantitative PCR and the 2(-Delta Delta C(T)) Method. *Methods*. 2001; 25 (4): 402–408. PMID: 11846609.
 22. Plenge U, Belhage B, Guadalupe-Grau A, Andersen PR, Lundby C, Dela F, Stride N, Pott FC, Helge JW, Boushel R. Erythropoietin treatment enhances muscle mitochondrial capacity in humans. *Front Physiol*. 2012; 13(3): 50. PMID: 22419911.
 23. Pokrovskij MV, Soldatov VO, Zatolokina MA et al. Svjaz' EPOR/CD131-oposredovannoj nejroprotekcii pri hronicheskoj jekspozicii jetanola u kryc s moduljaciej jekspressii genov autofagii, apoptoza, nejrovospaljenja i nejronal'noj regeneracii. *Jeksperimental'naja i klinicheskaja farmakologija*. 2021; 84 (2): 91–98. Russian].
 24. Su Y, Zhang Z, Li H, Ma J, Sun L, Shao S, Zhang Z, Hölscher C. A GLP-2 Analogue Protects SH-SY5Y and Neuro-2a Cells Against Mitochondrial Damage, Autophagy Impairments and Apoptosis in a Parkinson Model. *Drug Res (Stuttg)*. 2021; 71 (1): 43–50. PMID: 33022720.
 25. Li Q, Zhang T, Wang J, Zhang Z, Zhai Y, Yang GY, Sun X. Rapamycin attenuates mitochondrial dysfunction via activation of mitophagy in experimental ischemic stroke. *Biochem Biophys Res Commun*. 2014; 444 (2): 182–188. PMID: 24440703.
 26. Jang W, Kim HJ, Li H, Jo KD, Lee MK, Yang HO. The Neuroprotective Effect of Erythropoietin on Rotenone-Induced Neurotoxicity in SH-SY5Y Cells Through the Induction of Autophagy. *Mol Neurobiol*. 2016; 53 (6): 3812–3821. PMID: 26156288.

Литература

1. Logroscino G, Urso D, Savica R. Descriptive epidemiology of neurodegenerative diseases: What are the critical questions? *Neuroepidemiology*. 2022 Jun 21. Online ahead of print. PMID: 35728570.
2. Soldatov VO, Kukharsky MS, Belykh AE, Sobolev AM, Deykin AV. Retinal Damage in Amyotrophic Lateral Sclerosis: Underlying Mechanisms. *Eye Brain*. 2021; 13: 131–146. PMID: 34012311.
3. Angelova PR, Esteras N, Abramov AY. Mitochondria and lipid peroxidation in the mechanism of neurodegeneration: Finding ways for prevention. *Med Res Rev*. 2021; 41 (2): 770–784. PMID: 32656815.
4. Ludtmann MHR, Abramov AY. Mitochondrial calcium imbalance in Parkinson's disease. *Neurosci Lett*. 2018; 663: 86–90. PMID: 28838811.
5. Lou G, Palikaras K, Lautrup S, Scheibye-Knudsen M, Tavernarakis N, Fang EF. Mitophagy and Neuroprotection. *Trends Mol Med*. 2020; 26 (1): 8–20. PMID: 31375365.
6. Lemasters JJ. Selective mitochondrial autophagy, or mitophagy, as a targeted defense against oxidative stress, mitochondrial dysfunction, and aging. *Rejuvenation Res*. 2005; 8 (1): 3–5. doi: 10.1089/rej.2005.8.3.
7. Palikaras K, Lionaki E, Tavernarakis N. Mechanisms of mitophagy in cellular homeostasis, physiology and pathology. *Nat. Cell Biol*. 2018; 20 (9): 1013–1022. doi: 10.1038/s41556-018-0176-2.
8. Zuo Z, Jing K, Wu H, Wang S, Ye L, Li Z, Yang C, Pan Q, Liu WJ, Liu HF. Mechanisms and Functions of Mitophagy and Potential Roles in Renal Disease. *Front Physiol*. 2020; 11: 935. PMID: 32903665.
9. Moreau K, Luo S, Rubinsztein DC. Cytoprotective roles for autophagy. *Curr Opin Cell Biol*. 2010; 22 (2): 206–211. PMID: 20045304.
10. Cai Q, Ganesan D. Regulation of neuronal autophagy and the implications in neurodegenerative diseases. *Neurobiol Dis*. 2022; 162: 105582. PMID: 34890791.
11. Senousy MA, Hanafy ME, Shehata N, Rizk SM. Erythropoietin and Bacillus Calmette-Guérin Vaccination Mitigate 3-Nitropropionic Acid-Induced Huntington-like Disease in Rats by Modulating the PI3K/Akt/mTOR/P70S6K Pathway and Enhancing the Autophagy. *ACS Chem Neurosci*. 2022; 13(6): 721–732. PMID: 35226456.
12. Nichol A, French C, Little L, Haddad S, Presneil J, Arabi Y, Bailey M, Cooper DJ, Duranteau J, Huet O, Mak A, McArthur C, Pettilä V, Skrifvars M, Vallance S, Varma D, Wills J, Bellomo R. EPO-TBI Investigators; ANZICS Clinical Trials Group. Erythropoietin in traumatic brain injury (EPO-TBI): a double-blind randomised controlled trial. *Lancet*. 2015; 386 (10012): 2499–2506. PMID: 26452709.
13. Hemani S, Lane O, Agarwal S, Yu SP, Woodbury A. Systematic Review of Erythropoietin (EPO) for Neuroprotection in Human Studies. *Neurochem Res*. 2021; 46(4): 732–739. PMID: 33521906.
14. Robertson CS, Garcia R, Gaddam SS, Grill RJ, Cerami Hand C, Tian TS, Hannay HJ. Treatment of mild traumatic brain injury with an erythropoietin-mimetic peptide. *J Neurotrauma*. 2013; 30 (9): 765–74. PMID: 22827443.
15. Tan R, Tian H, Yang B, Zhang Bo, Dai C, Han Z, Wang M, Li Y, Wei L, Chen D, Wang G, Yang H, He F, Chen Z. Autophagy and Akt in the protective effect of erythropoietin helix B surface peptide against hepatic ischaemia/reperfusion injury in mice. *Sci Rep*. 2018; 8 (1): 14703.
16. Filomeni G, Graziani I, De Zio D, Dini L, Centonze D, Rotilio G, Ciriolo MR. Neuroprotection of kaempferol by autophagy in models of rotenone-mediated acute toxicity: possible implications for Parkinson's disease. *Neurobiol Aging*. 2012; 33 (4): 767–85. PMID: 20594614.
17. Sasaoka M, Ota T, Kageyama M. Rotenone-induced inner retinal degeneration via presynaptic activation of voltage-dependent sodium and L-type calcium channels in rats. *Sci Rep*. 2020; 10: 969. <https://doi.org/10.1038/s41598-020-57638-y>.
18. Benjamin AB, Ahenkorah J, Bismarck AH, Esther D, Addai FK. Improved method of producing satisfactory sections of whole eyeball by routine histology. *Microscopy Research and Technique*. 2014; 77 (2): 138–142. PMID: 24249388.
19. Goldberg MF, McLeod S, Tso M, Packo K, Edwards M, Bhutto IA, Baldeosingh, Eberhart C, Weber BHF, Luttly GA. Ocular Histopathology and Immunohistochemical Analysis in the Oldest Known Individual with Autosomal Dominant Vitreoretinopathology. *Ophthalmology Retina*. 2018; 2 (4): 360–378. PMID: 29774302.
20. Kubekina MV, Silaeva YYu, Bruter AV, Korshunova DS, Ilchuk LA, Okulova YD, Soldatova MO, Seryogina E, Kolesnik IM, Ukolova PA, Korokin MV, Deykin AV. Transgenic mice Cre-dependently expressing mutant polymerase-gamma: novel test-system for pharmacological study of mitoprotective drugs. *Research Results in Pharmacology*. 2021; 7 (3): 33–39.
21. Livak KJ. Analysis of relative gene expression data using real-time quantitative PCR and the 2(-Delta Delta C(T)) Method. *Methods*. 2001; 25 (4): 402–408. PMID: 11846609.
22. Plenge U, Belhage B, Guadalupe-Grau A, Andersen PR, Lundby C, Dela F, Stride N, Pott FC, Helge JW, Boushel R. Erythropoietin treatment enhances muscle mitochondrial capacity in humans. *Front Physiol*. 2012; 13(3): 50. PMID: 22419911.
23. Покровский М. В., Солдатов В. О., Затолокина М. А. и др. Связь EPOR/CD131-опосредованной нейропротекции при хронической экспозиции этанола у крыс с модуляцией экспрессии генов аутофагии, апоптоза, нейровоспаления и нейрональной регенерации. *Экспериментальная и*

- клиническая фармакология. 2021; 84 (2): 91-98.
24. Su Y, Zhang Z, Li H, Ma J, Sun L, Shao S, Zhang Z, Hölscher C. A GLP-2 Analogue Protects SH-SY5Y and Neuro-2a Cells Against Mitochondrial Damage, Autophagy Impairments and Apoptosis in a Parkinson Model. *Drug Res (Stuttg)*. 2021; 71 (1): 43–50. PMID: 33022720.
25. Li Q, Zhang T, Wang J, Zhang Z, Zhai Y, Yang GY, Sun X. Rapamycin attenuates mitochondrial dysfunction via activation of mitophagy in experimental ischemic stroke. *Biochem Biophys Res Commun*. 2014; 444 (2) :182–188. PMID: 24440703.
26. Jang W, Kim HJ, Li H, Jo KD, Lee MK, Yang HO. The Neuroprotective Effect of Erythropoietin on Rotenone-Induced Neurotoxicity in SH-SY5Y Cells Through the Induction of Autophagy. *Mol Neurobiol*. 2016; 53 (6): 3812–3821. PMID: 26156288.

PROGNOSTIC SIGNIFICANCE OF ORAL FLUID FLUORIDE MEASUREMENT IN ACUTE PERICORONITIS

Vagner VD¹, Sarf EA², Belskaya LV², Korshunov AS³✉, Kuryatnikov KN³, Bondar AA³, Meloyan AD³, Maksimenko KA³, Kasiy MN³

¹ Central Research Institute of Dentistry and Maxillofacial Surgery, Moscow, Russia

² Omsk State Pedagogical University, Omsk, Russia

³ Omsk State Medical University, Omsk, Russia

Oral fluid is a valuable substrate for assessing dental health and other aspects of physical status. New methods for early diagnosis and prognosis of dental diseases on the basis of oral fluid composition are in constant demand. Excessive fluoride concentrations, often overlooked by dental therapists, negatively affect organs and tissues of the oral cavity. This study aimed at development and approbation of a method for reliable measurement of fluoride ions in oral fluid by capillary electrophoresis to be used in patients with dental diseases. The fluoride ion concentrations were measured in health (2.16 ± 0.48 mg/L), in isolated acute pericoronitis (15.2 ± 2.7 mg/L) and in acute pericoronitis combined to multiple caries (18.9 ± 4.2 mg/L). By post-operative day 3, fluoride levels in the group with isolated acute pericoronitis dropped to normal values (2.28 ± 0.52 mg/L), whereas in the group with acute pericoronitis combined to multiple caries fluoride levels remained high (8.7 ± 1.9 mg/L; $p < 0.0001$). The developed protocol is efficient for studying fluoride ion concentrations in isolated and combined dental diseases.

Keywords: pericoronitis, multiple caries, fluorides, oral fluid, capillary electrophoresis

Author contribution: Vagner VD — planning of the study, literature analysis, data interpretation; Sarf EA — biochemical research, statistical analysis; Belskaya LV — planning of the study, biochemical research, manuscript preparation; Korshunov AS — planning of the study, literature analysis, data interpretation, collection of clinical samples, manuscript preparation; Kuryatnikov KN — collection of clinical samples, data interpretation, manuscript preparation; Bondar AA, Meloyan AD, Maksimenko KA, Kasiy MN — sample preparation, data analysis.

Compliance with ethical standards: the study was approved by ethical review board of the Omsk State Medical University (Protocol № 113 of 26 November 2019); all participants or their representatives provided informed consent for participation in the study.

✉ **Correspondence should be addressed:** Andrey S. Korshunov
Kosareva, 34, Omsk, 644043, Russia; andrey_k_180588@mail.ru

Received: 12.08.2022 **Accepted:** 26.08.2022 **Published online:** 28.08.2022

DOI: 10.24075/brsmu.2022.042

ПРОГНОСТИЧЕСКАЯ ЗНАЧИМОСТЬ ОПРЕДЕЛЕНИЯ ФТОРИД-ИОНОВ В РОТОВОЙ ЖИДКОСТИ ПРИ ОСТРОМ ПЕРИКРОНИТЕ

В. Д. Вагнер¹, Е. А. Сарф², Л. В. Бельская², А. С. Коршунов³✉, К. Н. Курятников³, А. А. Бондарь³, А. Д. Мелоян³, К. А. Максименко³, М. Н. Касий³

¹ Центральный научно-исследовательский институт стоматологии и челюстно-лицевой хирургии, Москва, Россия

² Омский государственный педагогический университет, Омск, Россия

³ Омский государственный медицинский университет, Омск, Россия

Разработка новых методов ранней диагностики и исхода стоматологических заболеваний по концентрации различных ионов в ротовой жидкости является перспективным направлением. По составу ротовой жидкости можно оценивать состояние не только стоматологического здоровья, но и всего организма в целом. Превышение концентрации фторид-ионов оказывает негативное влияние на органы и ткани полости рта, а контроль за его поступлением в организм врачами не проводится. Целью исследования было разработать и апробировать методику определения фторид-ионов в ротовой жидкости методом капиллярного электрофореза при стоматологических заболеваниях. Получены данные о концентрации фторид-ионов в норме ($2,16 \pm 0,48$ мг/л), при множественном кариесе и остром перикороните ($18,9 \pm 4,2$ мг/л), остром перикороните ($15,2 \pm 2,7$ мг/л). На третьи сутки после оперативного вмешательства значения в группе с острым перикоронитом пришли в норму ($2,28 \pm 0,52$ мг/л), при множественном кариесе и остром перикороните, даже после хирургического вмешательства, остались высокими ($8,7 \pm 1,9$ мг/л; $p < 0,0001$). Разработанная методика эффективна для изучения концентрации фторид-ионов при изолированных и сочетанных стоматологических заболеваниях.

Ключевые слова: перикоронит, множественный кариес, фториды, ротовая жидкость, капиллярный электрофорез

Вклад авторов: В. Д. Вагнер — планирование исследования, анализ литературы, интерпретация данных; Е. А. Сарф — проведение биохимических исследований, статистическая обработка данных; Л. В. Бельская — планирование исследования, проведение биохимических исследований, подготовка рукописи; А. С. Коршунов — планирование исследования, анализ литературы, интерпретация данных, набор клинического материала, подготовка рукописи; К. Н. Курятников — набор клинического материала, интерпретация данных, подготовка рукописи; А. А. Бондарь, А. Д. Мелоян, К. А. Максименко, М. Н. Касий — подготовка образцов для исследования, анализ данных.

Соблюдение этических стандартов: исследование одобрено этическим комитетом ФГБОУ ВО ОмГМУ Министерства здравоохранения РФ (протокол № 113 от 26 ноября 2019 г.); все участники исследования или их представители подписали добровольное информированное согласие.

✉ **Для корреспонденции:** Андрей Сергеевич Коршунов
ул. Косарева, д. 34, г. Омск, 644043, Россия; andrey_k_180588@mail.ru

Статья получена: 12.08.2022 **Статья принята к печати:** 26.08.2022 **Опубликована онлайн:** 28.08.2022

DOI: 10.24075/vrgmu.2022.042

The influence of fluorides on human health is a long-studied issue. The negative influence of fluorinated compounds on human body has been confirmed by advanced research in the fields of medicine, chemistry, occupational safety and nutritional health [1]. The known effects of fluorides on dental health include endemic diseases (fluorosis, caries) associated

with excessive intake/exposure or deficiency [2]. Fluoride ions can act on phosphoenolpyruvate kinase, thereby inhibiting glycolysis, which leads to reduced production of lactic acid and favors cariesogenic microflora in the oral cavity. The action of fluorine on other organs and tissues remains understudied [3]. Fluorides inhibit enzymatic activities through depletion of

cofactor ions of Mn, Ca, Fe and Mg. Humans receive fluorides with drinking water, foods, inhaled dust and gaseous fluorinated compounds. The average daily requirement of fluorides in adults is 2–3 mg [4]. Up to 70% of this amount enters the body with drinking water and about 30% is retrieved from foods. Fluorides play an important role in caries prophylaxis. Fluoride levels in the body have been linked to the morbidity of fluorosis, including endemic forms of the disease. Caries and fluorosis of both deciduous and definitive teeth, especially in children, have been associated with drinking water fluorination levels [5].

The influence of fluorine on the outcomes of dental conditions hallmarked by decay of hard tissues (caries, fluorosis) was elucidated in seminal publications both domestically and abroad. We have found no published evidence on a possible shift in fluoride ranges during complicated wisdom tooth eruption. Meanwhile, such shifts might prove clinically relevant given the hypomineralized condition of such teeth during eruption [6, 7]. The presence of inflammatory process during wisdom tooth eruption negatively affects oral homeostasis, and critically increased fluoride concentrations may exacerbate the consequences especially in the presence of other infectious foci in the oral cavity.

Fluoride-based medications are widely used in therapeutic dentistry as an affordable and accessible method of the focal enamel demineralization management. Fluoride ions prevent caries and inhibit metabolic processes in dental plaque bacteria through enzymatic interference, thus suppressing acidification and alleviating demineralization of carious lesions at early stages [8]. Still, such 'simple' low-molecular fluorides cannot effectively prevent caries due to the brevity of their stay at the tooth surface and low concentrations of the released fluorine. Administration of the low-efficient fluorides as tooth pastes, gels, rinses and coatings for local fluorination is one of additional factors of carious and non-carious tooth decay. The toothpastes and rinses containing antimicrobial components exert certain suppressive action on the microbial biofilm, but have no remineralizing effect [9]. This situation necessitates the use of deep fluorination. However, prescription of fluorine medications is conventionally based solely on dental status and unsupported by laboratory tests of fluoride content in the body. Importantly, fluorine belongs to chemical elements showing a sharp transition from physiologically beneficial concentrations to those promoting toxicosis [10], which accentuates the need for its reliable measurement in biological substrates [11]. The fluoride content can be assessed by their presence in blood, saliva, urine, bones and hair [12].

Oral fluid is a valuable substrate mirroring the overall physiological condition of the body [13–15]. Unlike capillary or venous blood sampling, the oral fluid sampling is non-invasive, which is definitely advantageous [16]. Biochemical composition of oral fluid is highly indicative of various shifts in homeostasis [17].

The utility of oral fluid for fluoride measurements is limited by the lack of unified protocol. Capillary electrophoresis is one of the most versatile methods for ion composition analysis [18, 19] increasingly applied in various fields of analytical chemistry [20]. The simplicity, accessibility and accuracy of this approach favor its use in clinical laboratories and make it applicable in various fields of medicine, notably dentistry, for diagnostics and monitoring.

Based on literature analysis, we have found it reasonable to study associations of dental diseases with fluoride concentrations in oral fluid. Elevated concentrations of these ions can interfere with maturation and mineralization of hard dental tissues and/or aggravate dental diseases.

This study aimed at development and approbation of a method for reliable measurement of fluoride ions in oral fluid by capillary electrophoresis to be used in patients with dental diseases exemplified by multiple caries and/or acute pericoronitis.

METHODS

Clinical study

The control group enrolled 200 individuals with satisfactory dental status (care index (CI) score of 0–4.4, mean 3.3 ± 0.4). Approbation of oral fluoride measurements on clinical samples involved two groups of patients: group 1 enrolled patients with acute pericoronitis and satisfactory dental status (CI score 0–4.4, mean 3.6 ± 0.5) aged 20–25 ($n = 20$); group 2 enrolled patients with acute pericoronitis against the background of multiple caries and CI scores over 6.6, mean 11.9 ± 0.6 , aged 20–25 ($n = 20$). Inclusion criteria were established in accordance with survey data: control group — satisfactory dental status, CI score 0–4.4, age 20–25 years, female; group 1 — acute pericoronitis, satisfactory dental status, CI score 0–4.4, age 20–25 years, female; group 2 — acute pericoronitis combined to multiple caries (CI score over 6.6), age 20–25 years, female. Exclusion criteria were as follows: age below 20 years or over 25 years, unsatisfactory oral hygiene, male, chronic diseases (somatic, inflammatory and/or infectious) with a negative impact on hard tissues of teeth and periodontium, drug and alcohol addiction, ulcerogenic medications. All patients were examined at the premises of the Department of General Dentistry of the Omsk Region State Healthcare Institution "City Clinical Dental Clinic № 1" in 2021–2022. The recruitment was accomplished during the appointed reception by a dental therapist upon confirmation of the diagnosis.

Oral fluid samples of the control group, collected fasting in sterile test tubes, were used to determine the normal reference range of oral fluoride levels. In patients of groups 1 and 2, the samples were collected similarly before surgical intervention for acute pericoronitis (extraction of teeth 38 and 48 at the stage of semi-retention beneath the mucosa and the hood as shown by X-ray scan) and subsequently on post-operative days 1 and 3. The samples were centrifuged at 7,000 rpm. Concentrations of fluoride ions were measured using two methods: capillary electrophoresis and photometry.

Capillary electrophoresis

The oral fluid capillary electrophoresis protocol was developed using a KAPEL-105M capillary electrophoresis system (Lumex; Russia) [21, 22] with instrumentation and preparation of capillaries for operation described previously [22]. The oral fluid aliquots (100 μ L) were diluted 20-fold with distilled water. By contrast with the previously published protocol [22], there was no need for protein precipitation prior to sample loading. The anions (chlorides, nitrites, nitrates, phosphates, fluorides and sulfates) were measured using a leading electrolyte containing CrO_3 (10 mM), diethanolamine (30 mM) and cetyltrimethylammonium hydroxide (2 mM).

Photometry

The method involves determination of the color change of the zircon-alizarin complex solution reflecting formation of a colorless, more stable complex compound of fluoride ions with zirconyl chloride (IV) [23]. Upon reaction with fluoride,

Table 1. Electropherogram parameters for fluoride measurement

Calibration solution №	Elution time, min	Peak height, mAU	Peak area	Concentration, mg/L
Solution 1	6.317	0.368	12.68	0.25
Solution 2	6.323	2.398	64.32	1.0
Solution 3	6.128	7.117	268.7	5.0
Solution 4	6.048	9.299	504.2	10.0

the zircon-alizarin complex releases alizarin, which turns the solution yellow. For each measurement, a 5 μ L aliquot of oral fluid was added to a 100 mL volumetric flask filled with distilled water, 5 mL of alizarin red C solution and 5 mL of acidic solution of zirconyl chloride prepared according to state standard (GOST) 23268.18-78. The solution was thoroughly mixed and incubated for 1 hour at room temperature. The optical density was measured in a spectrophotometer at 540 nm wavelength in cuvettes with 10 mm path length against a blank sample.

Statistics

Statistical processing of experimental data involved distribution tests, which confirmed normality of the distributions; so the confidence intervals were calculated using Student's t-test. The differences were assessed for a significance level of $p < 0.05$.

RESULTS

Development of the capillary electrophoresis protocol for fluoride ion measurement

The first step was calibration; the peak area calibration plot for fluoride is shown in Fig. 1. Since the protocol was intended for oral fluid as a substrate for fluoride measurements, the calibration used a solution of all inorganic anions possibly found in saliva (Fig. 2A). The insert illustrates the change in the peak area of fluoride ion depending on its concentration in the sample. Major parameters of the fluoride peaks, determined in electropherograms for a series of standard ion mixtures, are given in Table 1.

The analysis of oral fluid samples revealed no peaks for nitrite and nitrate ions (peaks 2 and 4, respectively). A typical electropherogram of salivary anions is given in Fig. 2B. The data were collected in three–four technical replicates for each sample to account for measurement error. To verify the correct identification of the fluoride ion peak, a series of experiments was carried out using the "added-detected" principle: a reference amount of a relevant additive with known concentration was introduced in the system (we used the registered standard sample of 1 mg/mL). The step-wise addition substantially increased the height and area of the peak identified with fluoride (Fig. 2B) and the measurement error did not exceed 10%.

To validate the developed method through comparison with a different protocol, the fluoride ion content of the samples was additionally determined by photometry. The concentrations were calculated using a pre-built calibration plot (Fig. 3). It should be noted that photometry assay covers just a narrow range of low fluoride concentrations, because at higher concentrations the absorbance-concentration curve is non-linear. Thus, the use of photometry requires serial dilutions of sample aliquots (Table 2) which negatively affects the accuracy.

The concentrations of fluoride ions determined by capillary electrophoresis matched those measured by spectrophotometry (Table 2). This result allows consideration of both methods for clinical purposes. However, clinical utility

of spectrophotometry assay is limited by the narrow range of suitable concentrations and the uncertainty of fold dilution required in each individual case. Photometry requires a dilution falling within the concentration range (Table 2), while capillary electrophoresis is suitable for non-diluted samples. Mean oral fluid fluoride content for the control group was 2.27 ± 1.07 mg/L, albeit the total range for this group was 0.16–8.7 mg/L. It would be more expedient and advisable to use a method that does not require adjusting the concentration of fluoride ions in a sample by pre-dilution. The developed method of capillary electrophoresis satisfies these requirements.

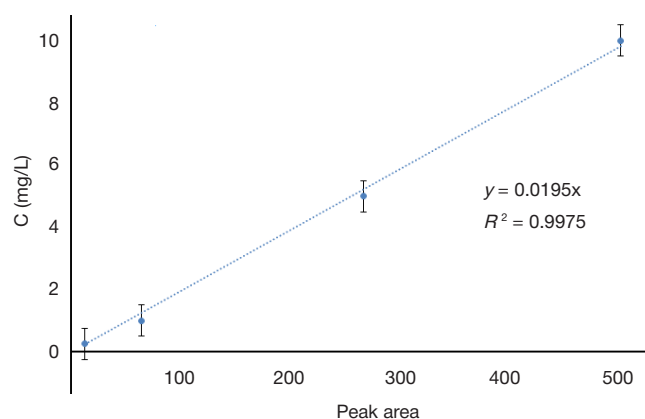


Fig. 1. Calibration curve for fluoride measurement by capillary electrophoresis, built in a standard range of 0.1–10 mg/L

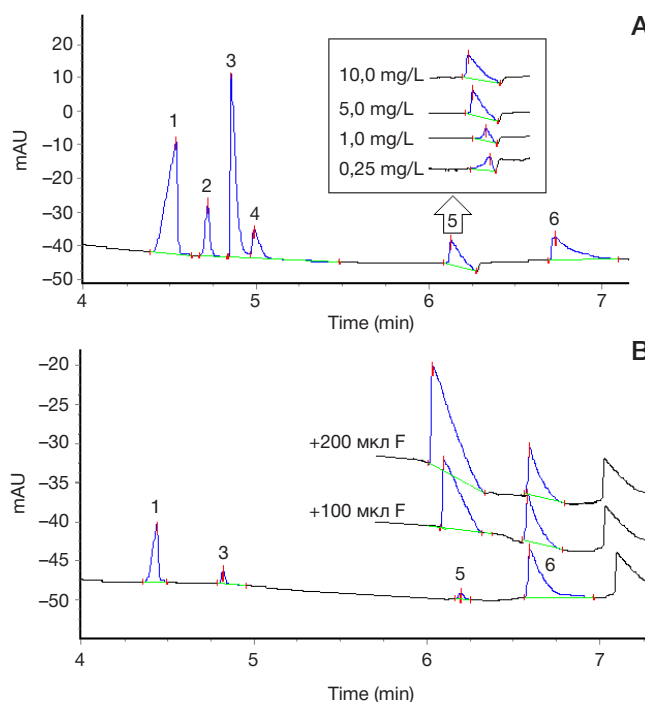


Fig. 2. A. Electropherogram for calibration solution containing a mixture of anions (1 — chlorides, 2 — nitrites, 3 — sulfates, 4 — nitrates, 5 — fluorides, 6 — phosphates). The insert shows fluoride ion peaks within the range of 0.25–10.0 mg/L. **B.** Electropherogram of saliva (100 μ L), pure or mixed with 100 μ L and 200 μ L aliquots of fluoride standard solution (diluted 20-fold)

Approbation of the oral fluid fluoride measurements on clinical samples of multiple caries and acute pericoronitis

For the control group, mean fluoride content constituted 2.16 ± 0.48 mg/L. The obtained ranges of oral fluid fluoride concentrations measured by capillary electrophoresis method encouraged using it in groups of patients with clinically unfavorable oral status (carious lesions, acute pericoronitis).

The highest oral fluoride levels were measured in patients before surgery for acute pericoronitis (isolated or combined to multiple caries: respectively, 15.2 ± 2.7 mg/L in group 1 and 18.9 ± 4.2 mg/L in group 2).

On post-operative day 1, fluoride concentrations decreased significantly to 9.4 ± 2.1 mg/L in group 1 and 11.4 ± 2.8 mg/L in group 2.

On post-operative day 3, fluoride concentrations in group 1 (isolated acute pericoronitis) reached the control group values (2.16 ± 0.48 mg/L), whereas fluoride concentrations in group 2 stayed high (8.7 ± 1.9 mg/L) indicating the persisting influence of multiple carious lesions combined to acute pericoronitis on oral fluoride levels. The identified differences were significant ($p < 0.0001$) (Fig. 4).

DISCUSSION

Analysis of literature on fluorine balance in the body identifies drinking water and foods as the main fluoride sources. Environmental factors, particularly professional intoxication in industrial facilities with high aerial content of fluorine and its chemical derivatives, should be considered as well. Fluorine content of various environmental objects has been elucidated in many studies [3, 4, 10]. Of note, environmental levels of fluorine depend on geography [11]; accordingly, the fluorine exposure varies geographically depending on the region of residence [24–26]. Many authors demonstrate correlations between fluoride levels and systemic diseases, though mostly indirectly, through environmental levels [27]. For example, a positive correlation has been demonstrated between fluoride content of drinking water and morbidity of diabetes, rheumatism, pyelonephritis and cervical erosion, whereas the fluorine/sulfate ratio correlates with morbidity of cerebrovascular, genitourinary, female reproductive, nervous and neurosensory disorders [27]. At the same time, data on possible disease-related shifts of fluoride content in biological fluids, including oral fluid, are sparse. As fluorine accumulates in dental tissues and is especially abundant at the enamel

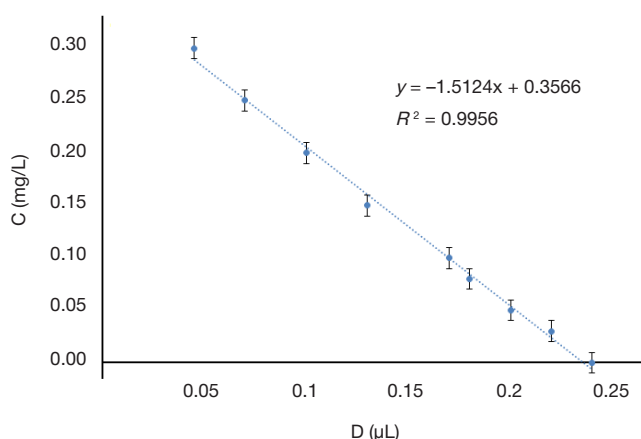


Fig. 3. Calibration curve for fluoride measurement by photometry

surface, salivary fluorine levels could be particularly informative. Fluoride concentrations in unstimulated saliva are a sum of their levels in ductal saliva, food and water [28]. Oral and dental diseases including fluorosis and caries are straightforwardly connected to oral levels of fluoride ions; accordingly, the timely determination and correction of fluoride intake is relevant to dental morbidity and prophylaxis. However, the lack of unified protocol of fluoride measurement and the diversity of available approaches hamper reliable comparison of data obtained by different authors (add in the inconvenience of using different units: mg/L, mmol/L, ppm, etc.) [11, 25, 29]. Environmental fluoride levels can be measured by capillary electrophoresis, potentiometry or photometry. These methods are suitable for oral fluid too, albeit most sources provide neither detailed description of the protocol, nor data confirming its validity [25]. Apart from the capillary electrophoresis and conventional photometry protocols used by us in this study, an alternative spectrophotometry assay is available, involving decolorization of trisodium 2-(4-sulfophenylazo)-1,8-dihydroxynaphthalene-3,6-disulfonate complex with fluoride ions detectable at 570 nm wavelength [29]. Potentiometric approaches are characterized by systematic errors and the necessity to get rid of impurities prior to measurements. Our methods, by contrast, allow measuring fluoride ions across the entire range of their salivary content both photometrically and by capillary electrophoresis. It should be noted that the latter approach allows simultaneous measurement of five other physiologically relevant inorganic ions (chlorides, nitrates, nitrites, sulfates and phosphates), which expands the scope of its application.

Table 2. Fluoride measurement for a selection of samples. CE, capillary electrophoresis

Sample	CE, mg/L	Photometry, mg/L				Δ , %
		Undiluted	Diluted 10-fold	Diluted 20-fold	Mean	
3	0.56	–	0.54	0.55	0.55	2.68
5	1.52	–	1.53	1.57	1.55	1.97
16	0.97	–	1.01	0.96	0.99	1.55
18	2.28	–	2.3	2.31	2.31	1.10
40	0.16	0.17	0.17	0.16	0.17	4.17
6	2.57	–	2.62	2.54	2.58	0.39
93	0.71	–	0.74	0.72	0.73	2.82
159	3.21	–	3.16	3.23	3.20	0.47
190	4.55	–	–	4.6	4.60	1.10
200	0.18	0.17	0.19	0.17	0.18	1.85

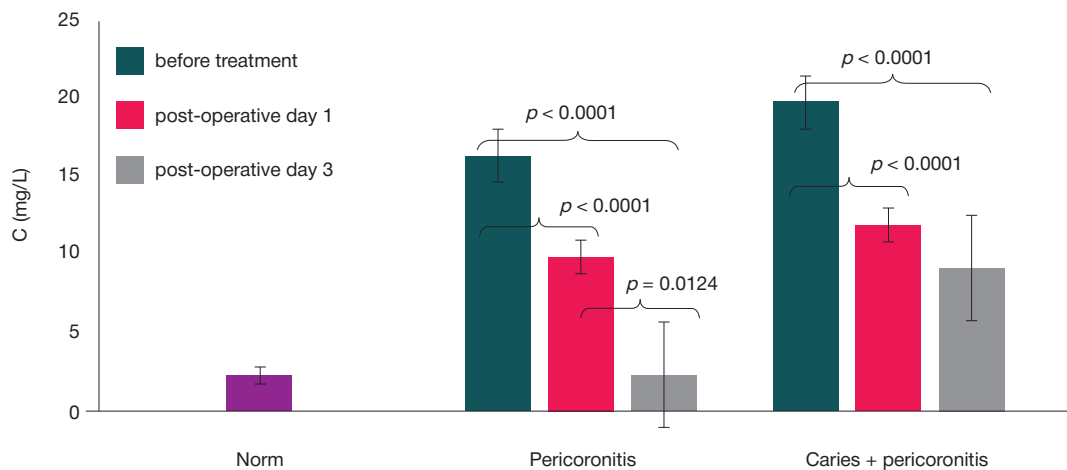


Fig. 4. Fluoride content for groups 1 and 2 before and after surgery (post-operative days 1 and 3) compared with the control group

Studies on oral fluid composition upon tooth fluorination procedure are fairly well elucidated in the literature [2, 8, 9], although the majority of studies focus on Ca/P ratio omitting the fluoride content.

Here we reveal substantially elevated oral fluoride levels in patients with inflammatory complications of the wisdom tooth eruption. Whether tooth eruption should be regarded as local or systemic process is an open issue [30]. The observed shift in physical and chemical salivary indicators suggests a profound systemic component. As long as in all cases of pericoronitis included in this study the eruption was almost complete, the observed increase in fluoride levels may reflect physiological response to this event, as wisdom teeth are known to be hypomineralized upon eruption and their enamel needs saturation with relevant ions to fortify the crystal lattice. Another factor causing the observed increase in oral fluoride levels is concomitant inflammation and bacterial flora expansion requiring appropriate treatment.

The limitations of the study include confinement to a single geographical area (Omsk region) as well as small size of both groups, necessitating further research on this problem.

CONCLUSIONS

Patients with pericoronitis combined to multiple caries reveal unfavorably high concentrations of fluoride ions in oral fluid, which stay elevated after surgical relief of acute pericoronitis. By contrast, in patients with isolated pericoronitis and CI score of 0–4.4, oral fluoride levels return to reference range by post-operative day 3. Despite the relevance of oral fluid as a source of fluoride, notably during teething, the retrieval should be regulatable and physiological, and proceed against the background of satisfactory oral hygiene and anti-inflammatory care. The capillary electrophoresis method is suitable for fluoride ion measurements in oral fluid.

References

- Kalyuzhnaya EEh, Prosekov AYu, Volobaev VP. Genotoksicheskie svojstva ftorid-ionov (obzor literatury). *Gigiena i sanitariya*. 2020; 3 (99): 253–58. DOI: 10.33029/0016-9900-2020-99-3-253-258. Russian.
- Pramanik S, Saha D. The genetic influence in fluorosis. *Environ Toxicol Pharmacol*. 2017; 56: 157–162. DOI: 10.1016/j.etap.2017.09.008.
- Savchenkov MF, Efimova NV, Manueva RS, Nikolaeva LA, Shin NS. Patologiya shhitovidnoj zhelezy u detskogo naseleniya pri sochetannom vozdeystvii deficita joda i ftoristogo zagryazneniya okruzhayushhej sredy. *Gigiena i sanitariya*. 2016; 12 (95): 1201–5. DOI: 10.1882/0016-9900-2016-95-12-1201-1205. Russian.
- Iordanishvili AK. Ftorydy: ix znachenie dlya zdorov'ya cheloveka v sovremennyx usloviyax i perspektivy ispol'zovaniya. *Chelovek i ego zdorov'e*. 2019; 2: 66–72. DOI: 10.21626/vestnik/2019-2/07. Russian.
- Iordanishvili AK, Barinov EX. Ftorydy i zdorov'e cheloveka: sovremennyye aspekty primeneniya. *Zdravooxranenie Yugry: opyt i innovacii*. 2022; 63 (7): 62–66. Russian.
- Vagner VD, Konev VP, Korshunov AS, Moskovskij SN, Kuryatnikov KN, Skurikhina A P. Vliyanie displazii soedinitel'noj tkani na sroki prorezyvaniya i stepen' mineralizacii zubov cheloveka. *Stomatologiya*. 2021; 100 (5): 7–14. DOI: 10.17116/stomat20211000517. Russian.
- Korshunov A, Vagner V, Konev V, Moskovskiy S, Kuryatnikov K, Skurikhina A, et al. Research of connective tissue dysplasia influence on teething. *Saudi Dent J*. 2022; 34 (5): 385–9. DOI: 10.1016/j.sdentj.2022.05.002.
- Xmyzova TG, Osyko AN, Kurkina VM, Nikitina TV. Primenenie ftoridnogo laka duraphat dlya lecheniya ochagovoj demineralizacii ehmalii. *Problemy nauki*. 2021; 5 (64): 72–74. Russian.
- Knappvost A. Pokazaniya k primeneniyu i mexanizmy kariesprofilakticheskogo dejstviya preparatov glubokogo ftorirovaniya — ehmal'-germetiziruyushhego i dentin-germetiziruyushhego likvidov. *Problemy stomatologii*. 2005; 3: 3–8.
- Alekseev LS, Mleva GA, Al-Amri Z. Tekniko-gigienicheskie aspekty ftorirovaniya pit'evoy vody. *Vestnik MGSU*. 2012; 3: 154–8. Russian.
- Mozgovaya LA, Sivak EYu, Sosnin DYu, Gavrilenko MS, Fokina NB, Mozgovaya SV. Osobennosti stomatologicheskogo statusa starshix shkol'nikov v zavisimosti ot mineral'nogo sostava pit'evoy vody. *Permskij medicinskij zhurnal*. 2021; XXXVIII (2): 79–87. Russian.
- Zajceva NV, Zemlyanova MA, Bulatova NI, Koldibekova YuV. Issledovanie i ocenka narushenij proteomnogo profilya plazmy krvi, obuslovlennyx povyshennoj koncentraciej ftorid-ionov v moche u detej. *Zdorov'e naseleniya i sreda obitaniya*. 2019; 7 (316): 23–27. DOI: 10.35627/2219-5238/2019-316-7-23-27. Russian.
- Khurshid Z, Warsi I, Moin SF, Slowey PD, Latif M, Zohaib S, et al. Biochemical analysis of oral fluids for disease detection. *Advances in Clinical Chemistry*. 2021; 100: 205–3. DOI: 10.1016/bs.acc.2020.04.005.
- Roblegg E, Coughran A, Sirjani D. Saliva: An all-rounder of our body. *Eur J Pharm Biopharm*. 2019; 142: 133–41. DOI: 10.1016/j.ejpb.2019.06.016.
- Kaczor-Urbanowicz KE, Wei F, Rao SL, Kim J, Shin H, Cheng J,

- et al. Clinical validity of saliva and novel technology for cancer detection. *Biochim Biophys Acta Rev Cancer*. 2019; 1872 (1): 49–59. DOI: 10.1016/j.bbcan.2019.05.007.
16. Dawes C, Wong DTW. Role of Saliva and Salivary Diagnostics in the Advancement of Oral Health. *J Dent Res*. 2019; 98 (2): 133–41. DOI: 10.1177/0022034518816961.
 17. Arunkumar S, Arunkumar JS, Krishna NB, Shakunthala GK. Developments in diagnostic applications of saliva in oral and systemic diseases — A comprehensive review. *Journal of Scientific and Innovative Research*. 2014; 3 (3): 372–87.
 18. Sursyakova VV, Rubajlova AI. Izuchenie meshayushhego vliyaniya organicheskix kislot na opredelenie ftorid-ionov metodom kapillyarnogo ehlektroforeza s primeneniem xromatnogo fonovogo ehlektrolita. *Zhurnal Sibirskogo federal'nogo universiteta*. 2017; 4: 573–79. DOI: 10.17516/1998-2836-0049. Russian.
 19. Belskaya LV, Sarf EA. Opredelenie sodержaniya organicheskix kislot v slyune bol'nyx rakom molochnoj zhelezy metodom kapillyarnogo ehlektroforeza. *Klinicheskaya laboratornaya diagnostika*. 2018; 63 (7): 419–22. Russian.
 20. Mori M, Ishikawa F, Tomoda T, Yamada S, Okamoto M, Itabashi H et al. Use of capillary electrophoresis with dual-opposite end injection for simultaneous analysis of small ions in saliva samples from wrestlers undergoing a weight training program. *Journal of Chromatography B*. 2016; 1012: 178–85.
 21. Komarova NV, Kamencev YaS. Prakticheskoe rukovodstvo po ispol'zovaniyu sistem kapillyarnogo ehlektroforeza «KAPEL'». SPb.: OOO «Veda», 2006; 212 s. Russian.
 22. Belskaya LV. Primenenie kapillyarnogo ehlektroforeza dlya opredeleniya mineral'nogo sostava slyuny cheloveka. *Byulleten' nauki i praktiki*. 2017; 2 (15): 132–40. Russian.
 23. Dorogova VB, Shayaxmetov SF, Merinov AV. Metodicheskie aspekty ximiko-analiticheskogo kontrolya sodержaniya ftora v biologicheskix substratax. *Sibirskij medicinskij zhurnal*. 2012; 7: 141–43. Russian.
 24. Xamadeeva AM, Nogina NV, Luchsheva LF, Bajmuratova LR. Osobennosti stomatologicheskogo zdorov'ya detej v regione s neblagopriyatnoj ehkologicheskoy situaciej na primere g. Chapaevska Samarskoj oblasti. *Dal'nevostochnyj medicinskij zhurnal*. 2018; 1: 67–72. Russian.
 25. Yavorskaya TE. Sravnitel'naya xarakteristika sostava i svojstv smeshannoj slyuny u detej shkol'nogo vozrasta. *Acta medica Eurasica*. 2016; 1: 30–40. Russian.
 26. Zajceva NV, Zemlyanova MA, Bulatova NI, Koldibekova YuV. Issledovanie i ocenka narushenij proteomnogo profilya plazmy krovi, obuslovlennyx povyshennoj koncentraciej ftorid-iona v moche u detej. *Zdorov'e naseleniya i sreda obitaniya*. 2019; 7 (316): 23–27. Russian.
 27. Anichkina NV. Issledovaniya biogeoximii ftora v komponentax geosistem. *Nauchnoe obozrenie. Biologicheskije nauki*. 2016; 3: 5–23. Russian.
 28. Talwar M, Tewari A, Chawla HS, Sachdev V. A comparative assessment of fluoride concentration available in saliva using daily prescribed topical fluoride agents. *Indian J Dent*. 2016; 7 (2): 76–80. DOI: 10.4103/0975-962X.184647.
 29. Sawan NM, Ben Gasseem AA, Aldegheishem A, Alsagob EI, Alshami AA. Screening of fluoride analysis as a biochemical parameter in the orthodontic treatment using fixed appliances. *Saudi J Biol Sci*. 2022; 29 (3): 1668–1672. DOI: 10.1016/j.sjbs.2021.10.065.
 30. Lacruz RS, Habelitz S, Wright JT, Paine ML. Dental enamel formation and implications for oral health and disease. *Physiol Rev*. 2017; 97 (3): 939–93. DOI: 10.1152/physrev.00030.2016.

Литература

1. Калюжная Е. Э., Просеков А. Ю., Волобаев В. П. Генотоксические свойства фторид-иона (обзор литературы). *Гигиена и санитария*. 2020; 3 (99): 253–58. DOI: 10.33029/0016-9900-2020-99-3-253-258.
2. Pramanik S, Saha D. The genetic influence in fluorosis. *Environ Toxicol Pharmacol*. 2017; 56: 157–162. DOI: 10.1016/j.etap.2017.09.008.
3. Савченко М. Ф., Ефимова Н. В., Мануева Р. С., Николаева Л. А., Шин Н. С. Патология щитовидной железы у детского населения при сочетанном воздействии дефицита йода и фтористого загрязнения окружающей среды. *Гигиена и санитария*. 2016; 12 (95): 1201–5. DOI: 10.1882/0016-9900-2016-95-12-1201-1205.
4. Иорданишвили А. К. Фториды: их значение для здоровья человека в современных условиях и перспективы использования. *Человек и его здоровье*. 2019; 2: 66–72. DOI: 10.21626/vestnik/2019-2/07.
5. Иорданишвили А. К., Баринев Е. Х. Фториды и здоровье человека: современные аспекты применения. *Здравоохранение Югры: опыт и инновации*. 2022; 63 (7): 62–66.
6. Вагнер В. Д., Конев В. П., Коршунов А. С., Московский С. Н., Курятников К. Н., Скурихина А. П. Влияние дисплазии соединительной ткани на сроки прорезывания и степень минерализации зубов человека. *Стоматология*. 2021; 100 (5): 7–14. DOI: 10.17116/stomat20211000517.
7. Korshunov A, Vagner V, Konev V, Moskovskiy S, Kuryatnikov K, Skurikhina A, et al. Research of connective tissue dysplasia influence on teething. *Saudi Dent J*. 2022; 34 (5): 385–9. DOI: 10.1016/j.sdentj.2022.05.002.
8. Хмызова Т. Г., Осыко А. Н., Куркина В. М., Никитина Т. В. Применение фторидного лака digarhat для лечения очаговой деминерализации эмали. *Проблемы науки*. 2021; 5 (64): 72–74.
9. Кнаппвост А. Показанию к применению и механизмы кариеспрофилактического действия препаратов глубокого фторирования — эмаль-герметизирующего и дентин-герметизирующего ликвидов. *Проблемы стоматологии*. 2005; 3: 3–8.
10. Алексеев Л. С., Ивлева Г. А., Аль-Амри З. Технико-гигиенические аспекты фторирования питьевой воды. *Вестник МГСУ*. 2012; 3: 154–8.
11. Мозговая Л. А., Сивак Е. Ю., Соснин Д. Ю., Гавриленко М. С., Фокина Н. Б., Мозговая С. В. Особенности стоматологического статуса старших школьников в зависимости от минерального состава питьевой воды. *Пермский медицинский журнал*. 2021; XXXVIII (2): 79–87.
12. Зайцева Н. В., Землянова М. А., Булатова Н. И., Кольдибекова Ю. В. Исследование и оценка нарушений протеомного профиля плазмы крови, обусловленных повышенной концентрацией фторид-иона в моче у детей. *Здоровье населения и среда обитания*. 2019; 7 (316): 23–27. DOI: 10.35627/2219-5238/2019-316-7-23-27.
13. Khurshid Z, Warsi I, Moin SF, Slowey PD, Latif M, Zohaib S, et al. Biochemical analysis of oral fluids for disease detection. *Advances in Clinical Chemistry*. 2021; 100: 205–3. DOI: 10.1016/bs.acc.2020.04.005.
14. Roblegg E, Coughran A, Sirjani D. Saliva: An all-rounder of our body. *Eur J Pharm Biopharm*. 2019; 142: 133–41. DOI: 10.1016/j.ejpb.2019.06.016.
15. Kaczor-Urbanowicz KE, Wei F, Rao SL, Kim J, Shin H, Cheng J, et al. Clinical validity of saliva and novel technology for cancer detection. *Biochim Biophys Acta Rev Cancer*. 2019; 1872 (1): 49–59. DOI: 10.1016/j.bbcan.2019.05.007.
16. Dawes C, Wong DTW. Role of Saliva and Salivary Diagnostics in the Advancement of Oral Health. *J Dent Res*. 2019; 98 (2): 133–41. DOI: 10.1177/0022034518816961.
17. Arunkumar S, Arunkumar JS, Krishna NB, Shakunthala GK. Developments in diagnostic applications of saliva in oral and systemic diseases — A comprehensive review. *Journal of Scientific and Innovative Research*. 2014; 3 (3): 372–87.
18. Сурсякова В. В., Рубайлова А. И. Изучение мешающего влияния органических кислот на определение фторид-ионов методом капиллярного электрофореза с применением хроматного фонового электролита. *Журнал Сибирского федерального университета*. 2017; 4: 573–79. DOI: 10.17516/1998-2836-0049.
19. Бельская Л. В., Сарф Е. А. Определение содержания

- органических кислот в слюне больных раком молочной железы методом капиллярного электрофореза. Клиническая лабораторная диагностика. 2018; 63 (7): 419–22.
20. Mori M, Ishikawara F, Tomoda T, Yamada S, Okamoto M, Itabashi H et al. Use of capillary electrophoresis with dual-opposite end injection for simultaneous analysis of small ions in saliva samples from wrestlers undergoing a weight training program. *Journal of Chromatography B*. 2016; 1012: 178–85.
 21. Комарова Н. В., Каменцев Я. С. Практическое руководство по использованию систем капиллярного электрофореза «КАПЕЛЬ». СПб.: ООО «Веда», 2006; 212 с.
 22. Бельская Л. В. Применение капиллярного электрофореза для определения минерального состава слюны человека. *Бюллетень науки и практики*. 2017; 2 (15): 132–40.
 23. Дорогова В. Б., Шаяхметов С. Ф., Меринов А. В. Методические аспекты химико-аналитического контроля содержания фтора в биологических субстратах. *Сибирский медицинский журнал*. 2012; 7: 141–43.
 24. Хамадеева А. М., Ногина Н. В., Лучшева Л. Ф., Баймуратова Л. Р. Особенности стоматологического здоровья детей в регионе с неблагоприятной экологической ситуацией на примере г. Чапаевска Самарской области. *Дальневосточный медицинский журнал*. 2018; 1: 67–72.
 25. Яворская Т. Е. Сравнительная характеристика состава и свойств смешанной слюны у детей школьного возраста. *Acta medica Eurasica*. 2016; 1: 30–40.
 26. Зайцева Н. В., Землянова М. А., Булатова Н. И., Кольдибекова Ю. В. Исследование и оценка нарушений протеомного профиля плазмы крови, обусловленных повышенной концентрацией фторид-иона в моче у детей. *Здоровье населения и среда обитания*. 2019; 7 (316): 23–27.
 27. Аничкина Н. В. Исследования биогеохимии фтора в компонентах геосистем. *Научное обозрение. Биологические науки*. 2016; 3: 5–23.
 28. Talwar M, Tewari A, Chawla HS, Sachdev V. A comparative assessment of fluoride concentration available in saliva using daily prescribed topical fluoride agents. *Indian J Dent*. 2016; 7 (2): 76–80. DOI: 10.4103/0975-962X.184647.
 29. Sawan NM, Ben Gasseem AA, Aldegheishem A, Alsagob EI, Alshami AA. Screening of fluoride analysis as a biochemical parameter in the orthodontic treatment using fixed appliances. *Saudi J Biol Sci*. 2022; 29 (3): 1668–1672. DOI: 10.1016/j.sjbs.2021.10.065.
 30. Lacruz RS, Habelitz S, Wright JT, Paine ML. Dental enamel formation and implications for oral health and disease. *Physiol Rev*. 2017; 97 (3): 939–93. DOI: 10.1152/physrev.00030.2016.

IN SILICO ALGORITHM FOR OPTIMIZATION OF PHARMACOKINETIC STUDIES OF [25Mg2+]PORPHYRIN-FULLERENE NANOPARTICLESFursov VV^{1,2} ✉, Zinchenko DI¹, Namestnikova DD², Kuznetsov DA^{2,3}¹ Mendeleev University of Chemical Technology, Moscow, Russia² Pirogov Russian National Research Medical University, Moscow, Russia³ Semenov Federal Research Center for Chemical Physics, Moscow, Russia

The search for effective pharmacophores to treat ischemic stroke is precipitated by the prevalence and high mortality of the condition. Optimization of preclinical scenarios for promising neuroprotectants by mathematical modeling using up-to-date computational platforms is a well-defined and urgent task. This study aimed to develop a drug-oriented model represented by an ordinary differential equation system to study pharmacokinetics of ²⁵Mg²⁺-releasing porphyrin-fullerene nanocationite PMC16 *in silico* using MATLAB and adjust computing model's adequateness using *in vivo* rat model. The developed five-compartment model predicts the distribution of nanoparticles in organs and tissues (e.g. the brain, the heart and the liver) for the purpose of experimental parameters optimization. The *in silico* produced pharmacokinetic curves show good agreement with the data obtained using *in vivo* rat model of ischemic stroke. The *in silico* and *in vivo* results indicate that PMC16 nanoparticles effectively cross the blood-brain barrier.

Keywords: ischemic stroke, penumbra, ²⁵Mg²⁺, nanocationites, pharmacokinetics, differential equations, mathematical modeling

Funding: the study was funded by the Ministry of Science and Higher Education of the Russian Federation, grant No. 075-15-2020-792 (Unique identifier RF-190220X0031)

Author contribution: Fursov VV — *in silico* study supervision, concept, hypothesis, structure, modeling, manuscript writing; Zinchenko DI — modeling, code, manuscript writing; Namestnikova DD — *in vivo* experiments; Kuznetsov DA — general supervision, data interpretation and analysis, planning of experiments.

Compliance with ethical standards: the study was approved by the ethical review board at the Pirogov Russian National Research Medical University (protocol № 140 of 15 December 2014) and the local committee for surveillance of the maintenance and use of laboratory animals (protocol № 13/2020 of 08 October 2020, protocol № 24/2021 of 10 December 2021).

✉ **Correspondence should be addressed:** Valentin V. Fursov
Ostrovityanova, 1, Moscow, 117997, Russia; vfursov@mail.ru

Received: 05.07.2022 **Accepted:** 18.07.2022 **Published online:** 22.07.2022

DOI: 10.24075/brsmu.2022.037

IN SILICO-МОДЕЛИРОВАНИЕ В ОПТИМИЗАЦИИ АЛГОРИТМОВ ФАРМАКОКИНЕТИЧЕСКИХ ИССЛЕДОВАНИЙ [25MG2+] ПОРФИРИН-ФУЛЛЕРЕНОВЫХ НАНОЧАСТИЦВ. В. Фурсов^{1,2} ✉, Д. И. Зинченко¹, Д. Д. Наместникова², Д. А. Кузнецов^{2,3}¹ Российский химико-технологический университет имени Д. И. Менделеева, Москва, Россия² Российский национальный исследовательский медицинский университет имени Н. И. Пирогова, Москва, Россия³ Федеральный исследовательский центр химической физики имени Н. Н. Семенова, Москва, Россия

Поиск эффективных фармакофоров для лечения ишемического инсульта актуален в связи с высокой распространенностью и смертностью от этого заболевания. Оптимизация сценариев доклинических исследований перспективных нейропротекторов средствами математического моделирования с использованием информационно-компьютерных технологий представляет собой отдельную актуальную задачу. Целью исследования было разработать препараториентированную математическую модель в виде системы ОДУ, реализовать ее *in silico* в виде программного кода на языке MATLAB и адаптировать к экспериментальным данным, полученным *in vivo* на крысах. В работе проведено исследование *in silico* фармакокинетики порфирина-фуллереновых нанокатионитов, высвобождающих ²⁵Mg²⁺ типа PMC16. Разработана пятикомпарментная математическая модель, которую можно использовать для прогнозирования распределения наночастиц в органах и тканях, расчета оптимальных дозировок, периодичности введения и т. д. Представлены расчетные кривые распределения PMC16 в мозге, печени и сердце. Достигнуто хорошее соответствие полученных *in silico* фармакокинетических кривых с результатами экспериментов *in vivo* на крысах, у которых моделировали инсульт. Доказано преодоление наночастицами PMC16 гематоэнцефалического барьера.

Ключевые слова: ишемический инсульт, пенумбра, ²⁵Mg²⁺, нанокатиониты, фармакокинетика, дифференциальные уравнения, математическая модель

Финансирование: работа выполнена при поддержке гранта Министерства науки и высшего образования Российской Федерации № 075-15-2020-792 (Уникальный идентификатор RF-190220X0031).

Вклад авторов: В. В. Фурсов — руководство *in silico* исследованием, идея, гипотеза, структура, моделирование, написание статьи; Д. И. Зинченко — моделирование, программный код, написание статьи; Д. Д. Наместникова — эксперимент *in vivo*; Д. И. Кузнецов — общее руководство проектом, анализ и обсуждение полученных данных, планирование эксперимента.

Соблюдение этических стандартов: исследование одобрено этическим комитетом ФГАОУ ВО РНИМУ им. Н. И. Пирогова Минздрава России (протокол № 140 от 15 декабря 2014 г.), а также университетской комиссией по контролю за содержанием и использованием лабораторных животных (протокол № 13/2020 от 08 октября 2020 г., протокол № 24/2021 от 10 декабря 2021 г.).

✉ **Для корреспонденции:** Валентин Владимирович Фурсов
ул. Островитянова, д. 1, г. Москва, 117997, Россия; vfursov@mail.ru

Статья получена: 05.07.2022 **Статья принята к печати:** 18.07.2022 **Опубликована онлайн:** 22.07.2022

DOI: 10.24075/vrgmu.2022.037

Stroke is the second most prevalent cause of death [1], hence the special relevance of effective pharmacophores for its treatment. Development and bench-to-bedside translation of pharmaceuticals is complex and lengthy, involving multiple preclinical and clinical steps. Optimization of such schemes by means of mathematical modeling using computer technologies is a well-defined task of applied bioinformatics.

Translational algorithms of computational pharmacology are increasingly recognized as integral tools in preclinical and clinical trials for innovative drugs. However, the expert judgments on this essential trend are non-uniform and depend on social/cultural background and economical/legal context.

New nanoparticle-based pharmacophores are a long-term focus of preclinical studies programs passed by the Shanghai Cooperation Organisation (SCO) for 2020–2025 [2, 3]. Significantly, this regional political and economical association of nine countries (China, Russia, Iran, India, Pakistan, Kazakhstan, Uzbekistan, Tajikistan and Kyrgyzstan) with a total budget of almost 26.8 billion USD currently provides support for ongoing developments in the field of preclinical studies optimization by emphasizing the influence of nanopharmacology models *in silico* [3, 4].

The apparent ethical and economical discrepancies between 'western' and 'eastern' perspectives on research, development and registration of new drugs [2, 3] signal an opportunity of modifying our attitude towards *in silico* methods in order to reduce both the costs and the lengths of pharmacophore translation. Sure enough, financial limitations and related obstacles [4] dictate a carefully weighted position with regard to a number of sensitive issues concerning translational medicine. On the other hand, we encounter the amassing experience of preclinical research optimization in Eurasian countries over the last 5–7 years.

For instance, recent translational projects controlled by SCO encompass current research on the neuroprotective potential of porphyrin-fullerene nanoparticles releasing $^{25}\text{Mg}^{2+}$. A remarkable aspect of this endeavour is the active use of *in silico* platforms designed to analyze allometric and *in vitro* data to predict the numerical values and variability levels for the most relevant pharmacokinetic and pharmacodynamic parameters [5–7].

After almost 15 years of studies on pharmacological effects of paramagnetic metal isotopes [4–11], three of them, ^{25}Mg , ^{43}Ca and ^{67}Zn , have been qualified as promising candidates for targeted delivery with the use of porphyrin-C60-based nanocarriers [8–11]. The above-mentioned reasons necessitate the use of *in silico* platforms with corresponding translational scenarios as appropriate [4, 5, 11, 12].

Modified algorithms of non-Markovian population dynamics, along with computational models based on ordinary differential equation (ODE) systems, are effective for predicting selective accumulation ^{25}Mg , ^{43}Ca , ^{60}Co and ^{67}Zn divalent metal isotopes released from PMC16 porphyrin-fullerene nanoparticles in brain cells [3].

This study aimed to develop a drug-oriented mathematical model in the ordinary differential equation system format for *in silico* implementation in MATLAB and adjust its adequateness using *in vivo* rat model.

METHODS

In silico model

The ODE system (1) used as a basis for the mathematical model implemented *in silico* was built analytically using

published biomedical evidence and our own experimental data concerning the *in vivo* effect of $^{25}\text{Mg}^{2+}$ -releasing porphyrin-fullerene nanoparticles (NPs) on the cerebral ischemic stroke pathogenesis. The code was written in MATLAB and implemented in MATLAB/SIMULINK version 2021b. The ODE system was solved using the Runge–Kutta midpoint method with the ode45 solver; $T_{1/2} = 9.0$ h, $T_{\text{max}} = 25$ h, $C_0 = 62$ $\mu\text{g}/\text{mL}$.

The behavior of the model in the parameter space was studied based on the theory of nonlinear dynamic systems with the method known as 'parametric analysis' (or 'bifurcation analysis' in synergetics) [14]. The method is effective for studying complex nonlinear processes in non-equilibrium systems of various types: physical, chemical, social, biological, etc., using their mathematical models on a computational experiment basis [14].

The mathematical model was built in the ODE system format by applying the five-compartment framework and choosing parameters to satisfy the *in vivo* experimental data. After reduction to a Cauchy problem by numerical method, the model was translated into machine code and further investigated by the parametric analysis of nonequilibrium processes and systems to bring it into line with the available experimental data.

The parametric analysis method [14] was further applied for studying the behavior of the model under various dynamic combinations of parameters to test the validity and adequacy of the proposed *in silico* platform, its power in solving pharmacokinetic problems, as well as the prospects of its use in optimization of the algorithms for preclinical studies.

In vivo experiment

NPs

The water-soluble PMC16-RX samples were courtesy of Dr N. Amirshahi, Amirkabir University of Technology, Tehran, Iran.

Animals

Wistar Albino Glaxo male rats ($n = 30$, purchased from BioPitomnik STEZAR facilities; Vladimir, Russia) of 180–220 g body weight were maintained on a standard fortified diet. The animals were fasted for 24 h before the experiment. Each experimental point involved 3 animals; each measurement was performed in 5–6 replicates. All manipulations involving animals (including withdrawal from the experiment) were performed in accordance with ARRIVE guidelines.

NP administration

NPs were administered to rats at 1.0 mg/kg and/or 20.0 mg/kg as a single intravenous injection using 15 mM Tris-HCl (pH 7.80) as a solvent. The animals were decapitated 12 h post-injection and brain tissue samples were homogenized in 5–7 volumes of 20 mM Tris-HCl (pH 8.0)/10 mM MgCl_2 /1.5 mM NaCl/2.0 mM EDTA/25 mM sucrose/2.0% Triton X-100 (w/w) using a glass/teflon Potter homogenizer at 1800 rpm (+4 °C).

Brain tissue homogenate fractionation

To isolate the S125 cytosolic fraction, the carefully washed homogenates were ultracentrifugated at 125,000 g for 4 h at +4 °C in a Spinco L5-65B ultracentrifuge (Beckman; USA), rotor SW 27.1. The S125 supernatants were collected and the protein content was measured by the conventional colorimetric Bradford assay.

Table 1. CZE system calibration: correlation of the internal standard content and optical density values of the identified PMC16 fractions (Rt = 7.0 min)

PMC16-RX, ng/mg S125 protein	(M + SEM), A ₃₄₀ /mL
1.0	0.09 + 0.02
5.0	0.33 + 0.08
10.0	0.61 + 0.09
25.0	1.84 + 0.08
50.0	3.87 + 0.11
100.0	5.32 + 0.50
200.0	8.55 + 0.72
1000.0	12.89 + 0.96

Note: CZE-analyzed samples comprised S125 acetone-soluble cytosolic pool mixed in a known proportion with NP (1.0–1000.0 ng/mg of the total cytosolic protein). Correlation coefficient $r = 0.86$; $n = 6$. NP retention time (effective migration) Rt = 7.0 min. CZE-analyzed sample: S125 acetone-soluble pool mixed in a known proportion with the target compound PMC16-RX (1.0–200.0 ng/mg of protein). Correlation coefficient $r = 0.86$; $n = 6$.

The S125 aliquots were mixed with 10 volumes of ice-cold acetone for subsequent overnight incubation at +4 °C. The precipitates were pelleted by centrifugation (20,000 rpm, 20 min, +4 °C) and discarded; the supernatants were collected and preserved for UV-spectrometry and CZE analysis.

To assess the NP extractability from biomaterial the acetone-insoluble pellets were dried at 25 °C and dissolved in 15 mM ammonium sulfate (pH 8.80)/0.1% SDS/2.5 mM EDTA/1.0% 2-mercaptoethanol (20 : 1, v/w) for subsequent 60 kHz ultrasonication at 40 °C for 60 min. The samples were subsequently analyzed by CZE (see below).

Ischemic stroke in vivo model

The stroke was modeled using conventional technique of the middle cerebral artery filament occlusion described elsewhere [15].

Original protocol of the capillary zonal electrophoresis (CZE)

The acetone-soluble S125 extracts were concentrated in a rotary evaporator to 0.2–0.3 mL volume and diluted with 30 mM ammonium phosphate (pH 8.80) 25 : 1, v/v. A 10 µl aliquot of this sample was injected into the receiver of a P/ACE MDQ Plus CZE analytical system (ALGIMED; Belarus) equipped with a UV-VIS 770 KS online fraction detector with a 440 nm monochromatic filter (Prince Technologies; Netherlands).

The CZE process was initiated and accomplished over 10 min at +6°C in a 50 µm (diameter) × 75 mm (effective length) quartz capillary containing UV-transparent silica gel saturated with SJX40 electrolyte pH 8.0 (SCLEX, BV; Netherlands).

Fractionation mode: 115 V/60 Hz/300 W/capillary. Block of planigraphic/temporal data analysis DAX DATE 220 LK (SCIEX BV; Netherlands). The calibration was carried out conventionally, using an internal standard in accordance with the algorithm recommended by the analytical system manufacturer (ALGIMED; Belarus); the calibration data are given in Table 1.

Pharmacokinetic distribution curves for PMC16 for different organs are given below; the confidence intervals were calculated using Student's method.

RESULTS

Our model is based on the common assumption that a nanoagent spreads throughout the body with the bloodstream, entering the heart, the liver, and the brain, and is eliminated naturally afterwards. At the same time, the post-ischemic inflammation area of the brain accumulates the nanoagent faster, which is explained by increased permeability of vascular walls in this area due to the

loosening of intercellular adhesions in the endothelium. The model is represented by ODE system (1) and illustrated in Fig. 1.

In ODE system (1) C_b , C_l , C_h , C_{is} , and C_{br} are concentrations of the nanoagent in the blood, the liver, the heart, intercellular spaces of the brain and brain cells, respectively. The 'intercellular spaces' compartment was added into consideration to emphasize the striking difference in permeability of the blood brain barrier for ischemic lesions compared with non-affected brain regions. The K_{is} constant is adjusted with regard to the size of ischemic lesion: the bigger the inflammation focus, the higher its value.

The K_b constant reflects the nanoagent elimination. The rest of the constants reflect the rates of transition of nanoagent molecules between the compartments. It is easy to see that summation across the system leaves us with the term $K_b C_b$ only, i.e. the nanoagent is completely eliminated from the body. For simplicity, the removal of the nanoagent through the liver is also included in K_b , but the metabolism takes time, which is reflected by the constants corresponding to the liver.

$$\begin{aligned}
 \frac{dC_b}{dt} &= -K_b C_b - K_{l+} C_b - K_{h+} C_b - K_{is+} C_b + K_{l-} C_l + K_{h-} C_h + K_{is-} C_{is} \\
 \frac{dC_l}{dt} &= K_{l+} C_b - K_{l-} C_l \\
 \frac{dC_h}{dt} &= K_{h+} C_b - K_{h-} C_h \\
 \frac{dC_{is}}{dt} &= K_{is+} C_b - K_{br+} C_{is} - K_{is-} C_{is} + K_{br-} C_{is} \\
 \frac{dC_{br}}{dt} &= K_{br+} C_{is} - K_{br-} C_{br}
 \end{aligned}
 \tag{1}$$

Knowing the half-life $T_{1/2}$ [5], we can estimate the elimination constant K_b as $\ln 2/T_{1/2}$.

We modeled a single intravenous injection of the substance at a 0.2 mg/µg dose. Although the uniform distribution of a pharmacophore from the injection site throughout the body is known to take time, we excluded the 'diffusion' factor from the model to simplify calculations, that is, assumed the nanoagent concentration uniformity immediately after administration.

The *in silico* modeling curves in comparison with *in vivo* experimental data are shown in Fig. 2.

The pharmacokinetics of the studied pharmacophore was simulated *in silico* over 24 h known to be the critical period of ischemic stroke development. With an increase in K_{h+} , the peak pharmacophore concentration in the myocardium shifts to the left and increases. According to published evidence [16], pharmacophore concentration rapidly peaks in the liver (within one hour) and declines rapidly, i.e. the liver clearance constant exceeds the absorption constant; at that, K_{h+} is smaller than K_{h-} . Upon a decrease in the clearance constant K_{l-} , the peak concentration of pharmacophore increases sharply. The corresponding constants describing pharmacodynamics for the brain require additional data for proper validation; nevertheless,

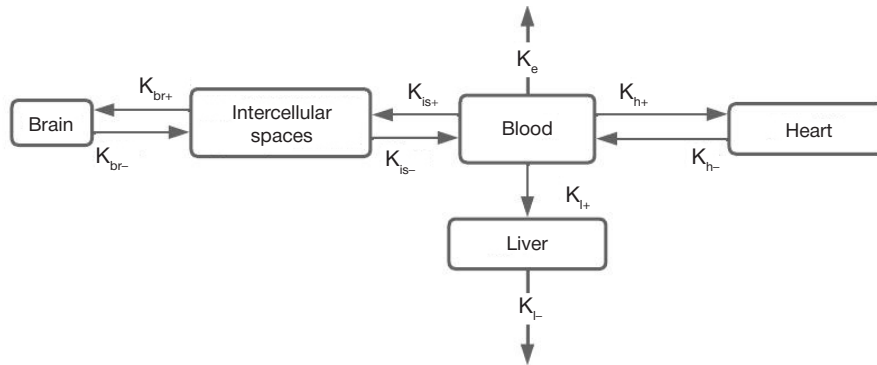


Fig. 1. A scheme of the five-compartment model of PMC16 pharmacokinetics

Fig. 2 shows that pharmacophore accumulation in the brain is lower compared with the liver and the myocardium, which is consistent with both the literature [16], and our own *in vivo* experiments. Fig. 2 shows the calculated and experimental pharmacokinetic curves for PMC16 in the brain, the liver and the heart. The calculated curves (shown in black) have a

classical shape and numerically fit into the confidence intervals of the experimental data collected *in vivo* for rat model, which proves the consistency between the mathematical model and the natural experiment.

Thus, we demonstrate experimentally that PMC16 crosses the blood-brain barrier to be internalized by the post-

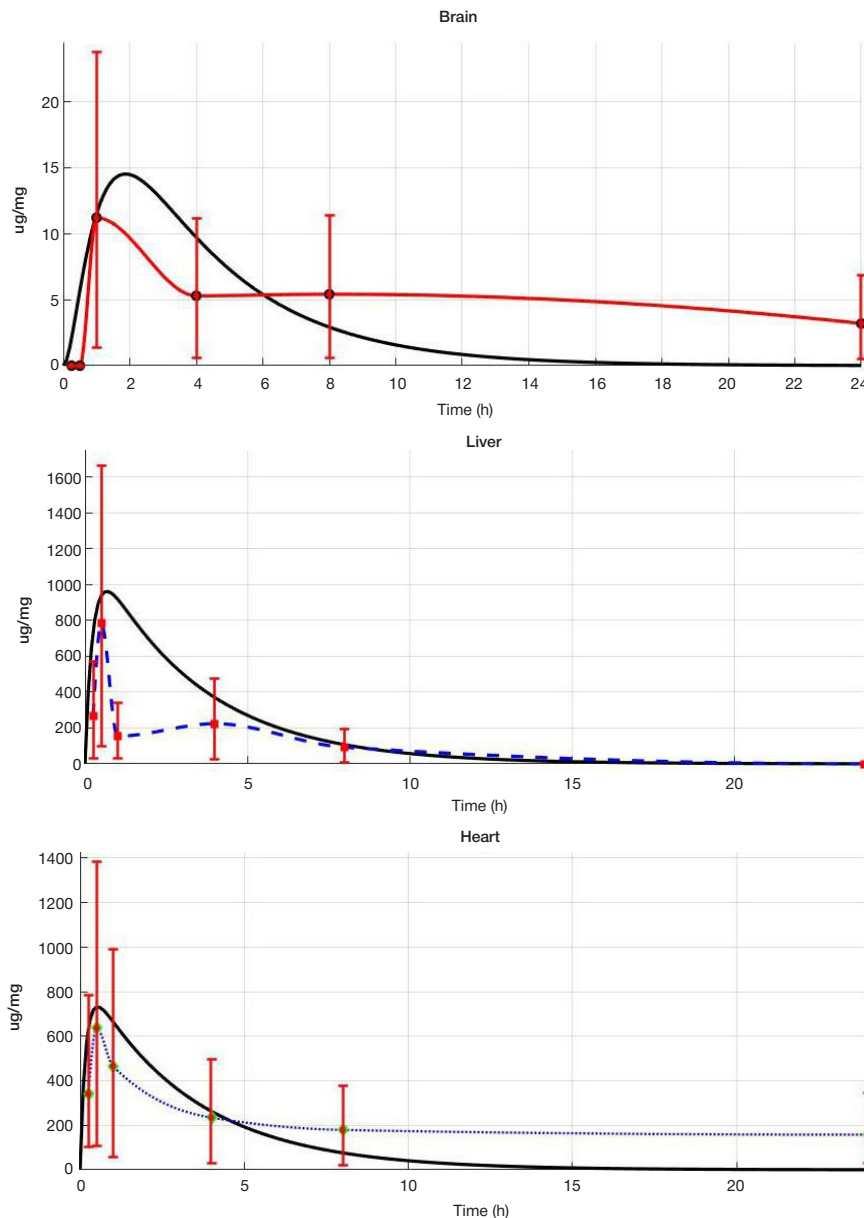


Fig. 2. Pharmacokinetic curves built using the model (shown in black) compared with experimental data for the brain, the liver and the heart ($K_{tm} = 0.50$; $K_p = 2$; $K_{ip} = 0.50$; $K_m = 6$; $K_{im} = 0.50$; $K_e = 0.077$; $K_{sp} = 0.70$; $K_{sm} = 0.70$; $K_{ism} = 0.10$; $K_{isp} = 0.10$)

Table 2. Permeability of the blood-brain barrier for PMC16-RX and pharmacophore internalization by brain cells

NP content in cytosol, ng/mg S125 protein (M ± SEM, n = 6)		
NON-AFFECTED BRAIN TISSUE	PENUMBRA	ISHEMIC LESION
7.83 ± 0.66	8.85 ± 0.74	4.11 ± 0.28

Note: 20 mg of PMC16-RX per 1.0 kg rat body weight intravenously, measured 12 h post-injection.

ischemic brain cells, delivering $^{25}\text{Mg}^{2+}$ ions that stimulate ATP hypersynthesis and thereby exert strong neuroprotective effects. At the same time, quantitative content of the studied pharmacophore in the brain, the heart and the liver differs. Our *in silico* model retrieves the same results, which confirms its prognostic potential and prospects in optimization of preclinical studies algorithms for porphyrin-fullerene nanocationites as promising neuroprotectants.

The distribution of PMC16 NPs in brain regions with regard to ischemic injury is given in Table 2.

DISCUSSION

The pharmacokinetics of porphyrin-fullerene nanoagents for preclinical research optimization is solvable *in silico* on a computational experiment basis [17, 18]. However, for comprehensive optimization of research algorithms, pharmacokinetics (PK) (i.e. computational output for the pharmacophore delivery to a particular organ, as has been done by us for PMC16 in this study) should be complemented by pharmacodynamics (PD) (i.e. a corresponding output for the development of therapeutic effect towards the studied pathology, e.g. ischemic stroke). We therefore consider building a complex PK/PD model as the ultimate prospective goal of our further research *in silico*.

Meanwhile, such studies are complicated not only by the scarcity of comprehensible mathematical models of ischemic stroke suitable for this purpose, but also by the lack of pharmacokinetic models for innovative pharmacophores, which may show distinct drug-specific pharmacokinetic patterns, especially under conditions of targeted delivery. The rapidly expanding field of nanopharmacology offers quite a number of such agents with excellent neuroprotective properties, albeit with pharmacokinetic patterns distinct from those of conventional pharmaceuticals [19].

These considerations are immediately applicable to the domestically produced PMC16, range regarded extraordinary promising in terms of ischemic stroke therapy. The invention of these pharmacophores was based on the fundamental discovery of the magnetic isotope effect exerted by $^{25}\text{Mg}^{2+}$. The magnetic isotope hyperactivates the magnesium-dependent ATP syntheses in a cell; moreover, such energy metabolism hyperactivation requires a tiny amount of these ions and can proceed even in the absence of oxygen, under conditions of profound tissue hypoxia [16]. These properties are exemplified by PMC-16 — a pharmaceutical nanoagent comprising a porphyrin-containing fullerene 'sphere' C60 (porphyrene-MC16) [20, 21].

The key issues in experimental validation of such *in silico* paradigm as ours include crossing of the blood-brain barrier by PMC16 and its capture (internalization) by brain cells. The task was accomplished (Fig. 2; Tables 1 and 2) to find both conditions fulfilled. Noteworthy, brain regions affected by the stroke were accessible to PMC16 as well (Table 2).

Thus, the relatively low 'mass quantity level' of NP capture by rat brain cells (Table 1) may have no correlation with the expected pharmacological effect of the agent, as the latter invariably involves the excessive ATP synthesis as a direct consequence of the $^{25}\text{Mg}^{2+}$ magnetic isotope effect phenomenon. At the same time, internalization of pharmacophore by target cells is definitely a priority in the advanced drug development.

A plain single-step ultracentrifugation (105,000–150,000 g) of mammalian tissue homogenates, usually pretreated with Triton X-100, ensures separation of cytosol from organelles, ribosomes, ribosomal subunits and membranous debris. The S125 fraction, a totality of soluble cytosolic compounds, is an excellent substrate to be used in pharmacophore internalization studies [3, 4, 10].

Although the obtained results are valuable as such, it should be noted that resolution and sensitivity of our CZE procedure are high enough to enable determination of the low-rate capture of PMC16-RX by rat brain, reaching estimated 4.0–8.0 ng per 1.0 mg of S125 total protein. Such content of NP, recorded 12 h after single intravenous injection of the drug, is distinctly above the background set by calibration (Table 1), which clearly indicates the penetration of the studied xenobiotic through the blood-brain barrier (Tables 1 and 2).

CONCLUSIONS

The developed *in silico* model describes the pharmacokinetics of PMC16 nanoparticles as promising neuroprotectants for the use in ischemic stroke therapy. The distribution of PMC16 in organs and tissues complies with a five-compartment mathematical model represented by an ordinary differential equation system and implemented computationally. The model can be fitted to specific properties of biological objects through the adjustment of numerical constants (parameters) of the model on the basis of *in vivo* experiments. The developed model is consistent with published evidence and newly collected experimental data and can be applied to optimize preclinical research scenarios for medical nanocationites PMC16 as neuroprotectants in ischemic stroke therapy.

References

- Global health estimates: Leading causes of death. World Health Organization. Available from (дата обращения: 25.05.22); <https://www.who.int/data/gho/data/themes/mortality-and-global-health-estimates/gho-leading-causes-of-death>.
- Li G, Liu Y, He R, et al. FDA decisions on new oncological drugs. *Lancet Oncology*. 2022; 23 (5): 583–5.
- Benjamin DJ, Prasad V, Lythgoe MP. FDA decisions on new oncological drugs. *Lancet Oncology*. 2022; 23 (5): 585–6.
- Das M. Biden's proposed investment in cancer research sparks concerns. *Lancet Oncology*. 2022; 23 (5): 576–80.
- Jun Z. SCO, a unique regional project. *St. Petersburg State Polytechnical University Journal*. 2016; 239 (1): 98–101.

6. Vasiliev AA, Spaper D, Ibragimov ZI. Ways to step up the international scientific and technological cooperation of the SCO countries. *Russian Asian Law Journal*. 2020; 13 (2): 92–6.
7. Kazemzadeh H, Mozafari M. Fullerene – based delivery systems. *Drug Discovery Today*. 2019; 24 (3): 898–05.
8. Kuznetsov D, Roumiantsev S, Fallahi M, et al. Non-Markovian population dynamics: does it help to optimize the chemotherapeutic strategy? *International Journal of Biomedical Science*. 2010; 6 (1): 20–6.
9. Bukhvostov AA, Dvornikov AS, Ermakov KV, Kuznetsov DA. Critical Study of Retinoblastoma Case: Shall We Get a Paramagnetic Trend in Chemotherapy? (2020) In: Quershi NA, editor. *Current Topics in Medicine and Medical Research*. Science Domain Publ., Ltd: Hoogley – London – New York, 2020; 1: 72–78.
10. Orlova MA, Osipova EY, Roumiantsev SA. Effect of 67Zn-nanoparticles in leukemic and normal lymphocytes. *British Journal of Medicine and Medical Research*. 2012; 2 (1): 21–30.
11. Buchachenko AL, Bukhvostov AA, Ermakov KV, et al. A specific role of magnetic isotopes. *Physics and biophysics beyond*. *Progress in Biophysics and Molecular Biology*. 2020; 155 (1): 1–20.
12. Fursov IV, Zinchenko DI, Fursov VV, Ananishnev VM. Технологии искусственного интеллекта в здравоохранении. *Создание In Silico — алгоритмов для оптимизации в экспериментальной нанофармакологии ишемического инсульта*. Сборник работ преподавателей, аспирантов и студентов. М.: Pero, 2022; с. 30–33. Russian.
13. Johansen RJ, Bukhvostov AA, Ermakov KV, Kuznetsov DA. Towards a computational prediction for the tumor selective accumulation of paramagnetic nanoparticles in retinoblastoma cells. *Bulletin of Russian State Medical University*. 2018; 6: 68–73. DOI: 10.24075/brsmu.2018.078. – EDN YZGOXB.
14. Kurkina ES. Моделирование нелинейных явлений в физико-химических системах: Автокколебания. Структуры. Волны. С подробными примерами в MATLAB. М.: LENAND, 2019; 248 с. Russian.
15. Gubsky IL, Namestnikova DD, Cherkashova EA, Chekhonin VP, Baklaushev VP, Gubsky LV, Yarygin KN. MRI guiding of the middle cerebral artery occlusion in rats aimed to improve stroke modeling. *Translational Stroke Research*. 2018; 9: 417–25.
16. Sarkar S, et al. Use of a magnesium isotope for treating hypoxia and a medicament comprising the same: заяв. пат. 12123245 США, 2008.
17. Fursov VV, Ananov AV, Ananov VN. Компьютерная математическая модель патологических изменений участка мозговой ткани при развитии инсульта. *Естественные и технические науки*. 2022; 5 (168): 173–7. Russian.
18. Fursov VV, et al. In silico studies on pharmacokinetics and neuroprotective potential of $^{25}\text{Mg}^{2+}$: releasing nanocationites — background and perspectives. *Pharmacogenetics*. 2021; p. 155.
19. Amirshakhi N, i dr. Порфирин-фуллереновые наночастицы для лечения гипоксических кардиопатий. *Российские нанотехнологии*. 2008; 3 (9–10): 125–35. Russian.
20. Sarkar S, Rezayat SM, Buchachenko AL, Kuznetsov DA, Orlova MA, Yurovskaya MA, Trushkov IV. (2007) Новые водорастворимые порфирин-фуллереновые соединения. Патент Европейского союза № 07009882.7/EP07009882 (рег.: Мюнхен, Германия). Russian.
21. Sarkar S, Rezayat SM, Buchachenko AL, Kuznetsov DA, Orlova MA, Yurovskaya MA, Trushkov IV. (2007) Использование изотопа магния для лечения гипоксии и лекарственного средства, содержащего его. Патент Европейского союза № 07009881.9/EP07009881 (рег.: Мюнхен, Германия). Russian.

Литература

1. Global health estimates: Leading causes of death. World Health Organization. Available from (дата обращения: 25.05.22): <https://www.who.int/data/gho/data/themes/mortality-and-global-health-estimates/ghe-leading-causes-of-death>.
2. Li G, Liu Y, He R, et al. FDA decisions on new oncological drugs. *Lancet Oncology*. 2022; 23 (5): 583–5.
3. Benjamin DJ, Prasad V, Lythgoe MP. FDA decisions on new oncological drugs. *Lancet Oncology*. 2022; 23 (5): 585–6.
4. Das M. Biden's proposed investment in cancer research sparks concerns. *Lancet Oncology*. 2022; 23 (5): 576–80.
5. Jun Z. SCO, a unique regional project. *St. Petersburg State Polytechnical University Journal*. 2016; 239 (1): 98–101.
6. Vasiliev AA, Spaper D, Ibragimov ZI. Ways to step up the international scientific and technological cooperation of the SCO countries. *Russian Asian Law Journal*. 2020; 13 (2): 92–6.
7. Kazemzadeh H, Mozafari M. Fullerene – based delivery systems. *Drug Discovery Today*. 2019; 24 (3): 898–05.
8. Kuznetsov D, Roumiantsev S, Fallahi M, et al. Non-Markovian population dynamics: does it help to optimize the chemotherapeutic strategy? *International Journal of Biomedical Science*. 2010; 6 (1): 20–6.
9. Bukhvostov AA, Dvornikov AS, Ermakov KV, Kuznetsov DA. Critical Study of Retinoblastoma Case: Shall We Get a Paramagnetic Trend in Chemotherapy? (2020) In: Quershi NA, editor. *Current Topics in Medicine and Medical Research*. Science Domain Publ., Ltd: Hoogley – London – New York, 2020; 1: 72–78.
10. Orlova MA, Osipova EY, Roumiantsev SA. Effect of 67Zn-nanoparticles in leukemic and normal lymphocytes. *British Journal of Medicine and Medical Research*. 2012; 2 (1): 21–30.
11. Buchachenko AL, Bukhvostov AA, Ermakov KV, et al. A specific role of magnetic isotopes. *Physics and biophysics beyond*. *Progress in Biophysics and Molecular Biology*. 2020; 155 (1): 1–20.
12. Фурсов И. В., Зинченко Д. И., Фурсов В. В., Ананишев В. М. Технологии искусственного интеллекта в здравоохранении. Создание in silico-алгоритмов для оптимизации в экспериментальной нанофармакологии ишемического инсульта. Сборник работ преподавателей, аспирантов и студентов. М.: Pero, 2022; с. 30–33.
13. Johansen RJ, Bukhvostov AA, Ermakov KV, Kuznetsov DA. Towards a computational prediction for the tumor selective accumulation of paramagnetic nanoparticles in retinoblastoma cells. *Bulletin of Russian State Medical University*. 2018; 6: 68–73. DOI: 10.24075/brsmu.2018.078. – EDN YZGOXB.
14. Куркина Е. С. Моделирование нелинейных явлений в физико-химических системах: Автокколебания. Структуры. Волны. С подробными примерами в MATLAB. М.: ЛЕНАНД, 2019; 248 с.
15. Gubsky IL, Namestnikova DD, Cherkashova EA, Chekhonin VP, Baklaushev VP, Gubsky LV, Yarygin KN. MRI guiding of the middle cerebral artery occlusion in rats aimed to improve stroke modeling. *Translational Stroke Research*. 2018; 9: 417–25.
16. Sarkar S, et al. Use of a magnesium isotope for treating hypoxia and a medicament comprising the same: заяв. пат. 12123245 США, 2008.
17. Фурсов В. В., Ананьев А. В., Ананьев В. Н. Компьютерная математическая модель патофизиологических изменений участка мозговой ткани при развитии инсульта. Естественные и технические науки. 2022; 5 (168): 173–7.
18. Fursov VV, et al. In silico studies on pharmacokinetics and neuroprotective potential of $^{25}\text{Mg}^{2+}$: releasing nanocationites — background and perspectives. *Pharmacogenetics*. 2021; p. 155.
19. Амиршахи Н. и др. Порфирин-фуллереновые наночастицы для лечения гипоксических кардиопатий. *Российские нанотехнологии*. 2008; 3 (9–10): 125–35.
20. Саркар С., Резаят С. М., Бучаченко А. Л., Кузнецов Д. А., Орлова М. А., Юровская М. А., Трушков И. В. (2007) Новые водорастворимые порфирин-фуллереновые соединения. Патент Европейского союза № 07009882.7/EP07009882 (рег.: Мюнхен, Германия).
21. Саркар С., Резаят С. М., Бучаченко А. Л., Кузнецов Д. А., Орлова М. А., Юровская М. А., Трушков И. В. (2007) Использование изотопа магния для лечения гипоксии и лекарственного средства, содержащего его. Патент Европейского союза № 07009881.9/EP07009881 (рег.: Мюнхен, Германия).